Experimental Diabetes Research

Inflammation and Oxidative Stress in Obesity, Metabolic Syndrome, and Diabetes

Guest Editors: Pietro Galassetti, Bo Andersen, and Dan Nemet

Inflammation and Oxidative Stress in Obesity, Metabolic Syndrome, and Diabetes

Experimental Diabetes Research

Inflammation and Oxidative Stress in Obesity, Metabolic Syndrome, and Diabetes

Guest Editors: Pietro Galassetti, Bo Andersen, and Dan Nemet

Editorial Board

Contents

Hindawi Publishing Corporation
Experimental Diabetes Research
Volume 2012, Article ID 943706, 2 pages
doi:10.1155/2012/943706

Editorial

Inflammation and Oxidative Stress in Obesity, Metabolic Syndrome, and Diabetes

Pietro Galassetti

ICTS Metabolism/Bionutrition Core, University of California, Irvine, CA 92697-1385, USA

Correspondence should be addressed to Pietro Galassetti, pgalasse@uci.edu

Received 12 December 2012; Accepted 12 December 2012

I do not think anybody even remotely connected with the field of diabetes, either as a researcher or as a health care provider, would have any serious objection to the concept that some degree of altered inflammatory activity or oxidative stress plays a serious role in multiple aspects of diabetes. Just to mention two of the best-known processes, a violent, acute inflammatory event leads to the destruction of beta cells at the onset of type 1 diabetes, and a chronic, subclinical proinflammatory state is at the base of the slow development of micro- and macrovascular complications accounting for the larger part of morbidity and mortality related to all forms of diabetes. This connection has led to a remarkable increase in research activity in this field in recent years. Running a PubMed search with "inflammation and diabetes" as search terms, for instance, returns 14,059 articles; "Oxidative stress and diabetes" 8850 articles; "inflammation and atherosclerosis" 11209 articles; and "inflammation and cardiovascular disease" 49245 articles. To a smaller extent, the very content of this special issue is a clear example of the variety and complexity of issues in the prevention, diagnosis, management, and therapy of diabetes, in which one or more inflammatory or oxidative stress component plays a critical role.

Inflammation and oxidative stress, however, are two extremely broad and comprehensive terms. This wealth of studies and results certainly clarified a large number of pathways, mediators and regulatory mechanisms, genes and post-transcriptional regulators of gene expression related to inflammation and oxidative stress. However, given the very large, and constantly growing, number of cell types and molecules involved, it often feels as though the rate at which new questions accumulate far exceeds the rate at which prior questions are definitively answered. We have now identified hundreds of cytokines and chemokines, whose full physiological function remains in many cases nebulous. Terms such as "pro" or "anti-inflammatory," earlier closely associated with individual inflammatory mediators (such as the classically defined proinflammatory interleukin-6), are now used more reluctantly, as the same molecules often display less clear-cut activity, or even shift from one end of the spectrum to the other, depending on the surrounding metabolic or cell-signaling milieu. More importantly, often only some components of the complex inflammatory network are altered in a specific pathological condition. Identifying what these components are, and using them as biomarkers of onset, progression or response to treatment of a given condition has become one the main focuses of inflammatory research. Again, however, the immense diversity of these biomarkers renders the task extremely difficult. Let us hypothesize, for the sake of discussion, that a group of cytokines, or certain leukocyte surface markers of activation, are definitively demonstrated to increase significantly in a population of diabetic patients (let us say young caucasian adult males with type 2 diabetes), and that their increase is proportional to the degree of early endothelia dysfunction in these subjects. While this piece of knowledge can lead to therapeutic and preventive efforts in this specific populations, it immediately raises the issue of whether the same biomarkers are as effective in other populations, that is, in different age groups, gender, ethnicities, different degrees of diabetes control, different duration of the disease, and so forth. In short, each set of chosen inflammatory biomarkers should be closely tailored to as well defined a subpopulation of subjects as possible, which would obviously require an enormous amount of research work. This work is feasible and should indeed be planned and systematically performed. It is obvious, however, that to cover all aspects of the interaction between altered inflammation, oxidative stress, and diabetes (with associated prediabetic states such as obesity and metabolic

syndrome), no single laboratory or group of laboratories can have the ability to perform all necessary studies. To really produce conclusive, reproducible, nonredundant results complementing each other and truly generating all interlocking pieces of an all-inclusive inflammatory jig-saw puzzle, a global scale, coordinated effort must be undertaken by a very large number of competent research groups, addressing in a synergistic, collaborative way the most pressing questions and then systematically chipping away at all collateral issues. Essential to this task is also the establishment of capillary informatics tools that would allow the immediate and complete exchange of data across groups, as soon as they are being gathered. While such an entity does not currently exist, at least not of the scale proposed here, many collaborations are indeed being formed across research groups, and the outlook for the future seems positive. In the meantime, I do not mean to discount the importance of many very good individual studies that are clarifying specific aspects of this broad issue. Given the immeasurable size of the task ahead, each new piece of information is precious, helpful, and welcome.

Pietro Galassetti

Hindawi Publishing Corporation
Experimental Diabetes Research
Volume 2012, Article ID 683680, 7 pages
doi:10.1155/2012/683680

Review Article

Aspects of Inflammation and Oxidative Stress in Pediatric Obesity and Type 1 Diabetes: An Overview of Ten Years of Studies

Brian Tran,[1] Stacy Oliver,[2] Jaime Rosa,[2] and Pietro Galassetti[1, 2, 3]

[1] *Insitute for Clinical and Translational Science, University of California, 843 Health Science Road, Irvine, CA 92697, USA*
[2] *Department of Pediatrics, School of Medicine, University of California, 100 Theory, Irvine, CA 92697, USA*
[3] *Department of Pharmacology, School of Medicine, University of California, 360 Med. Suzge II, Irvine, CA 92697, USA*

Correspondence should be addressed to Pietro Galassetti, pgalasse@uci.edu

Received 8 May 2012; Accepted 16 August 2012

Academic Editor: Dan Nemet

Obesity and type 1 diabetes (T1DM) are the two most common conditions of altered metabolism in children and adolescents. In both, similar long-term cardiovascular complications are known to occur, mediated in large part by underlying inflammatory and oxidative processes whose biochemical details remain relatively unclear. Through a series of experiments in these patient populations, over the last decade our laboratory has clarified a number of key issues in this field. Interestingly, while obese and type 1 diabetic children often differed in the specific type and magnitude of molecular alterations, in both groups a clear exaggeration of inflammatory and oxidative activation was detected when compared to healthy, age-matched controls. Our main findings include definition of resting and exercise-induced cytokine patterns and leukocyte profiles, patterns of activation of immune cells *in vitro*, and correlation of the magnitude of observed alterations with severity of obesity and quality of glycemic control. Further, we have identified a series of alterations in growth factor profiles during exercise that parallel inflammatory changes in obese children. This paper offers a concise overview of the salient results from this decade-long research effort.

1. Introduction

In a time when remarkable scientific advances have occurred in all fields of medicine, it seems sometimes anachronistic that in some areas, in which awareness of a given pathological condition and general knowledge of its pathophysiology have been established for decades, improvements in prevention, management, and avoidance of complications have not been as rapid and complete as could have been expected. This is especially true for conditions of altered metabolism in pediatric populations, such as obesity and diabetes, in which lack of a deep and thorough understanding of multiple disease aspects still prevents the widespread, effective control of health care and social problems associated with these conditions. In children and adolescents, obesity and type 1 diabetes (T1DM) are by far the two most common dysmetabolic conditions. While in recent decades obesity has been increasing at alarming rates in industrialized countries across all age groups, this phenomenon has been especially pronounced in children and adolescents. The obvious threat to which these populations are exposed is that if the condition is not corrected later in life, which unfortunately in the large majority of cases is not the case, onset and progression of related cardiovascular complications will occur at a proportionally earlier age, with enormous estimated social, health care, and emotional costs. Among obesity complications is of course also type 2 diabetes (T2DM). While this condition accounts for ~90% of all diabetes cases and is also occurring at much greater rates in pediatric ages than was used to only 20 years ago, it is still much less common than T1DM among children and adolescents. Paradoxically, while the recent increase in T2DM has been explained with the parallel obesity epidemic, the prevalence of T1DM has also been increasing in recent years, for reasons that remain unclear. Obesity and T1DM share a number of common features. Most importantly, in both conditions, long-term complications include severe impairment of the cardiovascular system. While this association has been clearly established empirically, much still remains to be learned about the specific pathogenetic

mechanisms regulating the development of these complications. Consensus exists among the leading research groups in this field that a major role is played by chronic subclinical levels of inflammation and oxidative stress which, in both conditions, through slow but persistent damaging action on the endothelial surface, eventually result in stiffening, narrowing, and occlusion of arteries of various caliber in a broad range of tissues. Inflammation and oxidative stress, however, are very extensive and complex processes encompassing the coordinated action of hundreds and possibly thousands of cellular and molecular mediators, including dozens of subtypes of immune cells (with shifting patterns of surface markers of activation), hundreds of cytokines, chemokines, growth factors, and their related receptors and binding proteins. Which components of this intricate network are activated at any given time, for how long, and to what degree, at any stage of obesity and T1DM, remains very poorly defined. Further, it is unclear to what degree any of the reported levels of exaggerated inflammation or oxidative stress are due to the presence of obesity or T1DM per se, or to an acute exacerbation of a specific aspect of each condition, such as acute hyperglycemia in T1DM or hyperlipidemia in obesity. To add a further layer of complication, most of what we know about interaction of metabolic dysregulation and inflammation/oxidative stress in obesity and T1DM is derived from studies in adults and may therefore not be applicable to pediatric populations in which the endogenous metabolic milieu changes rapidly and repeatedly during growth and development. Our group has therefore performed, over the last decade, a number of studies focused on the attempt to clarify key aspects of this interaction in pediatric populations. This paper is aimed at providing a broad overview of the main finding of these prolonged efforts.

Before we even start reporting our findings in these specific populations, however, it should be clear that this is only part of a broader context, in which inflammation, oxidative stress, and their interaction with exercise modulate health status in many more subject populations with related dysmetabolic conditions. Pediatric prediabetic states, for instance, may present with significant inflammatory alterations; in pre-type 2 diabetes, the enormous increase in circulating insulin may act by itself as a major inflammatory modulator, independent of obesity status [1]. In pre-type 1 diabetes, when autoantiobodies start increasing, a massive surge in inflammatory processes is preparing to explode which, if correctly identified in its exact time frame, holds great promise for preventive interventions that may block the evolution into frank diabetes [2]. Finally, even within the normal BMI range, positions close to the overweight range may be associated with less dramatic, but still clinically relevant differences in inflamamtiory status [3]. While all these conditions are important and definitely need to be explored in detail, their comprehensive evaluation is beyond the scope of this paper, which we will therefore keep focused on the two quantitatively largest pediatric dysmetabolic conditions, T1DM and obesity.

2. Inflammation in T1DM

Type 1 diabetes mellitus (T1DM) has long been associated with the development of cardiovascular disease (CVD). Numerous epidemiological studies have observed that diabetic subjects had extremely high risks of developing atherosclerosis, acute coronary events, and stroke relative to the general population [4, 5]. This risk is attenuated with very good glycemic control (DCCT); however, even very well-controlled patients retain considerably higher cardiovascular risk as compared to healthy matched controls.

Multiple lines of recent evidence indicate that the biochemical link between diabetes and later development of CVD includes the two parallel and related processes of increased inflammation and oxidative stress. T1DM is characterized as an inflammatory disease from several points of view. First, an acute, intense inflammatory reaction causes the very onset of the disease via lymphocyte-mediated destruction of pancreatic beta cells. After this first major inflammatory episode is resolved, a chronic state of whole-body low-grade inflammation appears to persist, which is periodically exacerbated by hyperglycemic fluctuations. In fact, elevated markers of inflammation [6], immune activation [7], and oxidative stress [8, 9] have been observed in the T1DM population. All of these factors are heavily associated with the initiation and progression of atherosclerosis and CVD [10]. However, the exact pathogenesis of these alterations is not well understood. This issue becomes particularly relevant when considering the disease in children, where the alterations have potential implications in the complex interaction of early onset of disease symptoms, growth, and development. Work in our laboratory over the last several years has continued with this line of inquiry; we have conducted a number of experiments designed to help isolate and characterize factors involved in the T1DM child's inflammatory state.

In an early study with 12 T1DM children and healthy controls, we observed a distinctly altered inflammatory cytokine profile for T1DM children. In particular, the T1DM group displayed markedly elevated interleukin 6 (IL-6), a molecule considered a classic proinflammatory mediator, but which, in specific context, has to be also hypothesized to exert opposite, antiinflammatory effects [11]. This finding was later confirmed in a larger study on 49 T1DM and 42 healthy controls, in which a more comprehensive inflammation and oxidative stress biomarker panel was performed. The T1DM group displayed not only elevated levels of IL-6, but also significantly higher plasma myeloperoxidase (MPO), an oxidative stress marker derived from neutrophils, monocytes, and macrophages. The latter observation is in agreement with prior studies indicating that chronic excessive activation of these cells lines is involved in the progression of atherosclerosis and cardiovascular disease in a number of dysmetabolic states [12, 13]. Additional evidence that inflammatory processes may be exaggerated in T1DM can also be found in a recent study that focused on observing gene expression of proinflammatory cytokines and chemokines in leukocytes following T-cell receptor and Fc receptor stimulation [14]. Leukocytes from T1DM children

displayed exaggerated gene expression for TNFSF 5, 7, and 9, CCL8, and CXCL10 compared to healthy controls.

One of the main issues driving our experimental design was the relative contribution of presence of diabetes per se, versus periodic hyperglycemic exacerbations, to the overall inflammatory status in these patients. Hyperglycemia is known to induce an acute state of inflammation, both in healthy and in diabetic subjects [15]. It had not been demonstrated, however, if this increased inflammatory state would persist after the hyperglycemic episode was resolved. This is especially relevant to T1DM children with poor glycemic control, where repeated hyperglycemic peaks are particularly common. In these subjects, the inability to fully correct for the proinflammatory effect of hyperglycemic episodes may result in chronically elevated inflammation, thus worsening its long-term damaging effects on the vascular system. We therefore measured a number of immune-modulatory cytokines in children with T1DM who were either normo- or hyperglycemic. Among these, IL-1α, IL-4, and IL-6 were significantly elevated in the hyperglycemic group not only while their glucose was high, but also for at least 2 hours after hyperglycemia had been corrected [16]. The presence of this sustained inflammatory state stressed the importance of preventing as opposed to correcting hyperglycemia and implied that additional therapeutic approaches, such as anti-inflammatory regimens, targeting this state in poorly controlled T1DM may be necessary to help prevent vascular complications.

A logical extension of the above experiments became the characterization of the nature of the hyperglycemic states (severity, durations, or distance in the past) that led to subsequent sustained inflammation. In a previous study, we divided 29 T1DM children in to 4 subgroups, based on their spontaneous morning glycemic level; we then normalized blood glucose in all subjects, kept them euglycemic for at least 2 hours, and then measured plasma IL-6. Not surprisingly, we observed that the group with the highest prior morning plasma glucose (>300 mg/dL) also had the highest IL-6 concentrations; the other three groups (prior glycemia of 200–300, 150–200, and <150 mg/dL, resp.) displayed progressively lower IL-6 levels, the lowest being identical to healthy controls. A subsequent study expanded these findings by incorporating the effect of prior hyperglycemia not only in the morning of the measurements, but also for the full previous three days. Participants wore a continuous glucose monitoring system recording glycemia every 5 minutes for a 3-day period while continuing their normal insulin regimen and conducting normal life activities (Figure 1). This allowed us to obtain additional information, including depth, duration, and repetition pattern of each hyperglycemic episode, as well as total time spent above arbitrary hyperglycrmic thresholds (i.e., 11 mM, the clinical definition of postprandial hyperglycemia). Among these variables, the average glycemia over the whole 3-day period correlated best with IL-6 levels at the end of the continuous measurements, after all subjects' glycemia had again been normalized for several hours. Again, children with the highest mean prior 3-day glycemia had the highest IL-6 levels and progressively lower IL-6 as their prior glycemia approached the physiological profile. Within subjects with similar mean 3-day glycemia, a greater proinflammatory effect was observed in those with the highest hyperglycemic peaks, indicating that optimal management strategies in these patients must be aimed not only at limiting the overall occurrence of hyperglycemia, but also at preventing its most dangerous characteristics (for example, the same overall amount of postprandial hyperglycemia can be achieved without a very high hyperglycemic peak if insulin administration is timed carefully and carbohydrate ingestion is spaced over a longer time).

One well-known therapeutic approach to reduce whole-body inflammation is exercise training. In the context of T1DM, the benefits are obvious: as stated previously, the potential risk for the development of CVD via a sustained state of inflammation is attenuated. Interestingly, a reduction in systemic inflammatory status occurs with long-term training [17, 18], while, somewhat paradoxically, individual bouts of exercise are in contrast acutely proinflammatory. This would normally not be an issue in the healthy subject, where the exercise-induced inflammation is well controlled, but in T1DM children, in whom our experiments have shown to be unable to fully correct for hyperglycemia-induced inflammation, the presence of this proinflammatory effect may mitigate the benefits of exercise or may even lead to deleterious effects over time. To address this issue, we conducted a number of experiments to clarify the effect of exercise on T1DM children.

Central to our exercise studies is the exercise protocol, which was specifically developed in our laboratory to both normalize work rate and maximize the physiological adaptive response, while also simulating real-life spontaneous physical activity. The test consisted of performing, on a stationary bike, a series of ten 2-minute exercise bouts at 80% of individual maximal aerobic capacity (VO2max, determined during a preliminary separate test), separated by 1-minute intervals. This sequence made it easier for children to tolerate the 30-minute challenge and produced a similar set of response as could be elicited by the stop-and-go pattern of a soccer or basketball game. This exercise protocol, now having been applied thousands of times to a variety of different experimental settings and in children with numerous health conditions, has been instrumental in ensuring that the physical exertion from exercise is normalized across different subjects.

Inflammation is a multifaceted condition, with many aspects mediated via activation of immune cells. Indeed, leukocyte counts physiologically increase acutely by ~50% during exercise. This effect seems not to be altered by the presence of diabetes, as demonstrated by a recent study from our laboratory in which we measured circulating leukocytes (neutrophils, lymphocytes, and monocytes), before and after the exercise challenge described above, in 45 healthy and 16 T1DM children. In both groups, all leukocyte measurements, including total and the subtypes, were significantly elevated at end exercise and returned to near baseline at 30 minutes after exercise. In pediatric diabetes therefore, an increased

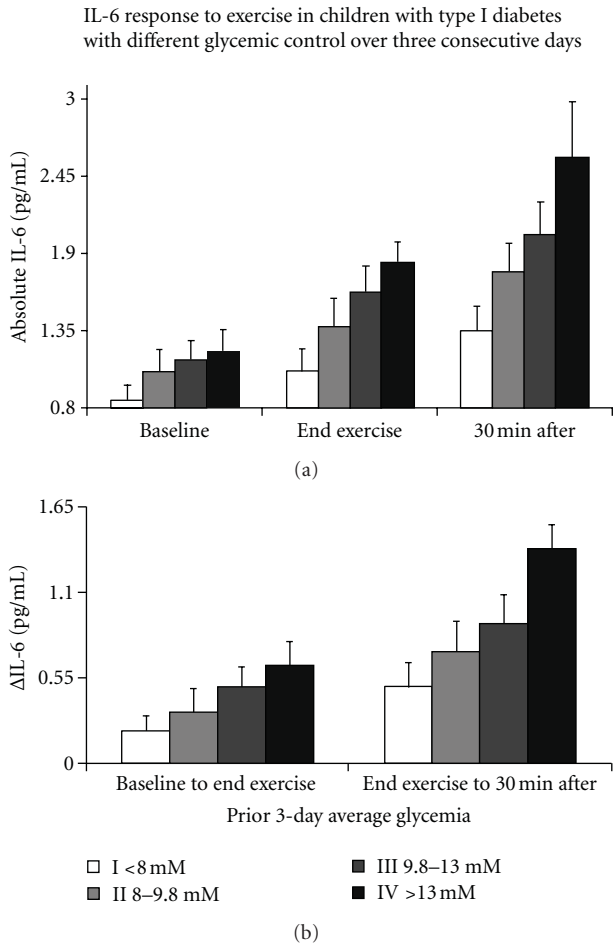

Figure 1: Plasma interleukin-6 (IL-6) in 47 children with type 1 diabetes before, at the end of, and 30 min after a standardized 30 minute intermittent exercise challenge (a) and exercise-induced IL-6 increments (b). While all children exercised in euglycemic conditions (and had been euglycemic for at least the two hours preceding exercise), they differed in average glycemic control during the previous three days and were therefore subdivided in four groups (11-12 subjects each) with increasing mean prior 3-day glycemia. Children in the group with the lowest mean glycemia (<8 mM, only slightly greater than comparable healthy controls) displayed the lowest IL-6 values at all time points; with greater mean prior glycemia, IL-6 values became progressively higher. Data are group means ± SE. $^*P < 0.05$ <8.0 mM group I.

contribution of circulating immune cells to systemic inflammation seems to be mediated, rather than by an increase in their number, by their levels of proinflammatory activation.

While several studies have measured cytokine response to exercise, especially IL-6, considerable inconsistency exists in the published literature as to the extent, and in some cases presence at all, of these responses (e.g., an increase or decrease in a specific cytokine from exercise). Coincidentally, many studies that looked into this effect simply measured two points (usually at baseline and after exercise), with conclusions that were based off of a linear interpolation of those points. Should cytokine levels actually fluctuate in a nonlinear manner during physical activity, two time points could have provided an incomplete view of the overall response to exercise. Thus, our group conducted a study to better clarify this issue [19]. Twenty one T1DM children and age-matched healthy controls underwent our standard exercise challenge. In this experiment, however, additional blood samples were drawn every 6 minutes during exercise and 4 times in 15-minute intervals after exercise. Testing revealed a relatively conserved, non linear pattern across various cytokines and chemokines. The control subjects generally exhibited an initial drop in circulating inflammatory mediators during exercise (possibly due to binding of existing molecules to the acutely increase numbers of circulating leukocytes), followed by a measurable rise at end of or after exercise (possibly due to new cytokine/chemokine molecules being secreted in response to exercise stimulus). T1DM subjects, for the majority of cytokines and chemokines, did not display the initial drop during exercise and instead exhibited an exaggerated and accelerated profile of inflammatory activation, with larger increases of mediators that peaked more rapidly during exercise. This was most clearly seen in the cytokines IL-6, tumor necrosis factor-α (TNF-α), and the chemokines monocyte chemoattractant protein-1 (MCP-1) and macrophage inflammatory protein-1α (MIP-1α). The practical meaning of this finding is that for the whole duration of exercise, at least in this particular format, T1DM children were exposed to a clearly more proinflammtory milieu, with greater concentrations of both proinflammatory mediators and of chemoattractants/activators for monocytes, known to play a key role in the early development of vascular atherosclerotic lesions.

3. Inflammation and Pediatric Obesity

Along with T1DM, obesity is among the most common dysmetabolic disorders in children. Modern society's increasingly sedentary lifestyles and growing ease of overnutrition have contributed to the prevalence and incidence of excessive adiposity, which has consistently risen in the US throughout the past four decades. In the latest NHANES conducted by the CDC, about 17% of children aged 9–17 were observed to be clinically obese [20], and other reports indicate that the prevalence may be even higher in the US population overall and certainly is within certain populations and at risk minorities [21]. Early-onset obesity has been clearly linked to a very high likelihood of life-long permanence of obesity, resulting in an exponential increase in the risk for CVD and other complications. The biochemical details and in-depth metabolic characteristics of pediatric obesity, however, which may differ substantially from adults and are at the very base of our ability to develop effective preventive and therapeutic strategies, remain very poorly understood. In this context, in our laboratory, we have therefore focused on identifying a number of physiological and pathological aspects of pediatric obesity, particularly as related to exercise.

The previously mentioned leukocytosis response study also included overweight children (BMI% > 85) [22]. These

subjects exhibited a pattern and magnitude of exercise-induced leukocytosis that was similar to healthy and T1DM children (i.e., all leukocyte subpopulations increased similarly in response to exercise and returned to near-baseline levels within 60 min after exercise cessation); as the study also included yet another group of children (with asthma), who also displayed a similar unaltered response pattern, the data indicate that leukocyte responses to exercise are a highly conserved adaptation mechanism that remains unaltered across a wide range of conditions. It should be noted, however, that the similarity in baseline leukocyte counts between overweight and healthy controls, observed in this study, was somewhat in contrast with a previous study, in which overweight children had higher baseline counts [23]. We believe that while this discrepancy may be due to differences in the severity of overweight/obesity, more severely obese children, therefore, may start exercising with higher basal leukocytes, and even maintaining a normal leukocyte response to exercise, they may be exposed to higher leukocyte levels at all times during and immediately after exercise, likely resulting in parallel increases in other indices of inflammation.

Additional support for this last concept was in fact provided by other studies in which multiple inflammatory mediators were measured in obese children during exercise. For instance, significantly larger levels of baseline and exercise-induced IL-6 were observed in overweight children by McMurray et al. [24]. A later study using our standardized exercise challenge, in which a broad panel of cytokines were measured at multiple time points during exercise, further supported this notion with significant elevations of TNF-α and IL-2 and parallel, marked elevation (albeit not statistically significant) of IL-6, IL-4, IL-5, IL-8, IL-10, andIL-13 in obese subjects (BMI% $>$ 95) [25]. In addition to inflammatory cytokines, key oxidative stress markers (MPO and F_2-isoprostanes) were also observed to be elevated in obese children both at baseline and throughout exercise [14, 26]. These studies suggest that chronic inflammation and oxidative stress, which in adults have been suggested as the biochemical link between obesity and its cardiovascular complications, are already markedly activated when obesity is established at a very early age.

In obesity, many changes in the inflammatory and oxidative response to exercise occur in the broader context of a more complex adaptive response which also include a series of hormones regulating availability of energy substrates and systemic anabolism (insulin, glucocorticoids, catecholamines, glucagon, and growth factors). While in adults these processes, if altered, are therefore likely to only affect exercise performance, in the growing child hormonal alterations, especially within the growth hormone (GH) insulin-like growth factor (IGF-1) axis, may have additional effects on growth and development. Indeed, several prior observations from other laboratories, derived from studies on adult populations, supported the concept that either the presence of obesity or the ingestion of a high-fat meal could reduce the GH response to exercise. In 1970, in fact,Hansen and Johansen [27], and in 1999, Kanaley et al. [28] showed that both subjects with upper-body or lower-body obesity had a significantly lower GH peak during a standardized exercise intervention, as compared to control. In a separate study, Cappon et al. displayed how in young healthy subject who performed an intense, 10 min exercise bout 45 min after ingesting a lipid-rich drink, the GH response was attenuated by over 50%, as compared to an identical exercise test, in the same subjects, performed either in fasting condition or after ingestion of an isocaloric carbohydrate-rich drink [29]. These observations. However, had not been confirmed in children until in our laboratory, using our standard exercise protocol, 25 obese children and healthy controls were studied. We observed that, much like in adults, the obese group displayed significantly lower circulating GH, epinephrine, norepinephrine, and dopamine. Other components of the GH-IGF-1 (IGF-1, IGF-, and GH-binding proteins) axis were not significantly different [30].

To determine whether the alterations in the GH response to exercise might become more pronounced in children with a greater severity of obesity, we repeated the same study on a larger subject pool (48 obese, 42 age-matched controls), with the obese subdivided in three subgroups with increasing BMI percentile (95–97th, 97–98.5th, and >98.5th BMI%) [31]. Interestingly, the more obese the children, the more blunted the GH response to exercise; this effect was also maintained both in early- and late-pubertal subjects.

Independent of obesity status, we also addressed the issue of whether, as shown in adults, a high-fat meal could attenuate exercise-induced GH secretion in children. This point may be very relevant to everyday life, as diet-induced obesity with frequent ingestion of high-fat nutrients is now particularly commonplace with the increased availability and convenience of fast food. A realistic scenario that may result from this trend is the practice of eating high-fat meals before physical activity (e.g., lunch before sports practice). We therefore studied a group of healthy children performing standardized exercise following a high-fat meal or placebo [30]. While basal growth hormone was similar across all subjects, the exercise-induced peak was found to be significantly lower after the high-fat meal. We then repeated the same study in obese children and observed that the combined effect of lipid ingestion and obesity almost completely suppressed the GH response to exercise, that is, reduced it to a much greater extent than could be expected by adding the separate effect of obesity and of fat ingestion alone, suggesting the presence of a synergistic effect of the two conditions [32].

4. Conclusions

While the picture of inflammatory and oxidative status in children with obesity and T1DM is by no means complete, we believe that a number of general conclusions can be drawn by our ten-year experience of studies in this field. First and foremost, it is clear that no matter what approach was taken (i.e., which mediators were measured, or what experimental protocol was utilized), differences across groups always reveled exaggerated inflammatory/oxidative

Table 1: Synopsis of key inflammatory/oxidative alteration in children with type 1 diabetes and obesity.

Inflammatory/oxidative alteration	Evidence
Pediatric type 1 diabetes mellitus	
Altered inflammatory status	Elevated baseline IL-6 (and other proinflammatory mediators); exaggerated gene expression of TNFSF 5, 7, and 9, CCL8, and CXCL10 following *ex vivo* leukocytic TCR and Fc receptor stimulation; exercise-induced changes in IL-6, TNF-α, MCP-1, and MIP-1α peak more rapidly and in greater magnitude
Altered oxidative stress	Elevated MPO and F_2-isoprostanes
Inflammatory status may be induced/exacerbated by hyperglycemic episodes	Elevated IL-1α, IL-4, and IL-6 in hyperglycemic T1DM children
Inflammation from hyperglycemia is not fully corrected for following reversion to euglycemia	Progressively elevated inflammatory markers based on past 3-day average glycemia
Inflammation may be mediated by level of immunologic proinflammatory activation, rather than cell numbers	Leukocytosis response is conserved as compared to healthy controls
	Pediatric obesity
Elevated inflammatory status	Elevated leukocytes and baseline and exercise-induced IL-6, TNF-α, and IL-2
Altered oxidative status	Elevated MPO and F_2-isoprostanes
Reduced exercise-induced growth hormone secretion in	
Healthy children	Cappon et al. 1993 [29]
Obese children	Oliver et al. 2010 [26, 31]
Markedly reduced exercise-induced GH secretion in Pediatric obesity following a high-fat meal	Oliver et al. 2012 [32]

activation in the obese and diabetic children as compared to healthy age-matched controls (Table 1).

Key inflammatory cytokines (IL-6, TNF-α) were among the biomarkers more consistently elevated; further, immune cells displayed greater reactivity in diabetic subjects, secreting larger amounts of inflammatory mediators in response to standard stimuli. When challenged with exercise, a stimulus that has the peculiar characteristic to exert a long-term anti-inflammatory effect, despite acute, proinflammatory responses to each individual exercise bout, obese, and diabetic children again displayed elevated and accelerated patterns of inflammatory activation. Far from indicating that exercise should be avoided in these children, these data rather indicate the necessity of better understanding the characteristics of each exercise format to be utilized in specific subgroup of individuals. Another clear finding of our studies is that while in both obese and diabetic children inflammatory and oxidative processes appeared consistently elevated, the individual factors that were altered differed across the two patient populations, suggesting complex underlying activating mechanisms. Further, the magnitude of inflammatory activation appeared to be proportional, in obese children, to the severity of obesity, and in T1DM children with the quality of glycemic control. Finally, we observed how inflammatory changes were paralleled by comparable alterations in related signaling systems, especially growth factors, with possible implications in the regulation of overall growth and development. As a whole, our data indicate how a better and more complete understanding of all aspects of the interaction between these two widespread pediatric dysmetabolic conditions, and the components of the underlying inflammatory and oxidative dysregulation, is at the very base of our future ability to successfully prevent, manage, and treat the related devastating cardiovascular complications.

Acknowledgments

The authors gratefully acknowledge Joanne Cheung for editorial and graphic assistance, as well as the nurses and staff of the UC Irvine Institute for Clinical and Translational Science for the outstanding support in the performance of human studies. The Galassetti Laboratory was supported with grants by the Juvenile Diabetes Research Foundation, the American Diabetes Foundation, and the NIH (1K24DK085223; NICHD-P01HD048721); the UCI-ICTS is funded via the NIH CTSA Award no. UL1 TR000153 (PI: Dan Cooper).

References

[1] P. Dandona, A. Aljada, and A. Bandyopadhyay, "Inflammation: the link between insulin resistance, obesity and diabetes," *Trends in Immunology*, vol. 25, no. 1, pp. 4–7, 2004.

[2] D. L. Eizirik, M. L. Colli, and F. Ortis, "The role of inflammation in insulitis and β-cell loss in type 1 diabetes," *Nature Reviews Endocrinology*, vol. 5, no. 4, pp. 219–226, 2009.

[3] D. A. Lawlor, L. Benfield, J. Logue et al., "Association between general and central adiposity in childhood, and change in these, with cardiovascular risk factors in adolescence: prospective cohort study," *BMJ*, vol. 341, article c6224, 2010.

[4] S. S. Soedamah-Muthu, J. H. Fuller, H. E. Mulnier, V. S. Raleigh, R. A. Lawrenson, and H. M. Colhoun, "High risk of cardiovascular disease in patients with type 1 diabetes in the U.K.: a cohort study using the general practice research database," *Diabetes Care*, vol. 29, no. 4, pp. 798–804, 2006.

[5] M. T. Schram, N. Chaturvedi, C. G. Schalkwijk, J. H. Fuller, and C. D. A. Stehouwer, "Markers of inflammation are cross-sectionally associated with microvascular complications and cardiovascular disease in type 1 diabetes—the EURODIAB Prospective Complications Study," *Diabetologia*, vol. 48, no. 2, pp. 370–378, 2005.

[6] S. Devaraj, M. R. Dasu, J. Rockwood, W. Winter, S. C. Griffen, and I. Jialal, "Increased toll-like receptor (TLR) 2 and TLR4 expression in monocytes from patients with type 1 diabetes: further evidence of a proinflammatory state," *Journal of Clinical Endocrinology and Metabolism*, vol. 93, no. 2, pp. 578–583, 2008.

[7] S. Devaraj, N. Glaser, S. Griffen, J. Wang-Polagruto, E. Miguelino, and I. Jialal, "Increased monocytic activity and biomarkers of inflammation in patients with type 1 diabetes," *Diabetes*, vol. 55, no. 3, pp. 774–779, 2006.

[8] S. I. Yamagishi, "Advanced glycation end products and receptor-oxidative stress system in diabetic vascular complications," *Therapeutic Apheresis and Dialysis*, vol. 13, no. 6, pp. 534–539, 2009.

[9] A. C. Maritim, R. A. Sanders, and J. B. Watkins, "Diabetes, oxidative stress, and antioxidants: a review," *Journal of Biochemical and Molecular Toxicology*, vol. 17, no. 1, pp. 24–38, 2003.

[10] T. A. Pearson, G. A. Mensah, R. W. Alexander et al., "Markers of inflammation and cardiovascular disease: application to clinical and public health practice: a statement for healthcare professionals from the centers for disease control and prevention and the American Heart Association," *Circulation*, vol. 107, no. 3, pp. 499–511, 2003.

[11] P. R. Galassetti, K. Iwanaga, M. Crisostomo, F. P. Zaldivar, J. Larson, and A. Pescatello, "Inflammatory cytokine, growth factor and counterregulatory responses to exercise in children with type 1 diabetes and healthy controls," *Pediatric Diabetes*, vol. 7, no. 1, pp. 16–24, 2006.

[12] G. Targher, L. Zenari, L. Bertolini, M. Muggeo, and G. Zoppini, "Elevated levels of interleukin-6 in young adults with type 1 diabetes without clinical evidence of microvascular and macrovascular complications," *Diabetes Care*, vol. 24, no. 5, pp. 956–957, 2001.

[13] A. B. Erbağci, M. Tarakçioğlu, Y. Coşkun, E. Sivasli, and E. S. Namiduru, "Mediators of inflammation in children with type I diabetes mellitus: cytokines in type I diabetic children," *Clinical Biochemistry*, vol. 34, no. 8, pp. 645–650, 2001.

[14] J. S. Rosa, M. Mitsuhashi, S. R. Oliver et al., "Ex vivo TCR-induced leukocyte gene expression of inflammatory mediators is increased in type 1 diabetic patients but not in overweight children," *Diabetes/Metabolism Research and Reviews*, vol. 26, no. 1, pp. 33–39, 2010.

[15] K. Esposito, F. Nappo, R. Marfella et al., "Inflammatory cytokine concentrations are acutely increased by hyperglycemia in humans: role of oxidative stress," *Circulation*, vol. 106, no. 16, pp. 2067–2072, 2002.

[16] J. S. Rosa, R. L. Flores, S. R. Oliver, A. M. Pontello, F. P. Zaldivar, and P. R. Galassetti, "Sustained IL-1α, IL-4, and IL-6 elevations following correction of hyperglycemia in children with type 1 diabetes mellitus," *Pediatric Diabetes*, vol. 9, no. 1, pp. 9–16, 2008.

[17] T. A. Lakka, H. M. Lakka, T. Rankinen et al., "Effect of exercise training on plasma levels of C-reactive protein in healthy adults: the HERITAGE Family Study," *European Heart Journal*, vol. 26, no. 19, pp. 2018–2025, 2005.

[18] A. Oberbach, A. Tönjes, N. Klöting et al., "Effect of a 4 week physical training program on plasma concentrations of inflammatory markers in patients with abnormal glucose tolerance," *European Journal of Endocrinology*, vol. 154, no. 4, pp. 577–585, 2006.

[19] J. S. Rosa, S. R. Oliver, M. Mitsuhashi et al., "Altered kinetics of interleukin-6 and other inflammatory mediators during exercise in children with type 1 diabetes," *Journal of Investigative Medicine*, vol. 56, no. 6, pp. 701–713, 2008.

[20] C. L. Ogden, M. D. Carroll, B. K. Kit, and K. M. Flegal, "Prevalence of obesity and trends in body mass index among US children and adolescents, 1999–2010," *The Journal of the American Medical Association*, vol. 307, pp. 483–490, 2012.

[21] "A school-based intervention for diabetes risk reduction," *The New England Journal of Medicine*, vol. 363, pp. 443–453, 2010.

[22] J. S. Rosa, C. D. Schwindt, S. R. Oliver, S. Y. Leu, R. L. Flores, and P. R. Galassetti, "Exercise leukocyte profiles in healthy, type 1 diabetic, overweight, and asthmatic children," *Pediatric Exercise Science*, vol. 21, no. 1, pp. 19–33, 2009.

[23] F. Zaldivar, R. G. McMurray, D. Nemet, P. Galassetti, P. J. Mills, and D. M. Cooper, "Body fat and circulating leukocytes in children," *International Journal of Obesity*, vol. 30, no. 6, pp. 906–911, 2006.

[24] R. G. McMurray, F. Zaldivar, P. Galassetti et al., "Cellular immunity and inflammatory mediator responses to intense exercise in overweight children and adolescents," *Journal of Investigative Medicine*, vol. 55, no. 3, pp. 120–129, 2007.

[25] J. S. Rosa, S. R. Oliver, R. L. Flores et al., "Altered inflammatory, oxidative, and metabolic responses to exercise in pediatric obesity and type 1 diabetes," *Pediatric Diabetes*, vol. 12, no. 5, pp. 464–472, 2011.

[26] S. R. Oliver, J. S. Rosa, G. L. Milne et al., "Increased oxidative stress and altered substrate metabolism in obese children," *International Journal of Pediatric Obesity*, vol. 5, no. 5, pp. 436–444, 2010.

[27] A. P. Hansen and K. Johansen, "Diurnal patterns of blood glucose, serum free fatty acids, insulin, glucagon and growth hormone in normals and juvenile diabetics," *Diabetologia*, vol. 6, no. 1, pp. 27–33, 1970.

[28] J. A. Kanaley, M. M. Weatherup-Dentes, E. B. Jaynes, and M. L. Hartman, "Obesity attenuates the growth hormone response to exercise," *Journal of Clinical Endocrinology and Metabolism*, vol. 84, no. 9, pp. 3156–3161, 1999.

[29] J. P. Cappon, E. Ipp, J. A. Brasel, and D. M. Cooper, "Acute effects of high fat and high glucose meals on the growth hormone response to exercise," *Journal of Clinical Endocrinology and Metabolism*, vol. 76, no. 6, pp. 1418–1422, 1993.

[30] P. Galassetti, J. Larson, K. Iwanaga, S. L. Salsberg, A. Eliakim, and A. Pontello, "Effect of a high-fat meal on the growth hormone response to exercise in children," *Journal of Pediatric Endocrinology and Metabolism*, vol. 19, no. 6, pp. 777–786, 2006.

[31] S. R. Oliver, J. S. Rosa, T. D. C. Minh et al., "Dose-dependent relationship between severity of pediatric obesity and blunting of the growth hormone response to exercise," *Journal of Applied Physiology*, vol. 108, no. 1, pp. 21–27, 2010.

[32] S. R. Oliver, S. R. Hingorani, J. S. Rosa, F. Zaldivar, and P. R. Galassetti, "Synergistic effect of obesity and lipid ingestion in suppressing the growth hormone response to exercise in children," *Journal of Applied Physiology*, vol. 113, no. 2, pp. 192–198, 2012.

Hindawi Publishing Corporation
Experimental Diabetes Research
Volume 2012, Article ID 815098, 7 pages
doi:10.1155/2012/815098

Clinical Study

Impact of Insulin Resistance on Silent and Ongoing Myocardial Damage in Normal Subjects: The Takahata Study

Taro Narumi,[1] Tetsuro Shishido,[1] Nobuyuki Kiribayashi,[1] Shinpei Kadowaki,[1] Satoshi Nishiyama,[1] Hiroki Takahashi,[1] Takanori Arimoto,[1] Takehiko Miyashita,[1] Takuya Miyamoto,[1] Tetsu Watanabe,[1] Yoko Shibata,[1] Tsuneo Konta,[1] Yoshiyuki Ueno,[2] Takeo Kato,[3] Takamasa Kayama,[4] and Isao Kubota[1]

[1] *Department of Cardiology, Pulmonology, and Nephrology, Yamagata University School of Medicine, 2-2-2 Iida-Nishi, Yamagata 990-9585, Japan*
[2] *Department of Gastroenterology, Yamagata University School of Medicine, Yamagata 990-9585, Japan*
[3] *Department of Neurology, Hematology, Metabolism, Endocrinology, and Diabetology, Yamagata University School of Medicine, Yamagata 990-9585, Japan*
[4] *Global Center of Excellence Program Study Group, Yamagata University School of Medicine, Yamagata 990-9585, Japan*

Correspondence should be addressed to Tetsuro Shishido, tshishid@med.id.yamagata-u.ac.jp

Received 9 March 2012; Revised 4 August 2012; Accepted 30 August 2012

Academic Editor: Dan Nemet

Background. Insulin resistance (IR) is part of the metabolic syndrome (Mets) that develops after lifestyle changes and obesity. Although the association between Mets and myocardial injury is well known, the effect of IR on myocardial damage remains unclear. *Methods and Results*. We studied 2200 normal subjects who participated in a community-based health check in the town of Takahata in northern Japan. The presence of IR was assessed by homeostasis model assessment ratio, and the serum level of heart-type fatty acid binding protein (H-FABP) was measured as a maker of silent and ongoing myocardial damage. H-FABP levels were significantly higher in subjects with IR and Mets than in those without metabolic disorder regardless of gender. Multivariate logistic analysis showed that the presence of IR was independently associated with latent myocardial damage (odds ratio: 1.574, 95% confidence interval 1.1–2.3) similar to the presence of Mets. *Conclusions*. In a screening of healthy subjects, IR and Mets were similarly related to higher H-FABP levels, suggesting that there may be an asymptomatic population in the early stages of metabolic disorder that is exposed to myocardial damage and might be susceptible to silent heart failure.

1. Introduction

The presence of metabolic disorders such as glucose intolerance and dyslipidemia is associated with the incidence of cardiovascular disease (CVD) and is a cause of mortality [1, 2]. It has been reported that the components of metabolic syndrome (Mets), which include abdominal obesity, hypertension, impaired insulin tolerance with high fasting glucose levels, and elevated levels of triglycerides [3–5], are risk factors for CVD [6, 7]. Epidemiological and experimental studies have provided evidence of the relationship between cardiac dysfunction and diabetes mellitus (DM) [8–11]. Furthermore, hyperglycemia, hypertension, and dyslipidemia are associated with ongoing myocardial damage. These findings imply that there is a significant association between the severity of Mets and organ damage [12, 13]. However, a correlation between insulin resistance (IR) and cardiac dysfunction in the general population has not been established to date.

Clinical studies have shown that heart-type fatty acid-binding protein (H-FABP), which is rapidly released into the circulation from the damaged myocardium, may be a marker for myocardial damage not only in patients with ischemic heart disease but also in those with chronic heart failure [14–17]. Because the levels of H-FABP are correlated with the incidence of cardiac events in heart failure patients, the assessment of H-FABP levels may be of value to estimate the potential existence of cardiac damage in the general population [18, 19]. The effect of IR on myocardial damage in normal subjects, however, remains to be clarified. The

purpose of this study was to investigate the association between IR and myocardial damage in healthy subjects.

2. Methods

2.1. Study Design. This study was part of the Molecular Epidemiological Study utilizing the Regional Characteristics of 21st Century Centers of Excellence (COE) Program and Global COE Program in Japan, as described in detail previously [20]. The study was approved by the institutional ethics committee and all participants provided written informed consent. The subjects included in the study were members of the general population with an age of 40 years and older from the town of Takahata in northern Japan. From June 2004 to November 2005, 1,380 men and 1,735 women were enrolled in the study. A total of 915 patients with incomplete data were excluded, and 2200 patients participated in the final study.

2.2. Clinical Assessments. The Takahata town study was based on a survey consisting of a self-administered questionnaire about lifestyle, blood pressure measurements, anthropometric measurements, and the collection of blood and urine specimens from the participants at annual health exams. Information concerning medical history, current medications, smoking habits, and alcohol intake was obtained from the self-reported questionnaire. Blood pressure was measured using a mercury manometer, with subjects resting in a seated position for at least 5 minutes before measurement.

2.3. Definition of Mets and IR. Mets was evaluated using the National Cholesterol Education program Adult Treatment Panel III (NCEP-ATP III) criteria [3]. The NCEP-ATP III criteria for abdominal obesity were modified by using body mass index (BMI) $\geq 25\,kg/m^2$ instead of the waist circumference because obesity is defined as BMI $\geq 25\,kg/m^2$ in Japan [21, 22]. Mets was defined on the basis of meeting at least 3 of the following 5 NCEP-ATP III criteria: BMI $\geq 25\,kg/m^2$, elevated triglyceride (TG) ≥ 150 mg/dL, reduced high-density lipoprotein cholesterol (HDLc) < 40 mg/dL in men and < 50 mg/dL in women, elevated fasting blood sugar (FBS) ≥ 110 mg/dL or previously diagnosed diabetes mellitus, elevated blood pressure [systolic blood pressure (sBP) ≥ 130 mmHg, and/or diastolic blood pressure (dBP) ≥ 85 mmHg] or use of antihypertensive medication. Insulin tolerance was evaluated with the homeostasis model assessment ratio [HOMA-R, HOMA-R = fasting insulin levels (IRI) $\times$ FBS $\times$ 1/405], and IR was defined as HOMA-R $>$ 2.5 [23].

2.4. Definition of Latent and Ongoing Myocardial Damage. The presence of latent and ongoing myocardial damage was defined as serum levels of heart type fatty acid binding protein (H-FABP) above 4.3 ng/mL as reported previously [16, 18].

2.5. Statistical Analysis. Data are presented as mean $\pm$ standard deviation (SD). Data that were not distributed normally were presented as medians and interquartile intervals. The unpaired Student's t-test and the chi-square test were used for comparisons between 2 groups of continuous and categorical variables, respectively. The Mann-Whitney U-test was used when data were not distributed normally. Comparisons of data among 3 groups categorized based on the presence of IR and Mets were performed by the Kruskal-Wallis test. Univariate and multivariate logistic analyses were performed to evaluate the association between IR and ongoing myocardial damage.

Table 1: Comparisons of clinical characteristics of 2200 subjects.

Age (years)*	69.1 ± 12.6
Gender (male/female)	973/1227
BMI (kg/m^2)*	23.0 ± 3.3
sBP (mm Hg)*	134 ± 16
dBP (mm Hg)*	79 ± 10
BNP (pg/mL)**	20.0 (10.9–35.8)
TC (mg/dL)**	200 (179–221)
TG (mg/dL)**	91 (68–125)
HDLc (mg/dL)*	59 ± 15
LDLc (mg/dL)*	124 ± 29
eGFR (mL/min/1.73 m^2)**	96 (82–110)
H-FABP (ng/mL)**	3.5 (2.6–4.7)

BMI: body mass index; BNP: brain natriuretic peptide; TC: total cholesterol; TG: triglyceride; HDLc: high density lipoprotein cholesterol; LDLc: low density lipoprotein cholesterol; H-FABP: heart type fatty acid binding protein; sBP: systolic blood pressure; dBP: diastolic blood pressure; Data are presented as *mean ± S.D; **median (interquartile range).

3. Results

3.1. Patient Characteristics. Table 1 lists the characteristics of the 2200 subjects. The proportion of men was 44.2%, and the mean age of the study subjects was 63 ± 10 years. Mean serum levels of brain natriuretic peptide (BNP) and H-FABP were 20.0 ng/L (interquartile range: 10.9–35.8) and 3.5 ng/mL (interquartile range: 2.6–4.7), respectively. Mean BMI was $23.0 \pm 3.3\,kg/m^2$; sBP and dBP were 134 ± 16 mmHg and 79 ± 10 mmHg, respectively. Serum FBS levels were 93 ± 12 mg/dL. Serum levels of total cholesterol (TC), TG, HDLc, and low-density lipoprotein cholesterol (LDLc) were 200 mg/dL (interquartile range: 179–221), 91 mg/dL (interquartile range: 68–125), 59 ± 15 mg/dL, and 124 ± 29 mg/dL, respectively. Estimated glomerular filtration rate was 96.0 mL/min/1.73 m^2 (interquartile range: 82–110).

3.2. Classification of Subjects by the Presence of IR. Subjects were divided into 3 groups according to the presence of IR and Mets, as shown in Table 2. IR was associated with female gender; high BMI; high sBP and dBP; high LDLc, TG, and TC levels; and low BNP and HDLc levels compared to subjects without IR. Mets was associated with male gender; high BMI; high sBP and dBP; high LDLc, TG, and TC levels; and low BNP and HDLc levels compared to subjects without Mets. Serum H-FABP levels were significantly higher in subjects

Table 2: Comparisons of clinical characteristics of patients with and without IR.

	IR (−)	IR (+)	Mets
Age	63 ± 10	63 ± 10	63 ± 10
Male	659 (46.2%)	169 (33.2%)*	145 (54.9%)*#
BMI	21.9 ± 2.8	24.4 ± 3.2*	26.1 ± 2.5*#
sBP	132 ± 16	136 ± 15*	134 ± 14*
dBP	78 ± 10	80 ± 10*	84 ± 8*#
BNP (pg/mL)	21.5 (12.1–37.4)	17.1 (9.5–30.5)*	17.5 (9.4–33.6)*
TC (g/dL)	197 (177–217)	204 (187–226)*	205 (182–229)*
TG (g/dL)	81 (63–106)	101 (77–128)*	171 (150–224)*#
HDL (g/dL)	61 ± 14	58 ± 13*	46 ± 12*#
LDL (g/dL)	122 ± 29	131 ± 28*	124 ± 30*#
eGFR (mL/min/1.73 m^2)	97 (82–112)	98 (83–111)	86 (74–102)*#
H-FABP (ng/mL)	3.5 (2.6–4.6)	3.6 (2.6–4.7)*	3.7 (2.8–5.1)*

BMI: body mass index; BNP: brain natriuretic peptide; TC: total cholesterol; TG: triglyceride; HDLc: high density lipoprotein cholesterol; LDLc: low density lipoprotein cholesterol; H-FABP: heart type fatty acid binding protein; sBP: systolic blood pressure; dBP: diastolic blood pressure; Data are presented as mean ± S.D or median (interquartile range). *$P < 0.05$ versus IR (−); #$P < 0.05$ versus IR (+).

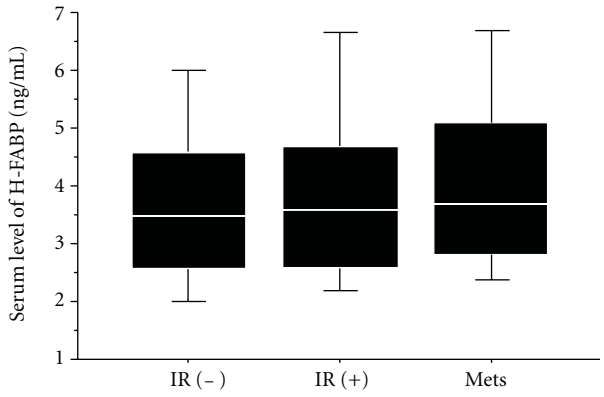

Figure 1: Serum levels of H-FABP in the study population. Subjects with and without insulin resistance (IR) and metabolic syndrome (Mets) were included. In comparison to IR (−) subjects, subjects with IR and Mets showed an increase in H-FABP levels. Data are expressed as mean ± SD. *$P < 0.05$ versus subjects without IR.

with IR and Mets than in those without IR. However, there was no significant difference between subjects with IR and those with Mets, as shown in Figure 1.

3.3. Classification by Gender. It is well known that serum H-FABP level and other blood parameters differ according to gender [18]. We therefore divided subjects into 2 groups according to gender, as shown in Table 3. Clinical characteristics were different between the 2 groups. However, serum H-FABP levels were significantly higher in subjects with IR and Mets than in those without IR in both groups regardless of gender, as shown in Tables 4 and 5.

3.4. Association between IR and Ongoing Myocardial Damage. To investigate the contribution of IR to the increase of H-FABP levels in the asymptomatic general population, 1936 subjects without Mets were examined by univariate and multivariate logistic analyses. In the univariate logistic analysis, the presence of IR, age, gender, sBP, and serum levels of BNP and LDLc were associated with latent and ongoing myocardial damage, as shown in Table 6. In the multivariate logistic analysis, the presence of IR was independently associated with the increase of H-FABP levels (OR: 1.6, 95% confidence interval 1.1–2.3) after adjusting for age, gender, serum BNP level, sBP, and serum LDLc level, as shown in Table 3. Furthermore, the percentage of subjects with latent and ongoing myocardial damage was significantly higher in those with IR than in those without IR (8.27% versus 11.20%, $P = 0.0478$), as shown in Figure 2.

Table 3: Comparisons of clinical characteristics in male and female subjects.

	Male	Female
Age (years)*	64.0 ± 10.2	62.7 ± 10.0†
BMI (kg/m^2)*	22.9 ± 3.0	23.1 ± 3.5
sBP (mm Hg)*	136 ± 16	133 ± 16†
dBP (mm Hg)*	82 ± 10	77 ± 9†
BNP (pg/mL)**	17.6 (9.3–36.1)	21.4 (12.4–35.3)
TC (mg/dL)**	191 (173–211)	206 (187–226)†
TG (mg/dL)**	95 (70–135)	89 (66–117)†
HDLc (mg/dL)*	56 ± 14	61 ± 14†
LDLc (mg/dL)*	119 ± 28	129 ± 28†
eGFR (mL/min/1.73 m^2)**	82 (72–90)	106 (97–124)†
H-FABP (ng/mL)**	3.7 (2.8–4.8)	3.4 (2.6–4.6)†

BMI: body mass index; BNP: brain natriuretic peptide; TC: total cholesterol; TG: triglyceride; HDLc: high density lipoprotein cholesterol; LDLc: low density lipoprotein cholesterol; H-FABP: heart type fatty acid binding protein; sBP: systolic blood pressure; dBP: diastolic blood pressure; Data are presented as *mean ± S.D; **median (interquartile range); †$P < 0.05$ versus male.

4. Discussion

The findings of the present study are as follows: (1) H-FABP levels increased in association with IR and Mets in normal

Table 4: Comparisons of clinical characteristics of patients with and without IR and Mets in male.

	IR (−)	IR (+)	Mets (+)
Age (years)	64 ± 10	64 ± 10	63 ± 8
BMI (kg/m^2)	22.0 ± 3.0	24.2 ± 2.8*	25.9 ± 2.3*#
sBP (mm Hg)	135 ± 16	138 ± 16*	142 ± 13*
dBP (mm Hg)	81 ± 10	83 ± 10	85 ± 9*
BNP (pg/mL)	19.8 (10.2–37.6)	13.8 (8.0–31.8)*	14.2 (8.0–28.7)*
TC (mg/dL)	189 (170–207)	197 (179–215)*	196 (173–224)*#
TG (mg/dL)	84 (64–111)	104 (79–135)*	184 (151–256)*
HDLc (mg/dL)	59 ± 14	54 ± 12*	43 ± 12*#
LDLc (mg/dL)	117 ± 28	128 ± 27*	123 ± 29*#
eGFR (mL/min/1.73 m^2)	83 (72–92)	76 (66–86)*	77 (67–89)*
H-FABP (ng/mL)	3.2 (2.4–4.5)	3.6 (2.7–4.8)*	3.8 (2.8–4.9)*

BMI: body mass index; BNP: brain natriuretic peptide; TC: total cholesterol; TG: triglyceride; HDLc: high density lipoprotein cholesterol; LDLc: low density lipoprotein cholesterol; H-FABP: heart type fatty acid binding protein; sBP: systolic blood pressure; dBP: diastolic blood pressure; Data are presented as mean ± S.D or median (interquartile range). *$P < 0.05$ versus IR (−); #$P < 0.05$ versus IR (+).

Table 5: Comparisons of clinical characteristics of patients with and without IR and Mets in female.

	IR (−)	IR (+)	Mets (+)
Age (years)	62 ± 10	62 ± 10	64 ± 8
BMI (kg/m^2)	22.0 ± 3.0	24.5 ± 3.4*	26.4 ± 2.7*#
sBP (mm Hg)	130 ± 16	135 ± 15*	144 ± 12*#
dBP (mm Hg)	75 ± 9	78 ± 9*	83 ± 8*#
BNP (pg/mL)	23.3 (14.0–37.0)	18.5 (10.8–30.5)*	19.8 (10.7–38.0)*
TC (mg/dL)	204 (185–223)	209 (190–232)*	212 (192–237)*
TG (mg/dL)	79 (62–102)	100 (76–123)*	166 (149–186)*#
HDLc (mg/dL)	64 ± 14	61 ± 13*	48 ± 11*#
LDLc (mg/dL)	127 ± 28	133 ± 29*	132 ± 29*
eGFR (mL/min/1.73 m^2)	107 (98–126)	104 (96–123)	101 (86–121)*
H-FABP (ng/mL)	3.3 (2.5–4.4)	3.6 (2.6–4.8)*	3.5 (2.7–5.2)*

BMI: body mass index; BNP: brain natriuretic peptide; TC: total cholesterol; TG: triglyceride; HDLc: high density lipoprotein cholesterol; LDLc: low density lipoprotein cholesterol; H-FABP: heart type fatty acid binding protein; sBP: systolic blood pressure; dBP: diastolic blood pressure; Data are presented as mean ± S.D or median (interquartile range). *$P < 0.05$ versus IR (−); #$P < 0.05$ versus IR (+).

subjects; (2) multivariate logistic analysis revealed that the presence of IR was an independent risk factor for myocardial injury in the general population; (3) the prevalence of high H-FABP was more prevalent in subjects with IR than in those without IR.

Although patients with IR are often asymptomatic, this condition can lead to a multitude of diseases [24]. The early detection of metabolic disorder is important for the prevention of new-onset CVD. Physicians can only treat patients in the symptomatic state because asymptomatic subjects, such as those with IR, do not generally present to clinics or hospitals. Our study showed that latent and ongoing myocardial damage may occur in the early stages of metabolic disease, such as those characterized by the presence of IR. This suggests that early detection of latent and ongoing myocardial damage through population screening is essential to prevent future cardiovascular disorders.

Serum BNP is an established and commonly used marker for the detection of myocardial damage during screening evaluations [25]. However, in the present study, we measured serum H-FABP to detect latent and ongoing myocardial damage for the following reasons. First, several cohort studies have shown that high BMI is inversely correlated to serum BNP level [26–28]. The hypothesized mechanism underlying this inverse relationship has been described previously. Increased expression of natriuretic peptide clearance receptor by adipose tissue, which is shown in obese subjects, results in increased clearance of serum BNP [29]. Similarly, we also observed an inverse relationship between serum BNP level and IR in the present study. Thus, serum BNP appears to be inadequate to detect latent and ongoing myocardial damage in the early stages of metabolic disorder. Second, previous reports showed that serum H-FABP is a useful and sensitive marker for screening patients with latent and ongoing myocardial damage [14, 17, 19]. It is well known that serum H-FABP is rapidly released into the circulation from damaged myocardium; hence, it is used as a marker of acute coronary syndrome. On the other hand, there is evidence that disturbances in cardiac microvascular circulation caused by metabolic disorders and left ventricular hypertrophy induce myocardial hypoxia and cardiomyocyte injury and impair cardiac function [30–32]. Moreover, not

Table 6: Univariate and multivariate logistic analysis for high serum level of H-FABP.

Variables	OR	95% CI	*P* value
Univariable analysis			
Age (per 5 years increase)	1.716	1.552–1.908	<0.0001
Male	1.396	1.022–1.905	0.0357
BMI	1.224	0.881–1.701	0.2288
BNP	1.004	1.002–1.006	0.0008
sBP	1.493	1.076–2.071	0.0164
dBP	1.110	0.784–1.570	0.5565
LDLc	0.682	0.468–0.995	0.0468
HDL (<40 mg/dL in male, <50 mg/dL in female)	1.532	0.774–3.035	0.2209
TG (above 150 mg/dL)	0.730	0.377–1.415	0.3514
TC (above 220 mg/dL)	0.960	0.670–1.377	0.8265
IR (presence of IR)	1.399	1.002–1.953	0.0487
Multivariable analysis			
Age (per 5 years increase)	1.707	1.531–1.908	<0.0001
Male	1.258	0.904–1.750	0.1726
BNP	1.022	0.719–1.454	0.9023
sBP	1.041	0.736–1.472	0.8219
IR (presence of IR)	1.574	1.100–2.251	0.0131

OR: odds ratio; CI: confidence interval; BMI: body mass index; BNP: brain natriuretic peptide; TC: total cholesterol; TG: triglyceride; HDLc: high density lipoprotein cholesterol; LDLc: low density lipoprotein cholesterol; H-FABP: heart type fatty acid binding protein; sBP: systolic blood pressure; dBP: diastolic blood pressure.

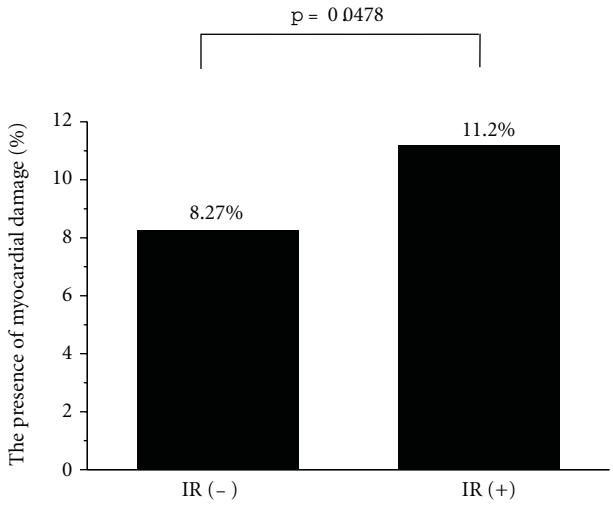

Figure 2: Comparison of latent and ongoing myocardial damage between subjects with and without IR. Latent and ongoing myocardial damage was defined as serum levels of heart type fatty acid binding protein (H-FABP) above 4.3 ng/mL. In comparison to IR (−) subjects, those with IR showed a higher incidence of myocardial damage.

only hypoxia, but also mechanical stretch, oxidative stress, inflammation, and apoptosis increase cardiomyocyte permeability, resulting in elevated levels of myocardial cytosolic markers in patients with heart failure [33–36]. Previously, we demonstrated that increased serum H-FABP level is associated with the exacerbation of chronic heart failure and thus provides prognostic information [15, 16]. These studies showed that patients with high serum levels of H-FABP had a significantly higher rate of cardiac events than those with normal H-FABP levels (34% versus 4%, $P < 0.001$). Furthermore, these studies suggested that serum H-FABP level was an independent predictor of future cardiac events ($\chi^2 = 7.397$, $P < 0.01$). Similarly, minimally increased levels of troponin T are associated with mortality and morbidity in patients with chronic heart failure [37, 38].

In this study, we demonstrated that H-FABP but not BNP was higher in subjects with IR and Mets than in those without these conditions, suggesting that measurement of H-FABP might be suitable to predict the occurrence of myocardial damage in subjects with metabolic disorder.

There were several limitations associated with our study. First, we modified the NCEP-ATP III criteria for abdominal obesity by using body mass index (BMI) $\geq 25\,kg/m^2$ instead of the waist circumference to evaluate metabolic syndrome. We used BMI instead of the waist circumference because the definition of waist circumference is unclear in Japan, especially in women [39]. On the other hand, BMI as a criterion for obesity has been clearly defined as BMI $\geq 25\,kg/m^2$ in the Japanese general population [21]. Second, we did not detect latent and ongoing myocardial damage by visual methods such as echocardiography or myocardial scintigraphy. The association between alterations in diastolic function and metabolic disorder has been reported [40], and the correlation between the results of myocardial scintigraphy and myocardial damage in subjects with diastolic dysfunction was also been shown [41]. In addition, prior reports have shown that H-FABP levels are correlated with the severity of myocardial injury evaluated by myocardial

scintigraphy [42]. Taken together, these findings suggest that the measurement of serum levels of H-FABP might be appropriate for a population-based study. Third, our data are cross-sectional and cannot demonstrate longitudinal progression of cardiovascular disorder and cannot establish causal relationship between IR and obvious heart disease. Future studies should be focused on assessing longitudinal progression.

5. Conclusion

The presence of IR is related to latent and ongoing myocardial damage in normal subjects, which suggests that myocardial damage occurs in the early state of metabolic disorder. Future studies should be aimed at developing effective strategies for the treatment of IR to prevent myocardial damage and improve clinical outcomes.

Acknowledgments

This study was supported, in part, by grants-in-aid for Scientific Research (nos. 21590923, 21790701, 23591028, 23790830, and 24659380) from the Ministry of Education Culture, Sport, Science and Technology, a grant-in-aid from the global century center of excellence (COE) program of the Japan Society for the Promotion of Science, and a grant-in-aid from the Japan Heart Foundation Research Grant.

References

[1] J. Lucove, S. Vupputuri, G. Heiss, K. North, and M. Russell, "Metabolic syndrome and the development of CKD in American Indians: the Strong Heart Study," *American Journal of Kidney Diseases*, vol. 51, no. 1, pp. 21–28, 2008.

[2] S. A. Hassan, A. Deswal, B. Bozkurt, D. Aguilar, D. L. Mann, and A. M. Pritchett, "The metabolic syndrome and mortality in an ethnically diverse heart failure population," *Journal of Cardiac Failure*, vol. 14, no. 7, pp. 590–595, 2008.

[3] J. I. Cleeman, "Executive summary of the third report of the National Cholesterol Education Program (NCEP) expert panel on detection, evaluation, and treatment of high blood cholesterol in adults (adult treatment panel III)," *Journal of the American Medical Association*, vol. 285, no. 19, pp. 2486–2497, 2001.

[4] C. M. Alexander, P. B. Landsman, S. M. Teutsch, and S. M. Haffner, "NCEP-defined metabolic syndrome, diabetes, and prevalence of coronary heart disease among NHANES III participants age 50 years and older," *Diabetes*, vol. 52, no. 5, pp. 1210–1214, 2003.

[5] Y. Matsuzawa, "Metabolic syndrome–definition and diagnostic criteria in Japan," *Journal of Atherosclerosis and Thrombosis*, vol. 12, no. 6, p. 301, 2005.

[6] H. Noda, H. Iso, I. Saito, M. Konishi, M. Inoue, and S. Tsugane, "The impact of the metabolic syndrome and its components on the incidence of ischemic heart disease and stroke: the Japan public health center-based study," *Hypertension Research*, vol. 32, no. 4, pp. 289–298, 2009.

[7] P. Bjorntorp, "'Portal' adipose tissue as a generator of risk factors for cardiovascular disease and diabetes," *Arteriosclerosis*, vol. 10, no. 4, pp. 493–496, 1990.

[8] T. Shishido, C. H. Woo, B. Ding et al., "Effects of MEK5/ERK5 association on small ubiquitin-related modification of ERK5: implications for diabetic ventricular dysfunction after myocardial infarction," *Circulation Research*, vol. 102, no. 11, pp. 1416–1425, 2008.

[9] T. B. Horwich and G. C. Fonarow, "Glucose, obesity, metabolic syndrome, and diabetes. Relevance to incidence of heart failure," *Journal of the American College of Cardiology*, vol. 55, no. 4, pp. 283–293, 2010.

[10] N. T. Le, Y. Takei, T. Shishido, C. H. Woo, E. Chang, K. S. Heo et al., "p90RSK targets the ERK5-CHIP ubiquitin E3 ligase activity in diabetic hearts and promotes cardiac apoptosis and dysfunction," *Circulation Research*, vol. 110, pp. 536–550, 2012.

[11] C. H. Woo, N. T. Le, T. Shishido et al., "Novel role of C terminus of Hsc70-interacting protein (CHIP) ubiquitin ligase on inhibiting cardiac apoptosis and dysfunction via regulating ERK5-mediated degradation of inducible cAMP early repressor," *The FASEB Journal*, vol. 24, no. 12, pp. 4917–4928, 2010.

[12] H. M. Lakka, D. E. Laaksonen, T. A. Lakka et al., "The metabolic syndrome and total and cardiovascular disease mortality in middle-aged men," *Journal of the American Medical Association*, vol. 288, no. 21, pp. 2709–2716, 2002.

[13] J. Rubin, K. Matsushita, C. M. Ballantyne, R. Hoogeveen, J. Coresh, and E. Selvin, "Chronic hyperglycemia and subclinical myocardial injury," *Journal of the American College of Cardiology*, vol. 59, pp. 484–489, 2012.

[14] K. Setsuta, Y. Seino, T. Ogawa, M. Arao, Y. Miyatake, and T. Takano, "Use of cytosolic and myofibril markers in the detection of ongoing myocardial damage in patients with chronic heart failure," *American Journal of Medicine*, vol. 113, no. 9, pp. 717–722, 2002.

[15] T. Arimoto, Y. Takeishi, R. Shiga et al., "Prognostic value of elevated circulating heart-type fatty acid binding protein in patients with congestive heart failure," *Journal of Cardiac Failure*, vol. 11, no. 1, pp. 56–60, 2005.

[16] T. Arimoto, Y. Takeishi, T. Niizeki et al., "Ongoing myocardial damage relates to cardiac sympathetic nervous disintegrity in patients with heart failure," *Annals of Nuclear Medicine*, vol. 19, no. 7, pp. 535–540, 2005.

[17] N. Morioka, Y. Shigematsu, M. Hamada, and J. Higaki, "Circulating levels of heart-type fatty acid-binding protein and its relation to thallium-201 perfusion defects in patients with hypertrophic cardiomyopathy," *American Journal of Cardiology*, vol. 95, no. 11, pp. 1334–1337, 2005.

[18] T. Niizeki, Y. Takeishi, N. Takabatake et al., "Circulating levels of heart-type fatty acid-binding protein in a general Japanese population—effects of age, gender and physiologic characteristics," *Circulation Journal*, vol. 71, no. 9, pp. 1452–1457, 2007.

[19] K. Setsuta, Y. Seino, T. Ogawa, T. Ohtsuka, K. Seimiya, and T. Takano, "Ongoing myocardial damage in chronic heart failure is related to activated tumor necrosis factor and Fas/Fas ligand system," *Circulation Journal*, vol. 68, no. 8, pp. 747–750, 2004.

[20] T. Konta, Z. Hao, H. Abiko et al., "Prevalence and risk factor analysis of microalbuminuria in Japanese general population: the Takahata study," *Kidney International*, vol. 70, no. 4, pp. 751–756, 2006.

[21] "New criteria for 'obesity disease' in Japan," *Circulation Journal*, vol. 66, pp. 987–992, 2002.

[22] T. Shishido, T. Konta, S. Nishiyama et al., "Suppressive effects of valsartan on microalbuminuria and CRP in patients with

metabolic syndrome (Val-Mets)," *Clinical and Experimental Hypertension*, vol. 33, no. 2, pp. 117–123, 2011.

[23] D. R. Matthews, J. P. Hosker, and A. S. Rudenski, "Homeostasis model assessment: insulin resistance and β-cell function from fasting plasma glucose and insulin concentrations in man," *Diabetologia*, vol. 28, no. 7, pp. 412–419, 1985.

[24] Z. T. Bloomgarden, "Insulin resistance concepts," *Diabetes Care*, vol. 30, no. 5, pp. 1320–1326, 2007.

[25] T. Kitahara, T. Shishido, S. Suzuki et al., "Serum midkine as a predictor of cardiac events in patients with chronic heart failure," *Journal of Cardiac Failure*, vol. 16, no. 4, pp. 308–313, 2010.

[26] A. Beleigoli, M. Diniz, M. Nunes, M. Barbosa, S. Fernandes, M. Abreu et al., "Reduced brain natriuretic peptide levels in class III obesity: the role of metabolic and cardiovascular factors," *Obesity Facts*, vol. 4, pp. 427–432, 2011.

[27] A. Clerico, A. Giannoni, S. Vittorini, and M. Emdin, "The paradox of low BNP levels in obesity," *Heart Failure Reviews*, vol. 17, pp. 81–96, 2012.

[28] T. J. Wang, M. G. Larson, D. Levy et al., "Impact of obesity on plasma natriuretic peptide levels," *Circulation*, vol. 109, no. 5, pp. 594–600, 2004.

[29] S. R. Das, M. H. Drazner, D. L. Dries et al., "Impact of body mass and body composition on circulating levels of natriuretic peptides: results from the Dallas Heart Study," *Circulation*, vol. 112, no. 14, pp. 2163–2168, 2005.

[30] M. L. Marcus, S. Koyanagi, and D. G. Harrison, "Abnormalities in the coronary circulation that occur as a consequence of cardiac hypertrophy," *American Journal of Medicine*, vol. 75, no. 3, pp. 62–66, 1983.

[31] M. Sano, T. Minamino, H. Toko et al., "p53-induced inhibition of Hif-1 causes cardiac dysfunction during pressure overload," *Nature*, vol. 446, no. 7134, pp. 444–448, 2007.

[32] Y. S. Yoon, S. Uchida, O. Masuo et al., "Progressive attenuation of myocardial vascular endothelial growth factor expression is a seminal event in diabetic cardiomyopathy: restoration of microvascular homeostasis and recovery of cardiac function in diabetic cardiomyopathy after replenishment of local vascular endothelial growth factor," *Circulation*, vol. 111, no. 16, pp. 2073–2085, 2005.

[33] S. D. Prabhu, "Cytokine-induced modulation of cardiac function," *Circulation Research*, vol. 95, no. 12, pp. 1140–1153, 2004.

[34] A. D. Robinson, K. B. Ramanathan, J. E. McGee, K. P. Newman, and K. T. Weber, "Oxidative stress and cardiomyocyte necrosis with elevated serum troponins: pathophysiologic mechanisms," *American Journal of the Medical Sciences*, vol. 342, no. 2, pp. 129–134, 2011.

[35] C. H. Davies, S. E. Harding, and P. A. Poole-Wilson, "Cellular mechanisms of contractile dysfunction in human heart failure," *European Heart Journal*, vol. 17, no. 2, pp. 189–198, 1996.

[36] G. Olivetti, R. Abbi, F. Quaini et al., "Apoptosis in the failing human heart," *New England Journal of Medicine*, vol. 336, no. 16, pp. 1131–1141, 1997.

[37] Y. Sato, T. Yamada, R. Taniguchi et al., "Persistently increased serum concentrations of cardiac troponin T in patients with idiopathic dilated cardiomyopathy are predictive of adverse outcomes," *Circulation*, vol. 103, no. 3, pp. 369–374, 2001.

[38] M. Egstrup, M. Schou, C. D. Tuxen, C. N. Kistorp, P. R. Hildebrandt, F. Gustafsson et al., "Prediction of outcome by highly sensitive troponin T in outpatients with chronic systolic left ventricular heart failure," *American Journal of Cardiology*, vol. 110, no. 4, pp. 552–557, 2012.

[39] K. Hara, Y. Matsushita, M. Horikoshi et al., "A proposal for the cutoff point of waist circumference for the diagnosis of metabolic syndrome in the Japanese population," *Diabetes Care*, vol. 29, no. 5, pp. 1123–1124, 2006.

[40] B. D. Powell, M. M. Redfield, K. A. Bybee, W. K. Freeman, and C. S. Rihal, "Association of obesity with left ventricular remodeling and diastolic dysfunction in patients without coronary artery disease," *American Journal of Cardiology*, vol. 98, no. 1, pp. 116–120, 2006.

[41] S. Katoh, T. Shishido, D. Kutsuzawa et al., "Iodine-123-metaiodobenzylguanidine imaging can predict future cardiac events in heart failure patients with preserved ejection fraction," *Annals of Nuclear Medicine*, vol. 24, no. 9, pp. 679–686, 2010.

[42] T. Arimoto, Y. Takeishi, T. Niizeki et al., "Cardiac sympathetic denervation and ongoing myocardial damage for prognosis in early stages of heart failure," *Journal of Cardiac Failure*, vol. 13, no. 1, pp. 34–41, 2007.

Hindawi Publishing Corporation
Experimental Diabetes Research
Volume 2012, Article ID 510902, 7 pages
doi:10.1155/2012/510902

Research Article

Circulating TGF-β1, Glycation, and Oxidation in Children with Diabetes Mellitus Type 1

Vladimír Jakuš,[1] Michal Sapák,[2] and Jana Kostolanská[3]

[1] *Institute of Medical Chemistry, Biochemistry and Clinical Biochemistry, Faculty of Medicine, Comenius University, Sasinkova 2, Bratislava 81108, Slovakia*
[2] *Department of Immunology, Faculty of Medicine, Comenius University, Sasinkova 2, Bratislava 81108, Slovakia*
[3] *National Institute for Certified Educational Measurements, Žehrianska 9, Bratislava 85107, Slovakia*

Correspondence should be addressed to Vladimír Jakuš, vladimir.jakus@fmed.uniba.sk

Received 28 March 2012; Revised 31 July 2012; Accepted 14 August 2012

Academic Editor: Pietro Galassetti

The present study investigates the relationship between diabetes metabolic control represented by levels of HbA1c, early glycation products-(fructosamine (FAM)), serum-advanced glycation end products (s-AGEs), lipoperoxidation products (LPO), advanced oxidation protein products (AOPP) and circulating TGF-β in young patients with DM1. The study group consisted of 79 patients with DM1 (8–18 years). 31 healthy children were used as control (1–16 years). Baseline characteristics of patients were compared by Student's t-test and nonparametric Mann-Whitney test (Statdirect), respectively. The correlations between the measured parameters were examined using Pearson correlation coefficient r and Spearman's rank test, respectively. A P value < 0.05 was considered as statistically significant. HbA1c was measured by LPLC, s-AGEs spectrofluorimetrically, LPO and AOPP spectrophotometrically and TGF-β by ELISA. Our results showed that parameters of glycation and oxidation are significantly higher in patients with DM1 than in healthy control. The level of serum TGF-β was significantly higher in diabetics in comparison with control: 7.1(3.6; 12.6) versus 1.6(0.8; 3.9) ng/mL. TGF-β significantly correlated with age and duration of DM1. There was not found any significant relation between TGF-β and parameres of glycation and oxidation. However, these results do not exclude the association between TGF-β and the onset of diabetic complications.

1. Introduction

Diabetes mellitus of Type 1 is one of the most frequent autoimmune diseases and is characterized by absolute or nothing short of absolute endogenous insulin deficiency which results in hyperglycemia that is considered to be a primary cause of diabetic complications. Diabetes mellitus leads to various chronic micro- and macrovascular complications. Diabetic nephropathy and cardiovascular disease are major causes of morbidity and mortality in patients with DM.

Persistent hyperglycemia is linked with glycation and glycoxidation. During glycation and glycoxidation, there are formed early, intermediate, and advanced glycation products (AGEs). Accumulation of AGEs has several toxic effects and takes part in the development of diabetic complications [1–3], such as nephropathy [4], neuropathy, retinopathy, and angiopathy [5]. Higher plasma levels of AGEs are associated also with incident cardiovascular disease and all-cause mortality in DM1 [6]. AGEs are believed to induce cellular oxidative stress through the interaction with specific cellular receptors [7].

It has been suggested that the chronic hyperglycaemia in diabetes enhances the production of reactive oxygen species (ROS) from glucose autoxidation, protein glycation, and glycoxidation, which leads to tissue damage [8–10]. Also, cumulative episodes of acute hyperglycaemia can be source of acute oxidative stress. A number of studies have summarized the relation between glycation and oxidation [11]. Uncontrolled production of ROS often leads to damage of cellular macromolecules (DNA, lipids, and proteins).

Some oxidation products or lipid peroxidation products may bind to proteins and amplify glycoxidation-generated

lesions. Lipid peroxidation of polyunsaturated fatty acids, one of the radical reaction *in vivo*, can adequately reflect increased oxidative stress in diabetes.

Advanced oxidation protein products (AOPPs) are formed during oxidative stress by the action of chlorinated oxidants, mainly hypochlorous acid and chloramines. In diabetes, the formation of AOPP is induced by intensified glycoxidation processes, oxidant-antioxidant imbalance, and coexisting inflammation [12]. AOPPs are supposed to be structurally similar to AGEs and to exert similar biological activities as AGEs, that is, induction of proinflammatory cytokines in neutrophils, as well as in monocytes, and adhesive molecules [13]. Accumulation of AOPP has been found in patients with chronic kidney disease [14]. Further possible sources of oxidative stress are decreased antioxidant defenses, or alterations in enzymatic pathways. AGEs and their receptor (RAGE) axis stimulate oxidative stress and generation and subsequently evoke fibrogenic reactions in renal tubular cells, thereby playing a role in diabetic nephropathy [15]. Growth factor TGF-β1 is one of profibrotic cytokines and is an important mediator in the pathogenesis of diabetic nephropathy [16, 17]. TGF-β1 stimulates the production of extracellular matrix components such as collagen-IV, fibronectin, and proteoglycans (decorin, biglycan). TGF-β1 may cause glomerulosclerosis and it is one of the causal factor in myointimal hyperplasia after baloon injury of carotid artery. It mediates angiotensin-II modulator effect on smooth muscle cell growth. Beside profibrotic activity, TGF-β1 has immunoregulatory function on adaptive immunity too. AGEs induce connective tissue growth factor-mediated renal fibrosis through TGF-β1-independent Smad3 signalling [18, 19].

The present study investigates the relationship between diabetes metabolic control represented by actual levels of HbA1c, early glycation products—(fructosamine (FAM)), serum-advanced glycation end products (s-AGEs), lipid peroxidation products (LPOs), advanced oxidation protein products (AOPPs), and circulating TGF-β in patients with DM1.

2. Materials and Methods

2.1. Patients and Design. The studied group consisted of 79 children and adolescents (8–18 years) with T1DM regularly attending the 1st Department of Pediatrics, Children Diabetological Center of the Slovak Republic, University Hospital, Faculty of Medicine, Comenius University, Bratislava. They had T1DM with duration at least for 5 years. The urine samples in our patients were collected 3 times overnight, microalbuminuria was considered to be positive when UAER was between 20 and 200 microgram/min. No changes (fundus diabetic retinopathy) were found by the ophthalmologist examining the eyes in subject without retinopathy. Diabetic neuropathy was confirmed by EMG exploration using the conductivity assessment of sensor and motor fibres of peripheral nerves. The controls file consists of 31 healthy children (1–16 years). The samples of EDTA capillary blood were used to determine of HbA1c and serum samples were used to determine of FAM, s-AGEs, LPO, and AOPP. The samples of serum were stored in −18°C/−80°C.

2.2. Determination of UAER. UAER was determined by means of immunoturbidimetric assay (Cobas Integra 400 Plus, Roche, Switzerland), using the commercial kit 400/400 Plus. The assay was performed as a part of patients routine monitoring in Department of Laboratory Medicine, University Hospital, Bratislava.

2.3. Determination of Fructosamine. For the determination of fructosamine we used a kinetic, colorimetric assay and subsequently spectrophotometrical determination at wavelength 530 nm. We used 1-deoxy-1-morpholino-fructose (DMF) as the standard. Serum samples were stored at −79°C and were defrost only once. This test is based on the ability of ketoamines to reduce nitroblue tetrazolium (NBT) to a formazan dye under alkaline conditions. The rate of formazan formation, measured at 530 nm, is directly proportional to the fructosamine concentration. Measurements were carried out in one block up to 5 samples. To 3 mL of 0.5 mmol/L NBT were added 150 microliters of serum and the mixture was incubated at 37°C for 10 minutes. The absorbance was measured after 10 min and 15 min of incubation at Novaspec analyzer II, Biotech (Germany).

2.4. Determination of Glycated Hemoglobin HbA1c. HbA1c was determined from EDTA capillary blood immediately after obtained by the low pressureliquid chromatography (LPLC, DiaSTAT, USA) in conjunction with gradient elution. Before testing hemolysate is heated at 62–68°C to eliminate unstable fractions and after 5 minutes is introduced into the column. Hemoglobin species elute from the cation exchange column at different times, depending on their charge, with the application of buffers of increasing ionic strength. The concentration of hemoglobins is measured after elution from the column, which is then used to quantify HbA1c by calculating the area under each peak. Instrument calibration is always carried out when introducing a new column set procedure (Bio-RAD, Inc., 2003).

2.5. Determination of Serum AGEs. Serum AGEs were determined as AGE-linked specific fluorescence, serum was diluted 20-fold with deionized water, the fluorescence intensity was measured after excitation at 346 nm, at emission 418 nm using a spectrophotometer Perkin Elmer LS-3, USA. Chinine sulphate (1 microgram/mL) was used to calibrate the instrument. Fluorescence was expressed as the relative fluorescence intensity in arbitrary units (A.U.).

2.6. Determination of Serum Lipoperoxides. Serum lipid peroxides were determined by iodine liberation spectrophotometrically at 365 nm (Novaspec II, Pharmacia LKB, Biotech, SRN). The principle of this assay is based on the oxidative activity of lipid peroxides that will convert iodide to iodine. Iodine can then simply be measured by means of a photometer at 365 nm. Calibration curves were obtained using cumene hydroperoxide. A stoichiometric relationship was

observed between the amount of organic peroxides assayed and the concentration of iodine produced [20].

2.7. Determination of Serum AOPP. AOPPs were determined in the plasma using the method previously devised by Witko-Sarsat et al. [21] and modified by Kalousová et al. [22]. Briefly, AOPPs were measured by spectrophotometry on a reader (FP-901, Chemistry Analyser, Labsystems, Finland) and were calibrated with chloramine-T solutions that in the presence of potassium iodide absorb at 340 nm. In standard wells, 10 microliters of 1.16 M potassium iodide was added to 200 microliters of chloramine-T solution (0–100 micromol/L) followed by 20 microliters of acetic acid. In test wells, 200 microliters of plasma diluted 1 : 5 in PBS were placed to cell of 9 channels, and 20 microliters of acetic acid was added. The absorbance of the reaction mixture is immediately read at 340 nm on the reader against a blank containing 200 microliters of PBS, 10 microliters of potassium iodide, and 20 microliters of acetic acid. The chloramine-T absorbance at 340 nm being linear within the range of 0 to 100 micromol/L, AOPP concentrations was expressed as micromoles per liter of chloramine-T equivalents.

2.8. Determination of Circulating TGF-β. Quantitative detection of TGF-β in serum was done by enzyme linked immunosorbent assay, using human TGF-β1 ELISA-kit (BMS249/2, Bender MedSystem). Brief description of the method: into washed, with anti-TGF-β1 precoated microplate were added prediluted (1 : 10) sera (100 microliters) and "HRP-Conjugate" (50 microliters) as a antihuman-TGF-β1 monoclonal antibody and incubated for 4 hour on a rotator (100 rpm). After microplate washing (3 times), "TMB Substrate Solution" (100 microliters) was added and was incubated for 10 minutes. Enzyme reaction was stopped by adding "Stop Solution" (100 microliters). The absorbance of each microwell was readed by HumaReader spectrophotometer (Human) using 450 nm wavelength. The TGF-β1 concentration was determined from standard curve prepared from seven TGF-β1 standard dilutions. Each sample and TGF-β1 standard dilution were done in duplicate.

2.9. Statistical Analysis. Shapiro-Wilk test was performed to the test the distribution of all continuous variables. Pearson's test with correlation coefficient r or Spearman's one with Spearman's rank correlation coefficient R in case of small count of variables was then used to association between parameters described within the text, in all studied patients. P values less than 0.05 were accepted as being statistically significant. All statistical analyses were carried out using Excel 2003, Origin 8 and BioSTAT 2009.

3. Results

3.1. Comparison of Clinical and Biochemical Parameters. Clinical and biochemical characteristics of the patients with DM1 without and with diabetic complications and controls are reported in Table 1.

As shown in Table 1, there were significantly higher levels of AGEs (Figure 1(a)), AOPP (Figure 1(b)), LPO (Figure 1(c)) and TGF-beta (Figure 1(d)) in patients with DM1 than in healthy control.

3.2. Correlations between Measured Parameters. HbA1c significantly correlated with duration of DM1 ($r = 0.294$; $P = 0.01$) and with FAM ($r = 0.601$; $P \ll 0.001$) (Figure 2(a)). S-AGEs significantly correlated with FAM ($r = 0.368$; $P < 0.01$).

AOPP has also significant correlation with FAM ($r = 0.440$; $P \ll 0.001$), HbA1c ($r = 0.455$; $P \ll 0.001$), and s-AGEs ($r = 0.540$; $P \ll 0.001$) (Figure 2(b)).

LPO significantly correlated with FAM ($r = 0.386$; $P < 0.01$), with s-AGEs ($r = 0.354$; $P = 0.02$) and very strong with AOPP ($r = 0.833$; $P \ll 0.001$) (Figure 2(c)).

TGF-β significantly correlated with age ($r = 0.460$; $P = 0.01$) and duration of DM1 ($r = 0.379$; $P < 0.05$). Relations with other parameters were not statistically significant.

4. Discussion

Many studies deal with the impact of glycative stress on the development of diabetic complications. We studied also glycative and oxidative stress parameters in regard to diabetic complications presence-absence and in with respect to glycemic compensation [23, 24]. In this work, we have focused on the study of relationship between clinical parameters, circulating markers of glycation, or oxidation and circulating cytokine TGF-β in young patients (children and adolescents) with DM1 without albuminuria (Table 1). Microalbuminuria is first clinical manifestation of albuminuria defined as urinary albumin excretion rate of 20 to 200 μg/min.

TGF-β1 has a very wide range of activities *in vitro*. For example, TGF-β regulates important cellular functions such as rate of proliferation and production of extracellular matrix proteins by wide range of cell types. As a result of the wide range of activities attributed to the TGF-β, a number of groups have investigated whether circulating levels of TGF-β1 might be altered in various disease states. With only one exception, all of these studies agree that TGF-β1 is found in detectable levels in plasma from healthy human subjects [25]. TGF-β levels are unaltered for example in normal pregnancy [26].

Moreover, plasma TGF-β1 concentration markedly differed (by as much as 10-fold) in subjects suffering from various diseases, including autoimmune diseases, atherosclerosis and various cancers, compared with control subjects [25]. If such a pathopysiological role of plasma TGF-β1 is proven, it could become both a prognostic indicator of future risk of disease and/or complications of disease and a target for therapeutic interventions.

TGF-β1 plays a pivotal role in the extracellular matrix accumulation and in the pathogenesis of diabetic nephropathy (Figure 3). TGF-β1 may participate in the development and progression of diabetic micro- and macrovascular complications [27–29]. The association between TGF-β1 and

Table 1: Clinical and biochemical parameters in all diabetic patients and healthy control.

Parameter	All patients with DM1	n	Controls	N
Age (r.)	15.2 ± 2.7	79	9.2 ± 4.9	31
Duration of DM (r.)	8.7 ± 3.0	79	—	—
UAER (μg/min)	37.8 ± 116.8	74	—	—
FAM (mmol/L)	2.85 ± 0.50	75	1.62 ± 0.35$^{\#}$	29
HbA1c (%)	9.51 ± 1.90	79	5.0 ± 0.39$^{\#}$	21
s-AGEs (A.U.)*	67.85 (61.6; 76.4)	70	58.2 (52.0; 65.5)$^{\#}$	29
AOPP (μmol/L)*	80.5 (44.9; 139.9)	59	58.5 (51.5; 66.9)$^{\#}$	12
LPO(nmol/mL)*	119 (100.3; 156.3)	48	99 (67; 106)$^{\#}$	11
TGF-β (ng/mL)*	7.1 (3.6; 12.6)	29	1.6 (0.8; 3.9)$^{\#}$	9

The results are presented as mean ± SD in normal distribution and as median (1st quartile, 3rd quartile) in data with abnormal distribution.*
$^{\#}$significant difference in comparison with DM1 patients.

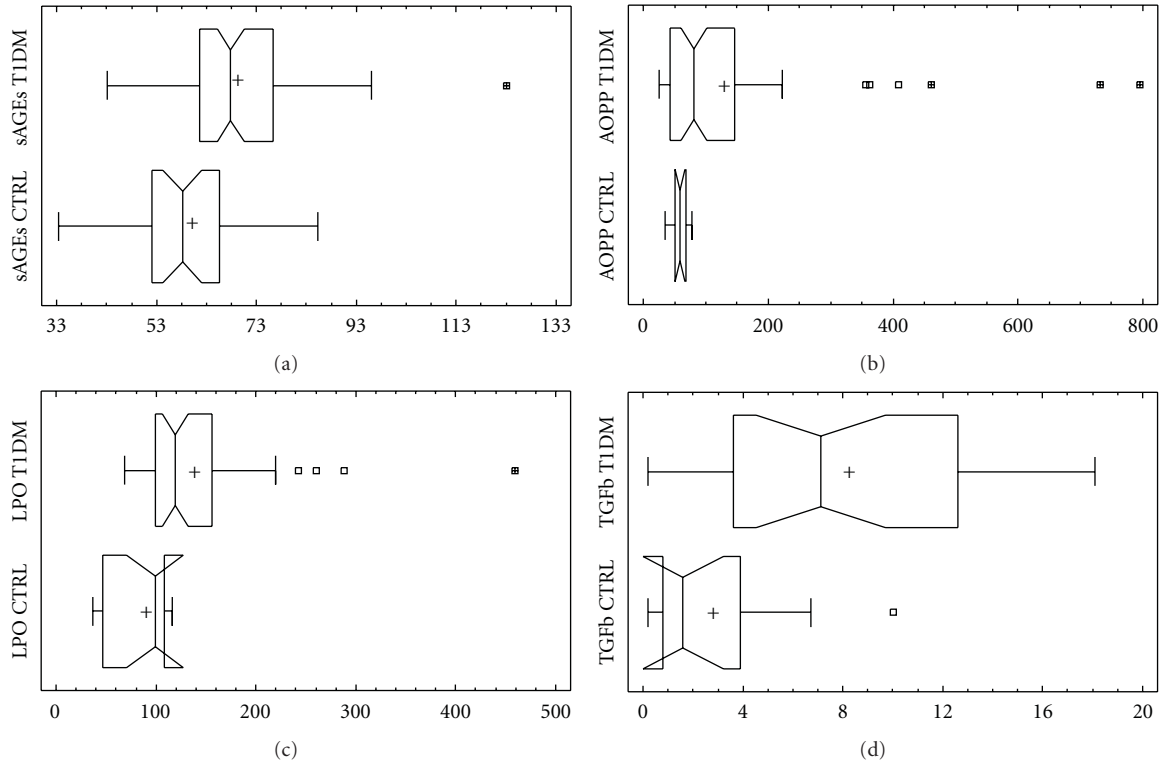

Figure 1: Comparison of (a) AGEs, (b) AOPP, (c) LPO and (d) TGF-β1 levels in diabetic patients and controls. Levels of AGEs are significantly higher in patients with DM1 than in healthy control (AGEs in serum 67.9 (61.6; 76.4) versus 58.2 (52.0; 65.0) A.U., $P < 0.001$*) (Figure 1(a)). Parameters of oxidative stress AOPP an LPO are significantly higher in patients with DM1 than in control (AOPP: 80.5 (44.9; 139.9) versus 51.5; 66.9) μmol/L, $P < 0.01$*) (Figure 1(b)) (LPO: 119.0 (100.3; 156.3) versus 99.0 (67.0; 106.0) nmol/mL, $P < 0.01$*) (Figure 1(c)). The level of serum TGF-β was significantly higher in diabetics in comparison with control (7.1 (3.6; 12.6) versus 1.6 (0.8; 3.9) ng/mL, $P < 0.01$*) (Figure 1(d)). *-Mann Whitney test.

cardiovascular disease in diabetic patients is controversial [30].

TGF-β1 is an important cytokine for the development of renal injury in patients with DM2 [31]. Higher serum levels of TGF-β1 were found in patients with DM2 [31–33]. In the study of patients with DM1 were also found alterations in level of circulating TGF-β1 [34, 35]. Elevated levels of circulating TGF-β1 were related to proliferative retinopathy and HbA1c [35]. AGEs play a critical role in diabetic nephropathy and vasculopathy and is associated with AGE deposition and receptor for AGE (RAGE) upregulation [18].

In our study the elevated levels of TGF-β1 in subjects with DM1 possibly indicate a tendency for renal and endothelial damage in such patients. Serum TGF-β1 can be probably one of diagnostic indicators for early diabetic vasculopathy. However, TGF-β correlated only with age and duration of DM1. There was not found any significant relation between circulating TGF-β and parameters of early

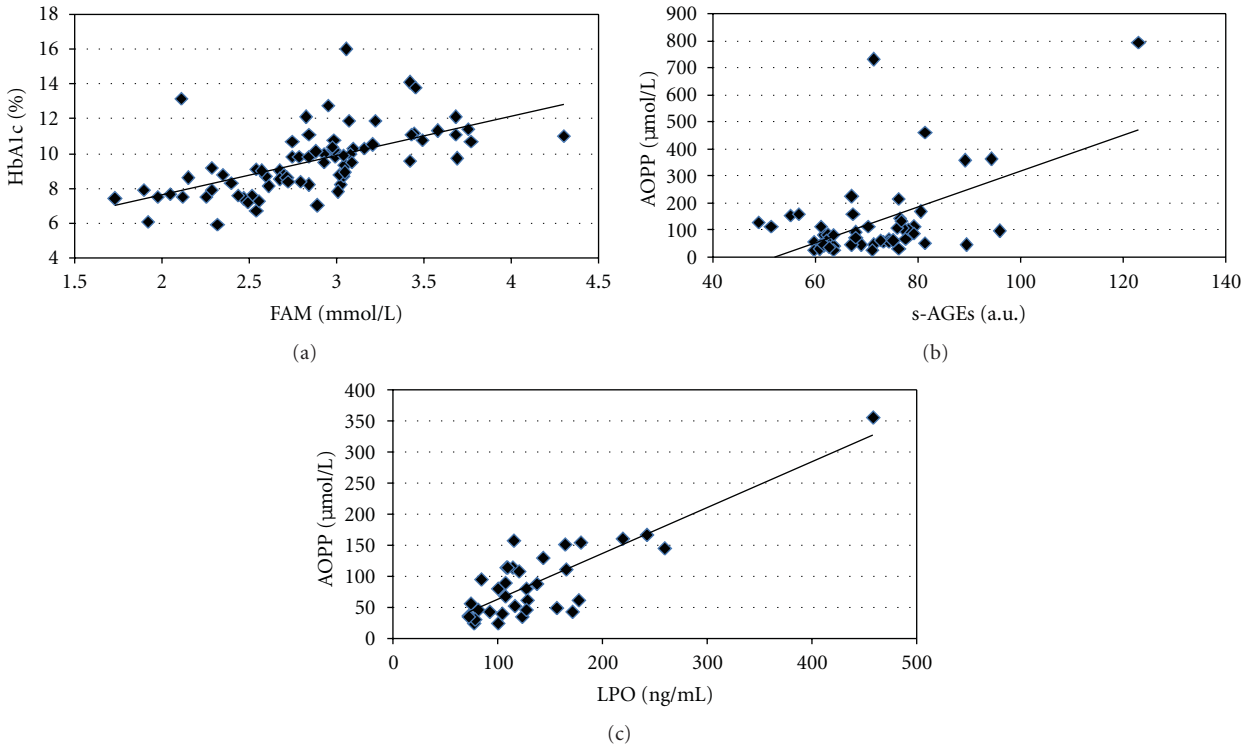

Figure 2: Significant correlations of (a) HbA1c and FAM ($r = 0.601$, $P \ll 0.001$; $n = 79$), (b) AOPP and s-AGEs ($r = 0.540$, $P \ll 0.001$; $n = 54$), and (c) AOPP and LPO ($r = 0.833$, $P \ll 0.001$; $n = 43$) in all diabetic patients.

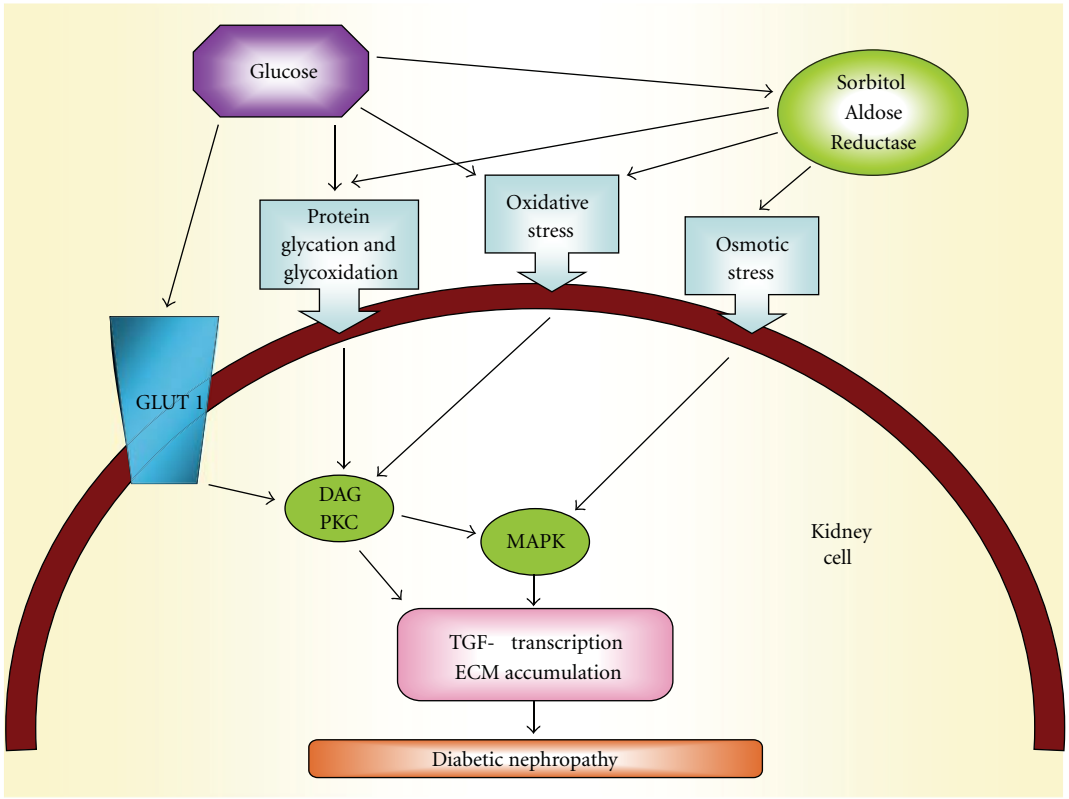

Figure 3: From hyperglycaemia to TGF-β transcription.

and advanced glycation and oxidation. Nevertheless, diabetic nephropathy was absent in our diabetic patients.

5. Conclusions

The level of TGF-β in serum of young patients with DM1 (children and adolescents) was significantly higher in the comparison with healthy control. TGF-β correlates only with age and duration of DM1. There was not found any significant relation between circulating TGF-β and parameters of early and advanced glycation and oxidation. However, these results do not exclude the association between TGF-β and the onset of diabetic complications.

Conflict of Interests

The authors report no conflict of interests.

Acknowledgments

This work was supported by Grant no. 1/0451/12 from the VEGA Agency. The authors are thankful to L. Barák, MD, E. Jančová, MD, J. Staník, MD, and A. Staníková, MD, for assistance with subject recruitment and assessment.

References

[1] P. J. Beisswenger, "Glycation and biomarkers of vascular complications of diabetes," *Amino Acids*, vol. 42, no. 4, pp. 1171–1183, 2012.

[2] V. Jakuš and N. Rietbrock, "Advanced glycation end-products and the progress of diabetic vascular complications," *Physiological Research*, vol. 53, no. 2, pp. 131–142, 2004.

[3] G. Pugliese, "Do advanced glycation end products contribute to the development of long-term diabetic complications?" *Nutrition, Metabolism & Cardiovascular Diseases*, vol. 18, no. 7, pp. 457–460, 2008.

[4] N. Kashihara, Y. Haruna, V. K. Kondeti, and Y. S. Kanwar, "Oxidative stress in diabetic nephropathy," *Current Medicinal Chemistry*, vol. 17, no. 34, pp. 4256–4269, 2010.

[5] S. Y. Goh and M. E. Cooper, "The role of advanced glycation end products in progression and complications of diabetes," *The Journal of Clinical Endocrinology & Metabolism*, vol. 93, no. 4, pp. 1143–1152, 2008.

[6] J. W. Nin, A. Jorsal, I. Ferreira et al., "Higher plasma levels of advanced glycation end products are associated with incident cardiovascular disease and all-cause mortality in type 1 diabetes: a 12-year follow-up study," *Diabetes Care*, vol. 34, no. 2, pp. 442–447, 2011.

[7] J. A. Mosquera, "Role of the receptor for advanced glycation end products (RAGE) in inflammation," *Investigacion Clinica*, vol. 51, no. 2, pp. 257–268, 2010.

[8] S. M. Son, "Role of vascular reactive oxygen species in development of vascular abnormalities in diabetes," *Diabetes Research and Clinical Practice*, vol. 77, no. 3, pp. S65–S70, 2007.

[9] R. Madonna and R. De Caterina, "Cellular and molecular mechanisms of vascular injury in diabetes—Part I: Pathways of vascular disease in diabetes," *Vascular Pharmacology*, vol. 54, no. 3–6, pp. 68–74, 2011.

[10] J. P. Kuyvenhoven and A. E. Meinders, "Oxidative stress and diabetes mellitus Pathogenesis of long-term complications," *European Journal of Internal Medicine*, vol. 10, no. 1, pp. 9–19, 1999.

[11] R. Boizel, G. Bruttmann, P. Y. Benhamou, S. Halimi, and F. Stanke-Labesque, "Regulation of oxidative stress and inflammation by glycaemic control: evidence for reversible activation of the 5-lipoxygenase pathway in type 1, but not in type 2 diabetes," *Diabetologia*, vol. 53, no. 9, pp. 2068–2070, 2010.

[12] A. Piwowar, "Advanced oxidation protein products. Part II. the significance of oxidation protein products in the pathomechanism of diabetes and its complications," *Polski Merkuriusz Lekarski*, vol. 28, no. 165, pp. 227–230, 2010.

[13] S. F. Yan, R. Ramasamy, and A. M. Schmidt, "Mechanisms of disease: advanced glycation end-products and their receptor in inflammation and diabetes complications," *Nature Clinical Practice Endocrinology and Metabolism*, vol. 4, no. 5, pp. 285–293, 2008.

[14] A. S. Bargnoux, M. Morena, S. Badiou et al., "Biologie des fonctions renales et de l' insuffisance renale," *Annales De Biologie Clinique*, vol. 67, no. 2, pp. 153–158, 2009.

[15] S. Maeda, T. Matsui, M. Takeuchi et al., "Pigment epithelium-derived factor (PEDF) inhibits proximal tubular cell injury in early diabetic nephropathy by suppressing advanced glycation end products (AGEs)-receptor (RAGE) axis," *Pharmacological Research*, vol. 63, no. 3, pp. 241–248, 2011.

[16] G. Wolf and F. N. Ziyadeh, "Cellular and molecular mechanisms of proteinuria in diabetic nephropathy," *Nephron—Physiology*, vol. 106, no. 2, pp. p26–p31, 2007.

[17] A. A. Elmarakby, R. Abdelsayed, J. Y. Liu, and M. S. Mozaffari, "Inflammatory cytokines as predictive markers for early detection and progression of diabetic nephropathy," *EPMA Journal*, vol. 1, no. 1, pp. 117–129, 2010.

[18] J. H. Li, X. R. Huang, H. J. Zhu et al., "Advanced glycation end products activate Smad signaling via TGF-beta-dependent and independent mechanisms: implications for diabetic renal and vascular disease," *The FASEB Journal*, vol. 18, no. 1, pp. 176–178, 2004.

[19] A. C. K. Chung, H. Zhang, Y. Z. Kong et al., "Advanced glycation end-products induce tubular CTGF via TGF-β-independent Smad3 signaling," *Journal of the American Society of Nephrology*, vol. 21, no. 2, pp. 249–260, 2010.

[20] M. El-Saadani, H. Esterbauer, M. El-Sayed, M. Goher, A. Y. Nassar, and G. Jurgens, "A spectrophotometric assay for lipid peroxides in serum lipoproteins using a commercially available reagent," *Journal of Lipid Research*, vol. 30, no. 4, pp. 627–630, 1989.

[21] V. Witko-Sarsat, M. Friedlander, C. Capeillère-Blandin et al., "Advanced oxidation protein products as a novel marker of oxidative stress in uremia," *Kidney International*, vol. 49, no. 5, pp. 1304–1313, 1996.

[22] M. Kalousová, J. Škrha, and T. Zima, "Advanced glycation end-products and advanced oxidation protein products in patients with diabetes mellitus," *Physiological Research*, vol. 51, no. 6, pp. 597–604, 2002.

[23] J. Kostolanska, V. Jakus, L. Barak, A. Stanikova, and I. Waczulikova, "Comparative study of serum/plasma glycation and lipid peroxidation of young patients with type 1 diabetes mellitus in relation to glycemic compensation and the occurrence of diabetic complications," *Bratislava Medical Journal*, vol. 111, no. 11, pp. 578–585, 2010.

[24] J. Kostolanská, V. Jakuš, L. Barák, and A. Staníková, "Impact of long-term glycemic control on changes of lipid profile in children and adolescents with 1 type diabetes mellitus," *Vnitrni Lekarstvi*, vol. 57, no. 6, pp. 533–539, 2011.

[25] D. J. Grainger, D. E. Mosedale, and J. C. Metcalfe, "TGF-β in blood: a complex problem," *Cytokine & Growth Factor Reviews*, vol. 11, no. 1-2, pp. 133–145, 2000.

[26] A. Szarka, J. Rigó, L. Lázár, G. Beko, and A. Molvarec, "Circulating cytokines, chemokines and adhesion molecules in normal pregnancy and preeclampsia determined by multiplex suspension array," *BMC Immunology*, vol. 11, article 59, pp. 1–9, 2010.

[27] B. F. Schrijvers, A. S. De Vriese, and A. Flyvbjerg, "From hyperglycemia to diabetic kidney disease: the role of metabolic, hemodynamic, intracellular factors and growth factors/cytokines," *Endocrine Reviews*, vol. 25, no. 6, pp. 971–1010, 2004.

[28] S. Hefini, A. Kamel, H. El-Banawy et al., "The role of BMP-7 and TGF-beta1 in diabetic nephropathy," *Journal of Medical Research Institute*, vol. 28, no. 3, pp. 235–243, 2007.

[29] M. van den Heuvel, W. W. Batenburg, and A. H. J. Danser, "Diabetic complications: a role for the prorenin-(pro)renin receptor-TGF-β1 axis?" *Molecular and Cellular Endocrinology*, vol. 302, no. 2, pp. 213–218, 2009.

[30] B. D. Schaan, A. S. Quadros, R. Sarmento-Leite, G. De Lucca, A. Bender, and M. Bertoluci, "'Correction:' Serum transforming growth factor beta-1 (TGF-beta-1) levels in diabetic patients are not associated with pre-existent coronary artery disease," *Cardiovascular Diabetology*, vol. 6, article 19, pp. 1–6, 2007.

[31] S. Ibrahim and L. Rashed, "Estimation of transforming growth factor-beta 1 as a marker of renal injury in type II diabetes mellitus," *Saudi Medical Journal*, vol. 28, no. 4, pp. 519–523, 2007.

[32] S. Yener, A. Comlekci, B. Akinci et al., "Serum transforming growth factor-beta 1 levels in normoalbuminuric and normotensive patients with type 2 diabetes. Effect of metformin and rosiglitazone," *Hormones*, vol. 7, no. 1, pp. 70–76, 2008.

[33] G. R. Huseynova, G. I. Azizova, and A. M. Efendiyev, "Quantitative changes in serum IL-8, TNF-α and TGF-β1 levels depending on compensation stage in type 2 diabetic patients," *International Journal of Diabetes and Metabolism*, vol. 17, no. 2, pp. 59–62, 2009.

[34] S. T. Azar, I. Salti, M. S. Zantout, and S. Major, "Alterations in plasma transforming growth factor β in normoalbuminuric type 1 and type 2 diabetic patients," *The Journal of Clinical Endocrinology & Metabolism*, vol. 85, no. 12, pp. 4680–4682, 2000.

[35] N. Chaturvedi, C. G. Schalkwijk, H. Abrahamian, J. H. Fuller, and C. D. Stehouwer, "Circulating and urinary transforming growth factor beta1, Amadori albumin, and complications of type 1 diabetes: the EURODIAB prospective complications study," *Diabetes Care*, vol. 25, no. 12, pp. 2320–2327, 2002.

Hindawi Publishing Corporation
Experimental Diabetes Research
Volume 2012, Article ID 504693, 11 pages
doi:10.1155/2012/504693

Research Article

Antioxidant Sol-Gel Improves Cutaneous Wound Healing in Streptozotocin-Induced Diabetic Rats

Yen-Hsien Lee,[1] Jung-Jhih Chang,[2] Chiang-Ting Chien,[3] Ming-Chien Yang,[1,2] and Hsiung-Fei Chien[4]

[1] *Graduate Institute of Applied Science and Technology, National Taiwan University of Science and Technology, Taipei 106, Taiwan*
[2] *Department of Materials Science and Engineering, National Taiwan University of Science and Technology, Taipei 106, Taiwan*
[3] *Department of Medical Research, National Taiwan University Hospital and National Taiwan University College of Medicine, Taipei 100, Taiwan*
[4] *Department of Surgery, National Taiwan University Hospital and National Taiwan University College of Medicine, Taipei 100, Taiwan*

Correspondence should be addressed to Ming-Chien Yang, myang@mail.ntust.edu.tw and Hsiung-Fei Chien, hfchien@ntu.edu.tw

Received 11 March 2012; Revised 28 May 2012; Accepted 12 June 2012

Academic Editor: Pietro Galassetti

We examined the effects of vitamin C in Pluronic F127 on diabetic wound healing. Full-thickness excision skin wounds were made in normal and diabetic Wistar rats to evaluate the effect of saline, saline plus vitamin C (antioxidant sol), Pluronic F127, or Pluronic F127 plus vitamin C (antioxidant sol-gel). The rate of wound contraction, the levels of epidermal and dermal maturation, collagen synthesis, and apoptosis production in the wound tissue were determined. *In vitro* data showed that after 6 hours of air exposure, the order of the scavenging abilities for HOCl, H_2O_2, and O_2^- was antioxidant sol-gel > antioxidant saline > Pluronic F127 = saline. After 7 and 14 days of wound injury, the antioxidant sol-gel improved wound healing significantly by accelerated epidermal and dermal maturation, an increase in collagen content, and a decrease in apoptosis formation. However, the wounds of all treatments healed mostly at 3 weeks. Vitamin C in Pluronic F127 hastened cutaneous wound healing by its antioxidant and antiapoptotic mechanisms through a good drug delivery system. This study showed that Pluronic F127 plus vitamin C could potentially be employed as a novel wound-healing enhancer.

1. Introduction

Wound healing represents a well-orchestrated reparative response that occurs after all surgical procedures or traumatic injury. Wound healing is a complex multifactorial process, involving inflammation, migration of different cell types, fibroplasia, collagen deposition, and wound contraction. During the inflammation phase, inflammatory cells significantly increased in the wound site [1] and produced burst amounts of reactive oxygen species (ROS) formation in the wound tissue [2] affecting wound healing.

Diabetes mellitus is one of the major contributors to chronic wound-healing problems, because minor skin wounds can lead to chronic, nonhealing ulcers and ultimately result in infection, gangrene, or even amputation. In critical ill diabetic patients, the antioxidant vitamin C in plasma was reported lower than nondiabetic critical ill patients [3]. In streptozotocin-induced and gene-induced diabetic mice, increased oxidative stress in the wounds has been noted [2]. Besides, increased oxidative stress promoted apoptosis formation in the damaged tissue and the increased apoptosis signaling also delayed the wound-healing process [4]. In addition, the diabetic rat skin was underhydroxylated in nascent collagen alpha chains (types I and III) [5]. Compromised collagen production associated with vitamin C deficiency results in impaired wound healing [6].

Vitamin C is an important water-soluble antioxidant, which may successfully scavenge ROS, protect against lipid damage, protein oxidation, and DNA oxidation [7]. Vitamin C can overcome the reduced proliferative capacity of elderly dermal fibroblast as well as increasing collagen synthesis in elderly cells [8]. Vitamin C promotes the hydroxylation,

which is required to stabilize the triple helical conformation of collagen [9]. Silvetti [10] has presented a safe and effective method of improving repair and controlling infection of wounds by daily topical application of a balanced solution of salts, amino acids, a high-molecular weight, D-glucose polysaccharide, and vitamin C. Vitamin C is water soluble but it is the most unstable of all water-soluble vitamins. Vitamin C reacts with the metallic ions of iron and copper and is easily destroyed by oxygen, alkalies, and high temperature [11].

Pluronic F127 is one member of a family of triblock copolymers of poly(ethylene oxide)-poly(propylene oxide)-poly(ethylene oxide), generically called poloxamers. At low temperatures, poly(propylene oxide) blocks have only weak hydrophobic properties. With increasing temperature, poly(ethylene oxide) blocks are dehrydrated and promote the aggregation to micelles and become gel form [12]. The incorporation of drugs into Pluronic micelles results in enhanced metabolic stability because of the outer hydrophilic poly(ethylene oxide) chains that protect drugs from external conditions. Pluronic F127 in a gel form has been used previously as a wound dressing [13] and as a drug delivery vehicle [14, 15]. In this study, we aimed to develop an antioxidant sol-gel preparation by incorporating vitamin C into Pluronic F127 and to apply the antioxidant sol-gel on cutaneous wounds in normal or diabetic rats. The parameters of wound closure rate, epidermal and dermal maturation, collagen synthesis, and apoptosis formation in wounds were evaluated. We hypothesized that the antioxidant ability of vitamin C in Pluronic F127 sol-gel was better than in saline solution, and antioxidant treatment will improve cutaneous wound healing in diabetic rats.

2. Materials and Methods

2.1. Animals. Female Wistar rats ($n = 6$ in most comparing group, $n = 5$ in ROS measurement), weighing 180 ± 20 g, were used to experiment. All rats were housed at a constant temperature and humidity in a room with an artificial 12-h light/dark cycle and allowed free access to food and water. All the surgical and experimental procedures were approved by Institutional Animal Care and Use Committee of National Taiwan University College of Medicine and College of Public Health and were in accordance with the guidelines of the National Science Council of Republic of China (NSC 1997).

2.2. Preparation of Antioxidant Sol-Gel. Pluronic F127 and vitamin C were purchased from Sigma-Aldrich Chemical Co. (USA). The Pluronic F127 (13% w/w) was dissolved in saline at 4°C by stirring into homogeneous sol-gel. Vitamin C powder was dissolved in the Pluronic F127 sol-gel (1 mg vitamin C/mL Pluronic F127 solution) as antioxidant sol-gel. The vitamin C powder was dissolved in saline (1 mg/mL) as vitamin C solution. We compared the *in vitro* antioxidant activities of 4 groups, that is, the saline, saline plus vitamin C (antioxidant saline), Pluronic F127, and Pluronic F127 plus vitamin C (antioxidant sol-gel) in this study. For this study, 200 μL samples exposed at 1 cm^2 area were determined their antioxidant ability at 0 and 6 hours after exposure to the air.

2.3. Measurement of ROS and Antioxidant Abilities [16]. To measure the production of ROS in the samples, chemiluminescence (CL) method was adopted using lucigenin (0.25 mM) as an amplifier for measuring superoxide (O_2^-) and luminol (0.25 mM) as an amplifier for measuring hydrogen peroxide (H_2O_2) and hypochlorous acid (HOCl). In brief, 0.2 mL of the samples (homogenized skin biopsies, vitamin C solution, Pluronic F127 sol, or antioxidant sol-gel) was placed in the plate for oxidative stress assay using a CL analyzer (Top Count System; Packard, Meriden, CT, USA). For H_2O_2 measurement, the sample and 0.5 mL of luminol were added on the dish, and the photon emission from the sample was count at 60-sec intervals at room temperature under atmospheric conditions. For measuring antioxidant abilities, after 120-sec incubation, 0.1 mL of 1 mM H_2O_2 was added. For hypochlorous acid (HOCl) measurement, the sample and 0.5 mL of luminol were added on the dish, and the photon emission from the sample was counted as previously. For measuring antioxidant abilities, after 60-sec incubation, 0.1 mL of 1 mM HOCl was added. For superoxide (O_2^-) measurement, the sample and 0.5 mL of 0.25 mM lucigenin were added on the dish, and the photon emission from the sample was counted as before. For measuring antioxidant abilities, after 60 sec incubation, 0.1 mL of 0.15% xanthine and 0.1 mL of 0.6% xanthine oxidase were added. For each sample, the assay was performed in triplicate, and the reactive oxidant level was expressed as CL counts.

2.4. Induction of Diabetic Rats and Wounding. Diabetes was induced by a single 65 mg/kg intraperitoneal injection of streptozotocin (STZ; Sigma, Inc., St. Louis, MO, USA), a toxin specific for insulin-producing cells, in normal saline. Blood glucose levels were measured using an acute glucometer. The diabetic state was confirmed 3 weeks after STZ injections by blood glucose levels above 300 mg/dL. Under brief anesthesia with intraperitoneal Nembutal (65 mg/kg), the dorsal skin of the animals was shaved and cleaned with povidone-iodine solution, and a full-thickness skin wound (approximately 1×1 cm^2) was created after marking the area with a wooden ink stamp before cutting the outlined skin. We applied 0.2 mL of antioxidant sol-gel, antioxidant saline, Pluronic F127, or saline on wounds twice per day for 21 days. Wound size was recorded with photographs, after anesthesia each time at 0, 7, 14, and 21 days after wounding. The wound size was then calculated with a free program called Image J. Animals were euthanized at each time point and the wound samples and adjacent normal skin were harvested and fixed in 10% paraformaldehyde for histological or snap-frozen in liquid nitrogen and stored at −80°C for further analysis. For detecting skin ROS, the intact skin (0.5 g) of diabetic rats as well as normal rats was biopsied, snap-frozen in liquid nitrogen, and homogenized by mortar and pestle, followed by adding 1 mL normal saline.

2.5. Wound-Healing Rate. The percentage of wound closure was calculated as follows by using the initial and final area

drawn on glass slides during the experiments:

$$\%\ \text{of wound contraction} = \frac{A_0 - A_t}{A_0} \times 100\%, \quad (1)$$

where A_0 is original wound area and A_t is the area of wound at days 7, 14, and 21, accordingly.

2.6. Hydroxyproline Analysis [17]. Wound tissues stored at −80°C were dried to a constant weight and hydrolyzed in 6 M HCl for 16 h at 120°C. Samples were dried on a hot plate and then washed three times with distilled water. The acid-free samples were reconstituted in 2.0 mL of acetate-citrate buffer (1.2% sodium acetate trihydrate, 5% citric acid, 12% sodium acetate, and 3.4% sodium hydroxide, pH 4–9). Five hundred microliters of 0.05 M chloramine-T was added to 1 mL of each sample, after which the samples were incubated for 15 min at room temperature, followed by the addition of 0.5 mL 15% perchloric acid and 15% 4-dimethyl aminobenzaldehyde in 1-propanol. After incubation at 60°C for 15 min, each sample was transferred to a microliter plate and the absorbance read at 550 nm. Hydroxyproline concentrations were calculated from the linear standard curve and presented as μg/g dry tissue weight.

2.7. Histological Analysis

2.7.1. Epidermal and Dermal Maturation Assessment. Wound bed biopsies were collected at days 7, 14, and 21 after wounding. Tissue samples were fixed in 10% buffered formalin, processed, and embedded in paraffin. Sections were stained with hematoxylin and eosin (H & E). Microscopic assessment of these slides was coded by a technician, and read-blinded to the sample identification. The sections were scored on a scale of 0–4 for epidermal healing (0 = no migration, 1 = partial migration, 2 = complete migration with partial keratinization, 3 = complete keratinization, and 4 = hypertrophic epidermis) and dermal healing (0 = no healing, 1 = inflammatory infiltrate, 2 = granulation tissue present-fibroplasias and angiogenesis, 3 = collagen deposition replacing granulation tissue > 50%, and 4 = hypertrophic fibrotic response) [18].

To investigate this further, differentiation of the neo-epidermis was studied by immunohistology using loricrin as late differentiation marker. Structural proteins, including involucrin and loricrin, are produced as skin matures imparting biomechanical strength to the epidermis [19, 20].

2.7.2. Immunohistochemistry Examination. After tissue sections were dewaxed and rehydrated conventionally, sections were incubated with 3% H_2O_2 for 30 minutes. The slides were washed with PBS (pH 7.4) twice. The sections were blocked with 5% BSA in TBS for 20 minutes. After the redundant liquid had been discarded, the sections were incubated with loricrin antibody (Abcam, Cambridge, UK) at 4°C overnight. After slides had been washed with PBS, the slides were incubated with rabbit secondary antibody for 1 hour, followed by incubation with streptavidin-HRP for 20 minutes. The antibody binding sites were visualized by incubation with DAB-H_2O_2 solution.

2.7.3. Masson's Trichrome Staining. Sections were dewaxed and rehydrated conventionally, placed in Weigert's hematoxylin stain for 1 h, rinsed under lukewarm water for 5 min, immersed in Masson solution for 15 min, and rinsed in deionized water before placing in phosphomolybdic acid for 10 min. Subsequently, sections were immersed in 2% aniline blue for 15 min, rinsed in 1% acetic acid, 95% ethanol, and absolute ethanol in turn, immersed in xylene for 10 min, and mounted with resin. Collagen fibers were stained blue, cytoplasm and erythrocyte were stained red, and nuclei were stained bluish brown.

2.7.4. TUNEL Assay. Apoptosis assay was performed using the TACS.XL DAB In Situ Apoptosis Detection Kit (Trevigen, Gaithersburg, MD, USA). Briefly, sections were blocked by incubation in 3% H_2O_2 in methanol for 5 minutes at 25°C. Then the sections were labeled with TdT labeling reaction mix at 37°C for 1 h. Nuclei exhibiting DNA fragmentation were visualized by incubation in 3′,3-diaminobenzidine (DAB) for 15 min.

2.8. Statistical Analysis. All values are expressed as mean ± SEM. For comparisons of parametric data, one-way analysis of variance and then the Student's unpaired t-test were conducted. $P < 0.05$ was recognized to indicate statistical significance. For nonparametric data, Kruskal-Wallis test with Dunn's posttest was done.

3. Results

3.1. Antioxidant Abilities in Antioxidant Sol-Gel. We showed that the CL counts of H_2O_2, HOCl, and O_2^- in Pluronic F127 and saline were similar, whereas the ROS levels in antioxidant sol-gel and antioxidant saline significantly decreased at 0 or 6 hours of air exposure (Figure 1). Our data indicated that the antioxidant sol-gel and antioxidant saline, not Pluronic F127, can directly scavenge ROS including H_2O_2, HOCl, and O_2^-. In addition, after 6 hours of air exposure, the antioxidant activities (except for O_2^-) in antioxidant sol-gel are stronger than those in antioxidant saline. This data implicates that Pluronic F127 can preserve parts of the antioxidant activities of vitamin C within after air exposure for a time period of such as 6 hours.

3.2. Wound Closure. Rats receiving STZ have significant elevation of blood glucose level (>300 mg/dL) after 3 weeks, which was sustained throughout the duration of the study. The wound healing of various treatments was evaluated in a full-thickness wound model. The wounds decreased in size gradually with time, closed at 2 weeks in normal rats and at 3 weeks in diabetic rats. We did not note any statistical difference in the wound closure of the normal rats with four kinds of treatment (Figure 2(a)). This was not unexpected since skin wounds of rats are known to heal efficiently and there is little room for improvement. However, in the diabetic

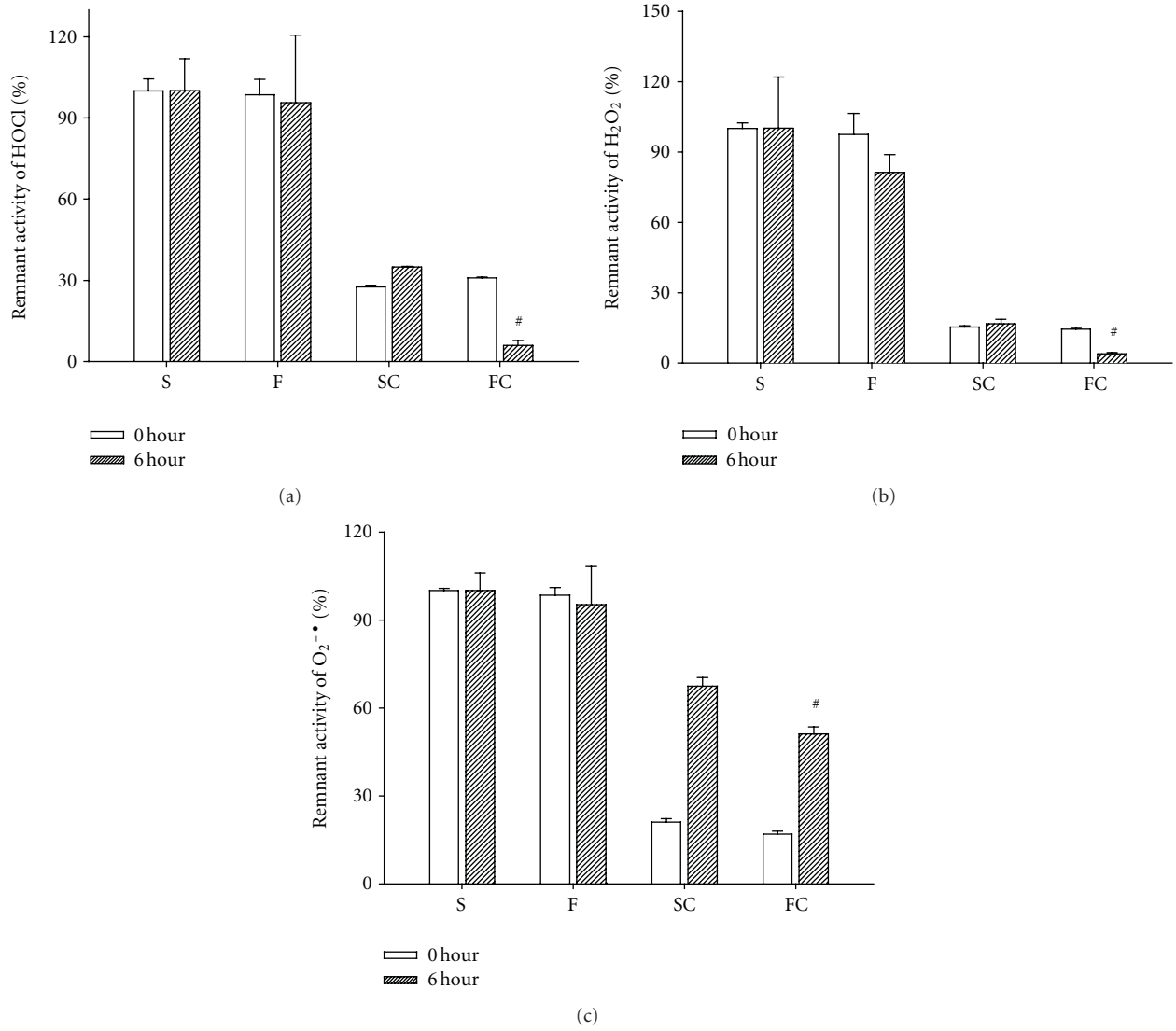

Figure 1: Scavenging abilities of saline (S), Pluronic F127 (F), antioxidant saline (SC), and antioxidant sol-gel (FC) for HOCl (a), H_2O_2 (b), and O_2^- (c) after 0 and 6 hours of preparation. Fresh-prepared (0 hour) antioxidant saline and antioxidant sol-gel significantly decreased HOCl, H_2O_2, and O_2^- counts when compared to saline. After 6 hours of air exposure, the antioxidant ability is significantly reserved in FC group when compared to SC group. Data are expressed as mean ± SEM. $^*P < 0.05$, $^\#P < 0.01$ when compared to saline group. S: saline control; F: Pluronic F127; SC: saline plus vitamin C; FC: Pluronic F127 plus vitamin C.

rats, periodical observation of animals at 7 days showed a significant increase ($P < 0.05$) in the rate of contraction of wounds in the antioxidant sol-gel and antioxidant saline groups when compared to saline group (Figure 2(b)). In the diabetic rats at 14 days, a significant ($P < 0.05$) wound closure was noted in the pluronic F127, antioxidant sol-gel, and antioxidant saline groups when compared to saline group (Figure 2(b)). However, the wound closure rate was displayed in a tendency of antioxidant sol-gel > antioxidant saline = Pluronic F127 ≥ saline in the diabetic wounds at 14 days after wounding. However, all groups attained full closure by the end of the third week.

3.3. ROS Amounts in the Diabetic Skins. As shown in Figure 3, three types of ROS including H_2O_2, HOCl, and O_2^- were all significantly increased in the intact skin of diabetic rats when compared with those in the skin of normal rats. These results directly evidence that diabetes increased oxidative stress in the skin before wounding.

3.4. Effect of Antioxidant Sol-Gel on Epidermal Maturation. With the help of hematoxylin & eosin stain (Figure 4) and the epidermal differentiation marker loricrin immunohistochemistry (Figure 7), the accelerated healing was noted in the epidermis of antioxidant saline or sol-gel-treated groups. Significant epidermal maturation indicated by migration of keratinization is indicated in an order of antioxidant sol-gel > antioxidant saline > Pluronic F127 > saline. Loricrin was abundant and finely granular in cells of the granular layer. The labeling was maximally present in the upper

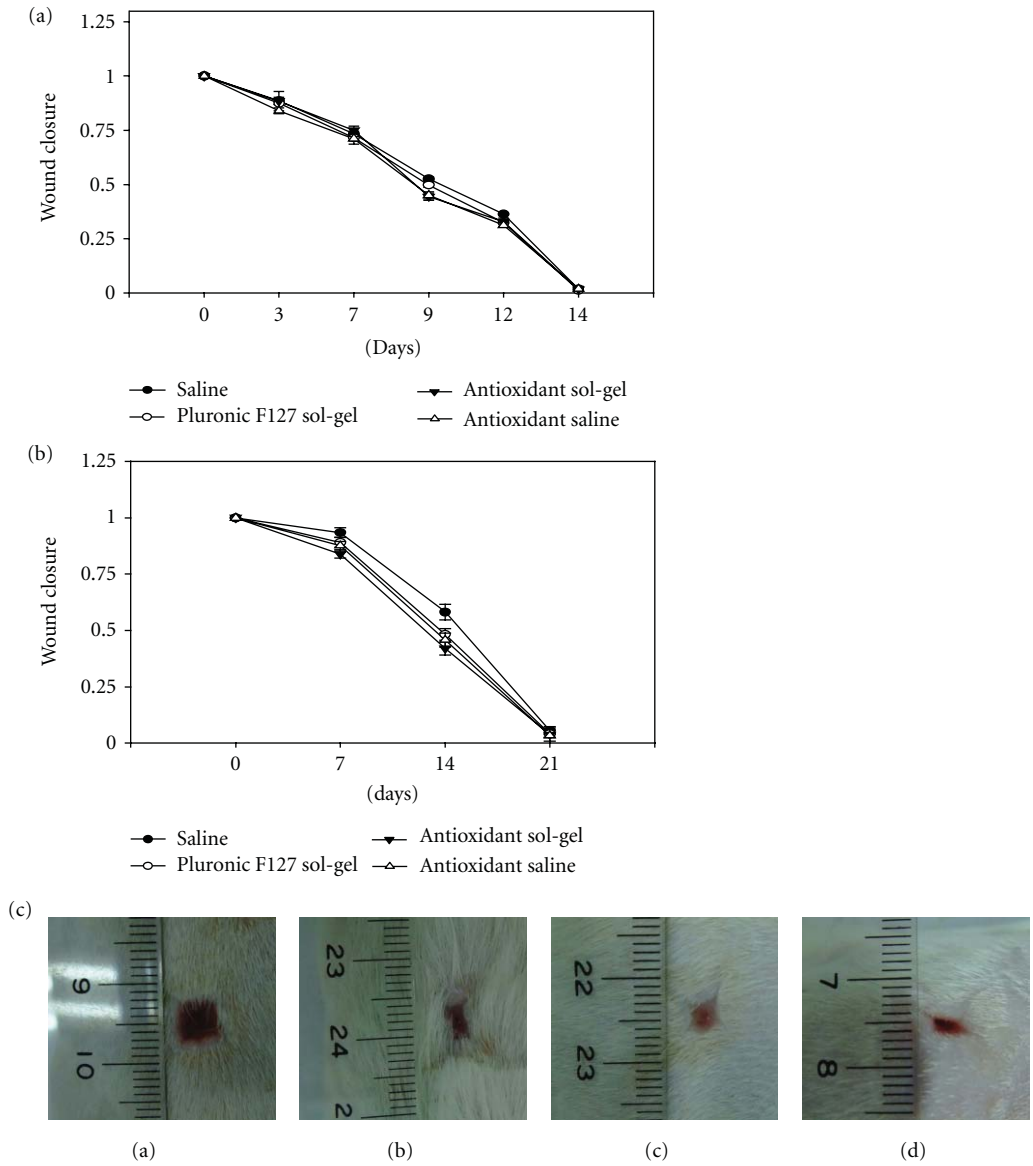

Figure 2: The effect of saline, Pluronic F127, antioxidant saline, and antioxidant Pluronic F127 on wound closure in the normal rats (a) and diabetic rats (b). Full-thickness skin wounds of 1.0 × 1.0 cm were measured from the time of wounding until closures. The skin defect was compared to the initial wound size to determine wound closure rate by tracing the wound. (a) Closure of full-thickness skin wounds of normal rats showed no significant difference in the healing rate between four groups of treatment. (b) Wound closure of diabetic skin showed that the antioxidant sol-gel-treated wounds closed faster than the saline-, sol- and antioxidant saline-treated wounds on days 7 and 14. Data is expressed as mean ± SEM for three separate experiments, each in quadruplicate. $^*P < 0.05$ when compared to saline control. (c) Representative pictures of skin wounds in group saline (a), Pluronic F127 (b), antioxidant saline (c), and antioxidant sol-gel (d) at day 7.

granular cells and suddenly decreased in the cornified layer, where a brick wall-like staining resulted.

3.5. Effect of Antioxidant Sol-Gel on Dermal Maturation. Normally, dermal recovery is assessed for three stages: proliferation, remodeling, and maturation. Histopathological examination with hematoxylin & eosin staining showed that the antioxidants sol-gel-treated wounds exhibited advancement in all these three stages. The histologic expression showed that dermal maturation was ranked in an order of antioxidant sol-gel > antioxidant saline > Pluronic F127 > saline (Figure 5(e)).

3.6. Effect of Antioxidant Sol-Gel on Masson's Trichrome Stain. Collagen deposition and cellular proliferation can be measured in the histological cross-sections of wounds with Masson's trichrome staining. Significant increase in blue collagen stain was found in the antioxidant sol-gel-treated group (Figure 6(d)) and antioxidant saline-treated group (Figure 6(c)) when compared to saline-treated group (Figure 6(a)).

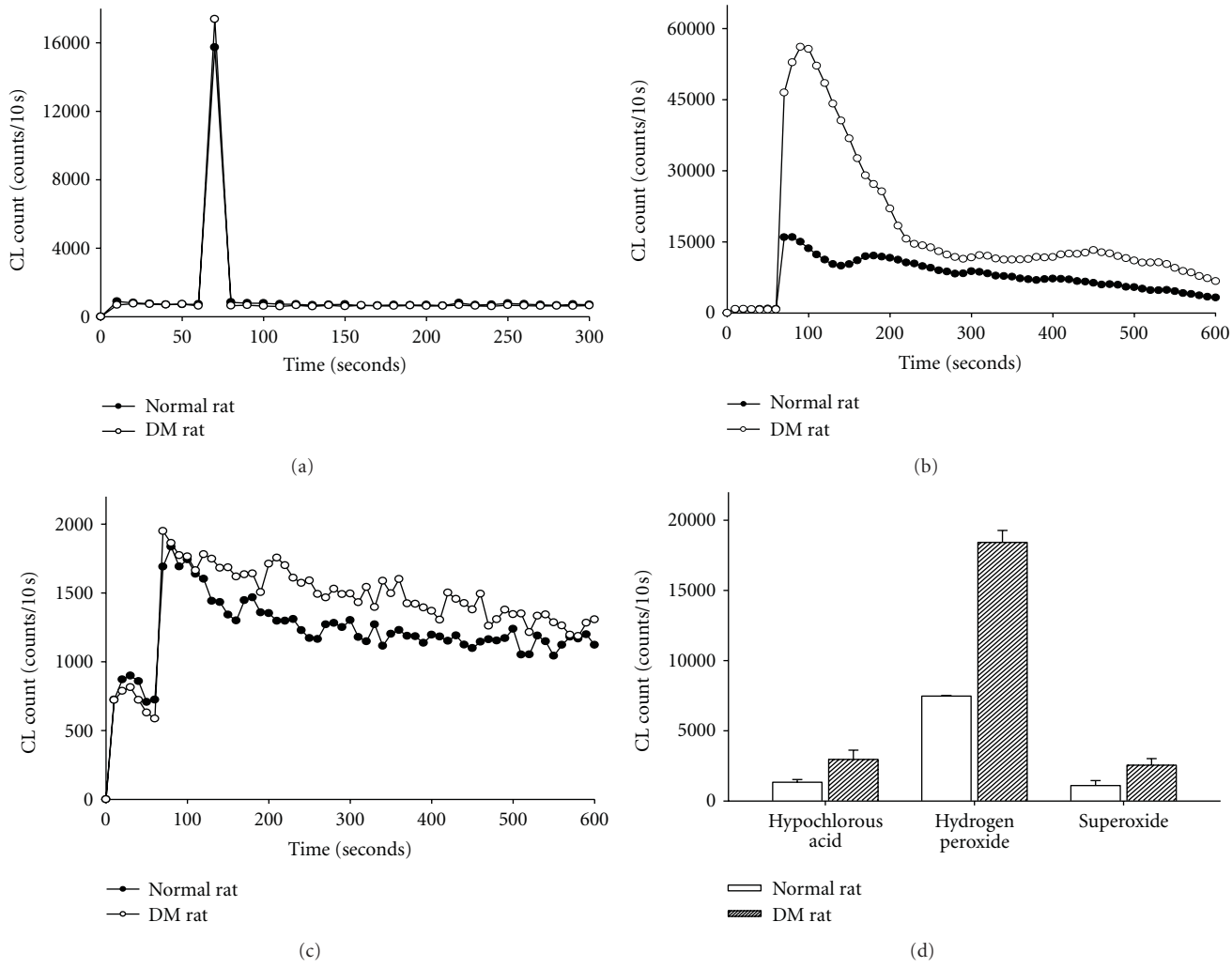

Figure 3: Representative data of HOCl, H_2O_2, and O_2^- contents are measured in the normal and diabetic rat skins. The level of HOCl (a), H_2O_2 (b), and O_2^- (c) counts is higher in the skin of diabetic rats than the normal rats. A summary data (d) shows that increased HOCl, H_2O_2, and O_2^- counts are found in diabetic rats when compared to the normal rats. Data are expressed as mean ± SEM in 5 rats each . $^*P < 0.05$ when compared to normal rats.

3.7. Hydroxyproline Estimation. Hydroxyproline is a major component of the protein collagen. Therefore, hydroxyproline content was used as an indicator to determine collagen content. As shown in Figure 6(f), hydroxyproline contents were significantly increased in the groups treated with antioxidant sol-gel (89.1 ± 2.3 μg/mg), antioxidant saline (78.2 ± 12.6 μg/mg), and Pluronic F127 sol group (60.5 ± 1.2 μg/mg) when compared with saline group (40.1 ± 3.1 μg/mg).

3.8. TUNEL Study. The apoptosis formation analyzed by TUNEL stain showed that a marked increase of apoptosis in the wound tissue of diabetic rats treated with topical saline 7 days, after injury. The topical application of antioxidant sol-gel or antioxidant saline significantly decreased the apoptosis production in the diabetic wounds (Figure 8). The potential of inhibiting apoptosis production was expressed in the order of antioxidant sol-gel > antioxidant saline > Pluronic F127 > saline (Figure 8(e)).

4. Discussion

The present study showed that the effect of *in vitro* drug release profiles indirectly indicated by the antioxidant activities demonstrated that the vitamin C from the Pluronic F127 was continuously released to depress H_2O_2, HOCl, and O_2^- amounts after 6 hours of air exposure at 37°C. The *in vivo* study further indicated that continuous release of vitamin C by using Pluronic F127 as a drug delivery vehicle exerted efficiently therapeutic potential on diabetic wound healing via its antioxidant and antiapoptotic effects. The antioxidant sol-gel is better than antioxidant saline in scavenging ROS, promoting collagen synthesis, epidermal and dermal maturation, and decreasing apoptosis production in the diabetic wound.

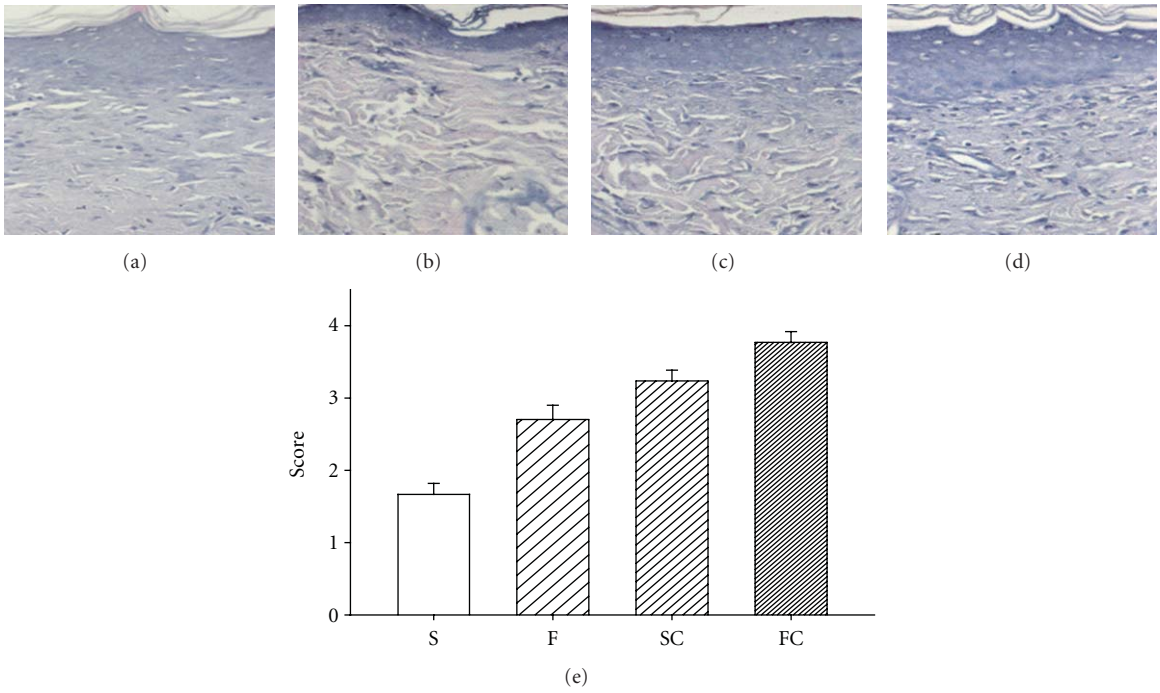

Figure 4: H & E stain in the saline control (a), Pluronic F127 (b), saline plus vitamin C (c), and Pluronic F127 plus vitamin C (d). Epidermal maturation was scored histologically from "no migration" (0) to "completed migration with keratinization" (4). The mean score of epidermal maturation is displayed in (e) . Significant epidermal maturation indicated by migration of keratinization was shown here in the groups of SC and FC when compared with the group of Saline 14 days after wounding (e). Data are expressed as mean ± SEM. *Four groups are significantly different when compared with Kruskal-Wallis test and posttest comparing all pairs of columns. S: saline control; F: Pluronic F127; SC: saline plus vitamin C; FC: Pluronic F127 plus vitamin C. Original magnifications taken at ×200.

Pluronics (also called Poloxamers) have been particularly interesting because this polymer shows a critical solution temperature (reverse sol-gel transition temperature) below the human physiological temperature and, thus, exists to a gel state in the body at 37°C. Yamaoka et al. [21] indicated that the copolymer films are biocompatible materials with controllable mechanical properties and biodegradability. In addition, Pluronic F127 caused relatively low inflammatory response and showed nontoxicity, and thus could be a good candidate material as a coatable wound dressing gel [22]. Hokett et al. [23] and Fowler et al. [24] had used Pluronics to ameliorate the wound-healing process in gingival and bony wounds, respectively. In the report of Khalil et al. [25] and also our study, normal rats treated with the Pluronic F127 alone showed results similar to the saline control animals without improving the wound-healing process. A 10% (w/w) Pluronic F127 has been added to the Jordanian traditional medicinal plants to modify the aqueous extract viscosity and to stabilize the oil dispersion. The applied Pluronic F127 continuously released the Jordanian traditional medicinal plants aqueous extract and significantly promoted the wound-healing process [25]. In our study, Pluronic F127 vehicle alone coating on wound did not show any inflammatory symptoms or toxicity and did not affect wound-healing process in the normal rats. This finding is consistent with a previous study [25]. As a drug delivery vehicle, we found that continuous vitamin C release from Pluronic F127 vehicle can partly sustain the scavenging ability against H_2O_2, HOCl, and O_2^- amount after 6 hours of air exposure.

Wound healing is a complex multifactorial process that results in the contraction and closure of the wound and restoration of a functional barrier. One of the leading causes of impaired wound healing is diabetes mellitus. In diabetic rats, a minor skin wound often leads to chronic, nonhealing ulcers and ultimately results in gangrene, even amputation. ROS and oxidative stress arise from inflammatory cells, which are strongly implicated in the pathogenesis of several diseases including chronic ulcers [26–28]. Rasik and Shukla [29] reported the decrease in antioxidants and the increase in oxidative stress delaying healing in excision cutaneous wounds in diabetic, aged, and immunocompromised animals. They further showed that skin levels of catalase, glutathione, vitamin C, and vitamin E in streptozotocin-induced diabetic rat were lower as compared to nondiabetics. In chronic wounds, fibroblast dysfunctions, such as increased apoptosis, premature senescence, senescence-like phenotype, or poor growth response in the absence of senescence markers may be due to excessive amounts of oxidative stress [4]. Our evidence in Figure 3 directly demonstrated that the skin levels of H_2O_2, HOCl, and O_2^- are significantly increased in the diabetic skin adjacent to the wounds when compared to the control skin of normal rats.

Several studies from rat dermal wound have shown that the treatment of antioxidants to depress ROS is beneficial

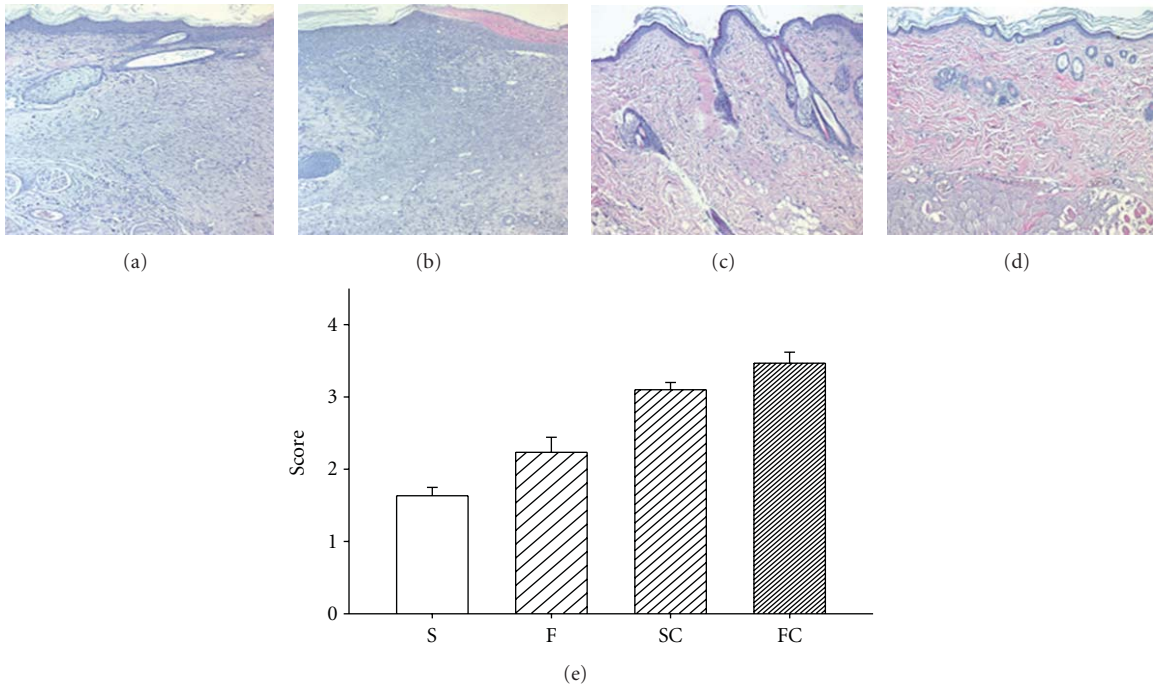

Figure 5: Effect of vitamin C on dermal maturation in diabetic rat wounds. Sections stained with H & E are displayed in the saline control (a), Pluronic F127 sol (b), saline plus vitamin C (c), and Pluronic F127 plus vitamin C (d). Histological evaluation of the 14-day wounds by H & E stain demonstrated enhanced healing characteristics including wound of proliferation, remodeling, and maturation in the antioxidant saline (c) or antioxidant sol-treated wound (d). Saline (a) or Pluronic 127 treatment (b) did not show any marked healing responses in the diabetic wounds. This advancement correlates with the fibroblast infiltration into the wounded area which was scored based on their maturity from reactive to normal. The mean score of dermal maturation is displayed in (e). The degree of dermal maturation is demonstrated in an order of FC > SC > F > S 14 days after wounding (e). Data are expressed as mean ± SEM. *Four groups are significantly different but not significant between saline and F127; vitamin C in saline and vitamin C in PF127. S: saline control; F: Pluronic F127; SC: saline plus vitamin C; FC: Pluronic F127 plus vitamin C. Original magnifications taken at ×100.

for wound healing. An improvement in the quality of wound healing has been attempted by slow delivery of antioxidants-like curcumin from collagen, which also acts as a supportive matrix for the regenerative tissue [30]. Biochemical parameters and histological analysis revealed that curcumin-incorporated collagen films increased wound reduction and enhanced cell proliferation and efficient free radical scavenging [30]. Another study [31] has shown that topical application of resveratrol accelerated wound contraction and closure associated with a more well-defined hyperproliferative epithelial region, higher cell density, enhanced deposition of connective tissue, and improved histological architecture. Study bySilvetti [10] has presented a safe and effective method of improving repair and controlling infection of wounds by daily topical application of a balanced solution of salts, amino acids, a high-molecular weight, D-glucose polysaccharide, and vitamin C. In skin, vitamin C has growth factor-like properties and is an important regulator for collagen synthesis of the extracellular matrix [8]. Vitamin C appears capable of overcoming the reduced proliferative capacity of elderly dermal fibroblasts, as well as increasing collagen synthesis in elderly cells by similar degrees as in newborn cells even though basal levels of collagen synthesis are age dependent [8]. By correcting a defect (underhydroxylation) in a posttranslational event and by increasing collagen production, dietary ascorbic acid improved the collagen status of a diabetes-perturbed connective tissue [5]. Our data from normal rats, with or without antioxidant showed no difference in wound closure rate. However, wound closure rates increased significantly in antioxidant sol-gel and antioxidant saline groups of the diabetic rats, indicating that increased vitamin C supplement improved the wound-healing process. We assumed that this therapeutic effect of vitamin C on diabetic wounds may be due to its inhibition of excess ROS production. This hypothesis was further supported by our finding that a significant increase of ROS including H_2O_2, HOCl, and O_2^- was found in the diabetic skins.

ROS can affect proliferative and cell survival signaling to alter apoptotic pathways in the skin diseases. Excess production of ROS in the skin can foster the development of dermatological diseases. One approach to prevent or treat these ROS-mediated disorders is based on the administration of various antioxidants in an effort to restore homeostasis. Many antioxidants have shown substantive efficacy in cell culture systems and in animal models of oxidant injury. On the other hand, increased apoptosis formation delayed wound healing [32]. Diabetes caused more than twofold

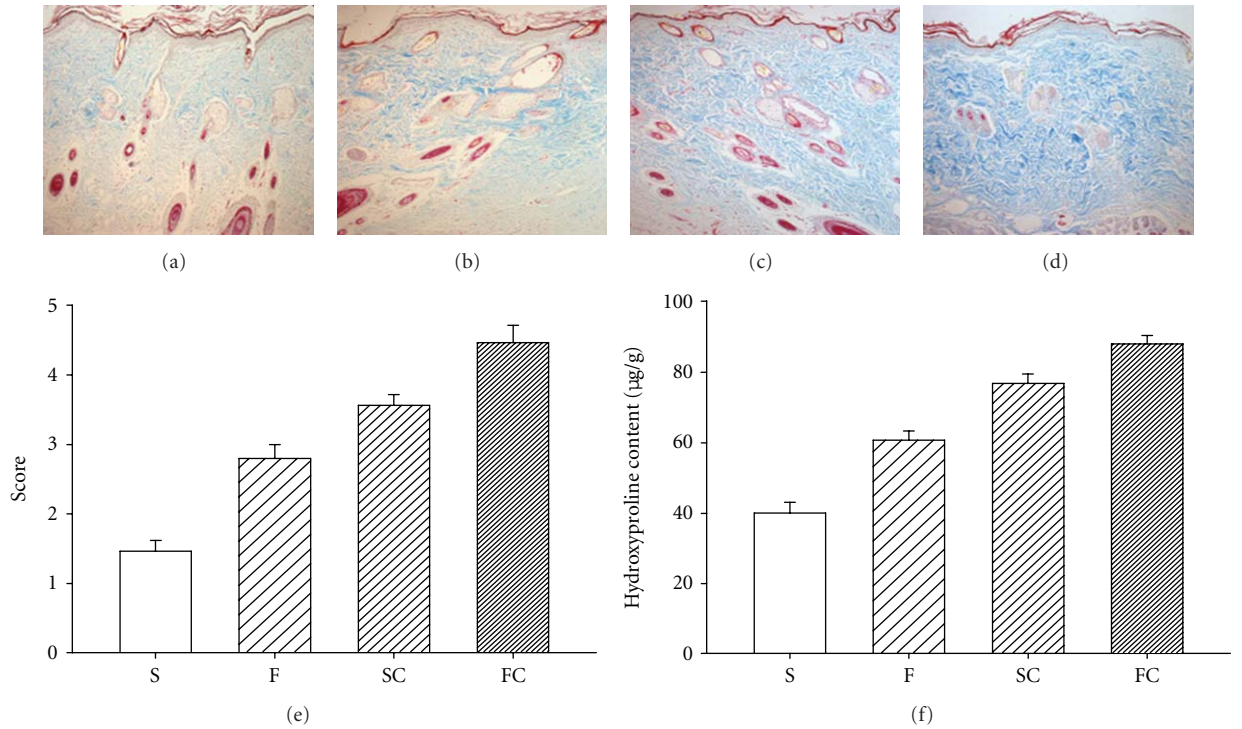

Figure 6: Effect of antioxidant sol-gel on collagen expression and collagen content at 14th day. Masson's trichrome staining of collagen in the saline control (a), Pluronic F127 sol (b), saline plus vitamin C (c), and Pluronic F127 plus vitamin C (d). The mean score of blue stain is displayed in (e). Four groups are significantly different when compared with Kruskal-Wallis test and posttest comparing all pairs of columns. Significant blue stain was demonstrated in an order of FC > SC > F > S. Increased hydroxyproline content was consistently increased in an order of FC > SC > F > S 14 days after wounding (f). Data are expressed as mean ± SEM. $^*P < 0.05$ when compared to saline group. S: saline control; F: Pluronic F127; SC: saline plus vitamin C; FC: Pluronic F127 plus vitamin C. Original magnifications taken at ×200.

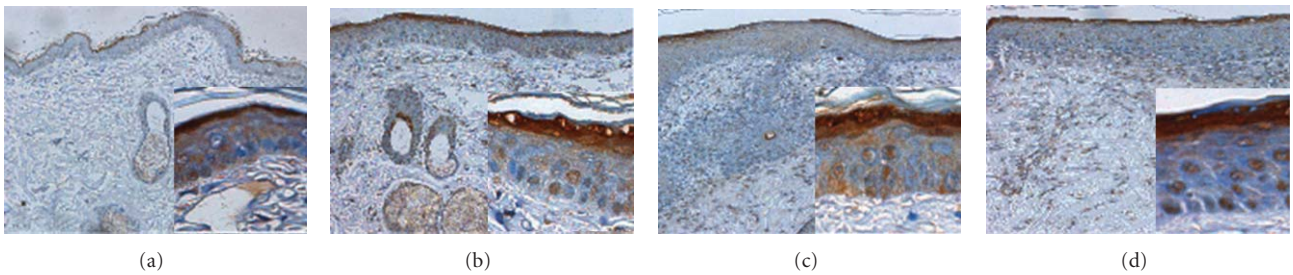

Figure 7: Immunohistochemical evidence of keratinization by loricrin at 14th day. Wounds treated with saline control (a), Pluronic F127 sol (b), saline plus vitamin C (c), and Pluronic F127 plus vitamin C (d) were demonstrated. Original magnifications taken at ×100 and ×200 as inset. Immunohistochemical staining by antiloricrin (epidermal differentiation marker) antibodies showed that loricrin was highly expressed in the upper granular cell layer, especially in the regenerated epidermis of Pluronic F127 plus vitamin C or saline plus vitamin C groups.

induction of 71 genes that directly or indirectly regulate apoptosis and significantly enhanced several caspases activity, and inhibiting apoptosis significantly improved several parameters of healing, including fibroblast density, enhanced mRNA levels of collagen I and III, and increased matrix formation [33]. This means that diabetes-enhanced apoptosis represents an important mechanism through which healing is impaired partly by diabetes-increased expression of proapoptotic genes and caspase activity. Fadini et al. [32] demonstrated that diabetes induced p66Shc expression and activation, subsequently produced H_2O_2 and delayed wound healing in mice with reduced granulation tissue thickness and vascularity, and increased apoptosis. They further found that the use of p66Shc knockout mice associated with a less enhancement of oxidative stress improved wound healing in diabetic animals. Therefore, a reduction of oxidative stress may reduce apoptosis formation and improve the impairment of wound-healing

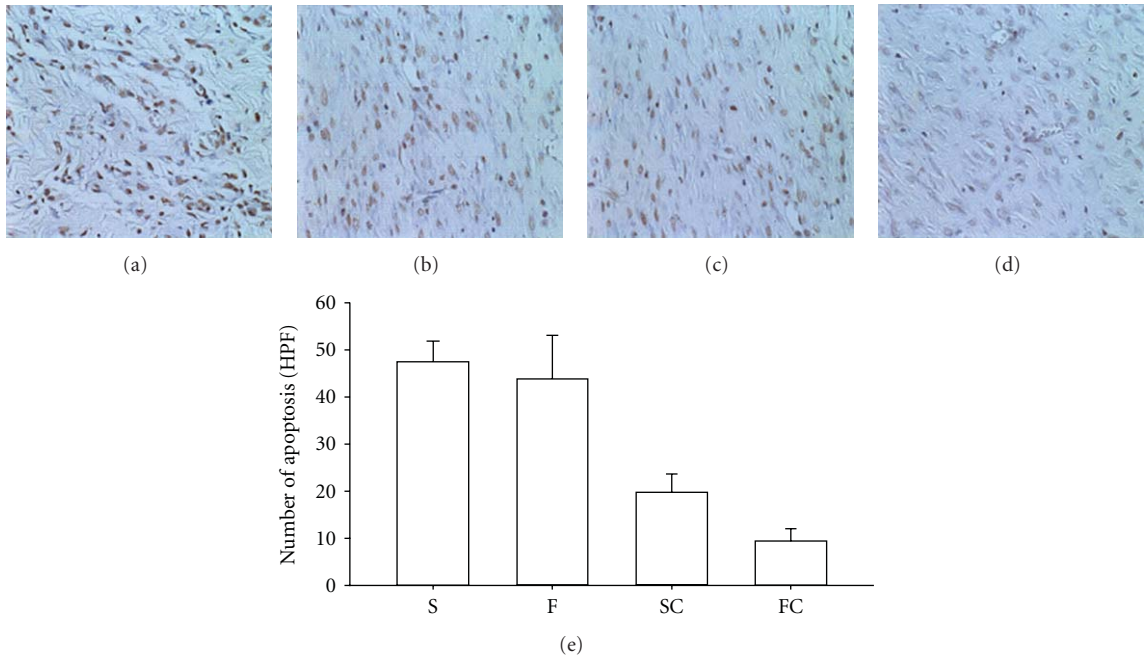

Figure 8: Effect of antioxidant sol-gel on apoptosis production of the healing skin in diabetic rats at 7th day. Apoptosis analyzed by TUNEL stain (brown color in the nucleus) was shown in the saline control (a), Pluronic F127 sol (b), saline plus vitamin C (c), and Pluronic F127 plus vitamin C (d). The data were expressed as the number of apoptosis (high power field) in each section (400x) is displayed in (e). The percentage of apoptosis appearance in the wounds is demonstrated in an order of FC > SC > F > S 14 days after wounding (e). Data are expressed as mean ± SEM. $^*P < 0.05$ when compared to saline group. S: saline control; F: Pluronic F127; SC: saline plus vitamin C; FC: Pluronic F127 plus vitamin C. Original magnifications taken at ×200.

process in diabetics. Based on our data, the antioxidant sol showed a strong scavenging activity for ROS and depressed diabetes-evoked apoptosis formation. This antioxidant sol clearly hastened the wound-healing process with the increased collagen synthesis, enhanced epidermal and dermal maturation, and the decreased apoptosis formation.

5. Conclusions

We demonstrate that vitamin C incorporated into Pluronic F127 exerts continuous effects of antioxidant and anti-apoptotic activities, which enhance epidermal and dermal maturation and collagen synthesis in the diabetic skins. The antioxidant sol-gel can decrease potentially harmful factors such as ROS production and apoptosis cell death present in chronic wound of the diabetic rats. These characteristics suggest a beneficial role for this preparation in helping rebalance the chronic wound environment and therefore promote healing.

Conflict of Interests

The authors report no conflict of interests.

Acknowledgments

This work was supported by Grants from the National Science Council of Taiwan (NSC 98-2320-B-002-043-MY3, 96-2221-E-002-256-MY3, and 98-2320-B002-016-MY3). The authors also want to thank Dr. Gunnar Johansson for critical reading of this paper and National Taiwan University Hospital the Third Core Lab for providing lab facilities.

References

[1] A. J. Singer and R. A. F. Clark, "Cutaneous wound healing," *The New England Journal of Medicine*, vol. 341, no. 10, pp. 738–746, 1999.

[2] J. D. Luo, Y. Y. Wang, W. L. Fu, J. Wu, and A. F. Chen, "Gene therapy of endothelial nitric oxide synthase and manganese superoxide dismutase restores delayed wound healing in type 1 diabetic mice," *Circulation*, vol. 110, no. 16, pp. 2484–2493, 2004.

[3] C. J. Schorah, C. Downing, A. Piripitsi et al., "Total vitamin C, ascorbic acid, and dehydroascorbic acid concentrations in plasma of critically ill patients," *American Journal of Clinical Nutrition*, vol. 63, no. 5, pp. 760–765, 1996.

[4] R. A. F. Clark, "Oxidative stress and "senescent" fibroblasts in non-healing wounds as potential therapeutic targets," *Journal of Investigative Dermatology*, vol. 128, no. 10, pp. 2361–2364, 2008.

[5] M. Schneir, N. Ramamurthy, and L. Golub, "Dietary ascorbic acid normalizes diabetes-induced underhydroxylation of nascent type I collagen molecules," *Collagen and Related Research*, vol. 5, no. 5, pp. 415–422, 1985.

[6] S. Briganti and M. Picardo, "Antioxidant activity, lipid peroxidation and skin diseases. What's new," *Journal of the European Academy of Dermatology and Venereology*, vol. 17, no. 6, pp. 663–669, 2003.

[7] G. Riccioni, T. Bucciarelli, B. Mancini, I. C. Di, V. Capra, and N. D'Orazio, "The role of the antioxidant vitamin supplementation in the prevention of cardiovascular diseases," *Expert Opinion on Investigational Drugs*, vol. 16, no. 1, pp. 25–32, 2007.

[8] C. L. Phillips, S. B. Combs, and S. R. Pinnell, "Effects of ascorbic acid on proliferation and collagen synthesis in relation to the donor age of human dermal fibroblasts," *Journal of Investigative Dermatology*, vol. 103, no. 2, pp. 228–232, 1994.

[9] D. R. Bickers and M. Athar, "Oxidative stress in the pathogenesis of skin disease," *Journal of Investigative Dermatology*, vol. 126, no. 12, pp. 2565–2575, 2006.

[10] A. N. Silvetti, "An effective method of treating long-enduring wounds and ulcers by topical applications of solutions of nutrients," *Journal of Dermatologic Surgery and Oncology*, vol. 7, no. 6, pp. 501–508, 1981.

[11] N. Collins, "Adding vitamin C to the wound management mix," *Advances in Skin & Wound Care*, vol. 17, no. 3, pp. 109–112, 2004.

[12] M. Bercea, R. N. Darie, L. E. Nita, and S. Morariu, "Temperature responsive gels based on Pluronic F127 and poly(vinyl alcohol)," *Industrial and Engineering Chemistry Research*, vol. 50, no. 7, pp. 4199–4206, 2011.

[13] I. R. Schmolka, "Artificial skin. I. Preparation and properties of pluronic F-127 gels for treatment of burns.," *Journal of Biomedical Materials Research*, vol. 6, no. 6, pp. 571–582, 1972.

[14] L. E. Bromberg and E. S. Ron, "Temperature-responsive gels and thermogelling polymer matrices for protein and peptide delivery," *Advanced Drug Delivery Reviews*, vol. 31, no. 3, pp. 197–221, 1998.

[15] P. K. Sharma, M. J. Reilly, D. N. Jones, P. M. Robinson, and S. R. Bhatia, "The effect of pharmaceuticals on the nanoscale structure of PEO-PPO-PEO micelles," *Colloids and Surfaces B*, vol. 61, no. 1, pp. 53–60, 2008.

[16] J. J. Chang, P. J. Lin, Y. H. Lee, M. C. Yang, and C. T. Chien, "The effect of covalent immobilization of sialic acid on the removal of lipopolysaccharide and reactive oxygen species for polyethylene terephthalate," *Polymer for Advanced Technologies*, vol. 22, pp. 1872–1878, 2011.

[17] L. Baoyong, Z. Jian, C. Denglong, and L. Min, "Evaluation of a new type of wound dressing made from recombinant spider silk protein using rat models," *Burns*, vol. 36, no. 6, pp. 891–896, 2010.

[18] C. C. Yates, D. Whaley, R. Babu et al., "The effect of multifunctional polymer-based gels on wound healing in full thickness bacteria-contaminated mouse skin wound models," *Biomaterials*, vol. 28, no. 27, pp. 3977–3986, 2007.

[19] Z. Nemes and P. M. Steinert, "Bricks and mortar of the epidermal barrier," *Experimental and Molecular Medicine*, vol. 31, no. 1, pp. 5–19, 1999.

[20] E. Candi, R. Schmidt, and G. Melino, "The cornified envelope: a model of cell death in the skin," *Nature Reviews Molecular Cell Biology*, vol. 6, no. 4, pp. 328–340, 2005.

[21] T. Yamaoka, Y. Takahashi, T. Fujisato et al., "Novel adhesion prevention membrane based on a bioresorbable copoly(ester-ether) comprised of poly-L-lactide and Pluronic: *in vitro* and *in vivo* evaluations," *Journal of Biomedical Materials Research*, vol. 54, pp. 470–479, 2001.

[22] S. H. Oh, J. K. Kim, K. S. Song et al., "Prevention of post-surgical tissue adhesion by anti-inflammatory drug-loaded pluronic mixtures with sol-gel transition behavior," *Journal of Biomedical Materials Research A*, vol. 72, pp. 306–316, 2005.

[23] S. D. Hokett, M. F. Cuenin, R. B. O'Neal et al., "Pluronic polyol effects on human gingival fibroblast attachment and growth," *Journal of Periodontology*, vol. 71, pp. 803–809, 2000.

[24] E. B. Fowler, M. F. Cuenin, S. D. Hokett et al., "Evaluation of pluronic polyols as carriers for grafting materials: study in rat calvaria defects," *Journal of Periodontology*, vol. 73, no. 2, pp. 191–197, 2002.

[25] E. A. Khalil, F. U. Afifi, and M. Al-Hussaini, "Evaluation of the wound healing effect of some Jordanian traditional medicinal plants formulated in Pluronic F127 using mice (Mus musculus)," *Journal of Ethnopharmacology*, vol. 109, no. 1, pp. 104–112, 2007.

[26] S. A. Abd-El-Aleem, M. W. J. Ferguson, I. Appleton et al., "Expression of nitric oxide synthase isoforms and arginase in normal human skin and chronic venous leg ulcers," *Journal of Pathology*, vol. 191, no. 4, pp. 434–442, 2000.

[27] M. Rojkind, J. A. Domínguez-Rosales, N. Nieto, and P. Greenwel, "Role of hydrogen peroxide and oxidative stress in healing responses," *Cellular and Molecular Life Sciences*, vol. 59, no. 11, pp. 1872–1891, 2002.

[28] R. Moseley, J. R. Hilton, R. J. Waddington, K. G. Harding, P. Stephens, and D. W. Thomas, "Comparison of oxidative stress biomarker profiles between acute and chronic wound environments," *Wound Repair and Regeneration*, vol. 12, no. 4, pp. 419–429, 2004.

[29] A. M. Rasik and A. Shukla, "Antioxidant status in delayed healing type of wounds," *International Journal of Experimental Pathology*, vol. 81, no. 4, pp. 257–263, 2000.

[30] D. Gopinath, M. R. Ahmed, K. Gomathi, K. Chitra, P. K. Sehgal, and R. Jayakumar, "Dermal wound healing processes with curcumin incorporated collagen films," *Biomaterials*, vol. 25, no. 10, pp. 1911–1917, 2004.

[31] S. Khanna, S. Roy, D. Bagchi, M. Bagchi, and C. K. Sen, "Upregulation of oxidant-induced VEGF expression in cultured keratinocytes by a grape seed proanthocyanidin extract," *Free Radical Biology and Medicine*, vol. 31, no. 1, pp. 38–42, 2001.

[32] G. P. Fadini, M. Albiero, L. Menegazzo et al., "The redox enzyme p66Shc contributes to diabetes and ischemia-induced delay in cutaneous wound healing," *Diabetes*, vol. 59, no. 9, pp. 2306–2314, 2010.

[33] H. A. Al-Mashat, S. Kandru, R. Liu, Y. Behl, T. Desta, and D. T. Graves, "Diabetes enhances mRNA levels of proapoptotic genes and caspase activity, which contribute to impaired healing," *Diabetes*, vol. 55, no. 2, pp. 487–495, 2006.

Hindawi Publishing Corporation
Experimental Diabetes Research
Volume 2012, Article ID 128694, 9 pages
doi:10.1155/2012/128694

Research Article

Decreased Skin-Mediated Detoxification Contributes to Oxidative Stress and Insulin Resistance

Xing-Xing Liu,[1] Chang-Bin Sun,[2] Ting-Tong Yang,[3] Da Li,[4] Chun-Yan Li,[1] Yan-Jie Tian,[1] Ming Guo,[5] Yu Cao,[4] and Shi-Sheng Zhou[1]

[1] *Department of Physiology, Medical College, Dalian University, Dalian 116622, China*
[2] *Department of Histology and Embryology, Medical College, Dalian University, Dalian 116622, China*
[3] *Department of Pathology, Xinxiang Medical College, Xinxiang 453003, China*
[4] *Department of Physiology, China Medical University, Shenyang 110001, China*
[5] *College of Environmental and Chemical Engineering, Dalian University, Dalian 116622, China*

Correspondence should be addressed to Shi-Sheng Zhou, zhouss@ymail.com

Received 21 February 2012; Revised 28 May 2012; Accepted 12 June 2012

Academic Editor: Pietro Galassetti

The skin, the body's largest organ, plays an important role in the biotransformation/detoxification and elimination of xenobiotics and endogenous toxic substances, but its role in oxidative stress and insulin resistance is unclear. We investigated the relationship between skin detoxification and oxidative stress/insulin resistance by examining burn-induced changes in nicotinamide degradation. Rats were divided into four groups: sham-operated, sham-nicotinamide, burn, and burn-nicotinamide. Rats received an intraperitoneal glucose injection (2 g/kg) with (sham-nicotinamide and burn-nicotinamide groups) or without (sham-operated and burn groups) coadministration of nicotinamide (100 mg/kg). The results showed that the mRNA of all detoxification-related enzymes tested was detected in sham-operated skin but not in burned skin. The clearance of nicotinamide and N^1-methylnicotinamide in burned rats was significantly decreased compared with that in sham-operated rats. After glucose loading, burn group showed significantly higher plasma insulin levels with a lower muscle glycogen level than that of sham-operated and sham-nicotinamide groups, although there were no significant differences in blood glucose levels over time between groups. More profound changes in plasma H_2O_2 and insulin levels were observed in burn-nicotinamide group. It may be concluded that decreased skin detoxification may increase the risk for oxidative stress and insulin resistance.

1. Introduction

Oxidative stress is a condition of oxidant/antioxidant imbalance in which the net amount of reactive oxygen species (ROS) exceeds the antioxidant capacity of the body [1, 2]. Increasing evidence suggests that oxidative stress might play a causal role in insulin resistance (IR) which is characterized by hyperinsulinemia [1–3]. One of the major sources of ROS is xenobiotics, which are exogenous chemicals such as heavy metals, drugs, insecticides, and food additives [3–5]. Another major source of ROS is endogenous toxic and bioactive compounds, such as catecholamines, the major stress hormones inactivated by catechol-*O*-methyltransferase (COMT) and monoamine oxidase (MAO) [6]. Thus, the efficiency of detoxification and elimination of xenobiotics and endogenous toxic compounds should be a crucial factor in oxidative stress and IR.

Xenobiotics are detoxified by xenobiotic/drug-metabolizing enzymes [7–9]. Thus, it is conceivable that any tissues/organs that are involved in xenobiotics detoxification/excretion and ROS clearance may play a role in oxidative stress and IR. The skin, which is the largest organ of the body, can degrade, inactivate, and eliminate numerous xenobiotics and endogenous toxic compounds through its xenobiotic/drug-metabolizing enzymes [7–9], ROS-scavenging system [10], and sweat glands [11–14]. It has been found that severe burns, which induce permanent structural tissue damage, are associated with longlasting IR, endoplasmic reticulum stress response, hypermetabolism, and elevation of cortisol, catecholamines, and cytokines

(i.e., they still persist after burns have healed) [15–17]. Moreover, impaired cutaneous vasodilation and sweating are found in grafted skin [18]. These lines of evidence raise the possibility that a decrease in the skin functions might play a role in the development of oxidative stress and IR. To test this hypothesis, the present study investigated the relationship between the skin detoxification and ROS generation and IR by examining burn-induced changes in the degradation and clearance of nicotinamide which is the precursor of nicotinamide-adenine dinucleotide and is known to induce IR [19, 20].

2. Materials and Methods

2.1. Animal Experiment

2.1.1. Glucose and Nicotinamide Loading Test. Animal experiment was conducted in accordance with institutional guidelines. Male Sprague-Dawley rats (180–220 g) were fed a standard rat chow. A 40% total body surface area full-thickness injury was inflicted on the back skin of the rat; sham-operated rats were subjected to an identical procedure, except that they were immersed in 25°C water, as previously described [20]. Rats were randomized into four groups: sham-operated group ($n = 8$), sham-nicotinamide group ($n = 8$), burn group ($n = 9$), and burn-nicotinamide group ($n = 9$). At 48 hours after burn injury or sham treatment and 12 h after fasting, all rats in the four groups received intraperitoneal injection of glucose (2 g/kg body weight) with (sham-nicotinamide group and burn-nicotinamide group) or without (sham-operated group and burn group) coinjection of nicotinamide (Sigma, St. Louis, MO, USA; 100 mg/kg body weight). Tail blood glucose level was monitored before and at 15, 30, and 60 min after glucose injection using a glucometer (OneTouch Ultra, LifeScan, Milpitas, CA, USA). At the same timepoints, samples of tail blood (200 μL) were collected for later determination of serum concentrations of insulin and hydrogen peroxide (H_2O_2). At the end of experiment (i.e., 1 h after glucose loading), blood sample was collected by eye bleed into EDTA tubes under urethane anesthesia (1.5 g/kg, ip); samples of liver, muscle (rectus femoris, biceps brachii, latissimus dorsi, and gastrocnemius), and back skin (in burned or sham-operated areas) were then harvested and stored in liquid nitrogen for later analysis. Plasma was separated by centrifugation (1500 g, 10 min) and stored at −80°C until assay.

2.1.2. Reverse Transcription Polymerase Chain Reaction (RT-PCR). Total RNA of rat back skin and muscle tissues (rectus femoris, biceps brachii, and latissimus dorsi) was extracted using Trizol (Invitrogen, Carlsbad, CA, USA) according to the manufacturer's protocol. The mRNA of nicotinamide *N*-methyltransferase (NNMT), aldehyde oxidase (AOX1), COMT, MAO (monoamine oxidase A), superoxide dismutase 2, glutathione peroxidase 1, catalase (CAT), peroxiredoxin 1 (PRDX1), and neutrophil cytosolic factor 1 (p47-phox) was detected by RT-PCR. Extracted RNA was reverse-transcripted in a 20 μL reaction with both oligo (dT) and random primers using PrimeScript RT Master Mix (Takara, Shiga, Japan). PCR amplification was performed in a Techne TC-512 gradient thermal cycler (Progene, Techne Ltd., Cambridge, UK), using specific primers listed in Table 1. PCR reaction conditions were as follows: 95°C for 10 min; 40 cycles of 95°C for 30 s, 60°C for 30 s, and 72°C for 45 s; followed by an extension reaction at 72°C for 10 min. The reaction products were analyzed by agarose gel electrophoresis and visualized by UV light after staining with ethidium bromide.

2.1.3. Assays of Insulin, H_2O_2, and Glycogen. Serum insulin levels were determined with ELISA (Rat/Mouse Insulin Kit; Millipore, St. Charles, MO, USA). Serum H_2O_2 concentrations were measured using an H_2O_2 Assay Kit (Beyotime Biotechnology, Jiangsu, China). Hepatic and muscle (gastrocnemius) glycogen contents were determined with Glycogen Assay Kits (Nanjing Jiancheng Bioengineering Institute, Nanjing, China). ELISA plates were read by microplate reader (Bio-Rad, Hercules, CA, USA).

2.1.4. Determination of Nicotinamide and N^1-Methylnicotinamide. High-performance liquid chromatography (HPLC) was used to measure plasma nicotinamide and N^1-methylnicotinamide, as previously described [20]. HPLC system consisted of an LC-9A pump (Shimadzu, Kyoto, Japan), a Rheodyne 7725i sample injector with a 20-μL sample loop (Rheodyne LLC, Rohnert Park, CA, USA), a Hypersil ODS C18 column (Thermo, Bellefonte, PA, USA) with a Waters 470 fluorescence detector (Milford, MA, USA). All chromatography was performed at room temperature.

2.2. Human Experiments.

All patients participating in the study signed an informed consent form before the liver and skin samples for the immunohistochemistry analysis. Human normal liver and skin samples were donated by individuals who underwent resection of liver cancer and breast cancer, respectively. This study has been approved by the Ethics Committee of Dalian University.

2.2.1. Immunohistochemistry. Histological examination of the resected livers and skin ensured the use of healthy tissue. Samples of liver and skin were plunged directly into liquid nitrogen and subsequently stored at −80°C until assay. The location of AOX1 in human skin was determined by immunohistochemical staining. Briefly, four-micrometer sections were deparaffinized in xylene and rehydrated through graded ethanol. After microwave antigen retrieval, immunoreactivity was detected by streptavidin-biotin-peroxidase complex method (Fuzhou Maixin, Fuzhou, China) with color development using 3, 3′-diaminobenzidine. The primary antibody was mouse anti-AOX1 (1 : 300; BD Biosciences, CA, USA). Substituting phosphate-buffered saline (PBS) for the primary antibody was used as the negative control. Sections were counterstained with Mayer's hematoxylin for 30 s. Sections of normal hepatic tissue were used as a positive control.

Table 1: Primer oligonucleotide sequences of selected genes.

Molecule (gene)		Primers
NNMT	Forward	5′-CAGAGCTGAGACACGATGGA
	Reverse	5′-GCAGGCAGAGAGAAGCTGAT
AOX1	Forward	5′-GTCCAGAAGCTTCCAGA
	Reverse	5′-GATGTTCACTGAGACCAAGA
COMT	Forward	5′-CTACTCAGCAGTGCGAATGG
	Reverse	5′-AAGTGTGTCTGGAAGGTAGCG
MAO	Forward	5′-GTGGCTCTTCTCTGCTTTGT
	Reverse	5′-AGTGCCAAGGGTAGTGTGTATCA
SOD	Forward	5′-CTCCCTGACCTGCCTTACGACT
	Reverse	5′-AAGCGACCTTGCTCCTTATTG
GPX1	Forward	5′-TCCACCGTGTATGCCTTCTCC
	Reverse	5′-CCTGCTGTATCTGCGCACTGGA
CAT	Forward	5′-GAGGCAGTGTACTGCAAGTTCC
	Reverse	5′-GGGACAGTTCACAGGTATCTGC
PRDX1	Forward	5′-GTGGATTCTCACTTCTGTCATCT
	Reverse	5′-GGCTTATCTGGAATCACACCACG
p47-phox	Forward	5′-AGCTCCCAGGTGGTATGATG
	Reverse	5′-TGTCAAGGGGCTCCAAAT

2.2.2. Western Blotting. Western blotting analysis of NNMT and AOX1 was performed according to standard protocols. Briefly, 30 μg human liver or skin protein was separated by 12% (for NNMT) and 8% (for AOX1) SDS polyacrylamide gels, respectively, and transferred to polyvinyl difluoride membranes (Millipore, MA, USA). The membranes were blocked in TBS containing 0.1% Tween-20 and 5% nonfat dry milk for 60 min at room temperature and incubated with antibody to NNMT (1 : 1000; Santa Cruz Biotechnology, CA, USA) and AOX1 (1 : 600; BD Biosciences, CA, USA) overnight at 4°C. Then, the membranes were washed by PBS-Tween followed by 1 h incubation at room temperature with horseradish peroxidase-conjugated secondary antibody (1 : 5000; Santa Cruz Biotechnology, CA, USA) and detected using the enhanced chemiluminescence (Amersham Life Science, NJ, USA). Human hepatic tissues were used as a positive control for the two antibodies.

2.3. Statistical Analysis. The data are presented as means ± SEM. Statistical differences in the data were evaluated by Student's t-test or one-way ANOVA as appropriate and were considered significant at $P < 0.05$.

3. Results

3.1. Burn-Induced Changes in Gene Expression in Rat Skin. We first compared the gene expression of xenobiotic/drug-metabolizing enzymes (including NNMT, AOX1, COMT, and MAO), ROS-scavenging enzymes (including SOD, GPX1, CAT, and PRDX1), and p47-phox, a component of the NADPH oxidase complex, between sham-operated rat skin and burned rat skin. The RT-PCR results showed that all of the enzymes tested were expressed in sham-operated rat skin, but there was no detectable expression of the enzymes in burned skin (Figure 1). These results suggest that full-thickness burn may lead to loss of the detoxification and antioxidant functions of the skin.

3.2. Burn-Induced Changes in the Degradation and Clearance of Nicotinamide. The observations that rat skin expresses nicotinamide-degrading enzymes suggest that the skin may play a role in nicotinamide clearance. Therefore, we investigated the effect of burn on the levels of plasma nicotinamide and N^1-methylnicotinamide, the toxic-methylated metabolite of nicotinamide [20]. Sham-nicotinamide group and burn-nicotinamide group showed significantly higher plasma nicotinamide levels compared with the other two groups, and the level of plasma nicotinamide in burn-nicotinamide group was significantly higher than that of sham-nicotinamide group (Figure 2(a)). These results suggest that the tolerance of burned rats to nicotinamide is decreased. Although there was no significant difference in plasma nicotinamide levels between sham-operated group and burn group (Figure 2(a)), the plasma N^1-methylnicotinamide level in burn group was much higher than that of sham-operated group (Figure 2(b)). Burn-nicotinamide group showed a significantly higher plasma level of N^1-methylnicotinamide than other groups (Figure 2(b)). These results indicate that burn decreases the clearance of N^1-methylnicotinamide.

3.3. Burn Enhances the H_2O_2-Generating and IR-Inducing Effects of Nicotinamide. Nicotinamide is known to induce oxidative stress, IR and glucose intolerance [19–21]. We therefore, examined the responses of rats of different groups to glucose load.

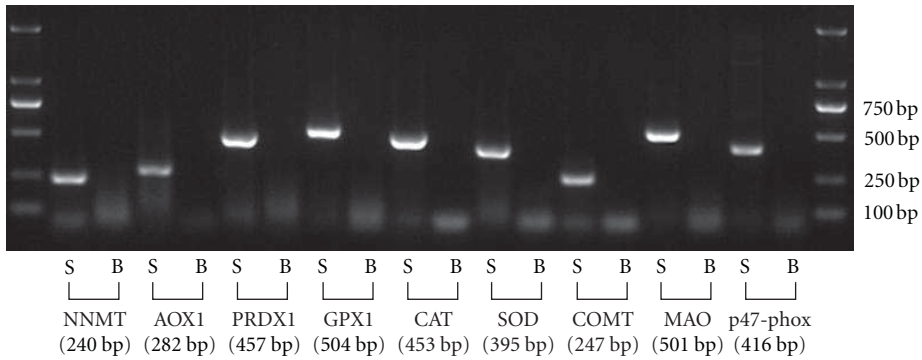

Figure 1: RT-PCR analysis of mRNA expression of xenobiotic/drug- and ROS-metabolizing enzymes in rat skin. S: sham-operated skin. B: burned skin. The data shown are representative of three separate experiments.

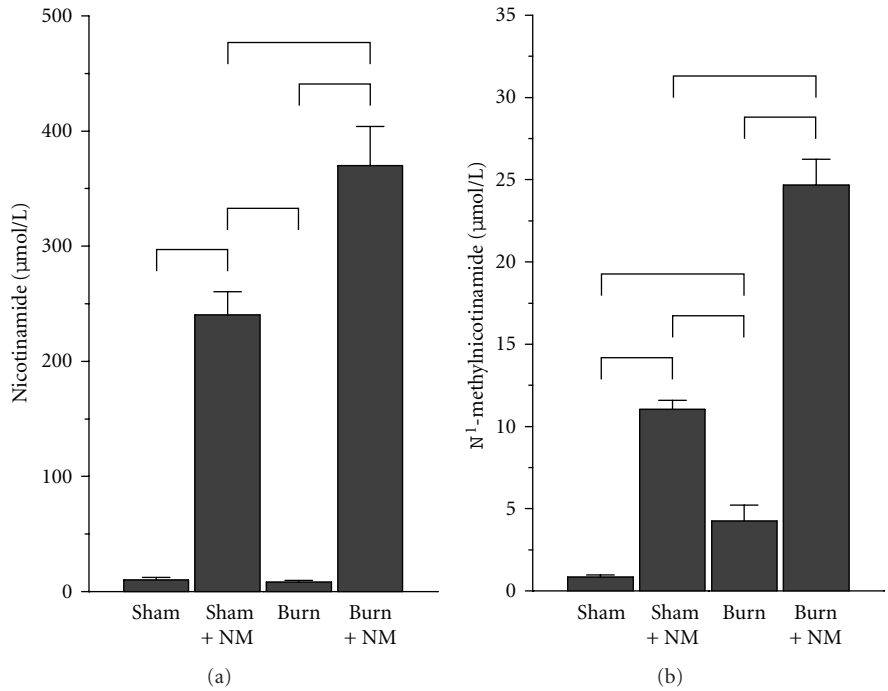

Figure 2: Plasma concentrations of nicotinamide and N^1-methylnicotinamide in different rat groups. Sham: sham-operated group; Sham + NM: sham-nicotinamide group; Burn: burn group; Burn + NM: burn-nicotinamide group. $^*P < 0.01$. Bar graph indicates mean ± SEM.

The results showed that there were no significant differences in the baseline serum concentration of H_2O_2 (a major component of ROS) between the groups.

Glucose load induced a decline in the plasma H_2O_2 level in sham-operated group, while the other three groups showed an increasing trend. The increasing trend was more profound in burn-nicotinamide group than in sham-nicotinamide group and burn group (Figure 3(a)).

The plasma insulin levels showed increasing trends in all groups with a peak at 15 or 30 min after glucose loading. The changes in plasma insulin were more profound in burn-nicotinamide group and burn group (Figure 3(b)), whereas there were no significant differences in the changing trends in blood glucose levels between groups (Figure 3(c)). These results indicate that burn can induce IR, which can be further enhanced by nicotinamide load.

There were no significant differences in liver glycogen contents either between sham-operated group and sham-nicotinamide group or between burn group and burn-nicotinamide group. However, the two burn groups showed significantly lower liver glycogen contents than that of the two sham groups (Figure 4(a)). It seems that the liver glycogen synthesis is affected by burn, but not by nicotinamide load. In contrast, the muscle glycogen levels were affected by both burn and nicotinamide load (Figure 4(b)).

To explore the mechanism underlying these different responses of liver and skeletal muscle to nicotinamide load, we detected the expression of NNMT and AOX1

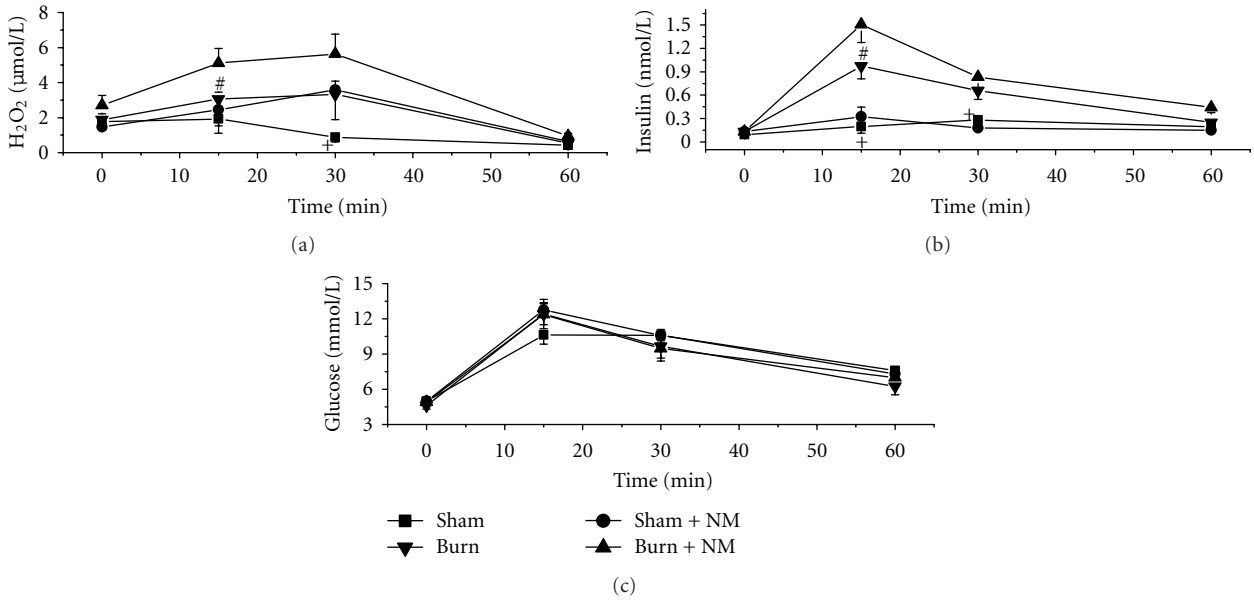

Figure 3: Serum H_2O_2 and insulin levels and blood glucose concentrations in different rat groups. Sham: sham-operated group; Sham + NM: sham-nicotinamide group; Burn: burn group; Burn + NM: burn-nicotinamide group. $^{*}P < 0.05$ and $^{**}P < 0.01$ versus sham-nicotinamide group, $^{\#}P < 0.05$ versus burn-nicotinamide group and $^{+}P < 0.01$ versus burn group at the same time point. Data were presented as means ± SEM.

in rat skeletal muscle. The RT-PCR results showed that rat skeletal muscle expressed NNMT, but did not express AOX1 (Figure 5). This suggests that the skeletal muscle could convert nicotinamide to N^1-methylnicotinamide, but could not detoxify N^1-methylnicotinamide.

3.4. Expression of NNMT and AOX1 in Human Skin. We then detected the expression of the NNMT and AOX1 in human skin. The results of western blotting showed that both NNMT and AOX1 were expressed in the human skin (Figure 6(a)). Immunohistochemical analysis showed that AOX1 was located in sweat glands (Figure 6(d)) and sebaceous glands (Figure 6(f)). These results suggest that human skin, like rat skin, may also be involved in the degradation of excessive nicotinamide.

4. Discussion

The main results of the present study are that: (1) the expression of xenobiotic/drug-metabolizing enzymes and ROS-scavenging enzymes was not detected in the full-thickness burned rat skin; (2) burn could decrease the clearance of excessive nicotinamide in rats, which was accompanied by increased H_2O_2 generation and abnormal response to glucose load, that is, elevated insulin levels and decreased glycogen levels in skeletal muscle; (3) rat skeletal muscle was found to express NNMT, but not AOX1; (4) the expression of NNMT and AOX1 was detected in human skin.

Excessive nicotinamide is primarily degraded to N^1-methylnicotinamide by NNMT and then further oxidized to pyridones by AOX1 [20]. Thus, it is expected that any tissues/organs that express NNMT and AOX1 may contribute to the body's total capacity to degrade excessive nicotinamide. The skin expresses NNMT, thus, burn-induced increase in the level of plasma nicotinamide might be due to a change in skin-mediated nicotinamide degradation. Plasma N^1-methylnicotinamide levels are determined not only by its generation from nicotinamide, but also by its conversion to pyridones. NNMT is widely expressed in human and rat tissues [22, 23], especially in skeletal muscle, while AOX1 is not expressed in the skeletal muscle (Figure 5). Skeletal muscle is the largest tissue in vertebrates. Obviously, the uninvolvement of skeletal muscle in N^1-methylnicotinamide degradation increases the importance of skin contribution in the conversion, which may account for nicotinamide load-induced more profound increase in plasma N^1-methylnicotinamide level in burned rats than in sham-operated rats.

Evidence suggests that IR may be the consequence of oxidative stress [1–3]. Indeed, our previous study has shown that coadministration of glucose and nicotinamide can induce IR due to excessive ROS generation caused by nicotinamide degradation in human subjects [21]. The data from the present study showed that decreased skin-mediated nicotinamide degradation could enhance the ROS generating and IR-inducing effects of nicotinamide. N^1-methylnicotinamide is a toxic intermediate of nicotinamide metabolism. The liver not only degrades nicotinamide to N^1-methylnicotinamide, but also further detoxifies N^1-methylnicotinamide to pyridones. Unlike the liver, the skeletal muscle can only convert nicotinamide to N^1-methylnicotinamide. This may thus lead to an accumulation of N^1-methylnicotinamide in muscle tissue and thus cause

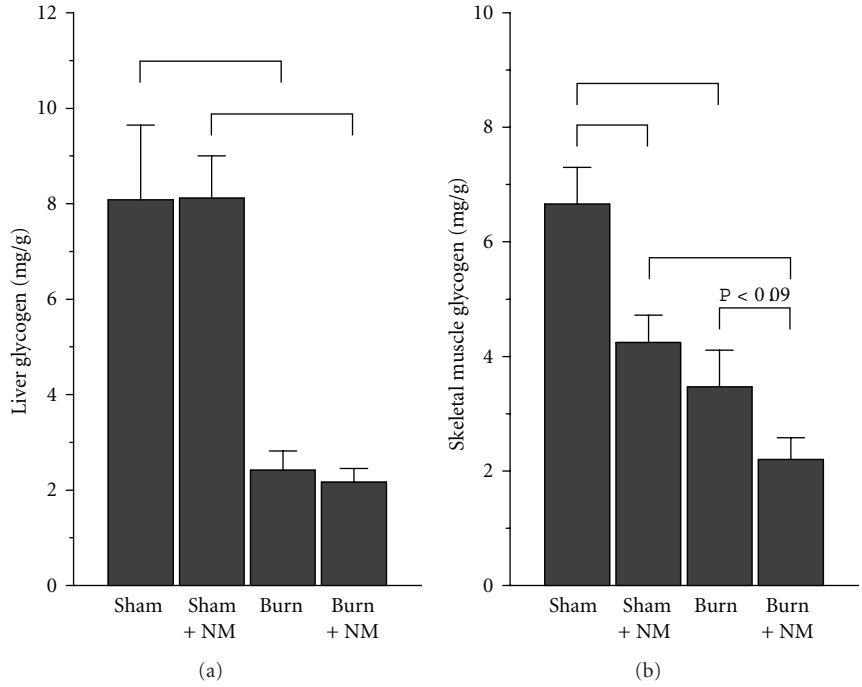

Figure 4: Glycogen contents of liver and skeletal muscle in different rat groups. Sham: sham-operated group; Sham + NM: sham-nicotinamide group; Burn: burn group; Burn + NM: burn-nicotinamide group. $^*P < 0.01$. Bar graph indicates mean ± SEM.

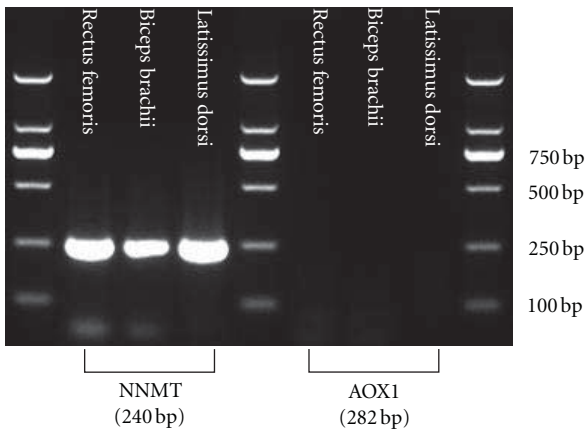

Figure 5: RT-PCR analysis of mRNA expression of NNMT and AOX1 in the muscle from sham-operated rat. The data shown are representative of three separate experiments.

a local toxic effect, which may explain why IR after nicotinamide load only occurs in the skeletal muscle, but not in the liver. The finding that burn alone decreased liver glycogen contents may involve other mechanisms that are beyond the scope of the present study.

It should be noted that besides nicotinamide-degrading enzymes, other xenobiotic/drug-metabolizing enzymes, such as cytochromes P450, flavin monooxygenases, MAO, COMT, glutathione-*S*-transferases, *N*-acetyltransferases, and sulfotransferases, are also expressed in the skin [7–9]. Numerous xenobiotics and endogenous bioactive/toxic substances are the substrates of skin xenobiotic/drug-metabolizing enzymes. The skin also expresses SOD, CAT, GPX1, and PRDX1, which can remove ROS, and thus help protect against oxidative damage [10, 24]. Moreover, human eccrine sweat glands, which total roughly one kidney, that is, 100 g, can excrete numerous xenobiotics, such as, metals and drugs [11, 13], and endogenous bioactive substances, such as, neurotransmitters, cytokines, and sterols [13, 25, 26]. Thus, it is conceivable that decreased skin function (e.g., due to burn injuries and cold ambient temperature) may increase the risk of an accumulation of toxic substances in the body and subsequent oxidative stress and IR.

Whether or not oxidative stress occurs not only depends on ROS production, but also on the body's total antioxidant capacity [1, 2]. The latter represents a sum of the antioxidant capacity of various organs. Each organ/tissue makes a distinctive contribution to the body's total antioxidant system. For example, the liver is mainly responsible for the biotransformation/detoxification of xenobiotics and endogenous toxic substances, while the kidney is mainly responsible for the elimination of toxic substances. Thus, a decrease in the functions of these organs is expected to increase the risk for oxidative stress and IR. Indeed, numerous studies have shown that patients with severe liver or kidney diseases are associated with oxidative stress and IR [27, 28]. The skin, like the liver and the kidneys, is one of the major contributors to the body's total antioxidant defense. Evidence has shown that (1) xenobiotics and endogenous toxic substances induce oxidative stress and IR [3]; (2) the skin is the largest organ involved in both the detoxification and excretion of xenobiotics and endogenous

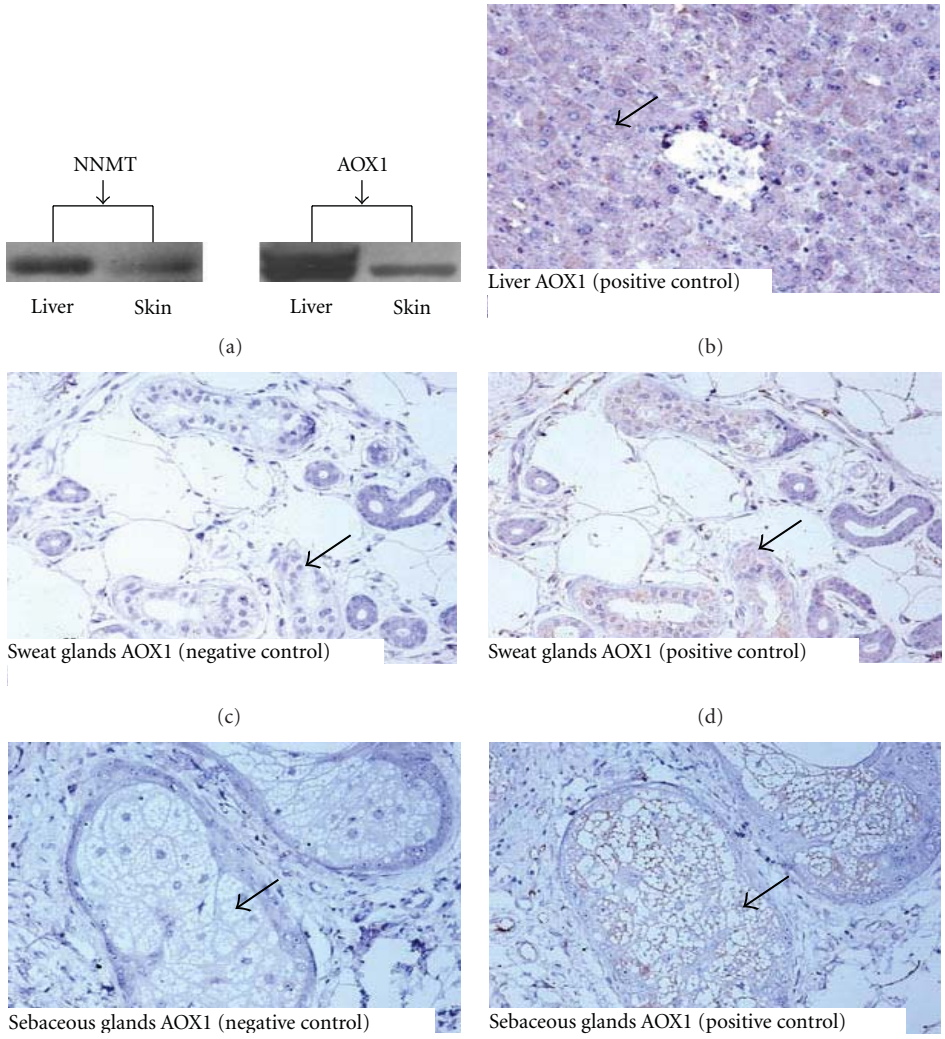

Figure 6: Expression of NNMT and location of AOX1 in human liver and skin. (a) western blotting results. ((b)–(f)) immunohistochemistry analysis of AOX1 expression. (b) positive control of AOX1 expression (human liver). ((d) and (f)), showing the location of AOX1 in sweat glands and sebaceous glands, respectively. ((c) and (e)) negative control for ((d) and (f)) respectively (without primary antibody). AOX1 was stained using a streptavidin-biotin-peroxidase complex method with diaminobenzidine substrate. Nuclei were counterstained with hematoxylin. Magnification: ×200.

toxic substances [29]; (3) sauna, which increases the elimination of toxic substances [30], can improve cardiovascular, autoimmune, toxicant-induced, and other chronic health problems [25]; (4) there are sustained impairments in cutaneous vasodilation and sweating in grafted skin [18]; (5) there is an accumulation of endogenous toxic substances (e.g., cortisol, catecholamines, and cytokines) in the circulation of postburn patients [17]; (6) there is a decrease in the skin-mediated biotransformation of xenobiotics, as shown by the present study; (7) post-burn patients are associated with persistent endoplasmic reticulum stress and IR [15, 17]. Thus, post-burn oxidative stress and IR might involve decreased skin detoxification and excretion.

The above hypothesis is also supported by the observations in nonburn trauma and surgery. Both burn trauma and nonburn trauma (including major surgery), which are accompanied with increased sympathetic activity and redistribution of blood flow away from certain nonvital organs, such as the skin, gastrointestinal tract, and kidneys [31], are associated with IR during the acute phase. However, unlike burn trauma, the IR induced by nonburn trauma and surgery is transient and disappears after nonburn trauma or surgery [32], suggesting the following relationship: a permanent decrease in the skin function is associated with sustained IR, while a transient decrease in the function of intact skin is associated with transient IR. Moreover, the observation that there is an elevation in IR-inducing substances [33] and blood pressure [34] and worse symptoms of IR-related diseases [35, 36] in winter might also imply a close association between the skin function and IR, since low ambient temperature exposure reduces the blood flow to the skin and the skin temperature [37].

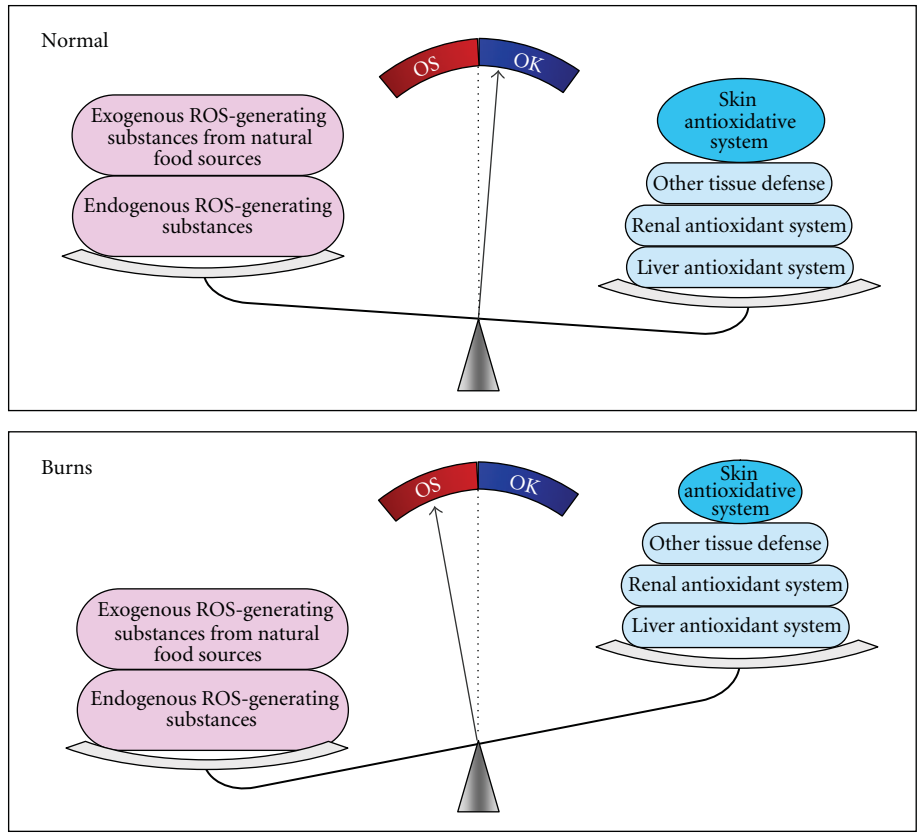

Figure 7: Proposed role of skin in oxidative stress and IR. The body's total antioxidant capacity, consisting of biotransformation system, excretion system, and reactive oxygen species clearance system, depends on the functions of body's tissues/organs. A decrease in the skin contribution, such as induced by severe burn and cold ambient environment, decreases the body's total antioxidant capacity and thus increases the risk for oxidative stress and subsequent IR. OK: the body's total antioxidant capacity > ROS generation; OS: oxidative stress, that is, ROS generation > the body's total antioxidant capacity.

In conclusion, the skin is one of the major components of the body's antioxidant defense system. Factors that decrease the skin function may lead to a decrease in the clearance of xenobiotics and endogenous toxic substances and subsequent increase in ROS generation, which may contribute to the development of IR. The proposed role of the skin in oxidative stress and IR is summarized in Figure 7.

Conflict of Interests

The authors have no conflict of interests to declare.

Authors' Contribution

S.-S. Zhou was responsible for the study concept, design, direction and supervision, drafted the manuscript, and obtained funding; X.-X. Liu and C.-B. Sun contributed equally to this work; X.-X. Liu, C.-B. Sun, T.-T. Yang, D. Li, C.-Y. Li and Y.-J. Tian contributed to the data acquisition and analysis/discussion. Y. Cao participated in the design of the study and performed the statistical analysis. M. Guo participated in the HPLC experiments.

Acknowledgments

This research was supported by the National Natural Science Foundation of China (no. 31140036) and the Foundation of Key Laboratory of Education Department of Liaoning Province (no. 2009S005).

References

[1] E. J. Henriksen, M. K. Diamond-Stanic, and E. M. Marchionne, "Oxidative stress and the etiology of insulin resistance and type 2 diabetes," *Free Radical Biology and Medicine*, no. 5, pp. 993–999, 2011.

[2] N. Houstis, E. D. Rosen, and E. S. Lander, "Reactive oxygen species have a causal role in multiple forms of insulin resistance," *Nature*, vol. 440, no. 7086, pp. 944–948, 2006.

[3] S. S. Zhou, Y. M. Zhou, D. Li, and Y. Z. Lun, "Dietary methyl-consuming compounds and metabolic syndrome," *Hypertension Research*, vol. 34,

[4] S. Mena, A. Ortega, and J. M. Estrela, "Oxidative stress in environmental-induced carcinogenesis," *Mutation Research—Genetic Toxicology and Environmental Mutagenesis*, vol. 674, no. 1-2, pp. 36–44, 2009.

[5] M. Valko, H. Morris, and M. T. D. Cronin, "Metals, toxicity and oxidative stress," *Current Medicinal Chemistry*, vol. 12, no. 10, pp. 1161–1208, 2005.

[6] G. Eisenhofer, I. J. Kopin, and D. S. Goldstein, "Catecholamine metabolism: a contemporary view with implications for physiology and medicine," *Pharmacological Reviews*, vol. 56, no. 3, pp. 331–349, 2004.

[7] E. L. Giller Jr., J. G. Young, X. O. Breakefield, C. Carbonari, M. Braverman, and D. J. Cohen, "Monoamine oxidase and catechol-O-methyltransferase activities in cultured fibroblasts and blood cells from children with autism and the Gilles de la Tourette syndrome," *Psychiatry Research*, vol. 2, no. 2, pp. 187–197, 1980.

[8] A. Pannatier, P. Jenner, B. Testa, and J. C. Etter, "The skin as a drug-metabolizing organ," *Drug Metabolism Reviews*, vol. 8, no. 2, pp. 319–343, 1978.

[9] C. K. Svensson, "Biotransformation of drugs in human skin," *Drug Metabolism and Disposition*, vol. 37, no. 2, pp. 247–253, 2009.

[10] L. Korkina and S. Pastore, "The role of redox regulation in the normal physiology and inflammatory diseases of skin," *Frontiers in Bioscience*, vol. 1, pp. 123–141, 2009.

[11] H. L. Johnson and H. I. Maibach, "Drug excretion in human eccrine sweat," *Journal of Investigative Dermatology*, vol. 56, no. 3, pp. 182–188, 1971.

[12] F. O. Omokhodion and J. M. Howard, "Trace elements in the sweat of acclimatized persons," *Clinica Chimica Acta*, vol. 231, no. 1, pp. 23–28, 1994.

[13] K. Sato, "The physiology, pharmacology, and biochemistry of the eccrine sweat gland," *Reviews of Physiology Biochemistry and Pharmacology*, vol. 79, pp. 51–131, 1977.

[14] J. L. Stauber and T. M. Florence, "A comparative study of copper, lead, cadmium and zinc in human sweat and blood," *Science of the Total Environment*, vol. 74, pp. 235–247, 1988.

[15] G. G. Gauglitz, D. N. Herndon, G. A. Kulp, W. J. Meyer III, and M. G. Jeschke, "Abnormal insulin sensitivity persists up to three years in pediatric patients post-burn," *Journal of Clinical Endocrinology and Metabolism*, vol. 94, no. 5, pp. 1656–1664, 2009.

[16] M. G. Jeschke, C. C. Finnerty, D. N. Herndon, J. Song, D. Boehning, R. G. Tompkins et al., "Severe injury is associated with insulin resistance, endoplasmic reticulum stress response, and unfolded protein response," *Annals of Surgery*, vol. 255, no. 2, pp. 370–378, 2012.

[17] M. G. Jeschke, G. G. Gauglitz, G. A. Kulp et al., "Long-term persistance of the pathophysiologic response to severe burn injury," *PLoS ONE*, vol. 6, no. 7, Article ID e21245, 2011.

[18] S. L. Davis, M. Shibasaki, D. A. Low et al., "Sustained impairments in cutaneous vasodilation and sweating in grafted skin following long-term recovery," *Journal of Burn Care and Research*, vol. 30, no. 4, pp. 675–685, 2009.

[19] C. J. Greenbaum, S. E. Kahn, and J. P. Palmer, "Nicotinamide's effects on glucose metabolism in subjects at risk for IDDM," *Diabetes*, vol. 45, no. 11, pp. 1631–1634, 1996.

[20] S. S. Zhou, D. Li, W. P. Sun et al., "Nicotinamide overload may play a role in the development of type 2 diabetes," *World Journal of Gastroenterology*, vol. 15, no. 45, pp. 5674–5684, 2009.

[21] D. Li, W. P. Sun, Y. M. Zhou et al., "Chronic niacin overload may be involved in the increased prevalence of obesity in US children," *World Journal of Gastroenterology*, vol. 16, no. 19, pp. 2378–2387, 2010.

[22] S. Aksoy, C. L. Szumlanski, and R. M. Weinshilboum, "Human liver nicotinamide N-methyltransferase. cDNA cloning, expression, and biochemical characterization," *Journal of Biological Chemistry*, vol. 269, no. 20, pp. 14835–14840, 1994.

[23] R. Seifert, J. Hoshino, and H. Kröger, "Nicotinamide methylation. tissue distribution, developmental and neoplastic changes," *Biochimica et Biophysica Acta*, vol. 801, no. 2, pp. 259–264, 1984.

[24] H. Steiling, B. Munz, S. Werner, and M. Brauchle, "Different types of ROS-scavenging enzymes are expressed during cutaneous wound repair," *Experimental Cell Research*, vol. 247, no. 2, pp. 484–494, 1999.

[25] W. J. Crinnion, "Sauna as a valuable clinical tool for cardiovascular, autoimmune, toxicant—induced and other chronic health problems," *Alternative Medicine Review*, vol. 16, no. 3, pp. 215–225, 2011.

[26] T. Takemura, P. W. Wertz, and K. Sato, "Free fatty acids and sterols in human eccrine sweat," *British Journal of Dermatology*, vol. 120, no. 1, pp. 43–47, 1989.

[27] C. A. Peralta, M. Kurella, J. C. Lo, and G. M. Chertow, "The metabolic syndrome and chronic kidney disease," *Current Opinion in Nephrology and Hypertension*, vol. 15, no. 4, pp. 361–365, 2006.

[28] S. Watanabe, R. Yaginuma, K. Ikejima, and A. Miyazaki, "Liver diseases and metabolic syndrome," *Journal of Gastroenterology*, vol. 43, no. 7, pp. 509–518, 2008.

[29] S. S. Zhou, D. Li, Y. M. Zhou, and J. M. Cao, "The skin function: a factor of anti-metabolic syndrome," *Diabetology & Metabolic Syndrome*, vol. 4, no. 1, p. 15, 2012.

[30] J. Krop, "Chemical sensitivity after intoxication at work with solvents: response to sauna therapy," *Journal of Alternative and Complementary Medicine*, vol. 4, no. 1, pp. 77–86, 1998.

[31] B. A. Foex, "Systemic responses to trauma," *British Medical Bulletin*, vol. 55, no. 4, pp. 726–743, 1999.

[32] H. S. Bagry, S. Raghavendran, and F. Carli, "Metabolic syndrome and insulin resistance: perioperative considerations," *Anesthesiology*, vol. 108, no. 3, pp. 506–523, 2008.

[33] D. Kanikowska, J. Sugenoya, M. Sato et al., "Seasonal variation in blood concentrations of interleukin-6, adrenocorticotrophic hormone, metabolites of catecholamine and cortisol in healthy volunteers," *International Journal of Biometeorology*, vol. 53, no. 6, pp. 479–485, 2009.

[34] K. J. Radke and J. L. Izzo, "Seasonal variation in haemodynamics and blood pressure-regulating hormones," *Journal of Human Hypertension*, vol. 24, no. 6, pp. 410–416, 2010.

[35] P. Doró, R. Benko, M. Matuz, and G. Soós, "Seasonality in the incidence of type 2 diabetes: a population-based study," *Diabetes Care*, vol. 29, no. 1, p. 173, 2006.

[36] F. Kamezaki, S. Sonoda, Y. Tomotsune, H. Yunaka, and Y. Otsuji, "Seasonal variation in metabolic syndrome prevalence," *Hypertension Research*, vol. 33, no. 6, pp. 568–572, 2010.

[37] O. Talpash, "Skin reactions to cold," *Canadian Family Physician*, vol. 22, pp. 40–42, 1976.

Hindawi Publishing Corporation
Experimental Diabetes Research
Volume 2012, Article ID 120645, 10 pages
doi:10.1155/2012/120645

Research Article

Early Degenerative Effects of Diabetes Mellitus on Pancreas, Liver, and Kidney in Rats: An Immunohistochemical Study

Mehmet Haligur,[1] Senay Topsakal,[2] and Ozlem Ozmen[1]

[1] *Department of Pathology, Faculty of Veterinary Medicine, University of Mehmet Akif Ersoy, 15030 Ortulu Yerleskesi, Burdur, Turkey*
[2] *Department of Endocrinology and Metabolism, Faculty of Medicine, University of Pamukkale, 20070 Kinikli, Denizli, Turkey*

Correspondence should be addressed to Mehmet Haligur, mhaligur@mehmetakif.edu.tr

Received 3 March 2012; Revised 11 May 2012; Accepted 14 May 2012

Academic Editor: Pietro Galassetti

Liver and kidney commonly affected by diabetes in chronic cases but pathogenetic mechanisms are not fully understood in early stages of the disease. The aim of this study was to investigate the immunohistochemical expression of caspase-3, cyclooxygenase (COX)-1 and-2, calcium sensing receptor (CSR), and hypoxia inducible factor-1α (HIF-1α) in pancreas, liver, and kidney in streptozotocin (STZ) induced DM. Study group ($n = 6$) were received streptozotocin (50 mg/kg) and control group ($n = 6$) physiologic saline. The blood glucose and ketonuria were measured, and necropsy was performed on them on third, fourth, and fifth days. Immunohistochemistry revealed that marked increase in caspase-3 reaction pancreas, liver, and kidney in the study group than control group. COX-1 slightly increased in these organs in study group compared to controls. Immunohistochemically COX-2 reaction was markedly positive in liver and kidney, but slightly increased in pancreas. The most increased reaction was observed in CRS and all organs were markedly positive. HIF-1α expression was also increased but the reaction was more severe in pancreas than liver and kidney. This study indicated that degeneration starts in organs in early stages of the disease and the most effective route for degeneration related to increase of calcium influx and hypoxia upon cells in DM.

1. Introduction

Diabetes mellitus is a metabolic disorder that results from a reduction of insulin available for normal function of many cells in the body. In some cases, increased concentrations of glucagon contribute to development of persistent hyperglycemia. In addition to chronic hyperglycemia, DM is characterized by disturbance of carbohydrate, fat, and protein metabolism resulting from defects in insulin secretion, insulin action, or both. The diseases can also be recognized during less overt stages, most usually by the presence of glucose intolerance. The effects of DM include long-term damage, dysfunction, and failure of various organs, especially the eyes, kidneys, livers, hearts, and blood vessels [1].

In the pathogenesis of DM, several factors are responsible for the decreased availability of insulin. Hyperglycemia, and its attendant effects upon cells, underlies the pathogenic lesions of DM [2]. Cellular damages can be demonstrated by numerous markers by immunohistochemistry. For example, caspases are a family of cysteine proteases mainly involved in the apoptotic pathway [3]. Caspase-3 is one of the effector caspases that has been implicated as a key protease cleaving multiple cellular substrates, including components related to DNA repair and regulation, to bring the cell to its demise [4, 5]. Cyclooxygenase enzymes also play an important role at cellular damages. Three different COX enzymes existed, now known as COX-1, COX-2, and COX-3, they are responsible for formation of important biological mediators called prostanoids, including prostaglandins, prostacyclin, and thromboxane. Pharmacological inhibition of COX can provide relief from the symptoms of inflammation and pain [6]. In diabetes, direct evidence that cytoplasmic Ca^{2+} triggers exocytosis of the insulin granules is obtained from experiments using β cell of which the plasma membrane is permeabilized in these cells, the membrane potential is dissipate and the cytosolic concentration of small molecules can be controlled [7]. Calcium sensing receptor is a G protein-coupled receptor (GPCR) and regulation of extracellular and

intracellular calcium homeostasis related to CSR. It has also been found in a wide variety of organs not involved in systemic calcium homeostasis that it plays important roles in cellular damages [8–10]. Hypoxia-inducible factor-1α has central role in degeneration and a transcriptional activator that promotes angiogenesis [11, 12]. HIF-1α expression is also induced under normoxic conditions when cells are stimulated with growth factors, inflammatory cytokines, lactate, or prostaglandins [13–15].

DM is a complex disease and causes numerous cellular damages in different organs. A number of pathogenetic advances have been made during the past decade but numerous mechanisms need to be clarified. The pathogenetic mechanisms are likely interactive and linked in DM. For that reason, mechanism of cellular damage is not fully understood. This preliminary study was designed to explore the cellular distribution and the underlying mechanisms of hypoxia and calcium influx in experimental diabetes.

2. Material and Methods

Twelve female Sprague-Dawley rats, weighing 125 to 150 g and aged 2 months, were maintained at the Experimental Animal Housing Unit of the University of Akdeniz. They were randomly allocated into 2 groups, as follows: study group that treated with STZ and control group. Both groups were composed of 6 rats and were allowed free access to water and food. Rats were fasted before the STZ injection. A single intraperitoneal injection of 50 mg/kg STZ (Sigma Chemical Co, St. Louis, Mo) dissolved immediately before administration in freshly prepared 50 mmol/L citrate buffer (pH 4.0) that was given on day 0. Control animals received an equivalent volume of physiologic saline. Urine samples were collected at 3rd, 4th, and 5th days. At the third day, two rats form, study group and two rats from the control group were anesthetized with ether before blood and tissue samples were obtained. The blood glucose concentration was measured in blood from jugular vein in the morning from 2 rats in each group before euthanasia, and then necropsy was performed on them after the third day. The MS9 blood counting equipment was used for hematological analysis of the blood drawn in EDTA tubes. Glucose levels were analyzed in serum samples using IDEXX VetTest equipment and reagents. Pancreas, liver, and kidney tissue samples were collected and fixed in 10% buffered formalin. After routine procedure, tissues were blocked in paraffin and cut to 5 μm thickness. Tissue sections were stained with hematoxylin-eosin (HE) and examined microscopically. Afterward, pancreas, liver, and kidney samples were immunostained with caspase-3 (rabbit polyclonal, Cat. no. 250573, Abbiotec-San Diego, USA), COX-1 (Epitope Specific rabbit antibody, Cat. no. RR-10687-P0, Thermo scientific, Fremont, USA), COX-2 (Cat. no: RM-9121-S0, Thermo scientific, Fremont, USA), CSR (Rb pAb to CSR, ab62653-100, Abcam Lot: 433372, Cambridge, UK), and HIF-1α (H1α67, Sc-53546, Santa Cruz Biotechnology Inc. CA, USA) according to the manufactures' instructions. In this study, avidin-biotin complex peroxidase (ABC-P) method was used for immunohistochemistry. Paraffin blocks were sectioned at 5 μm for immunohistochemical examination, and sections were attached to glass slides coated with poly-L-lysine. The slides were dried overnight at 37°C to optimize adhesion. Sections were deparaffinized through xylene, and tissues were rehydrated in sequentially graduated ethyl alcohol. Slides were incubated in hydrogen peroxide in methanol for 10 min to reduce nonspecific background staining due to endogenous peroxidase. The sections were washed twice, in phosphate buffer solution (PBS). Then, tissues were boiled in 1 : 100 citrate buffer solution for10 min and cooled for 20 min. The cooled tissues were washed four times in PBS prior to application of blocking serum for 5 min. Then, primary antibody was applied; tissues were incubated for 30 min at room temperature. They were rinsed 4 times in PBS, given an application of biotinylated anti-polyvalent antibody and incubated for 10 min at room temperature. After being washed three times in PBS, streptavidin peroxidase was applied and the samples were incubated for 10 min at room temperature, and then rinsed 4 times in PBS. Tissues were further incubated for 20 min at room temperature in a solution of DAB (3, 30 diaminobenzidine) chromogen. After being washed in PBS, tissues were counter stained with Mayer's haematoxylin, washed in water, and coverslips were applied with mounting media. For negative control, primary antibody was not added to the sections.

In order to evaluate the percentage of immunopositive cells, 100 cells calculated in 10 different microscopic high-powered fields of each slide were examined under the 40x objective of a trinocular microscope (Nikon E600) and microphotography apparatus. The count of positive cells one high-power field for each marker was noted and compared with control groups.

In the statistical evaluations, Students t test was used. Calculations were made using the SPSS 13.0 program pack. $P < 0.05$ was accepted as statistically significant.

Table 1: Blood and urine values of the rats in groups.

Study group	Blood glucose (mmol/L)	Ketonuria
3rd day	10.15 ± 2.18	—
4th day	11.84 ± 1.84	+
5th day	9.91 ± 1.69	+
Control group		
3rd day	4.05 ± 1.42	—
4th day	5.67 ± 0.94	—
5th day	6.07 ± 0.86	—
Reference values	2.28–7.50	—

The differences between the means of groups are statistically significant ($P < 0.05$).

3. Results

Hyperglycemia and ketonuria was initially observed in both rats in study group 3 days after administration. There were no glucosuria and ketonuria in the control group. Biochemical results of blood and urine were shown in Table 1. No macroscopical changes were observed in organs

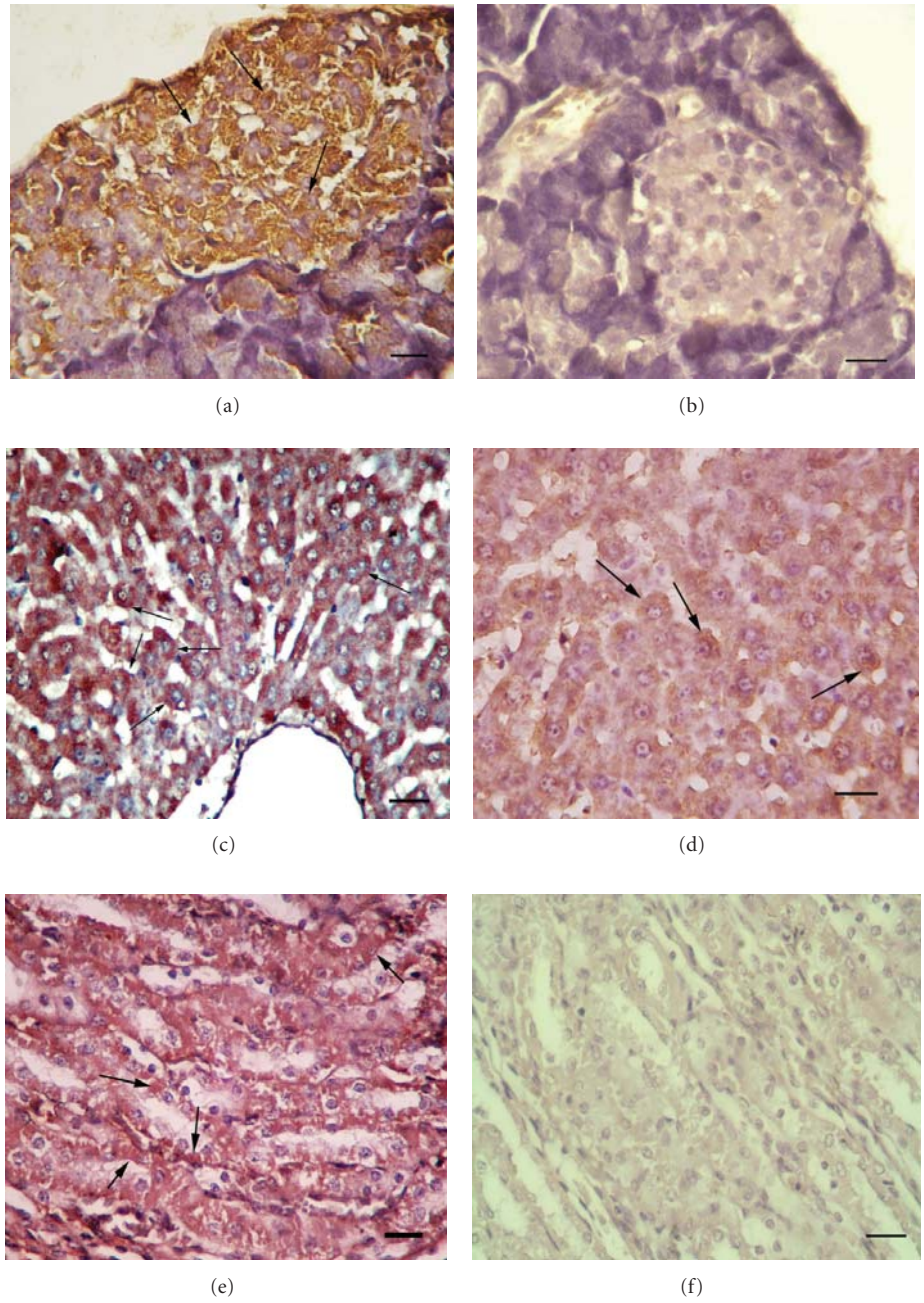

Figure 1: *Caspase-3 reactions*. (a) Immunopositive reaction in Langerhans islets cells (arrows) in study group, Bar = 50 μm; (b) no immunoreaction in control group, Bar = 50 μm; (c) marked reaction in hepatocytes in study group (arrows), Bar = 100 μm. (d) Slight immunoreaction in some hepatocytes (arrows) in control group, Bar = 50 μm; (e) Strong reactions in tubular cells in kidney (arrows), Bar = 100 μm. (f) A few immunopositive cells in kidney in control group, Bar = 100 μm. ABC-P method with Hematoxyline counterstaining were used for all tissue. The right column belongs to study group and left column belongs to control group.

in both groups. At the histopathological examination of pancreas, degenerative and necrotic beta cells were seen in Langerhans islets in study group. At microscopical examination slight degenerative changes were observed in liver and tubular epithelial cells of the kidney. Immunohistochemical observation of caspase-3, COX-1, COX-2, CSR, and HIF-1α immunostained sections revealed severe damage in these organs in early stages of the DM. Statistical results of immunohistochemical observation were shown in graphic. Caspase-3 immunopositive cell numbers were markedly increased in pancreatic islets in study group. In addition to pancreas, caspase-3 immunopositive reaction was higher in liver hepatocyte in study group than controls and strong immunoreactions were observed in kidney tubular epithelial cells (Figures 1(a), 1(b), 1(c), 1(d), 1(e), and 1(f)). Slight increases in COX-1 reaction were observed in pancreas, liver,

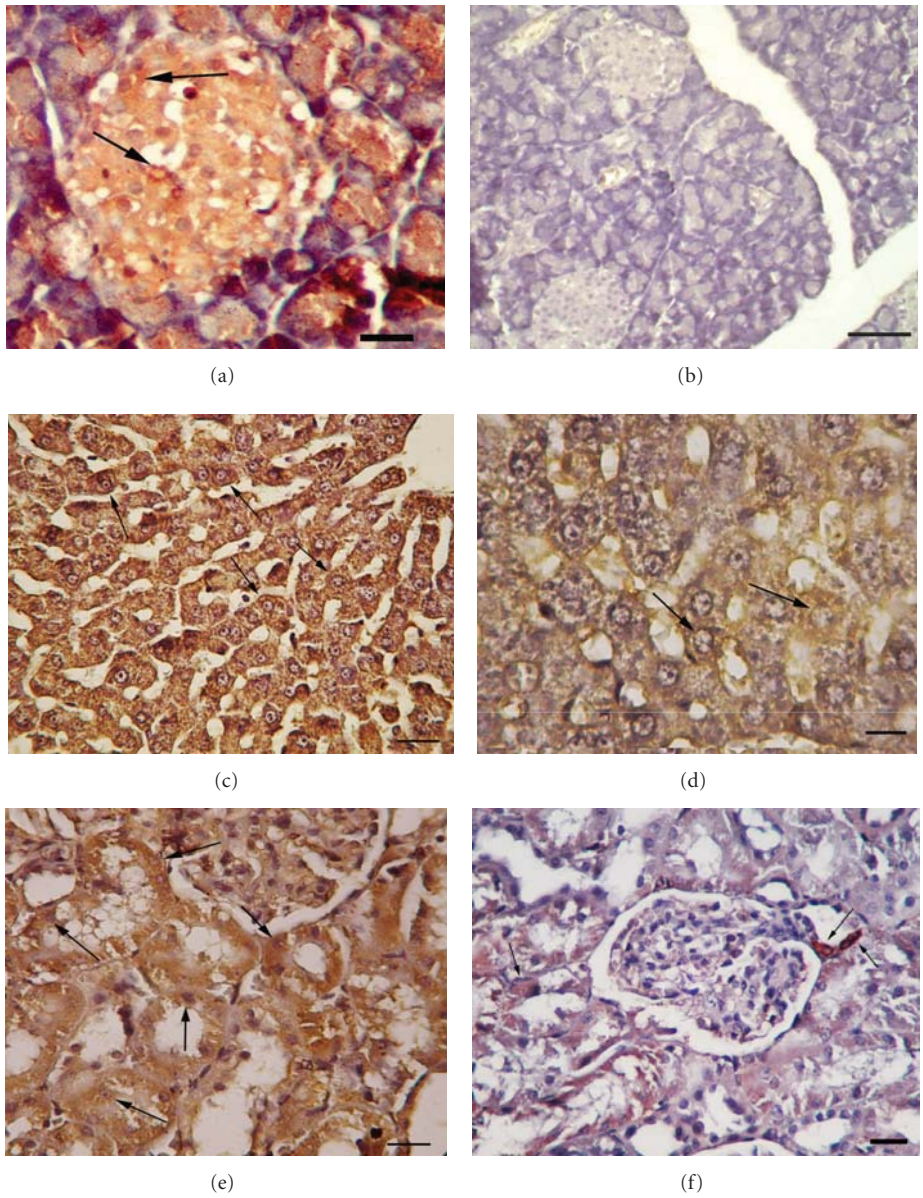

Figure 2: *COX-2 reactions.* (a) Severe positive immunoreaction in endocrine islets of pancreas in study group (arrows), Bar = 50 μm. (b) No immunoreaction in Langerhans islets of pancreas in control group, Bar = 100 μm. (c) Moderate immunoreaction in hepatocyte in study group (arrows), Bar = 100 μm. (d) A few immunoreactions in liver (arrows) in control group, Bar = 50 μm. (e) Strong immunopositive reaction in nonmacula densa area in kidney (arrows) in study group, Bar = 100 μm. (f) A few immunoreactions in kidney tubul cells in macula densa (arrows) in control group, Bar = 100 μm. ABC-P method with hematoxylin counterstaining was used for all tissues. The right column belongs to study group and left column is belong to control group.

and kidney in study group's rats. In kidneys, immunohistochemical examination revealed that the expression of COX-1 localized on collecting tubules. COX-2 immunoreactive cells were markedly increased in study rats compared with controls in all examined organs. In control group, COX-2 positive immunostaining was observed in individual kidney tubular epithelial cells. Marked immunopositivity was demonstrated in macula densa and nonmacula densa tubules of kidney in study group (Figures 2(a), 2(b), 2(c), 2(d), 2(e), and 2(f)). In both groups, CSR immunopositive immunoreactions were noticed in cytoplasm of cells in the organs. But reaction was prominent in study group. Immunopositive reaction was also observed in nucleus of the some cells in Langerhans islets of pancreas. Similar CSR reaction was noticed in hepatocytes and both proximal and distal tubular epithelial cells of the kidney (Figures 3(a), 3(b), 3(c), 3(d), 3(e), and 3(f)). HIF-1α immunoreactions markedly increased in the study group while the controls were negative. Langerhans islets of pancreas exhibited markedly HIF-1α immunopositive reactions. Slight immunoreaction was detected in hepatocytes of the liver. Strong HIF-1α reaction was observed in both proximal and distal tubular epithelial

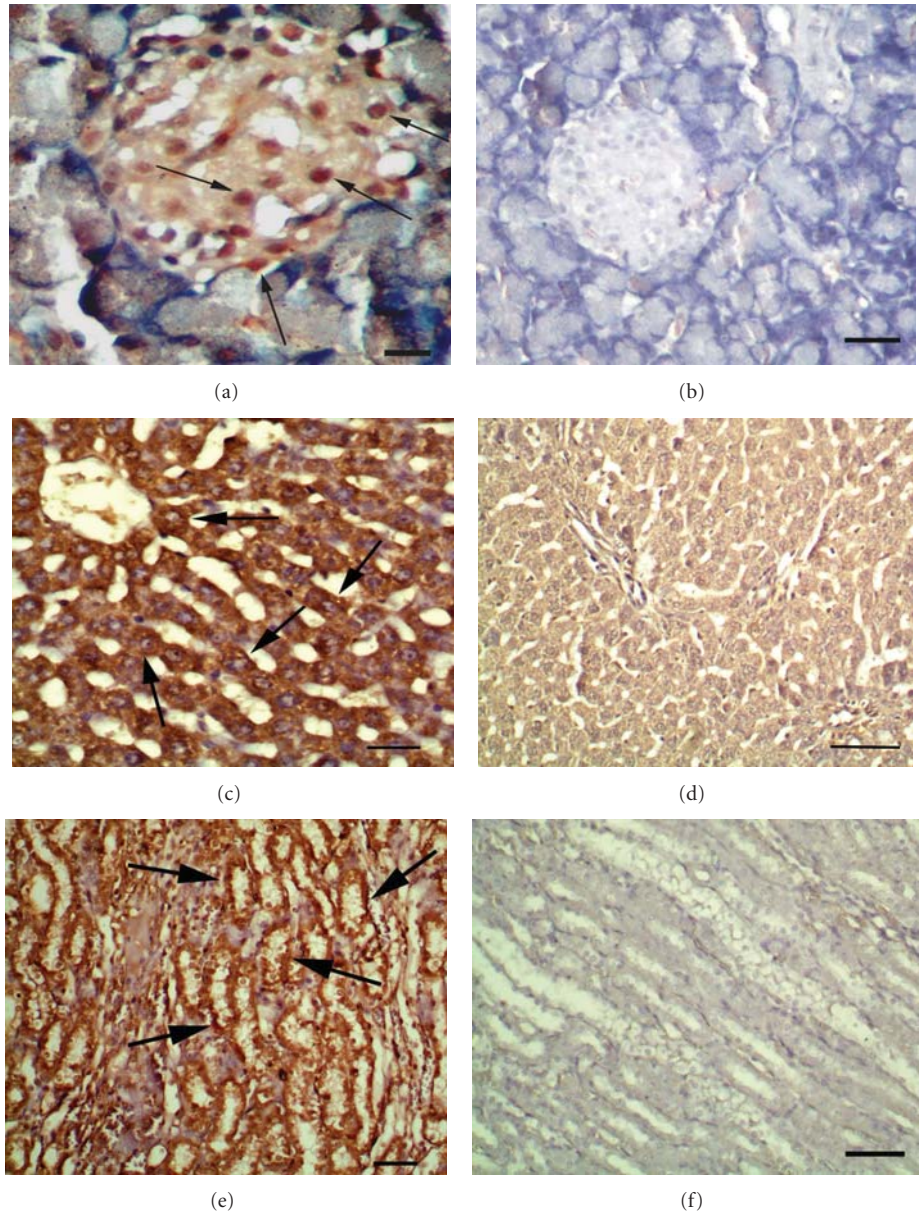

Figure 3: *CSR reactions*. (a) Severe expression in nucleus and cytoplasms of endocrine islets of pancreas in study group (arrows), Bar = 50 μm. (b) No immunoreaction in Langerhans islets of pancreas in control group, Bar = 100 μm. (c) Severe immunopositive reaction in hepatocyte in study group (arrows), Bar = 100 μm. (d) A few immunoreactions in liver (arrows) in control group, Bar = 100 μm. (e) Strong immunopositive reaction in tubular epithelial cells in kidney (arrows) in study group, Bar = 200 μm. (f) Very slight immunoreactions in kidney in control group, Bar = 200 μm. ABC-P method with Hematoxyline counterstaining was used for all tissues. The right column belongs to study group and left column belongs to control group.

cells of the kidney in study group (Figures 4(a), 4(b), 4(c), 4(d), 4(e), and 4(f)). Positive immunoreactivity was noted by an intense brown color (DAB). All of the markers were gradually increased related to days from induction of DM in this study (Figures 5(a), 5(b), 5(c), 5(d), and 5(e)).

4. Discussion

STZ administration to mature rats induces severe and permanent diabetes, with a decrease in insulin levels, to produce a cytotoxic model of diabetes very similar to type I DM. Streptozocin damages β cells of the islets of Langerhans in the pancreas [16]. Streptozotocin-induced diabetes in the rats is being employed extensively for studies into the immunopathogenesis of DM [17]. Although several studies have examined the underlying immune cellular and molecular changes during disease in this model, investigations on the early stages and cell injury in different organs have been limited. Cell damage is the main reason of necrosis and numerous agents can cause this process. The main reason of

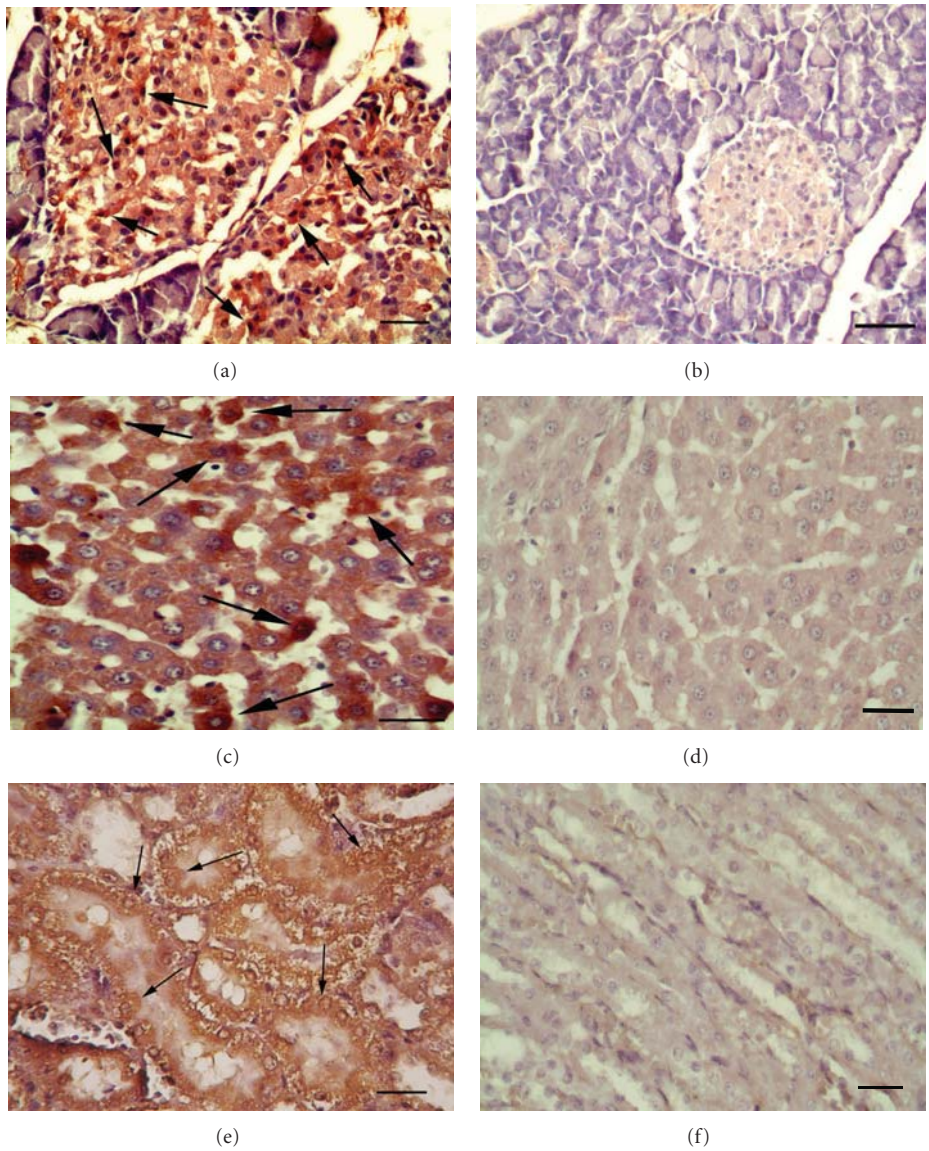

Figure 4: *HIF reactions*. (a) Severe expression in endocrine islets of pancreas in study group (arrows), Bar = 100 μm. (b) Slight immunoreaction in Langerhans islets of pancreas in control group, Bar = 100 μm. (c) Severe immunopositive reaction in hepatocyte in study group (arrows), Bar = 50 μm. (d) A few immunoreactions in liver in control group, Bar = 50 μm. (e) Strong immunopositive reaction in tubular epithelial cells in kidney (arrows) in study group, Bar = 50 μm. (f) Very slight immunoreactions in kidney in control group, Bar = 100 μm. ABC-P method with Hematoxyline counterstaining was used for all tissues. The right column belongs to study group and left column belongs to control group.

cellular injury is hypoxia and it is commonly seen. Calcium is main player of the cell damage and activates both plasma membrane and mitochondrial injuries which are cell damage pathways. COX enzymes play a major role in cellular damage process. Cell death is the last stage of the cellular damage and it can occur by apoptosis or necrosis. Caspase-3 is the main marker of the apoptosis [18]. This study planned to examine the role of calcium, hypoxia, and apoptosis in early stages of DM in different cells by using HIF-1α, COX-1 and -2, CSR and Caspase-3 by immunohistochemical method.

DM results from the progressive destruction of beta cells of Langerhans islets [19]. Multiple mechanisms have been proposed as effectors of beta cell destruction [20, 21]. Although DM is a chronic and progressive disease, initial lesions can be seen in very early stages. Previous studies reported that initial lesions occur after 3 days of DM induction in rats [22, 23]. Similar findings were observed in this study, and glucosuria was detected three days after streptozotocin treatment. Tissue sections of pancreas, liver, and kidney were examined histopathologically and immunohistochemically at 3rd, 4th, and 5th days. This study demonstrated that increased expression of caspase-3, COX-1 and -2, CSR, and HIF-1α in islet of Langerhans, liver, and kidney in streptozotocin induced DM in rats. These results supported

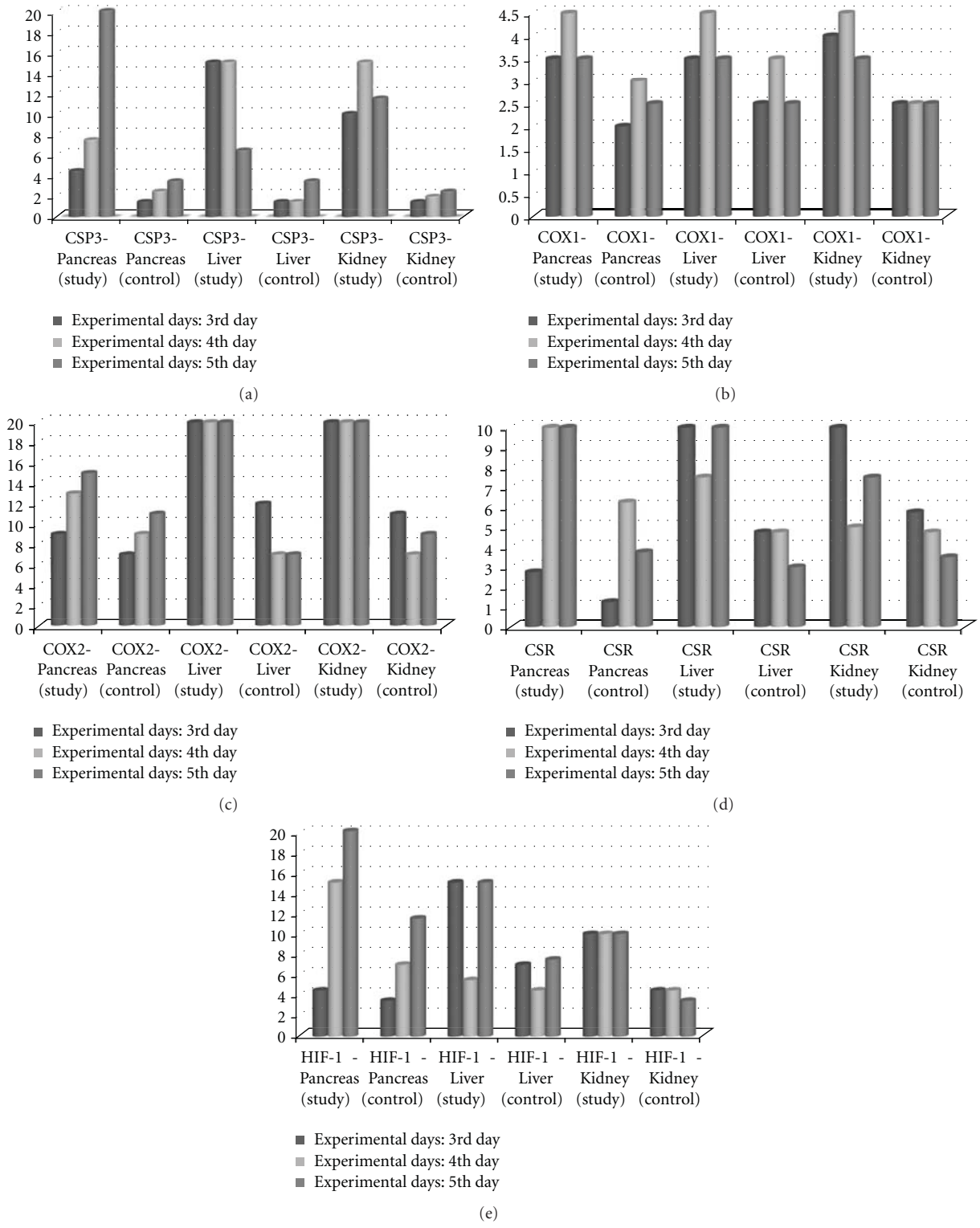

Figure 5: Statistical analysis results of (a) Caspase-3, (b) COX-1, (c) COX-2, (d) CSR, and (e) HIF-1αimmunopositive cell numbers.

the idea that cellular damages due to DM can occur in very early stages of the disease. Our results showed that different mechanisms may play role in diabetes like as hypoxia, apoptosis, and calcium influx in degenerative changes in cells.

Caspases are cysteine-aspartyl specific proteases that play a key role in apoptosis [24]. Caspase-3 is one of the effector caspases downstream of apoptotic pathways. Gene targeting strategies have provided valuable tools to study

the physiologic function of individual caspases in vivo and have shown their roles not only in apoptosis but also in other fundamental cellular processes [4]. Several in vitro studies have suggested that caspase dependent apoptotic pathways are essential for β cell apoptosis [25]. The underlying mechanism of tubular changes in kidney in diabetes, however, is unclear. One attractive mechanism is apoptosis, which has been demonstrated to mediate cell death in a variety of renal diseases, including diabetic nephropathy [26]. Indeed, apoptosis was detected in renal proximal tubular cells of different species including experimental animals and patient with diabetes, suggesting that tubular apoptosis may precede tubular atrophy in diabetes [27, 28]. In this study, apoptotic activity in pancreatic islets was also observed in the study group's rats and was an agreement with previous studies. At the same time we also observed increased apoptotic activity in the hepatocytes and kidney tubular cells. This study showed that possible mechanism of occurrence of liver and kidney problem in diabetes may be related to the increased apoptotic activity.

Many studies using streptozotocin-induced type 1 diabetic rats have shown an increase in COX-2 production in kidney [23]. Therefore, in the present study, the kidneys of study and control rats were investigated histologically and immunohistochemically, and changes in the renal expression of COX-2 during the DM induction were marked in the study group compared to control group. Marked increase in COX-2 expressions was observed in the renal proximal tubules and macula densa in the study group as compared with the control group. Only slight increases were observed in COX-1 expression in the study group. These results were corresponding to previous observations [23]. The possible cause of the increased COX-2 protein expression in kidneys of study group rats may be related to that the tissue changes also have a pathophysiological impact in modulating renal hemodynamics in diabetes.

Calcium is known to be an important intracellular messenger. Ca^{2+} plays a key role in numerous cellular processes, such as maintaining membrane potential and controlling hormonal secretion and cellular proliferation and differentiation [8]. The mechanisms governing extracellular calcium homeostasis maintain its near constancy to ensure continual availability of calcium ions for their multiple intra- and extracellular functions. CSR expression has an important role in many physiological situations. It is involved in calcium metabolism regulation in many cells such as parathyroid [29], bone [30], kidney cells [31], fibroblasts [32], antral gastrin cells [33], epithelial cells [34], oligodendrocytes [30], renal cells, retina, osteoclasts and osteoblasts, vessels smooth muscle cells, and on some brain cells [8]. In this study CSR expression was demonstrated in pancreas, liver, and kidney in diabetes-induced rats. Expression of the CSR was more prominent in the study group than the control group. Marked increase was observed in both nucleus and cytoplasm of the cells of Langerhans islets of pancreas in the study group. Little expression was seen in the control group and only in cytoplasm. Strong immunopositive reaction was observed in collective tubules of kidney compared to the controls. Hepatocytes also expressed CSR in both groups, and reaction was more prominent in the study group.

Hypoxia is the main regulator of HIF-1α expression and function in some conditions such as diabetes pathogenesis [35, 36]. HIF-1α is one of the important members of the bHLH-PAS family [37] and functions as an obligate dimer with other family members, including aryl hydrocarbon receptor (AhR) nuclear translocator (ARNT) [38]. HIF-1α degradation occurred by HIF prolyl hydroxylases. HIF-1α degradation can be considered cellular oxygen sensors, because their activity varies in the range of physiologic/pathologic oxygen tensions [39]. It is very important to detect HIF activation in tissue sections by immunohistochemical methods in detection of nuclear HIF-1α [40]. HIF activity can be modulated by a number of factors such as hydrogen peroxide and superoxide [41]. Diabetes can cause increased production of reactive oxygen species [42]. In the renal medulla, NAD(P)H oxidase activity can cause increased superoxide in the thick ascending limbs of the loop of Henle [43]. Superoxide may both intensify renal medullary hypoxia and reduce hypoxia adaptation in diabetes [44]. In this study, although HIF-1α-negative in the control group's pancreas, increase reaction was seen in the liver and kidney in the study group. The most marked reaction of HIF-1α was observed in Langerhans islets of the pancreas.

5. Conclusion

As a result, this study showed that marked immunoreaction can be seen in the pancreas, liver and kidney with caspase-3, COX-1, COX-2, CSR, and HIF-1α in diabetes-induced rats. These reactions became prominent related to days after induction. The possible cause of the increase may be related to cellular damage by different routes. Increase of severity of the immunoreactions related to days also supported this idea. The most marked reaction was observed in Langerhans islets of pancreas with all of the markers in this study. But liver, and kidney can be affected in very early stages of the disease. These results indicated that cellular damage in DM showed both hypoxia and calcium influx in the cells. Apoptosis can cause marked lesions in organs. This study showed that although diabetes is a chronic disease, its affects can be seen in cells in early stages.

References

[1] P. H. Bennett and W. C. Knowler, "Definition, diagnosis and classification of diabetes mellitus and glucose homeostasis," in *Joslin's Diabetes Mellitus*, C. R. Kahn, G. C. Weir, G. L. King, A. M. Jacobson, A. C. Moses, and R. J. Smith, Eds., pp. 331–339, Lippincott, Williams and Wilkins, 2005.

[2] N. F. Cheville, "Response to cellular injury," in *Ultrastructural Pathology*, pp. 5–31, Willey- Blackwell, Ames, Iowa, USA, 2009.

[3] N. A. Thornberry and Y. Lazebnik, "Caspases: enemies within," *Science*, vol. 281, no. 5381, pp. 1312–1316, 1998.

[4] M. Woo, R. Hakem, M. S. Soengas et al., "Essential contribution of caspase 3/CPPp32 to apoptosis and its associated

nuclear changes," *Genes and Development*, vol. 12, no. 6, pp. 806–819, 1998.

[5] X. Zhang, G. Barile, S. Chang et al., "Apoptosis and cell proliferation in proliferative retinal disorders: PCNA, Ki-67, caspase-3, and PARP expression," *Current Eye Research*, vol. 30, no. 5, pp. 395–403, 2005.

[6] I. Morita, "Distinct functions of COX-1 and COX-2," *Prostaglandins and Other Lipid Mediators*, vol. 68-69, pp. 165–175, 2002.

[7] T. Tamagawa, H. Niki, and A. Niki, "Insulin release independent of a rise in cytosolic free Ca^{2+} by forskolin and phorbol ester," *FEBS Letters*, vol. 183, no. 2, pp. 430–432, 1985.

[8] E. M. Brown and R. J. Macleod, "Extracellular calcium sensing and extracellular calcium signaling," *Physiological Reviews*, vol. 81, no. 1, pp. 239–297, 2001.

[9] N. Chattopadhyay, A. Mithal, and E. M. Brown, "The calcium-sensing receptor: a window into the physiology and pathophysiology of mineral ion metabolism," *Endocrine Reviews*, vol. 17, no. 4, pp. 289–307, 1996.

[10] E. M. Brown, "Extracellular Ca^{2+} sensing, regulation of parathyroid cell function, and role of Ca^{2+} and other ions as extracellular (first) messengers," *Physiological Reviews*, vol. 71, no. 2, pp. 371–411, 1991.

[11] M. C. Brahimi-Horn and J. Pouysségur, "Harnessing the hypoxia-inducible factor in cancer and ischemic disease," *Biochemical Pharmacology*, vol. 73, no. 3, pp. 450–457, 2007.

[12] G. L. Semenza, "Life with oxygen," *Science*, vol. 318, no. 5847, pp. 62–64, 2007.

[13] E. Laughner, P. Taghavi, K. Chiles, P. C. Mahon, and G. L. Semenza, "HER2 (neu) signaling increases the rate of hypoxia-inducible factor 1α (HIF-1α) synthesis: novel mechanism for HIF-1-mediated vascular endothelial growth factor expression," *Molecular and Cellular Biology*, vol. 21, no. 12, pp. 3995–4004, 2001.

[14] R. Fukuda, B. Kelly, and G. L. Semenza, "Vascular endothelial growth factor gene expression in colon cancer cells exposed to prostaglandin E2 is mediated by hypoxia-inducible factor 1," *Cancer Research*, vol. 63, no. 9, pp. 2330–2334, 2003.

[15] T. K. Hunt, R. S. Aslam, S. Beckert et al., "Aerobically derived lactate stimulates revascularization and tissue repair via redox mechanisms," *Antioxidants and Redox Signaling*, vol. 9, no. 8, pp. 1115–1124, 2007.

[16] B. Portha, C. Levacher, L. Picon, and G. Rosselin, "Diabetogenic effect of streptozotocin in the rat during the perinatal period," *Diabetes*, vol. 23, no. 11, pp. 889–895, 1974.

[17] G. L. Wilson and E. H. Leiter, "Streptozotocin interactions with pancreatic β cells and the induction of insulin-dependent diabetes," *Current Topics in Microbiology and Immunology*, vol. 156, pp. 27–54, 1990.

[18] B. J. Slauson and D. O. Cooper, "Pathology—the study of disease," in *Mechanisms of Disease A Textbook of Comparative General Pathology*, pp. 1–15, Mosby, St. Louis, Mo, USA, 2002.

[19] G. S. Eisenbarth, J. Connelly, and J. S. Soeldner, "The "natural" history of type I diabetes," *Diabetes/Metabolism Reviews*, vol. 3, no. 4, pp. 873–891, 1987.

[20] A. Rabinovitch, "Free radicals as mediators of pancreatic islet β-cell injury in autoimmune diabetes," *Journal of Laboratory and Clinical Medicine*, vol. 119, no. 5, pp. 455–456, 1992.

[21] D. Mathis, L. Vence, and C. Benoist, "β-cell death during progression to diabetes," *Nature*, vol. 414, no. 6865, pp. 792–798, 2001.

[22] O. Ozmen, S. Topsakal, S. Sahinduran, and M. Ozcelik, "Effect of insufficient insulin treatment in streptozotocin-induced diabetes mellitus," *Pancreas*, vol. 34, no. 3, pp. 354–358, 2007.

[23] R. Komers, J. N. Lindsley, T. T. Oyama et al., "Immunohistochemical and functional correlations of renal cyclooxygenase-2 in experimental diabetes," *Journal of Clinical Investigation*, vol. 107, no. 7, pp. 889–898, 2001.

[24] E. M. Creagh, H. Conroy, and S. J. Martin, "Caspase-activation pathways in apoptosis and immunity," *Immunological Reviews*, vol. 193, pp. 10–21, 2003.

[25] K. Maedler, G. A. Spinas, R. Lehmann et al., "Glucose induces beta-cell apoptosis via upregulation of the Fas receptor in human islets," *Diabetes*, vol. 50, no. 8, pp. 1683–1690, 2001.

[26] M. L. Brezniceanu, F. Liu, C. C. Wei et al., "Attenuation of interstitial fibrosis and tubular apoptosis in db/db transgenic mice overexpressing catalase in renal proximal tubular cells," *Diabetes*, vol. 57, no. 2, pp. 451–459, 2008.

[27] F. Liu, M. L. Brezniceanu, C. C. Wei et al., "Overexpression of angiotensinogen increases tubular apoptosis in diabetes," *Journal of the American Society of Nephrology*, vol. 19, no. 2, pp. 269–280, 2008.

[28] D. Kumar, J. Zimpelmann, S. Robertson, and K. D. Burns, "Tubular and interstitial cell apoptosis in the streptozotocin-diabetic rat kidney," *Nephron*, vol. 96, no. 3, pp. e77–e88, 2004.

[29] E. M. Brown, G. Gamba, D. Riccardi et al., "Cloning and characterization of an extracellular Ca^{2+}-sensing receptor from bovine parathyroid," *Nature*, vol. 366, no. 6455, pp. 575–580, 1993.

[30] N. Chattopadhyay, T. Yamaguchi, and E. M. Brown, "Ca^{2+} receptor from brain to gut: common stimulus, diverse actions," *Trends in Endocrinology and Metabolism*, vol. 9, no. 9, pp. 354–359, 1998.

[31] D. Riccardi, W. S. Lee, K. Lee, G. V. Segre, E. M. Brown, and S. C. Hebert, "Localization of the extracellular Ca^{2+}-sensing receptor and PTH/PTHrP receptor in rat kidney," *American Journal of Physiology*, vol. 271, no. 4, pp. F951–F956, 1996.

[32] S. E. McNeil, S. A. Hobson, V. Nipper, and K. D. Rodland, "Functional calcium-sensing receptors in rat fibroblasts are required for activation of SRC kinase and mitogen-activated protein kinase in response to extracellular calcium," *Journal of Biological Chemistry*, vol. 273, no. 2, pp. 1114–1120, 1998.

[33] J. M. Ray, P. E. Squires, S. B. Curtis, M. R. Meloche, and A. M. J. Buchan, "Expression of the calcium-sensing receptor on human antral gastrin cells in culture," *Journal of Clinical Investigation*, vol. 99, no. 10, pp. 2328–2333, 1997.

[34] N. Chattopadhyay, C. Ye, D. P. Singh et al., "Expression of extracellular calcium-sensing receptor by human lens epithelial cells," *Biochemical and Biophysical Research Communications*, vol. 233, no. 3, pp. 801–805, 1997.

[35] D. Feldser, F. Agani, N. V. Iyer, B. Pak, G. Ferreira, and G. L. Semenza, "Reciprocal positive regulation of hypoxia-inducible factor 1α and insulin-like growth factor 2," *Cancer Research*, vol. 59, no. 16, pp. 3915–3918, 1999.

[36] P. H. Maxwell, "HIF-1's relationship to oxygen: simple yet sophisticated," *Cell Cycle*, vol. 3, no. 2, pp. 156–159, 2004.

[37] R. J. Kewley, M. L. Whitelaw, and A. Chapman-Smith, "The mammalian basic helix-loop-helix/PAS family of transcriptional regulators," *International Journal of Biochemistry and Cell Biology*, vol. 36, no. 2, pp. 189–204, 2004.

[38] J. E. Gunton, R. N. Kulkarni, S. Yim et al., "Loss of ARNT/HIF1β mediates altered gene expression and pancreatic-islet dysfunction in human type 2 diabetes," *Cell*, vol. 122, no. 3, pp. 337–349, 2005.

[39] A. C. R. Epstein, J. M. Gleadle, L. A. McNeill et al., "C-elegans EGL-9 and mammalian homologs define a family of dioxygenases that regulate HIF by prolyl hydroxylation," *Cell*, vol. 107, no. 1, pp. 43–54, 2001.

[40] C. Rosenberger, S. Mandriota, J. S. Jürgensen et al., "Expression of hypoxia-inducible factor-1α and -2α in hypoxic and ischemic rat kidneys," *Journal of the American Society of Nephrology*, vol. 13, no. 7, pp. 1721–1732, 2002.

[41] J. Pouysségur and F. Mechta-Grigoriou, "Redox regulation of the hypoxia-inducible factor," *Biological Chemistry*, vol. 387, no. 10-11, pp. 1337–1346, 2006.

[42] L. E. Fridlyand and L. H. Philipson, "Oxidative reactive species in cell injury: mechanisms in diabetes mellitus and therapeutic approaches," *Annals of the New York Academy of Sciences*, vol. 1066, pp. 136–151, 2005.

[43] N. Li, F. X. Yi, J. L. Spurrier, C. A. Bobrowitz, and A. P. Zou, "Production of superoxide through NADH oxidase in thick ascending limb of Henle's loop in rat kidney," *American Journal of Physiology*, vol. 282, no. 6, pp. F1111–F1119, 2002.

[44] A. A. Banday, A. Marwaha, L. S. Tallam, and M. F. Lokhandwala, "Tempol reduces oxidative stress, improves insulin sensitivity, decreases renal dopamine D1 receptor hyperphosphorylation, and restores D1 receptor-G-protein coupling and function in obese Zucker rats," *Diabetes*, vol. 54, no. 7, pp. 2219–2226, 2005.

Hindawi Publishing Corporation
Experimental Diabetes Research
Volume 2012, Article ID 847246, 8 pages
doi:10.1155/2012/847246

Research Article

Increased Hypothalamic Inflammation Associated with the Susceptibility to Obesity in Rats Exposed to High-Fat Diet

Xiaoke Wang,[1,2] Aiguo Ge,[2] Mengjie Cheng,[2] Fangfang Guo,[2] Min Zhao,[2] Xiaoqi Zhou,[2] Liegang Liu,[2] and Nianhong Yang[2]

[1] *Department of Occupational and Environment Health, School of Public Health, Nantong University, Nantong 226019, China*
[2] *Department of Nutrition and Food Hygiene, MOE Key Lab of Environment and Health, School of Public Health, Tongji Medical College, Huazhong University of Science & Technology, 13 Hangkong Road, Wuhan 430030, China*

Correspondence should be addressed to Nianhong Yang, zynh@mails.tjmu.edu.cn

Received 8 February 2012; Accepted 14 May 2012

Academic Editor: Pietro Galassetti

Inflammation has been implicated in the hypothalamic leptin and insulin resistance resulting defective food intake during high fat diet period. To investigate hypothalamic inflammation in dietary induced obesity (DIO) and obesity resistant (DIO-R) rats, we established rat models of DIO and DIO-R by feeding high fat diet for 10 weeks. Then we switched half of DIO and DIO-R rats to chow food and the other half to high fat diet for the following 8 weeks to explore hypothalamic inflammation response to the low fat diet intervention. Body weight, caloric intake, HOMA-IR, as well as the mRNA expression of hypothalamic TLR4, NF-κB, TNF-α, IL-1β, and IL-6 in DIO/HF rats were significantly increased compared to DIO-R/HF and CF rats, whereas IL-10 mRNA expression was lower in both DIO/HF and DIO-R/HF rats compared with CF rats. Switching to chow food from high fat diet reduced the body weight and improved insulin sensitivity but not affecting the expressions of studied inflammatory genes in DIO rats. Take together, upregulated hypothalamic inflammation may contribute to the overeating and development of obesity susceptibility induced by high fat diet. Switching to chow food had limited role in correcting hypothalamic inflammation in DIO rats during the intervention period.

1. Introduction

The prevalence of obesity is growing rapidly and has become a major public health problem worldwide [1]. Associated with the pathogenesis of type 2 diabetes, hyperlipidemia and the increased risk of cardiovascular mortality [2, 3], obesity can only develop when energy intake exceeds energy expenditure. Dietary fat has been shown to influence eating behavior and the development of obesity [4, 5]. However, both human beings and rodents appear to be different in developing obesity when they exposed to high-fat diet, described as dietary induced obesity (DIO) and dietary induced obesity resistant (DIO-R) [6, 7]. The potential mechanism relating the susceptibility to obesity induced by high-fat diet has not been clearly elucidated.

Obesity is considered to be a chronic low-grade inflammatory state [8]. Many studies have revealed that increased inflammatory response in hypothalamus produces insulin and leptin resistance contributing to the defective food intake both in genetic or dietary fat-induced obesity [9–11]. Recently, considerable evidence suggests the inflammatory response to dietary fat is mediated by TLR (Toll-like receptor) signaling, which result in the activation of NF-κB and production of inflammatory cytokines, such as IL-1β, IL-6, and TNF-α [12–14]. TLRs are pattern-recognition receptors which provide the first line of host defense, and four members of the TLR family including TLR1, 2, 4, and 6, are reported to recognize lipid containing motifs [12, 13]. Emerging study proposed that TLR4 acts as a predominant molecular target for saturated fatty acids in the hypothalamus and triggers the intracellular signaling network that induces an inflammation response and that ultimately results to overeating and obesity [15]. Moreover, genetic deletion designed to disrupt TLR4 signaling protects against high-fat diet-induced obesity [16]. Recent investigations also demonstrated that hypothalamic IKKB/NF-κB was upregulated by high-fat diet and associated

with diminished hypothalamic insulin and leptin signal transduction [17, 18]. Further, experimental and genetic interventions that block the hypothalamic NF-κB signaling reversed hypothalamic insulin and leptin resistance and was associated with reduced food intake and weight loss in the high-fat-induced obesity [17]. These data collectively implicated that the activation of hypothalamic inflammation is necessary and sufficient for the control of food intake and likely involved in the mechanism underlying the pathogenesis of obesity susceptibility during high-fat diet feeding.

We have previously shown that upregulated hypothalamic NPY and Y1, Y2, and Y5 receptor gene expressions were closely associated with being predisposed to obesity and overeating of DIO rats [19]. To our knowledge, no studies have been carried out to investigate the involvement of hypothalamic inflammation on the different susceptibility to obesity between DIO and DIO-R rats and their responses to chow food. The main aim of the present study is to compare the expressions of TLR4, NF-κB, and inflammatory cytokine in the hypothalamus between DIO and DIO-R rats for investigating the underlying mechanism related to obesity susceptibility induced by high-fat diet and their respective responses to low-fat dietary intervention.

2. Materials and Methods

2.1. Animals, Diets, and Experimental Protocols. The experimental protocol was approved by the Animal Care and Use Committee of Huazhong University of Science and Technology. Fifty-five six-week-old outbred male SD rats (purchased from Shanghai Sippr-BK Laboratory Animal Co. Ltd.) weighing 150–160 g were housed individually with regulated temperature (22 ± 5°C) and humidity (50 ± 10%) on a daily cycle of 12 h light and darkness (08:00–20:00 h). All rats were allowed ad libitum access to water and food throughout the experimental period.

After a week acclimation, tail blood was collected and serum was stored under −80°C for further assay. Then the rats were randomly divided into two groups: the HF group ($n = 45$) was placed on a high-fat diet containing 4.62 kcal/g (49.85% fat, 20.00% protein, and 30.15% carbohydrate) and the CF group ($n = 10$) remained on normal laboratory chow food (purchased from Tongji Medical College Laboratory Animal Center, Wuhan, China) containing 3.29 kcal/g (13.68% fat, 21.88% protein, and 64.44% carbohydrate). Dietary intake was recorded daily and body weight was measured weekly in the morning throughout the study. After 10 weeks of free access to their corresponding diet, rats in HF group with body weights more than $\bar{x} + 1.96$ s of CF group were designated as DIO and those with body weight less than $\bar{x} + 1.0$ s of CF group were designated as DIO-R rats. Then one half of the DIO and DIO-R rats were switched to chow food and the other half were kept on HF diets for the following 8 weeks. All rats were provided water and food ad libitum. Terminally, all animals were killed after 12 h fasting between 08:00 and 11:00. Trunk blood was collected and centrifuged and serum was stored for further use. Perirenal and epididymal white adipose tissue was dissected and weighed. Hypothalamus was located and isolated according to brain coronal plane iconography of rat and related articles [20, 21]. Samples of hypothalamic tissues were snap frozen in liquid nitrogen immediately and stored at −80°C for RNA extraction.

2.2. Fasting Serum Glucose and Insulin Assay. Serum glucose level was assayed by an enzymatic kit (Nanjing Jiancheng Bioengineering Institute, Nanjing, China) and serum insulin level was measured by radioimmunoassay kits (Beijing Chemclin Biotechnology Corporation Limited, Beijing, China). HOMA-IR was calculated by (fasting serum glucose × fasting serum insulin)/22.5. All the analyses were conducted in duplicate.

2.3. RNA Preparation and mRNA Quantification by Real-Time PCR. Total RNA was isolated from hypothalamic tissue using the Trizol Reagent Kit (Invitrogen, USA) following the manufacturer's instruction. The total amount of RNA was measured by spectrophotometry at an absorbance of 260 nm and designated the purity valid if the ratio of A260/A280 was in the range from 1.8 to 2.0. The integrity of the RNA was checked by denaturing agarose gel electrophoresis and ethidium bromide staining. 3.0 μg of the total RNA was reverse transcribed by revert Aid First Strand cDNA synthesis kit (Fermentas, CA, USA). The abundances of TLR4, NF-κB, TNF-α, IL-1β, IL-6, IL-10, and glyceraldehyde-3-phosphate dehydrogenase (GAPDH) mRNA were analyzed by real-time polymerase chain reaction (PCR) in the 7900 HT real-time PCR system (Applied Biosystems, Foster, CA, USA). Real-time PCR was performed using the SYBR Premix Ex Taq (TaKaRa Bio Inc.) according to the manufacturer's instructions. Reactions were performed in a total volume of 10 μL containing 1 μL cDNA, 0.2 μL ROX reference Dye, 0.2 μM of each primer and 5 μL of the SYBR Green reaction mix. The amplification protocol was as follows: 95°C/10 s (95°C/5 s, 60°C/30 s) × 40. Following amplification, a dissociation curve analysis was performed to insure purity of PCR product. The specific sense and antisense primers were shown as follows. TLR4 (110 bp), sense: 5′-GCA GAA AAT GCC AGG ATG ATG-3′, antisense: 5′-AAG TAC CTC TAT GCA GGG ATT CAA G −3′; NF-κB (167 bp), sense: ATC TGT TTC CCC TCA TCT TTC, antisense: GTG CGT CTT AGT GGT ATC TGT G; TNF-α (145 bp): sense: 5′-GGA AAG CAT GAT CCG AGA TG-3′, antisense: 5′-CAG TAG ACA GAA GAG CGT GGT G-3′, IL-1β (131 bp): sense: 5′-TGT GAT GTT CCC ATT AGA C-3, antisense: 5′-AAT ACC ACT TGT TGG CTT A-3′; IL-6 (100 bp), sense: 5′ TTG CCT TCT TGG GAC TGA TG 3′, antisense: 5′ ACT GGT CTG TTG TGG GTG GT 3′′; IL-10 (102 bp): sense: 5′-AGG GTT ACT TGG GTT GC-3′, antisense: 5′-ATG CTC CTT GAT TTC TGG-3′; GAPDH (140 bp): sense: 5'-GCA AGT TCA ACG GCA CAG-3′, antisense: 5′-GCC AGT AGA CTC CAC GAC AT-3′. Standard curves for each primer pair were generated by serial dilutions of cDNA from a reference sample and used for regression analyses. All PCR assays were performed in triplicate. The variance of the triplicate measurements was <1%. Results were analyzed using the standard curve method

Table 1: Fasting serum level of glucose, insulin, and HOMA-IR.

	DIO/HF	DIO/CF	DIO-R/HF	DIO-R/CF	CF
FPG (mmol/L)					
0 W	2.61 ± 0.14	2.93 ± 0.10	2.94 ± 0.29	2.86 ± 0.14	2.94 ± 0.04
10 W	5.16 ± 0.12[ab]	5.27 ± 0.11[ab]	4.24 ± 0.09	4.10 ± 0.13	4.12 ± 0.07
18 W	4.96 ± 0.10	4.73 ± 0.20	4.62 ± 0.21	4.60 ± 0.09	4.84 ± 0.10
FINS (μIU/mL)					
0 W	27.02 ± 1.01	23.50 ± 1.29	25.12 ± 1.18	23.70 ± 1.62	23.01 ± 1.13
10 W	54.59 ± 1.39[ab]	55.31 ± 1.06[ab]	43.47 ± 1.31[a]	45.98 ± 1.36[a]	30.18 ± 1.18
18 W	60.16 ± 2.52[abc]	43.55 ± 2.69	45.87 ± 1.01	41.17 ± 2.12	31.66 ± 1.83
HOMA-IR					
0 W	3.24 ± 0.51	3.16 ± 0.20	3.18 ± 0.42	3.11 ± 0.39	3.14 ± 0.03
10 W	12.56 ± 0.85[ab]	12.64 ± 1.12[ab]	8.32 ± 0.08	8.37 ± 1.02	6.52 ± 1.96
18 W	13.36 ± 1.06[abc]	9.25 ± 1.42	9.31 ± 1.03	8.52 ± 1.19	6.91 ± 0.45

Data was shown as mean ± SEM. [a]$P < 0.05$ compared with the CF group; [b]$P < 0.05$ compared with the DIO-R/HF group; [c]$P < 0.05$ compared with their perspective CF intervention group. FPG: fasting serum glucose; FINS: fasting serum insulin; DIO: dietary induced obesity; DIO-R: dietary induced obesity resistant; CF: chow food; DIO/HF: DIO on HF; DIO/CF: DIO on CF; DIO-R/HF: DIO-R on HF; DIO-R/CF: DIO-R on CF.

[22] by the SDS (sequence detection systems) software. The data was expressed as the relative levels of mRNA after normalized with GAPDH.

2.4. Statistical Analysis. The results were expressed as mean ± SEM. Statistical comparisons were assessed by multivariate analysis (MANOVA), followed by Bonferroni post hoc analysis using the SPSS 13.0 statistical package (SPSS Inc., Chicago, IL, USA). In all analyses, a two-tailed probability of less than 5% ($P < 0.05$) was considered to be statistically significant.

3. Results and Discussion

At the end of 10 weeks, rats fed high-fat diet had a wide distribution in body weight and weight gain. 18 of the 45 were designated as DIO and 12 of which were DIO-R and the remains with weight between DIO and DIO-R were excluded from experiments. As presented in Figure 1(a), the body weight in DIO rats was significantly higher than DIO-R or CF rats beginning from 3 weeks to 10 weeks, whereas no significant difference was observed between DIO-R and CF rats throughout the experiment period. During the following 8 weeks, changing the diet to standard chow from high-fat diet reduced the weight gain in DIO rats but not in DIO-R rats (Figure 1(b)). At the end of the experiment, the percentage of fat mass in DIO/HF rats was significantly higher than that in DIO-R/HF and CF rats, while DIO/CF and DIO-R/CF had a lower percentage of fat mass compared with their counterparts on high-fat diet, no significant difference was found between DIO/CF, DIO-R/CF, and CF rats (Figure 1(c)).

Cumulative food intake and energy intake during the first 10 weeks and the following 8 weeks were compared among groups. Over the first 10 weeks, DIO rats had greater food intake than DIO-R rats though they all had free access to high-fat diet (Figure 1(d)). When food intake was calculated as energy intake for the different energy density between chow food and high-fat diet, DIO rats had greater energy intake than DIO-R and CF rats, whereas no significant difference was found between DIO-R and CF groups (Figure 1(e)). After shifting to chow food from high-fat diet, the food intake in both DIO/CF and DIO-R/CF were increased compared with their respective counterpart continued on high-fat diet (Figure 1(f)). No significant difference in energy intake was found among groups during the intervention period (Figure 1(g)).

At the initiation of this experiment, there were no differences among groups in serum glucose, insulin, and HOMA-IR. The serum glucose, insulin, and HOMA-IR in DIO rats were higher than DIO-R and CF rats, no difference was found between DIO-R and CF rats after 10 weeks. Switching to standard chow from the high-fat diet, serum insulin and HOMA-IR in DIO/CF rats were finally reduced compared with DIO/HF rats and similar to that in CF rats, while no difference was found between DIO-R/CF and DIO-R/HF rats (Table 1).

As shown in Figures 2(a) and 2(b), the hypothalamic expression of genes encoding TLR4 and NF-κB mRNA were significantly increased in DIO/HF rats as compared to DIO-R/HF and CF rats, no significant difference was detected between DIO-R/HF and CF rats. Changing the diet from the high-fat diet to chow food did not affect the level of hypothalamic TLR4 and NF-κB mRNA expression both in DIO and DIO-R rats. Hypothalamic TNF-α, IL-1β, and IL-6 mRNA expressions in DIO/HF rats were higher compared with the DIO-R/HF and CF rats, no difference was found between DIO-R/HF and CF rats. Switching diet to chow food from high-fat diet did not affect the TNF-α, IL-1β, and IL-6 expression in hypothalamus of DIO rats (Figures 2(c), 2(d) and 2(e)). The anti-inflammatory cytokine IL-10 mRNA expression was lower both in DIO/HF and DIO-R/HF rats compared with CF rats, but only restored in DIO-R/HF rats by switching to chow food (Figure 2(f)).

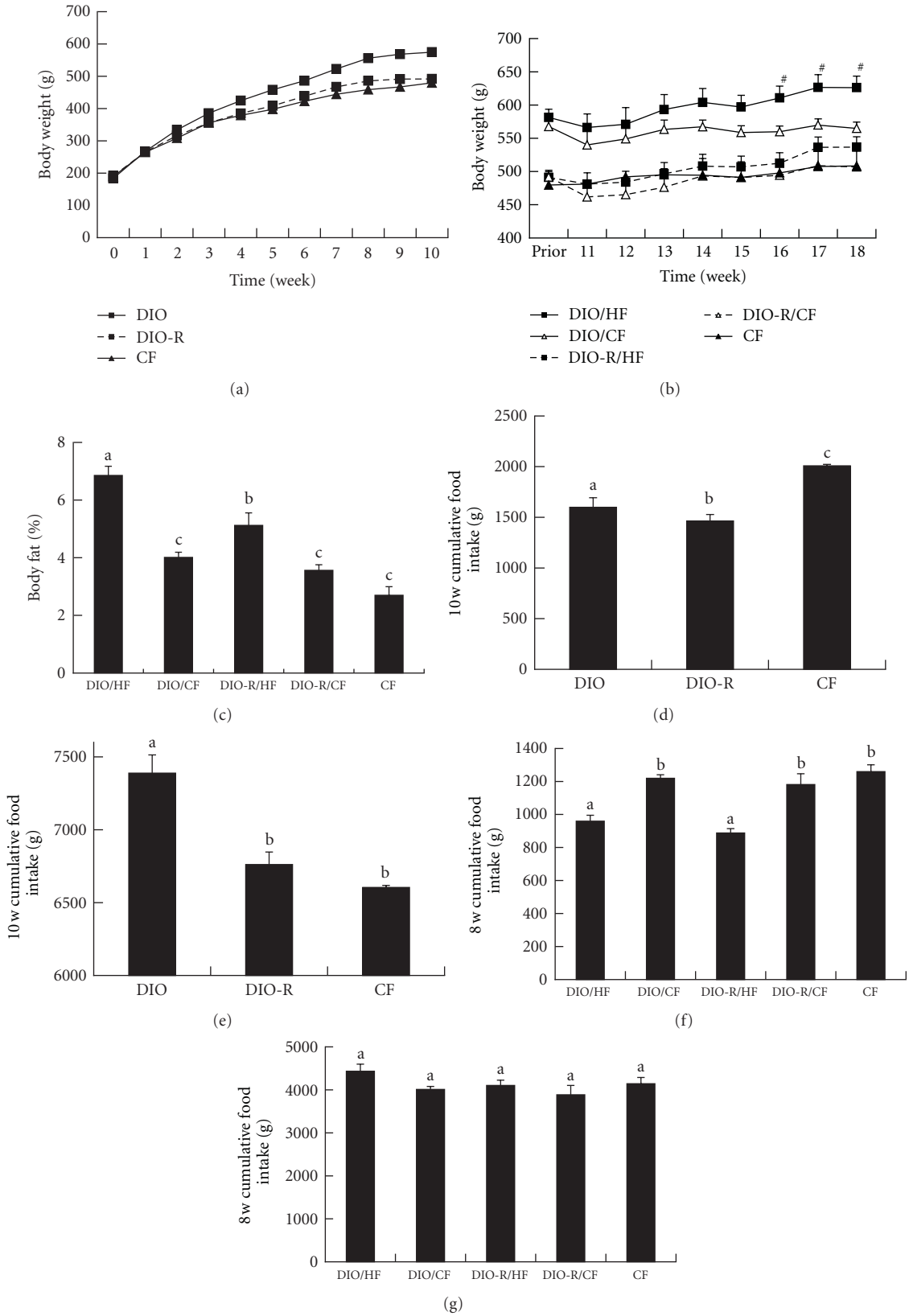

Figure 1: Body weight in DIO, DIO-R, and CF groups during the 10 weeks (a) and the change over 8 weeks dietary intervention (b) was observed weekly. Body fat in each group was measured at 18th (c). Cumulative food intake (d and f), cumulative energy intake (e and g) were obtained in different periods and results expressed as mean ± SEM. $^{*}P < 0.05$ for DIO versus DIO-R or CF; $^{\#}P < 0.05$ for DIO/HF versus DIO/CF. Groups sharing different letters above the bars mean statistically significant differences ($P < 0.05$), while those denoted by the same letters are insignificant. DIO: dietary induced obesity; DIO-R: dietary induced obesity resistant; CF: chow food; DIO/HF: DIO on HF; DIO/CF: DIO on CF; DIO-R/HF: DIO-R on HF; DIO-R/CF: DIO-R on CF.

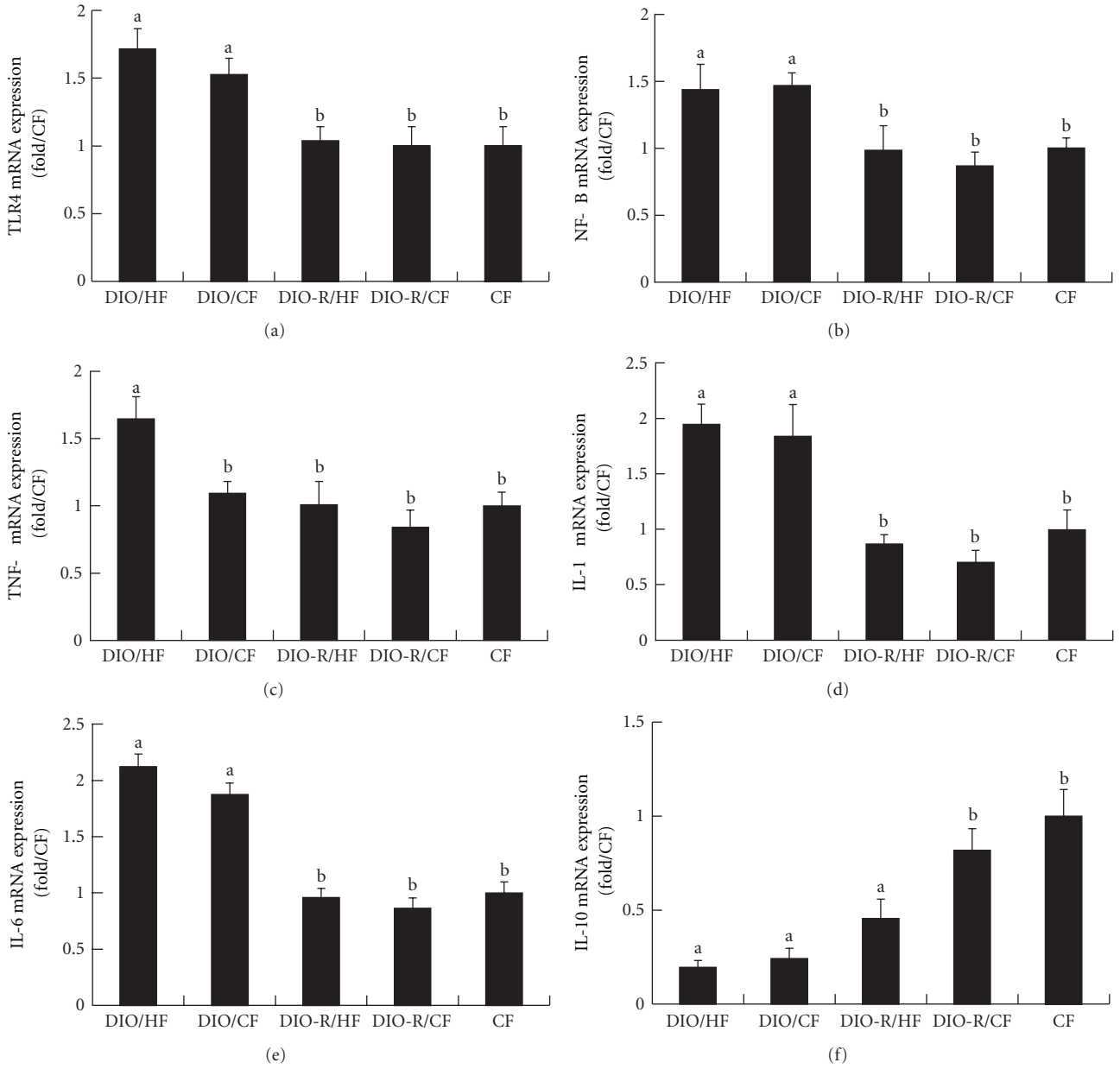

Figure 2: Relative mRNA expression of TLR4 (a), NF-κB (b), TNF-α (c), IL-1β (d), IL-6 (e), and IL-10 (f) in hypothalamus was measured by real-time PCR in each group at 18th week. All results were normalized to GAPDH and expressed as arbitrary units. Data was shown as mean ± SEM. Groups sharing different letters above the bars mean statistically significant differences ($P < 0.05$), while those denoted by the same letters are insignificant. DIO: dietary induced obesity; DIO-R: dietary induced obesity resistant; CF: chow food; DIO/HF: DIO on HF; DIO/CF: DIO on CF; DIO-R/HF: DIO-R on HF; DIO-R/CF: DIO-R on CF.

This study compared hypothalamic inflammation between high-fat diet-induced obese and obese-resistant rats and their responses to chow food intervention. The main finding is as follows: (1) DIO/HF rats but not DIO-R/HF rats exhibited significant increase in TLR4, NF-κB, TNF-α, IL-1β, and IL-6 mRNA expression as well as energy intake when compared to CF controls. (2) Switching from high-fat diet to chow food failed to affect hypothalamic TLR4, NF-κB, TNF-α, IL-1β, and IL-6 mRNA expression both in DIO and DIO-R rats except an increased IL-10 mRNA expression in DIO-R rats. (3) DIO/CF rats remained higher hypothalamic TLR4, NF-κB, TNF-α, IL-1β, and IL-6 mRNA expression than DIO-R/CF rats.

It is generally accepted that obesity results from the complex interaction of genetic components that predispose to obesity and environment which facilitates the development of obese phenotype [23]. Although high-fat diet is among the most important environment factors leading to obesity, both rodent and human beings showed different susceptibility to obesity in response to a high-fat diet [6, 24]

and models of diet-induced obesity are commonly used to study the human obesity in the context of an environment where energy-dense foods and diets are highly available. Our present study confirmed that the outbred SD rats exhibited different phenotype after exposed to high-fat diet. The increased energy intake appeared to be primarily responsible for the increased weight gain in DIO rats on high-fat diet ad libitum, while DIO-R rats exposed to high-fat diet compensated for the increased energy density of the high-fat diet by eating significantly less, similar to the previous studies [25, 26].

There is an intimate relationship between the immune and metabolic systems during the evolutionary period and might allow nutrients to act through pathogen-sensing pathway for storing energy and fighting off the infection [27]. In the presence of abundance nutritional surplus, this once advantageous immune-metabolic system contributes to the excess energy intake and adiposity. TLRs, especially TLR4, were shown to act as the receptor both for pathogens and saturated fatty acid [28, 29], giving rise to interaction between immune response and metabolic system. Recently, investigators proposed that activated hypothalamic TLR4/NF-κB and the production of inflammatory cytokines were implicated in the defective food intake after exposure to dietary fat [9, 15, 17]. In the present study, we found that hypothalamic TLR4, NF-κB, TNF-α, IL-1β, and IL-6 mRNA expressions were significantly higher in DIO/HF rats compared with DIO-R/HF and CF rats. Similar to the results in our study, Zhang et al. [17] have shown that the hypothalamic NF-κB activity was 5- to 6-fold higher in $ob^{+/+}$ mice (a hyperphagic obesity) compared with the wild type controls even both fed normal chow, implicating that higher inflammation response in hypothalamus was associated with obesity susceptibility. An observation from a pair-feeding model showed that the rats fed the high-fat diet had higher IKKB expression and reduced IκBα expression in hypothalamus compared with the rats that consumed the same amount of calories from the low-fat diet [18], which conflicts with the result in our study that there is no significant difference in hypothalamic inflammation between DIO-R/HF rats and CF rats even though they consumed the same amount of calories. One potential explanation for this phenomenon is the use of a different rat model and DIO-R/HF rats may have the inherent physicochemical properties to normal the central inflammatory response for governing energy balance. Combined with insulin resistance and increased energy intake in DIO/HF rats, these findings suggested that upregulated hypothalamic inflammation may lead DIO/HF rats to consume more energy and obtains more weight than DIO-R/HF rats when fed with the same high-fat diet ad libitum, while DIO-R/HF rats could appropriately adjust caloric intake by preventing increased hypothalamic inflammation. And the reason why DIO-R/HF rats could automatically prevent the increased hypothalamic inflammatory response in DIO-R/HF rats needs further study.

Low-fat diet has been investigated extensively for reversibility of chronic high-energy diet-induced obesity [30, 31]. However, the result was controversial for the genetic background, duration of high-fat diet and food palatability [32]. In the present study, DIO rats switched to chow (DIO/CF), lost their body weight, and finally improved insulin sensitivity, concurring with the previous study [33–35], whereas there was no significant alteration in either hypothalamic inflammatory or anti-inflammatory cytokine between the DIO/HF and DIO/CF groups. Combined with no difference in energy intake between the DIO/HF and DIO/CF groups during the intervention period, this result implicates that the weight loss and improved insulin sensitivity in DIO/CF rats may be mediated mainly through reduced fat content in chow food, independent of the total energy intake by correcting hypothalamic inflammation. Previous studies have revealed that hypothalamic leptin resistance was associated with inflammation [15, 36] and reversed by 20 weeks of low-fat diet feeding [33], suggesting that the hypothalamic inflammation could be improved by low-fat diet. However, the studied hypothalamic inflammation genes were not altered after chow food intervention in the present study. One potential explanation is that 8 weeks intervention period in our study is not enough to ameliorate the hypothalamic inflammation and additional research of prolonged intervention is warranted.

It is believed that inflammation produced by hypertrophied adipose tissues is a strong driving force for the development of type 2 diabetes [37, 38]. Recent studies demonstrated that hypothalamic inflammation induced by chronic high-fat diet could not only cause feeding and body weight changes, but also employ body weight-independent manners to cause systemic glucose intolerance [17, 39]. The mechanism underlying is possibly related to induction of central leptin and insulin resistance. Further studies are needed to elucidate the role of hypothalamic inflammation in the induction of central leptin and insulin resistance.

4. Conclusions

Taken together, this study showed that the DIO rats appear to have higher energy intake and greater fat storage and body weight than the DIO-R rats when both have free access to high-energy-density diet. Excessive energy intake and body weight gain in DIO rats was attributed to the activated hypothalamic inflammation induced by high-fat diet. Switching to low-fat chow failed to recover hypothalamic inflammation, although body weight and fat pad were decreased and insulin sensitivity was improved in DIO/CF rats. The limitation of this study is that we assessed the contribution of inflammation response to feeding behavior and obesity phenotype after DIO and DIO-R had already occurred. The inflammatory response evolved over time after exposure to high-fat diet and early response in hypothalamus which may trigger distinct intermediate responses that in turn lead to different late responses. Further studies with different feeding periods and regimes are warranted.

Abbreviations

DIO: Dietary induced obesity
DIO-R: Dietary induced obesity resistant
CF: Chow food

DIO/HF:	DIO on HF
DIO/CF:	DIO on CF
DIO-R/HF:	DIO-R on HF
DIO-R/CF:	DIO-R on CF
TLR4:	Toll-like receptor-4
NF-κB:	Nuclear factor κB
TNF-α:	Tumor necrosis factor-α
IL-1β:	Interleukin-1β
IL-6:	Interleukin-6
IL-10:	Interleukin-10
Real-time PCR:	Real-time polymerase chain reaction.

Conflict of Interests

The authors declare that they have no conflict of interests.

Funding

The study sponsors had no involvement in design; in collection, analysis, or interpretation of data; in writing of the report; or in the decision to submit the paper for publication.

Acknowledgments

The study was supported by National Natural Science Foundation of China (NSFC30671765) and Natural Science Foundation of Hubei Province (NSFH 2009CDB253).

References

[1] D. Yach, D. Stuckler, and K. D. Brownell, "Epidemiologic and economic consequences of the global epidemics of obesity and diabetes," *Nature Medicine*, vol. 12, no. 1, pp. 62–66, 2006.

[2] Y. Wang, E. B. Rimm, M. J. Stampfer, W. C. Willett, and F. B. Hu, "Comparison of abdominal adiposity and overall obesity in predicting risk of type 2 diabetes among men," *American Journal of Clinical Nutrition*, vol. 81, no. 3, pp. 555–563, 2005.

[3] J. Ärnlöv, E. Ingelsson, J. Sundström, and L. Lind, "Impact of body mass index and the metabolic syndrome on the risk of cardiovascular disease and death in middle-aged men," *Circulation*, vol. 121, no. 2, pp. 230–236, 2010.

[4] G. A. Bray and B. M. Popkin, "Dietary fat intake does affect obesity," *American Journal of Clinical Nutrition*, vol. 68, no. 6, pp. 1157–1173, 1998.

[5] B. E. Levin and R. E. Keesey, "Defense of differfing body weight set points in diet-induced obese and resistant rats," *American Journal of Physiology*, vol. 274, no. 2, pp. R412–R419, 1998.

[6] C. Bouchard and A. Tremblay, "Genetic influences on the response of body fat and fat distribution to positive and negative energy balances in human identical twins," *Journal of Nutrition*, vol. 127, no. 5, supplement, pp. 943S–947S, 1997.

[7] B. E. Levin, J. Triscari, S. Hogan, and A. C. Sullivan, "Resistance to diet-induced obesity: food intake, pancreatic sympathetic tone, and insulin," *American Journal of Physiology*, vol. 252, no. 3, pp. R471–R478, 1987.

[8] J. P. Bastard, M. Maachi, C. Lagathu et al., "Recent advances in the relationship between obesity, inflammation, and insulin resistance," *European Cytokine Network*, vol. 17, no. 1, pp. 4–12, 2006.

[9] C. T. De Souza, E. P. Araujo, S. Bordin et al., "Consumption of a fat-rich diet activates a proinflammatory response and induces insulin resistance in the hypothalamus," *Endocrinology*, vol. 146, no. 10, pp. 4192–4199, 2005.

[10] J. B. C. Carvalheira, E. B. Ribeiro, E. P. Araújo et al., "Selective impairment of insulin signalling in the hypothalamus of obese Zucker rats," *Diabetologia*, vol. 46, no. 12, pp. 1629–1640, 2003.

[11] J. K. Howard, B. J. Cave, L. J. Oksanen, I. Tzameli, C. Bjoørbæk, and J. S. Flier, "Enhanced leptin sensitivity and attenuation of diet-induced obesity in mice with haploinsufficiency of Socs3," *Nature Medicine*, vol. 10, no. 7, pp. 734–738, 2004.

[12] S. Akira, S. Uematsu, and O. Takeuchi, "Pathogen recognition and innate immunity," *Cell*, vol. 124, no. 4, pp. 783–801, 2006.

[13] S. Akira and K. Takeda, "Toll-like receptor signalling," *Nature Reviews Immunology*, vol. 4, no. 7, pp. 499–511, 2004.

[14] M. S. Hayden and S. Ghosh, "Shared principles in NF-κB signaling," *Cell*, vol. 132, no. 3, pp. 344–362, 2008.

[15] M. Milanski, G. Degasperi, A. Coope et al., "Saturated fatty acids produce an inflammatory response predominantly through the activation of TLR4 signaling in hypothalamus: implications for the pathogenesis of obesity," *Journal of Neuroscience*, vol. 29, no. 2, pp. 359–370, 2009.

[16] D. M. L. Tsukumo, M. A. Carvalho-Filho, J. B. C. Carvalheira et al., "Loss-of-function mutation in toll-like receptor 4 prevents diet-induced obesity and insulin resistance," *Diabetes*, vol. 56, no. 8, pp. 1986–1998, 2007.

[17] X. Zhang, G. Zhang, H. Zhang, M. Karin, H. Bai, and D. Cai, "Hypothalamic IKKβ/NF-κB and ER stress link overnutrition to energy imbalance and obesity," *Cell*, vol. 135, no. 1, pp. 61–73, 2008.

[18] K. A. Posey, D. J. Clegg, R. L. Printz et al., "Hypothalamic proinflammatory lipid accumulation, inflammation, and insulin resistance in rats fed a high-fat diet," *American Journal of Physiology*, vol. 296, no. 5, pp. E1003–E1012, 2009.

[19] C. Wang, N. Yang, S. Wu, L. Liu, X. Sun, and S. Nie, "Difference of NPY and its receptor gene expressions between obesity and obesity-resistant rats in response to high-fat diet," *Hormone and Metabolic Research*, vol. 39, no. 4, pp. 262–267, 2007.

[20] Y. S. Allen, T. E. Adrian, and J. M. Allen, "Neuropeptide Y distribution in the rat brain," *Science*, vol. 221, no. 4613, pp. 872–879, 1983.

[21] B. Beck, "Intracerebroventricular injection of proinsulin C-peptide does not influence food consumption in male long-evans rats," *Hormone and Metabolic Research*, vol. 38, no. 5, pp. 314–316, 2006.

[22] A. Larionov, A. Krause, and W. R. Miller, "A standard curve based method for relative real time PCR data processing," *BMC Bioinformatics*, vol. 6, article 62, 2005.

[23] L. Perusse and C. Bouchard, "Gene-diet interactions in obesity," *American Journal of Clinical Nutrition*, vol. 72, no. 5, supplement, pp. 1285S–1290S, 2000.

[24] B. E. Levin, J. Triscari, and A. C. Sullivan, "Metabolic features of diet-induced obesity without hyperphagia in young rats," *American Journal of Physiology*, vol. 251, no. 3, pp. R433–R440, 1986.

[25] B. E. Levin, S. Hogan, and A. C. Sullivan, "Initiation and perpetuation of obesity and obesity resistance in rats," *American Journal of Physiology*, vol. 256, no. 3, pp. R766–R771, 1989.

[26] M. R. Ricci and B. E. Levin, "Ontogeny of diet-induced obesity in selectively bred sprague-dawley rats," *American Journal of Physiology*, vol. 285, no. 3, pp. R610–R618, 2003.

[27] L. Sondergaard, "Homology between the mammalian liver and Drosophila fat body," *Trends in Genetics*, vol. 9, no. 6, p. 193, 1993.
[28] R. Medzhitov, "Toll-like receptors and innate immunity," *Nature Reviews Immunology*, vol. 1, no. 2, pp. 135–145, 2001.
[29] M. B. Fessler, L. L. Rudel, and J. M. Brown, "Toll-like receptor signaling links dietary fatty acids to the metabolic syndrome," *Current Opinion in Lipidology*, vol. 20, no. 5, pp. 379–385, 2009.
[30] A. Kendall, D. A. Levitsky, B. J. Strupp, and L. Lissner, "Weight loss on a low-fat diet: consequence of the imprecision of the control of food intake in humans," *American Journal of Clinical Nutrition*, vol. 53, no. 5, pp. 1124–1129, 1991.
[31] H. Wang, L. H. Storlien, and X. F. Huang, "Effects of dietary fat types on body fatness, leptin, and ARC leptin receptor, NPY, and AgRP mRNA expression," *American Journal of Physiology*, vol. 282, no. 6, pp. E1352–E1359, 2002.
[32] J. O. Hill, J. Dorton, M. N. Sykes, and M. Digirolamo, "Reversal of dietary obesity is influenced by its duration and severity," *International Journal of Obesity*, vol. 13, no. 5, pp. 711–722, 1989.
[33] P. J. Enriori, A. E. Evans, P. Sinnayah et al., "Diet-induced obesity causes severe but reversible leptin resistance in arcuate melanocortin neurons," *Cell Metabolism*, vol. 5, no. 3, pp. 181–194, 2007.
[34] X. F. Huang, X. Xin, P. McLennan, and L. Storlien, "Role of fat amount and type in ameliorating diet-induced obesity: insights at the level of hypothalamic arcuate nucleus leptin receptor, neuropeptide Y and pro-opiomelanocortin mRNA expression," *Diabetes, Obesity and Metabolism*, vol. 6, no. 1, pp. 35–44, 2004.
[35] I. S. Lee, G. Shin, and R. Choue, "Shifts in diet from high fat to high carbohydrate improved levels of adipokines and pro-inflammatory cytokines in mice fed a high-fat diet," *Endocrine Journal*, vol. 57, no. 1, pp. 39–50, 2010.
[36] A. Kleinridders, D. Schenten, A. C. Könner et al., "MyD88 signaling in the CNS is required for development of fatty acid-induced leptin resistance and diet-induced obesity," *Cell Metabolism*, vol. 10, no. 4, pp. 249–259, 2009.
[37] G. S. Hotamisligil, "Inflammation and metabolic disorders," *Nature*, vol. 444, no. 7121, pp. 860–867, 2006.
[38] G. S. Hotamisligil, "Endoplasmic reticulum stress and the inflammatory basis of metabolic disease," *Cell*, vol. 140, no. 6, pp. 900–917, 2010.
[39] A. P. Arruda, M. Milanski, A. Coope et al., "Low-grade hypothalamic inflammation leads to defective thermogenesis, insulin resistance, and impaired insulin secretion," *Endocrinology*, vol. 152, no. 4, pp. 1314–1326, 2011.

Hindawi Publishing Corporation
Experimental Diabetes Research
Volume 2012, Article ID 905683, 7 pages
doi:10.1155/2012/905683

Research Article

Effects of Rosiglitazone with Insulin Combination Therapy on Oxidative Stress and Lipid Profile in Left Ventricular Muscles of Diabetic Rats

Servet Kavak,[1] Lokman Ayaz,[2] and Mustafa Emre[3]

[1] *Department of Biophysics, Faculty of Medicine, Yüzüncü Yıl University, 65100 Van, Turkey*
[2] *Department of Biochemistry, Faculty of Medicine, Mersin University, 33343 Mersin, Turkey*
[3] *Department of Biophysics, Faculty of Medicine, Çukurova University, 01330 Adana, Turkey*

Correspondence should be addressed to Servet Kavak, skavak@yyu.edu.tr

Received 13 February 2012; Accepted 1 May 2012

Academic Editor: Pietro Galassetti

Purpose. In this study, we tested the hypothesis that rosiglitazone (RSG) with insulin is able to quench oxidative stress initiated by high glucose through prevention of NAD(P)H oxidase activation. *Methods and Materials*. Male albino Wistar rats were randomly divided into an untreated control group (C), a diabetic group (D) that was treated with a single intraperitoneal injection of streptozotocin (45 $mgkg^{-1}$), and rosiglitazone group that was treated with RSG twice daily by gavage and insulin once daily by subcutaneous injection (group B). HbA1c and blood glucose levels in the circulation and malondialdehyde and 3-nitrotyrosine levels in left ventricular muscle were measured. *Result*. Treatment of D rats with group B resulted in a time-dependent decrease in blood glucose. We found that the lipid profile and HbA1c levels in group B reached the control group D rat values at the end of the treatment period. There was an increase in 3-nitrotyrosine levels in group D compared to group C. Malondialdehyde and 3-nitrotyrosine levels were found to be decreased in group B compared to group D ($P < 0.05$). *Conclusion*. Our data suggests that the treatment of diabetic rats with group B for 8 weeks may decrease the oxidative/nitrosative stress in left ventricular tissue of rats. Thus, in diabetes-related vascular diseases, group B treatment may be cardioprotective.

1. Introduction

Hyperglycemia induces protein glycation, systemic low grade inflammation, and endothelial dysfunction [1]. As a consequence, diabetes is one of the main risk factor for cardiovascular disease. Hyperglycemia-induced endothelial dysfunction is characterized by an enhanced production of reactive oxygen species (ROS), which are important actors in the development of vascular damage. Consistently, antioxidant agents are able to rescue hyperglycemia-induced vascular dysfunction [1, 2].

Insulin resistance is a fundamental abnormality in the pathogenesis of type-2 diabetes. A number of different mechanisms have been proposed to explain the mechanism of insulin resistance. Recent information suggests that a common feature of the development of insulin resistance is an increased production of ROS and that reduction in ROS production results in improved insulin sensitivity [3].

Rosiglitazone, a member of the thiazolidinediones (TZD) class of antidiabetic agents, is an agonist of the nuclear hormone receptor peroxisome proliferator gamma (PPARγ). Expression of these receptors is most abundant in adipose tissue where they play a central role in adipogenesis and lipid metabolism [4].

Thiazolidinediones (TZD) are used clinically in diabetic patients by virtue of their insulin-sensitizing action, conveyed by the activation of the nuclear transcription factor PPARγ [5]. In addition, these agents have remarkable pleiotropic activities: by improving endothelial function and systemic inflammation, they are expected to exert direct beneficial effects on cardiovascular risk, which are not mediated by the improvement in glucose metabolism. In this regard, pioglitazone was shown to abolish ROS production in 3T3-L1 adipocytes [6], whereas RSG reduced NADPH-stimulated superoxide production in aortas from diabetic mice [7], and

troglitazone diminished ROS generation in leukocytes from obese subjects [8]. However, the molecular mechanism by which TZDs attenuate oxidative stress is not clear.

PPAR-γ activation reduced O^{2-} generation and NADPH oxidase expression in vascular endothelial cells in vitro and increased NO production through PPARγ-dependent mechanisms [9].

In this study, treatment of insulin and rosiglitazone may decrease oxidative stress in diabetic rats, which may be cardioprotective in setting diabetic vascular disease, Therefore, the aim of the present study was to dissect the molecular mechanisms underlying the effects of RSG on hyperglycemia-induced ROS production.

2. Material and Method

2.1. Animal Handling and Treatment Protocol. Twenty-four healthy male Wistar albino male rats (250–320 g) were selected for the study. All animal procedures were performed according to the Guide for the Care and Use of Laboratory Animals of the US National Institutes of Health and approval of the ethics committee of our institution was obtained before the commencement of the study. The diabetic rat model used in our experiments was based on partial damage of pancreatic beta-cells resulting from a single administration of streptozotocin (45 mg/kg, STZ, Sigma Chemical Co., USA) intravenously (dissolved in 0.01 M sodium citrate, pH adjusted to 4.5). This model of experimental diabetes is associated with partial deficits in insulin secretion and consequential hyperglycaemia, without changes in peripheral insulin resistance [10]. STZ-injected animals were accepted as diabetic if blood glucose levels were more than 200 mg/dL [11, 12] using a glucometer (Aquo-Check, Roche) after a one-week period and at least three high blood glucose levels.

We used three groups randomly constituted four groups: (1) Nondiabetic control animals (C): rats orally fed with standard rat nutrients and water, and (2) diabetic group (D), and (3) rosiglitazone with insulin group (B) treated diabetic animals group (B) rats treated with 4 mg/kg/day RSG two times a day by gavage and Insulin Treatment Protocols eight weeks after the initial STZ injections, diabetic animals were randomly divided into one group. One group of these animals was placed on an insulin regimen (NPH Ilentin II, intermediate acting) for 8 weeks. Insulin doses were individually adjusted so as to maintain euglycemic states and varied between 1 uU/kg (s.c.), given once per day between 9:00 AM. Animals were fed with standard rat nutrient and water without restriction throughout the experiment. Rosiglitazone-treated groups were given group B for 8 weeks and blood glucose levels as well as body weights were measured once weekly.

2.1.1. Isolation of Left Ventricular Muscles. Wistar albino rats were anesthetized with dietyl ether. Hearts were rapidly removed and the left ventricular muscles were dissected. The muscle was mounted in a Petri cup (about 2 mL volume) and perfused continuously (6–8 mL min^{-1}) with oxygenated (95% O_2 and 5% CO_2) krebs buffer, (constituents in mmol L^{-1}: 113 NaCl, 4.7 KCL, 1.2 $MgSO_4 \cdot 7H_2O$, 1.9 $CaCl_2 \cdot 2H_2O$, 1.2 KH_2PO_4, 25 $NaHCO_3$ 11.5 glucose, pH 7,4) solution at a constant flow rate.

2.2. Biochemical Analysis

2.2.1. Measurements of HbA1c and Lipid Parameters. Blood plasma HbA1c was determined immunoturbidimetrically (*Pfeiffer M*). Triacylglycerol (TAG), total cholesterol (TC), and high-density lipoprotein-cholesterol (HDL-C) were analyzed by glycerophosphate oxidase, peroxidase/4-aminophenazone (GPO/PAP), cholesterol oxidase, peroxidase/4-aminophenazone (CHOD/PAP), and direct COHD/PAP enzymatic colorimetric methods, respectively. The very low density lipoprotein-cholesterol (VLDL-C) and low density lipoprotein-cholesterol (LDL-C) was calculated according to the equation described by Friedewald et al. [13]. All these parameters were determined by Cobas Integra 800 biochemical analyzer (Roche Diagnostics, GmbH, Mannheim, Germany).

2.2.2. Measurement of Malondialdehyde. A tissue specimen of 50 mg was homogenized in 0.15 mol/L KCL. After the homogenate had been centrifuged at 1600 rpm, the MDA levels in tissue homogenate supernatant were determined by the thiobarbituric acid (TBA) reaction according to Yagi [14]. The principle of the method is based on measuring absorbance of the pink color produced by the interaction of TBA with MDA at 530 nm. Values were expressed as nmol/mL.

2.2.3. Measurement of 3-Nitroyrosine. 3-NT and tyrosine were obtained from Sigma Chemical (St. Louis, USA). H_2O_2, sodium acetate, citrate, NaOH, HCL, H_3PO_4, KH_2PO_4, and K_2HPO_4 were purchased from Merck Chemical (Deisenhofen, Germany). All organic solvents were HPLC grade. The tissues were homogenized in ice-cold phosphate-buffered saline (pH 7.4). Equivalent amounts of each sample were hydrolyzed in 6 N HCI at 100°C for 18–24 h, and then samples were analyzed on an Agilent 1100 series HPLC apparatus (Germany). The analytical column was a 5 μm pore size Spherisorb ODS-2 C_{18} reverse-phase column (4.6 × 250 mm; HICHROM, Waters Spherisorb, UK). The guard column was a C_{18} cartridge (HICHROM, Waters Spherisorb, UK). The mobile phase was 50 mmol/L sodium acetate/50 mmol/L citrate/8% (v/v) methanol, and pH 3.1. HPLC analysis was performed under isocratic conditions at a flow rate of 1 mL min^{-1} and UV detector set at 274 nm. 3-NT and tyrosine peaks were determined according to their retention times and the peaks were confirmed by spiking with added exogenous 3-NT [15] and tyrosine (10 μmol/L). 3-NT levels were expressed as 3-NT/total tyrosine.

2.3. Statistical Analysis. The results were expressed as mean ± standard deviation (SD). Kruskal-Wallis (which is nonparametric) test was used for the comparison of groups. When significant differences were observed ($P < 0.05$), Tukey multiple comparison test was used to determine

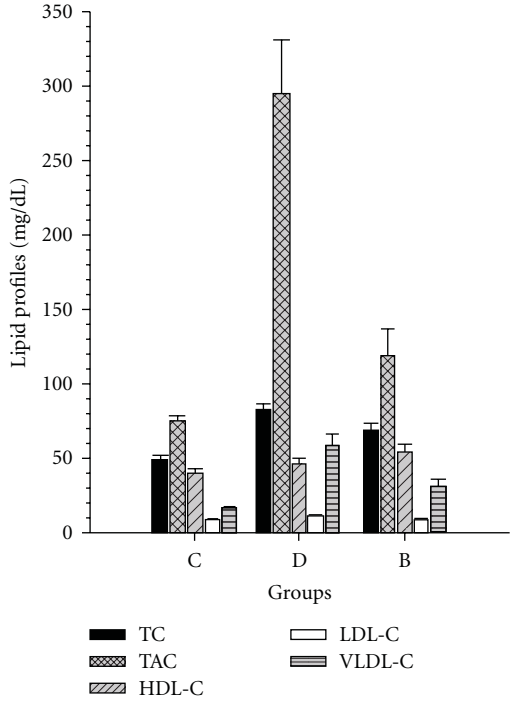

Figure 1: The effects of rosiglitazone with insulin combine on lipid prolifies. C: control rats, D: diabetic rat, group B: rosiglitazone with insulin-treated diabetic rats. Data are expressed as mean + SEM. $^{*}P < 0.001$ in D compared with group B, C. TAG: triacylglycerol, TC: total cholesterol, HDL-C: high-density lipoprotein-cholesterol VLDL-C; very low-density lipoprotein-cholesterol, LDL-C; low-density lipoprotein-cholesterol.

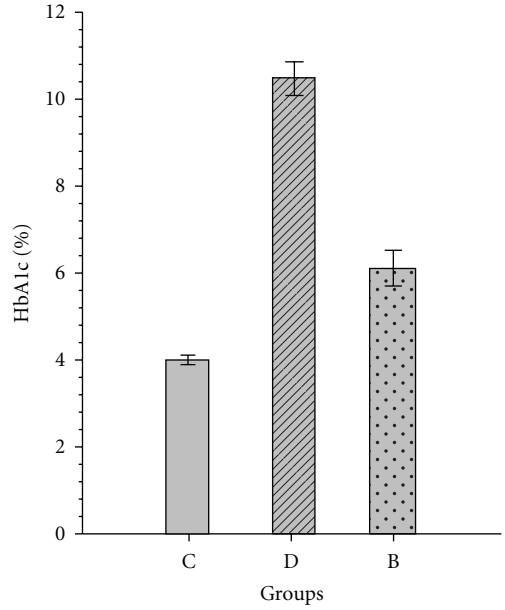

Figure 2: The effects of rosiglitazone with insulin combine on HbA1c. C: control rats, D: diabetic rat, group B: rosiglitazone with insulin-treated diabetic rats. Data are expressed as mean + SEM. $^{*}P < 0.001$ in D compared with groups B and C. HbA1c: hemoglobin A1c.

the difference between groups. Statistical analyses were carried out using the SPSS statistical software package (SPSS for Windows version 13.0, SPSS Inc., Chicago, Illinois, USA).

3. Results

3.1. Effects of Rosiglitazone with Insulin Combination on HbA1c and Lipid Profiles Tolerance in Control and Diabetic Rats. TAG: triacylglycerol, TC: total cholesterol, HDL-C: high-density lipoprotein-cholesterol, VLDL-C: very low-density lipoprotein-cholesterol, LDL-C: low-density lipoprotein-cholesterol levels of study groups are shown in Figures 1 and 2. Group B had significant effects on HbA1c and lipid profiles in diabetic rats ($P < 0.05$). HbA1c and TC, TAG and VLDL levels were significantly increased in diabetic group compared with C group ($P < 0.05$). LDL-C levels were not significantly different between groups (Figures 1 and 2).

3.2. Effects of Rosiglitazone with Insulin Combination on Blood Glucose in Control and Diabetic Rats. Treatment of D rats with group B resulted in a time-dependent decrease in blood glucose levels. The reduction in blood glucose became significant by week 2 of treatment compared to the diabetic groups ($P < 0.05$) (Table 1). At the end of the study period, the diabetic group had lower body weights than the control group ($P < 0.05$). Treatment of diabetic rats with group B for 8 weeks showed a significant increase (27.3%) in the body weight compared to the diabetic group ($P < 0.05$). On the other hand, D rats for 8 weeks resulted in a significant decrease (39.9%) in the body weight compared to the control group ($P < 0.05$) (Table 2).

3.3. Effects of Rosiglitazone with Insulin Combination Therapy on Malondialdehyde Levels in Control and Diabetic Rats. Treatment of diabetic rats with RSG (4 mg/kg/day) for 8 weeks brought about a significant decrease at MDA levels compared with the C groups ($P < 0.001$). MDA levels in D + RSG group were not significantly compared with the B groups. In the diabetic group, MDA levels were found to be increased compared with the C ($P < 0.04$), D + RSG, D + INS, group B ($P < 0.001$) groups and the differences between these groups were significant. MDA levels were not statistically significant between the C and B groups. MDA levels in the C group were significantly different compared to the group B ($P < 0.003$) (Figure 3).

3.4. Effects of Rosiglitazone with Insulin Combination Therapy on 3-Nitroyrosine Levels in Control and Diabetic Rats. 3-NT levels in the C group were not significantly different compared to the D + RSG and D + INS groups. In diabetic group, 3-NT levels were found to be increased when compared with C and B groups and the differences between these groups were significant, respectively ($P < 0.005$). There were no statistically significant differences between the B groups. Treatment of diabetic rats with group B (4 mg/kg/day and 1 uU/kg^{-1}) for 8 weeks brought about a significant decrease

Table 1: Blood glucose levels in the study groups.

	Weeks								
Groups	0	1	2	3	4	5	6	7	8
C (mg/dL)	99.1 ± 1.1	101.2 ± 1.9	102.0 ± 1.7	99.6 ± 1.7	99.1 ± 1.2	98.8 ± 1.7	99.4 ± 1.4	101.1 ± 2.7	100.7 ± 1.6
D (mg/dL)	102.5 ± 1.8	275.8 ± *10.0	301.9 ± *4.8	306.9 ± *10.1	318.5 ± *16.3	319.6 ± *11.8	321.5 ± *9.3	322.2 ± *9.7	335.7 ± *16.7
B (mg/dL)	92.2 ± 3.1	306.3 ± 7.8	273.5 ± †22.7	272.2 ± †20.1	262.9 ± †18.5	261.5 ± †28.2	169.0 ± †29.1	200.3 ± †12.9	202.1 ± †6.4

C: control rats, D: diabetic rat, B: rosiglitazone with insulin combine-treated diabetic rats. Data are presented as mean ± SEM. †$P < 0.05$ in B groups compared with D; *$P < 0.05$ in D compared with C in the same group in the same week.

Table 2: Body weight levels in the study groups.

	Weeks								
Groups	0	1	2	3	4	5	6	7	8
C (gr)	100.0 ± 0.8	100.8 ± 0.8	101.1 ± 0.7	102.7 ± 0.7	107.6 ± 2.2	107.5 ± 0.8	109.3 ± 0.7	111.2 ± 0.8	112.6 ± 0.9
D (gr)	100.0 ± 1.8	91.5 ± 1.3	86.8* ± 1.3	75.5* ± 2.8	75.0* ± 1.7	73.5* ± 1.5	70.9* ± 1.5	71.6* ± 1.6	72.7* ± 1.8
B (gr)	100.0 ± 2.0	94.0 ± 2.1	89.1 ± 1.4	91.0† ± 1.2	95.3† ± 2.5	96.0† ± 2.4	97.0† ± 1.8	99† ± 2.3	100.0† ± 2.1

C: control rats, D: diabetic rat, B: rosiglitazone with insulin combine-treated diabetic rats. Data are presented as mean ± SEM. †$P < 0.05$ in B groups compared with D; *$P < 0.05$ in D compared with C in the same group in the same week.

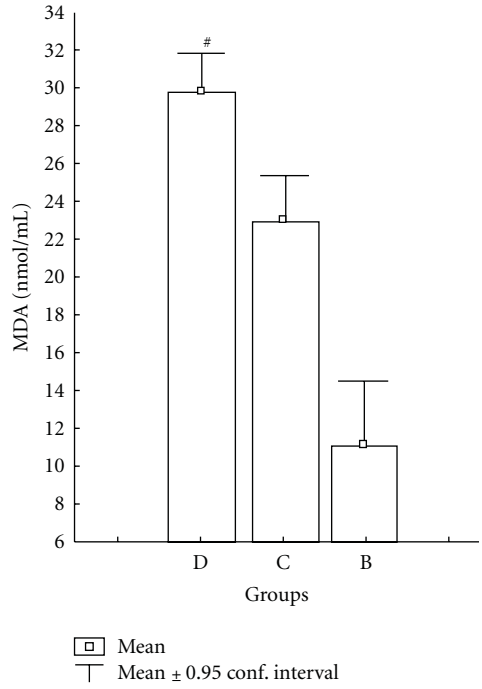

Figure 3: Effects of rosiglitazone with insulin combination therapy on the MDA levels of rat left ventricular. C: control rats, D: diabetic rat, group B: rosiglitazone with insulin combine-treated diabetic rats. Data are presented as mean ± SEM. *#$P < 0.05$ in D group compared with C and group B compared with D.

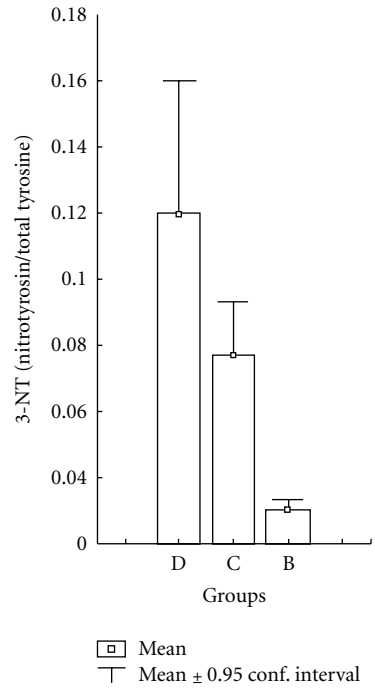

Figure 4: Effects of D + RSG + INS on the 3-nitrotyrosine/total tyrosine levels of rat left ventricular. C: control rats, D: diabetic rat, group B: rosiglitazone with insulin combine-treated diabetic rats. *$P < 0.05$ in D group compared with groups B and C.

at 3-NT levels compared with the C and B groups ($P < 0.0011$). There were no statistically significant differences between the B groups (Figure 4).

4. Discussion

In this study, we have demonstrated that group B prevents glucose-induced oxidative stress in cardiac cells, an effect independent from PPARγ, but distinctively dependent on activated protein kinase (AMPK) activation. We also showed that the ability of RSG to quench oxidative stress is conveyed through the inhibition of NADPH oxidase. Furthermore, we demonstrated that, downstream of AMPK activation, the effect of RSG + INS on glucose-induced NADPH oxidase-derived ROS production is mediated by the inhibition of the diacylglycerol (DAG)-*protein kinase C* (PKC) pathway.

In this study, we investigated the effect of RSG, a member of the TZD family, on lipid profile and oxidative status in STZ-induced diabetes mellitus rats. Many studies have reported that TZDs act through PPARγ-dependent mechanisms, and this is also true in endothelial cells. For instance, RSG increased NO production in human umbilical vein endothelial cells through a transcriptional mechanism unrelated to eNOS expression but dependent on PPARγ activation [16]. Interestingly, this effect has been attributed to the inhibition of NO quenching by NADPH oxidase-derived ROS [17].

Rosiglitazone is an agonist of the PPAR-γ, which is found in insulin-dependent glucose-requiring tissues such as adipose tissue, skeletal muscle, left ventricular muscle, and liver tissue [18, 19]. The end result of PPAR-γ activation is a reduction in hepatic glucose production and increased insulin dependent glucose uptake in fat and skeletal tissues [8, 19, 20].

Calkin et al. [21] observed that RSG had a significant effect on HbA1c in diabetic mice. In addition, previous studies have reported that the administration of RSG induced a significant decrease in serum glucose levels [18, 22]. In our study, in group B-treated diabetic rats mean blood glucose significantly decreased rapidly from 335 to 202.1 mg/dL between weeks 0 and 8. The blood glucose levels started to be reduced at 2th week of treatment compared to the level of diabetic groups. Malinowski and Bolesta [23] found that treatment of RSG responses began to be observed at 4th week and were maximal at 12th week. With regard to this report, RSG may indicate its full effect on blood glucose at 12th week. In our previous studies, it was indicated that the effects of treatment with RSG on the body weight of diabetic rats was significant [18], but treatment of diabetic rats with RSG (4 mg/kg/day) was caused a significant increase compared with diabetic rats by the end of the treatment period [24]. In our study, statistically significant increases in body weight were observed group B-treated diabetic rats. These weight changes may be function increased adipocyte differentiation, which is one of the primary effects of group B. The clinical significance of these modest weight changes will require further evaluation in a long-term study.

We found a graded and significant elevation of glucose levels from the initial phase through the sacrifice in D group with and without RSG and we believe that it could be secondary to the development of some degree of insulin resistance although this was not evaluated in the present study. The insulin-resistant state is commonly associated with lipoprotein abnormalities such as hypertriglyceridemia, high levels of VLDL, small dense LDL [25], and low levels of HDL-cholesterol [26], which are risk factors for coronary heart disease. The hypoglycemic and hypotriglyceridemic action of TZDs is through the activation of PPAR-gama leading to increased insulin sensitivity of peripheral tissues and lipoprotein lipase activity in the adipose tissue [27]. Zhaohui et al. [28] did not show a reduction of blood glucose level in hypercholesterolemic rabbits receiving RSG for 6 weeks, as in the present study. Furthermore, we also observed a significant elevation of triglycerides and HDL-C at the time of euthanasia in RSG group. The effects of TZDs on triglycerides have been somewhat more variable. Decreases in triglyceride levels have been more frequently observed with pioglitazone than with rosiglitazone. We cannot rule out that these effects on glucose and triglycerides were due to chance, as our evaluation period was short and the sample was relatively. These findings are quite controversial in the literature [28–30].

Boyle et al. [31] found that RSG reduced TAG, but increased total cholesterol, LDL-C, and reduced HDL-C. In contrast, pioglitazone reduced TAG, total cholesterol, and LDL-C and increased HDL-C. Conversely, in their study, Myerson et al. [32] observed reduced plasma fatty acid concentrations and hepatic TAG content after RSG therapy. Within that TZD group, marked differences have been reported as regards the effect of different members on lipid profiles in patients with type-2 diabetes. In the present study, the administration of RSG + INS, a member of the TZD family, decreased TC, TAG, and VLDL-C, LDL-C levels in STZ diabetic rat.

Bagi et al. [33] reported that the reduced activity of catalase may result in enhanced hydroxyl radical production leading to enhanced lipid peroxidation in diabetes. Even short-term activation of PPAR-γ by RSG reduces NAD(P)H oxidase and enhances catalase activity causing a reduction of superoxide and hydroxyl radical production, thereby enhancing NO mediation of coronary vasodilation and reducing lipid peroxidation in diabetes. These findings suggest that activation of PPAR-gamma may exert an antioxidant activity by favorably altering the expression of specific enzymes participating in the production and/or elimination of reactive oxygen species.

Radi et al. [34] found that elevated levels of MDA were brought down to the normal values by treatment with RSG. In the present study, we have found that compared with controls, in diabetic rats, the serum level of MDA (a marker of in vivo lipid peroxidation) was significantly elevated, which was reduced by group B treatment (Figure 3). On the basis of study findings, we observed that even short-term RSG treatment of rats with diabetes would, by reducing oxidative stress. These results suggest that RSG + INS is capable of reducing oxidative stress in rats with diabetes. Patients with diabetes have modified levels of various markers of oxidative stress, indicating an overproduction of free radicals, which have a key role in the development of diabetic vascular complications [35]. When focusing on diabetic vascular disease, it is the fine balance between the levels of superoxide (O_2^-), peroxynitrite ($ONOO^-$), and NO, that is, the key in determining the extent of vascular damage. It is noteworthy that TZD show intracellular antioxidant activity. This property may reflect "preventative" action since these agents do not show direct antioxidant scavenging activity on free radicals, but block several mechanisms that in hyperglycaemic or hyperlipidaemic conditions lead to the generation of oxidative stress. It has been observed that PPAR-γ ligands inhibit the expression of inducible NO synthase (iNOS) and, consequently, $ONOO^-$ production, in mesangial cells and in cerebellar granule cells [36]. Similarly, in mice with rheumatoid arthritis, pioglitazone and RSG

have been shown to reduce the expression of iNOS and nitrotyrosine deposition [37].

It seems that this is the first study to investigate the effect of group B on oxidative/nitrosative effect in left ventricular of diabetes mellitus rats.

In summary, the present study demonstrates that in diabetes, treatment with rosiglitazone with insulin combined caused rapid reductions in oxidative stress that are not associated with corrections of major metabolic derangements. Our results clarify that mechanisms of TZD-induced vascular protection include suppression of specific NADPH oxidase subunit expression and ventricular muscle superoxide production similar to previously reported direct effects of PPARγ ligands on vascular endothelial cells in vitro [38]. The mechanisms of PPARγ-induced suppression of NADPH oxidase subunits remain to be defined and constitute an area of active investigation in our lab. We also postulate that improvements in endothelial dysfunction caused by sustained PPARγ activation in diabetes as well as in other disorders associated with endothelial dysfunction may be related to direct effects of PPARγ activation on endothelial nitric oxide synthase activity [39] mediated by TZD-induced alterations in post-translational mechanisms regulating eNOS activity [40].

5. Conclusions

Ongoing studies in our laboratory will determine if direct TZD-mediated activation of PPARγ coordinately regulates the production of O^{2-} and nitric oxide at the level of the vascular wall to modulate the development of endothelial dysfunction. These studies could further clarify the vascular protective effects of PPARγ ligands and Thus, in diabetes-related vascular diseases RSG treatment may be cardioprotective.

Conflict of Interests

The authors fully disclose that there is no financial or ethical conflict of interests.

Acknowledgments

This project is supported by a Grant from Çukurova University Scientific Research Project Coordination Unit, (TF 2006 D3) Turkey. The authors thank Professor Dr. Lülüfer Tamer.

References

[1] A. Ceriello and E. Motz, "Is oxidative stress the pathogenic mechanism underlying insulin resistance, diabetes, and cardiovascular disease? The common soil hypothesis revisited," *Arteriosclerosis, Thrombosis, and Vascular Biology*, vol. 24, no. 5, pp. 816–823, 2004.

[2] D. Aronson and E. J. Rayfield, "How hyperglycemia promotes atherosclerosis: molecular mechanisms," *Cardiovascular Diabetology*, vol. 1, article 1, 2002.

[3] N. Houstis, E. D. Rosen, and E. S. Lander, "Reactive oxygen species have a causal role in multiple forms of insulin resistance," *Nature*, vol. 440, no. 7086, pp. 944–948, 2006.

[4] A. J. Vidal-Puig, R. V. Considine, M. Jimenez-Linan et al., "Peroxisome proliferator-activated receptor gene expression in human tissues: effects of obesity, weight loss, and regulation by insulin and glucocorticoids," *Journal of Clinical Investigation*, vol. 99, no. 10, pp. 2416–2422, 1997.

[5] H. Yki-Jarvinen, "Thiazolidinedione," *The New England Journal of Medicine*, vol. 351, pp. 1106–1118, 2004.

[6] N. Houstis, E. D. Rosen, and E. S. Lander, "Reactive oxygen species have a causal role in multiple forms of insulin resistance," *Nature*, vol. 440, no. 7086, pp. 944–948, 2006.

[7] A. C. Calkin, J. M. Forbes, C. M. Smith et al., "Rosiglitazone attenuates atherosclerosis in a model of insulin insufficiency independent of its metabolic effects," *Arteriosclerosis, Thrombosis, and Vascular Biology*, vol. 25, no. 9, pp. 1903–1909, 2005.

[8] P. D. Miles, K. Higo, O. M. Romeo, M. K. Lee, K. Rafaat, and J. M. Olefsky, "Troglitazone prevents hyperglycemia-induced but not glucosamine-induced insulin resistance," *Diabetes*, vol. 47, no. 3, pp. 395–400, 1998.

[9] I. Barroso, M. Gurnell, V. E. Crowley et al., "Dominant negative mutations in human PPARγ associated with severe insulin resistance, diabetes mellitus and hypertension," *Nature*, vol. 402, no. 6764, pp. 880–883, 1999.

[10] V. Bonnevie-Nielsen, M. W. Steffes, and A. Lernmark, "A major loss in islet mass and b-cell function precedes hyperglycemia in mice given multiple low doses of streptozotocin," *Diabetes*, vol. 30, no. 5, pp. 424–429, 1981.

[11] B. Ramesh and K. V. Pugalendi, "Influence of umbelliferone on membrane-bound ATPases in streptozotocin-induced diabetic rats," *Pharmacological Reports*, vol. 59, no. 3, pp. 339–348, 2007.

[12] S. P. Sawant, A. V. Dnyanmote, K. Shankar, P. B. Limaye, J. R. Latendresse, and H. M. Mehendale, "Potentiation of carbon tetrachloride hepatotoxicity and lethality in type 2 diabetic rats," *Journal of Pharmacology and Experimental Therapeutics*, vol. 308, no. 2, pp. 694–704, 2004.

[13] W. T. Friedewald, R. I. Levy, and D. S. Fredrickson, "Estimation of the concentration of low-density lipoprotein cholesterol in plasma, without use of the preparative ultracentrifuge," *Clinical Chemistry*, vol. 18, no. 6, pp. 499–502, 1972.

[14] K. Yagi, "Lipid peroxides and related radicals in clinical medicine," in *Free Radicals in Diagnostic Medicine*, D. Armstrong, Ed., pp. 1–15, Plenum, New York, NY, USA, 1994.

[15] A. Ünlü, N. Türkozkan, B. Çimen, U. Karabýçak, and H. Yaman, "The effects of Escherichia coli-derived lipopolysaccharides on plasma levels of malondialdehyde and 3-nitrotyrosine," *Clinical Chemistry and Laboratory Medicine*, vol. 39, pp. 491–493, 2001.

[16] D. S. Calnek, L. Mazzella, S. Roser, J. Roman, and C. M. Hart, "Peroxisome proliferator-activated receptor γ ligands increase release of nitric oxide from endothelial cells," *Arteriosclerosis, Thrombosis, and Vascular Biology*, vol. 23, no. 1, pp. 52–57, 2003.

[17] J. Hwang, D. J. Kleinhenz, B. Lassègue, K. K. Griendling, S. Dikalov, and C. M. Hart, "Peroxisome proliferator-activated receptor-γ ligands regulate endothelial membrane superoxide production," *American Journal of Physiology*, vol. 288, no. 4, pp. C899–C905, 2005.

[18] S. Kavak, L. Ayaz, M. Emre, T. Inal, L. Tamer, and I. Günay, "The effects of rosiglitazone on oxidative stress and lipid profile in left ventricular muscles of diabetic rats," *Cell Biochemistry and Function*, vol. 26, no. 4, pp. 478–485, 2008.

[19] B. M. Spiegelman, "PPAR-γ: adipogenic regulator and thiazolidinedione receptor," *Diabetes*, vol. 47, no. 4, pp. 507–514, 1998.

[20] R. Kahn, "Consensus development conference on insulin resistance: 5-6 November 1997," *Diabetes Care*, vol. 21, no. 2, pp. 310–314, 1998.

[21] A. C. Calkin, J. M. Forbes, C. M. Smith et al., "Rosiglitazone attenuates atherosclerosis in a model of insulin insufficiency independent of its metabolic effects," *Arteriosclerosis, Thrombosis, and Vascular Biology*, vol. 25, no. 9, pp. 1903–1909, 2005.

[22] P. Iozzo, K. Hallsten, V. Oikonen et al., "Effects of metformin and rosiglitazone monotherapy on insulin-mediated hepatic glucose uptake and their relation to visceral fat in type 2 diabetes," *Diabetes Care*, vol. 26, no. 7, pp. 2069–2074, 2003.

[23] J. M. Malinowski and S. Bolesta, "Rosiglitazone in the treatment of type 2 diabetes mellitus: a critical review," *Clinical Therapeutics*, vol. 22, no. 10, pp. 1151–1168, 2000.

[24] J. Chaudhry, N. N. Ghosh, K. Roy, and R. Chandra, "Antihyperglycemic effect of a new thiazolidinedione analogue and its role in ameliorating oxidative stress in alloxan-induced diabetic rats," *Life Sciences*, vol. 80, no. 12, pp. 1135–1142, 2007.

[25] M. R. Taskinen, "Insulin resistance and lipoprotein metabolism," *Current Opinion in Lipidology*, vol. 6, no. 3, pp. 153–160, 1995.

[26] G. M. Reaven, Y. D. Chen, J. Jeppesen, P. Maheux, and R. M. Krauss, "Insulin resistance and hyperinsulinemia in individuals with small, dense, low density lipoprotein particles," *Journal of Clinical Investigation*, vol. 92, no. 1, pp. 141–146, 1993.

[27] B. Staels and J. Auwers, "Role of PPAR in the pharmacological regulation of lipoprotein metabolism by fibrates and thiazolidinediones," *Current Pharmaceutical Design*, vol. 3, no. 1, pp. 1–14, 1997.

[28] W. Zhao-hui, L. Feng, and L. Xiao-mei, "Effect of PPARγ agonist rosiglitazone on regression of the atherosclerotic plaques in rabbits," *Yao Xue Xue Bao*, vol. 40, no. 11, pp. 1051–1053, 2005.

[29] Z. Levi, A. Shaish, N. Yacov et al., "Rosiglitazone (PPARγ-agonist) attenuates atherogenesis with no effect on hyperglycaemia in a combined diabetes-atherosclerosis mouse model," *Diabetes, Obesity and Metabolism*, vol. 5, no. 1, pp. 45–50, 2003.

[30] L. Tao, H. R. Liu, E. Gao et al., "Antioxidative, antinitrative, and vasculoprotective effects of a peroxisome proliferator-activated receptor-γ agonist in hypercholesterolemia," *Circulation*, vol. 108, no. 22, pp. 2805–2811, 2003.

[31] P. J. Boyle, A. B. King, L. Olansky et al., "Effects of pioglitazone and rosiglitazone on blood lipid levels and glycemic control in patients with type 2 diabetes mellitus: a retrospective review of randomly selected medical records," *Clinical Therapeutics*, vol. 24, no. 3, pp. 378–396, 2002.

[32] A. B. Mayerson, R. S. Hundal, S. Dufour et al., "The effects of rosiglitazone on insulin sensitivity, lipolysis, and hepatic and skeletal muscle triglyceride content in patients with type 2 diabetes," *Diabetes*, vol. 51, no. 3, pp. 797–802, 2002.

[33] Z. Bagi, A. Koller, and G. Kaley, "PPARγ activation, by reducing oxidative stress, increases NO bioavailability in coronary arterioles of mice with Type 2 diabetes," *American Journal of Physiology*, vol. 286, no. 2, pp. H742–H748, 2004.

[34] R. Radi, A. Denicola, B. Alvarez, G. Ferrer-Sueta, and H. Rubbo, "The biological chemistry of peroxynitrite," in *Introduction and Overview*, J. L. Ignarro, Ed., pp. 57–82, Academic Press, 2000.

[35] C. D. Filippo, S. Cuzzocrea, F. Rossi, R. Marfella, and M. D'Amico, "Oxidative stress as the leading cause of acute myocardial infarction in diabetics," *Cardiovascular Drug Reviews*, vol. 24, no. 2, pp. 77–87, 2006.

[36] M. Ricote, A. C. Li, T. M. Willson, C. J. Kelly, and C. K. Glass, "The peroxisome proliferator-activated receptor-γ is a negative regulator of macrophage activation," *Nature*, vol. 391, no. 6662, pp. 79–82, 1998.

[37] T. Shiojiri, K. Wada, A. Nakajima et al., "PPARγ ligands inhibit nitrotyrosine formation and inflammatory mediator expressions in adjuvant-induced rheumatoid arthritis mice," *European Journal of Pharmacology*, vol. 448, no. 2-3, pp. 231–238, 2002.

[38] J. Hwang, D. J. Kleinhenz, B. Lassègue, K. K. Griendling, S. Dikalov, and C. M. Hart, "Peroxisome proliferator-activated receptor-γ ligands regulate endothelial membrane superoxide production," *American Journal of Physiology*, vol. 288, no. 4, pp. C899–C905, 2005.

[39] D. S. Calnek, L. Mazzella, S. Roser, J. Roman, and C. M. Hart, "Peroxisome proliferator-activated receptor γ ligands increase release of nitric oxide from endothelial cells," *Arteriosclerosis, Thrombosis, and Vascular Biology*, vol. 23, no. 1, pp. 52–57, 2003.

[40] J. A. Polikandriotis, L. J. Mazzella, H. L. Rupnow, and C. M. Hart, "Peroxisome proliferator-activated receptor γ ligands stimulate endothelial nitric oxide production through distinct peroxisome proliferator-activated receptor γ-dependent mechanisms," *Arteriosclerosis, Thrombosis, and Vascular Biology*, vol. 25, no. 9, pp. 1810–1816, 2005.

Hindawi Publishing Corporation
Experimental Diabetes Research
Volume 2012, Article ID 859395, 8 pages
doi:10.1155/2012/859395

Research Article

A Comparison of Inflammatory and Oxidative Stress Markers in Adipose Tissue from Weight-Matched Obese Male and Female Mice

Karen J. Nickelson,[1] Kelly L. Stromsdorfer,[1] R. Taylor Pickering,[1] Tzu-Wen Liu,[1] Laura C. Ortinau,[1] Aileen F. Keating,[2] and James W. Perfield II[1,3]

[1] *Department of Nutrition and Exercise Physiology, University of Missouri-Columbia, 256 William Stringer Wing, Columbia, MO 65211, USA*
[2] *Department of Animal Science, Iowa State University, Ames, IA 50011, USA*
[3] *Department of Food Science, University of Missouri-Columbia, 256 William Stringer Wing, Columbia, MO 65211, USA*

Correspondence should be addressed to James W. Perfield II, perfieldj@missouri.edu

Received 9 February 2012; Accepted 16 April 2012

Academic Editor: Pietro Galassetti

Expansion of intra-abdominal adipose tissue and the accompanying inflammatory response has been put forward as a unifying link between obesity and the development of chronic diseases. However, an apparent sexual dimorphism exists between obesity and chronic disease risk due to differences in the distribution and abundance of adipose tissue. A range of experimental protocols have been employed to demonstrate the role of estrogen in regulating health benefits; however, most studies are confounded by significant differences in body weight and adiposity. Therefore, the purpose of this study was to compare weight-matched obese male and female mice to determine if the sex-dependent health benefits remain when body weight is similar. The development of obesity in female mice receiving a high-fat diet was delayed; however, subsequent comparisons of weight-matched obese mice revealed greater adiposity in obese female mice. Despite excess adiposity and enlarged adipocyte size, obese females remained more glucose tolerant than weight-matched male mice, and this benefit was associated with increased expression of adiponectin and reductions in immune cell infiltration and oxidative stress in adipose tissue. Therefore, the protective benefits of estrogen persist in the obese state and appear to improve the metabolic phenotype of adipose tissue and the individual.

1. Introduction

Obesity is widely regarded as an independent risk factor for a range of chronic diseases including type 2 diabetes and cardiovascular disease [1, 2]. Low-grade systemic inflammation has been put forward as a unifying link between obesity and the onset of these obesity-associated diseases [3–5]. Expansion of intra-abdominal adipose tissue is associated with increased infiltration and activation of immune cells, and these events are a significant contributor to the systemic inflammation that occurs with obesity [6, 7]. While an exact explanation for the accumulation of immune cells in adipose tissue is unknown, one potential contributing factor is elevated oxidative stress [8, 9]. Therefore, decreasing intra-abdominal obesity and/or reducing adipose tissue oxidative stress and inflammation will positively influence chronic disease risk.

Clear sex-based differences exist in adipose tissue distribution, inflammation, and ultimately the probability of developing a chronic disease [10–12]. Specifically, females tend to have a higher body fat content with the fat localized subcutaneously while males have less total body fat and their adipose tissue predominates in the visceral region. Furthermore, animal studies have demonstrated that diet-induced obesity and insulin resistance occur much more rapidly in male rodents as compared to females [13–15]. Estrogen is a major factor involved in this sexual dimorphism as it promotes subcutaneous fat accumulation, has anti-inflammatory properties, and is a strong regulator of appetite and energy expenditure [10, 12, 16, 17]. To help elucidate

the effects of estrogen on obesity, adipose tissue distribution, inflammation, and insulin resistance studies have utilized models of ovariectomy with or without repletion of estrogen and/or compared male and female mice provided a high-fat diet [13–15, 18]. While the outcome measures of these studies varied, they all clearly demonstrate a beneficial effect of estrogen. However, these studies were also confounded by body weight differences as intact females or animals receiving estrogen were typically smaller and had smaller adipose tissue depots.

Therefore, the purpose of the current study was to compare weight-matched obese male and female mice to determine if the sex-dependent improvements in metabolic health occur independent of differences in body weight. Following chronic exposure to a high-fat diet, a glucose tolerance test was performed and differences in markers for inflammatory and oxidative stress were assessed in adipose tissue. Our data demonstrate that glucose tolerance remains improved in obese female mice independent of a difference in body weight. Furthermore, despite increases in total adiposity and gonadal adipocyte size, the obese female mice displayed lower expression of markers for immune cells and oxidative stress which are consistent with an improved metabolic phenotype.

2. Methods

2.1. Animals and Animal Care. The University of Missouri Animal Care and Use committee approved all procedures involving mice. Animals were maintained at a controlled temperature (22°C) and a 12-hour light: 12-hour dark cycle. Six-to eight-week old male and female C57BL/6 mice were individually housed and fed either a chow (Purina 5001; 4.5 g/100 g fat) or high-fat diet (HFD; Research Diets D12492; 35 g/100 g fat) for the duration of the experiment. Body weight was measured weekly and mice were kept on treatment until the average body weight of the HFD group was 45 g. At this point, glucose tolerance testing and tissue collection were performed on the HFD group and their age-matched chow-fed counterparts.

2.2. Glucose Tolerance Testing. Once the HFD-fed group reached a body weight of 45 g; a glucose tolerance test was performed in both HFD and chow-fed animals. Following an overnight fast, a baseline blood sample was taken from the tail vein at time 0. Then an intraperitoneal injection of glucose (1 g/kg BW) was administered and blood glucose concentrations were determined using a handheld glucometer at 30, 60, 90, and 120 minutes postinjection. Glucose area under the curve (AUC) calculations were performed using GraphPad Prism 4 software.

2.3. Tissue Collection. One week after the glucose tolerance tests were performed, animals were fasted 10–12 hours and blood glucose was measured via a tail nick. Animals were then euthanized by CO_2 asphyxiation followed by exsanguination via cardiac puncture. Plasma was separated by centrifugation, aliquoted, and frozen for future analysis. Gonadal and subcutaneous adipose tissues were excised, weighed, and snap frozen for gene expression analysis or fixed for histological analysis.

2.4. Histological Analysis of Adipose Tissue. A portion of the gonadal adipose tissue was fixed in 4% paraformaldehyde, embedded in paraffin, sectioned, and stained with hematoxylin and eosin (H&E). Digital images were acquired with an Olympus BX51 light microscope using an Olympus DP70 camera. Dead adipocytes were quantified by identification of crown-like structures (CLSs) within histologic sections of adipose tissue. The percentage of CLS present in gonadal adipose tissue was calculated and used for comparison among experimental groups. Adipocyte volume was calculated using the cross-sectional area obtained from perimeter tracings using Image J software (Sun Microsystems, Santa Clara, CA, USA).

2.5. Plasma Analysis. An estradiol EIA kit (Cayman Chemical Company) was used to determine fasting (overnight) plasma estradiol concentrations of female mice.

2.6. Real-Time Quantitative PCR. Total mRNA was extracted from adipose using RNeasy lipid tissue kits with on-column DNase digestion (Qiagen). Purity and concentration were determined with a Nanodrop 1000 spectrophotometer (Thermo Scientific). 1 μg of RNA was used to synthesize cDNA with a reverse transcriptase polymerase chain reaction kit (Applied Biosystems) and diluted to 10 ng/μL. Expression of mRNA was determined using SYBR green qRT-PCR on an Applied Biosystems StepOne Plus RT-PCR system. Fold difference for gene expression was calculated using $2^{-\Delta\Delta CT}$ using the endogenous control gene RPS-3.

2.7. Statistical Analysis. Treatment differences were analyzed by one-way analysis of variance (ANOVA) with main effect significance set at $P < 0.05$. Significant main effects were followed by a Tukey's multiple comparison test. Values are reported as mean ± standard error.

3. Results

3.1. Onset of Obesity Is Delayed in Female Mice Receiving High-Fat Diet. Male and female C57BL/6 J mice received either a low-fat chow diet or a HFD. The HFD induced a more rapid body weight gain in male mice which achieved the target body weight of 45 g in 21 weeks, while female mice required an additional 17 weeks of HFD to reach the same body weight (Table 1). This experimental design ensured that mice would be studied at a body weight associated with established obesity and insulin resistance [6] and that body weight would not be a confounding variable. However, due to the delayed body weight gain in female HFD mice age did emerge as an unaccounted for variable. Interestingly, despite having similar body weights, the adiposity of the female HFD mice was greater than the male HFD group as both gonadal and subcutaneous adipose tissue masses were significantly increased (Table 1). Fasting blood glucose

Table 1: Characteristics of male and female C57BL/6 mice receiving a standard rodent chow or a high-fat diet (HFD).[1]

	Male chow	Male HFD	Female chow	Female HFD
Body weight (g)	28.8 ± 0.28^{b}	45.3 ± 1.0^{a}	24.8 ± 0.45^{b}	46.5 ± 2.0^{a}
Age[2] (weeks)	21	21	38	38
Gonadal AT[3] (g)	0.51 ± 0.28^{c}	2.25 ± 0.17^{b}	0.44 ± 0.05^{c}	3.74 ± 0.35^{a}
Subcutaneous AT (g)	0.32 ± 0.01^{c}	2.29 ± 0.24^{b}	0.27 ± 0.02^{c}	3.34 ± 0.28^{a}
Blood glucose (mg/dL)	99 ± 8^{b}	142 ± 11^{a}	108 ± 8^{b}	116 ± 5^{ab}
Plasma estradiol (pg/mL)	—	—	92.5 ± 1.53	92.7 ± 0.35

[1] Data are presented as means ± SE; means with different superscripts differ $P < 0.05$; $n = 5$–8.
[2] Age at which the HFD-fed group reached a body weight of 45 g and metabolic testing and tissue collection occurred.
[3] AT; adipose tissue.

concentrations were elevated by obesity in the male mice but not the female mice. Obesity also did not alter plasma estradiol concentrations in the female mice (Table 1).

3.2. Obese Female Mice Have Improved Glucose Tolerance as Compared to Weight-Matched Obese Male Mice. When the average body weight of HFD-fed male and female mice reached 45 g, an intraperitoneal glucose tolerance test was performed on that experimental group and their age-matched chow-fed counterparts. Glucose area under the curve calculations revealed better glucose tolerance in the female HFD group as compared to the male HFD mice (Figure 1). This improvement is especially noteworthy since there was no difference in body weight between these two groups and also, the HFD females had greater total fat mass (Table 1). Further, despite the age difference, glucose tolerance was similar between male chow and female chow mice (Figure 1).

3.3. Immune Cell Infiltration and Oxidative Stress Markers Are Reduced in the Adipose Tissue of Obese Female Mice. In order to better understand the observed glucose tolerance differences, we characterized markers of inflammation and oxidative stress in gonadal adipose tissue. In the current study, gonadal adipose tissue mass was greater in female HFD mice as compared to the male HFD group (Table 1). Consistent with an increased mass of adipose tissue, relative mRNA expression of leptin in gonadal adipose tissue was elevated in both male HFD and female HFD groups with no difference between genders observed (Figure 2). Interestingly, gonadal adipose tissue mRNA expression of adiponectin was reduced in male HFD mice but remained unchanged in female HFD mice (Figure 2). Adiponectin expression is often correlated with smaller adipocyte size. Therefore, gonadal adipocyte size was quantified, and surprisingly female HFD mice had a larger average adipocyte size as compared to male HFD mice (Figure 3). This apparent disconnect between adipocyte size and adiponectin expression may help explain the improvements in glucose tolerance.

Increases in adipocyte size also are correlated with an increased presence of immune cells in adipose tissue [6, 19]. Crown-like structures (CLSs) are clusters of proinflammatory immune cells that localize to dead adipocytes within adipose tissue [20]. Consistent with previous reports [6, 21], gonadal adipose tissue from the male HFD group contained elevated numbers of CLS (Figure 3). Interestingly, the presence of CLS in the gonadal adipose tissue of female HFD mice was reduced by greater than 50% when compared to the male HFD group (Figure 3). In support of this observed reduction, mRNA expression of the macrophage markers F480 and CD11c were also decreased in female HFD compared to male HFD mice (Figure 4). However, there was no difference in the relative expression of the inflammatory cytokines IL-6 and TNF-α or the chemokine MCP-1 (Figure 4). Obesity caused a reduction in the relative mRNA expression of eNOS in male HFD gonadal adipose tissue while there was no change in the female HFD group (Figure 4). Furthermore, the oxidative stress markers HO-1, p40phox, and prdx1 were increased in male HFD gonadal adipose tissue, and this increase was attenuated in gonadal adipose tissue from female HFD mice (Figure 4). Importantly, when gonadal adipose tissue from male chow and female chow mice was compared, adipocyte size was smaller in female mice, but there were no differences in any of the other variables that were measured (Figures 2, 3, and 4). Overall, adipocyte size and adipose tissue masses were greater in weight-matched female HFD mice as compared to male HFD mice. However, female HFD mice had reduced immune cell infiltration and oxidative stress, and this may be due, in part, to increased adiponectin expression.

Subcutaneous adipose tissue has been reported to be metabolically different than gonadal adipose tissue [22] and therefore the gene expression profile of this tissue was also investigated. Subcutaneous adipose tissue mRNA expression of CD11c and F480 was increased in male HFD mice as compared to the female HFD group (Figure 5). Obesity also caused an increase in MCP-1 expression in this tissue; however, the increase was greater in the male HFD animals as compared to the female HFD mice. The expression of the inflammatory cytokines IL-6 and TNF-α was increased in both male HFD and female HFD mice (Figure 5). Similar to the results reported for gonadal adipose tissue, mRNA expression of oxidative stress markers in subcutaneous adipose tissue was elevated in male HFD mice as compared to the female HFD group (Figure 5). In contrast to the gonadal adipose tissue, we did not observe any differences in adiponectin expression in subcutaneous adipose tissue (data not shown). No appreciable differences in subcutaneous mRNA expression for any of the genes investigated were observed between male chow and female chow groups (Figure 5).

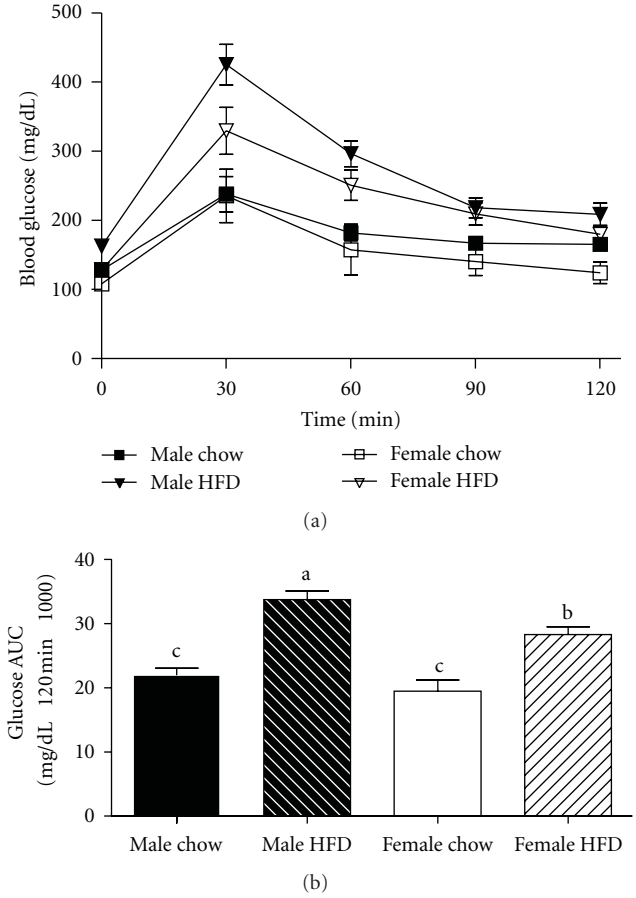

Figure 1: Obese female mice (female HFD) have improved glucose tolerance when compared to weight-matched obese male mice (male HFD). Male and female C57BL/6 mice were fed either a standard rodent chow or a high-fat diet (HFD) from 6 weeks of age until the HFD-fed group achieved a body weight of 45 g. At that time, a glucose tolerance test was performed in both chow- and HFD-fed males (21 weeks old) or females (38 weeks old) and blood glucose change over time plotted (a). Corresponding blood glucose area under the curve (AUC) was calculated (b), data are reported as mean ± SE and means with different superscripts differ by $P < 0.05$. $n = 5$–8 per group.

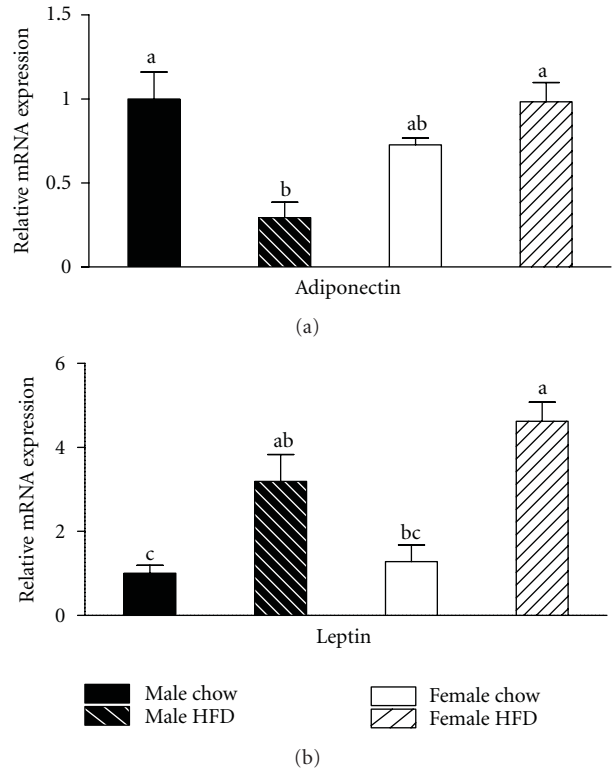

Figure 2: Adiponectin mRNA expression in gonadal adipose tissue is reduced by obesity in male mice but not weight-matched obese female mice. Male and female C57BL/6 mice were fed either a standard rodent chow or a high-fat diet (HFD) from 6 weeks of age until the HFD-fed group achieved a body weight of 45 g. At that time, both chow- and HFD-fed males (21 weeks old) or females (38 weeks old) were sacrificed and qRT PCR performed on gonadal adipose tissue. Relative mRNA expression of adiponectin was reduced by obesity in male mice, while obesity had no effect on adiponectin expression in female mice (a). Consistent with an obese phenotype, mRNA expression of leptin was elevated in both male HFD and female HFD mice (b). Data are reported as mean ± SE; $n = 5$–8 per group; means with different superscripts differ by $P < 0.05$.

4. Discussion

While numerous studies have demonstrated the benefits of estrogen in obesity prevention and chronic disease risk management [13–17, 23], our study is novel in that weight-matched obese male and female mice were evaluated to determine if endogenous estrogen provides health benefits in the obese state that are independent of body weight differences. As observed from the circulating estradiol levels, these female mice had not entered ovarian senescence. Postmenopausal mice have been shown to display a more severe obese phenotype relative to their cycling, age-matched controls [24], further supporting that estradiol provides protection against HFD-induced obesity and alternations in glucose metabolism. Consistent with previous reports [13–15], we observed that male mice were more susceptible to HFD-induced obesity as compared to the female HFD group. Therefore, we recognize that age is a potential confounding variable that was not accounted for in the current study design as it took 17 weeks longer for the female HFD group to reach the target body weight of 45 g. This target body weight was selected because it has been shown to be a period of established obesity, adipose tissue inflammation, and insulin resistance in male mice [6].

Regardless of the difference in age, obese female mice had improved glucose clearance during a glucose tolerance test as compared to weight-matched obese males. This improvement in glucose metabolism was supported by the observation that obesity caused an increase in fasting blood glucose concentrations in males but not females when compared to their chow-fed littermates. These data demonstrate that chronic exposure to a HFD can induce an obese phenotype in female mice; however, the development

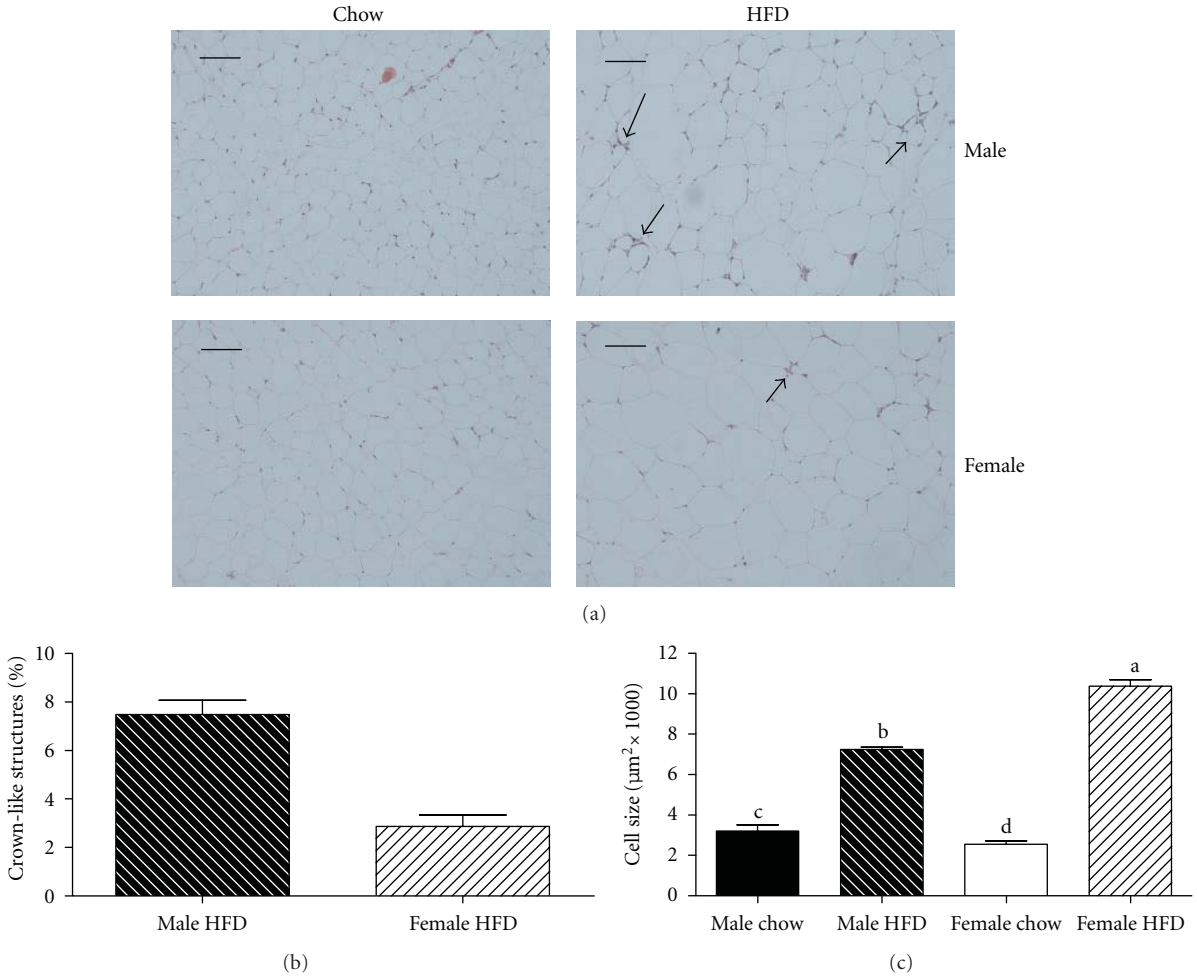

Figure 3: Obese female mice have larger adipocytes and reduced prevalence of crown-like structures in gonadal adipose tissue when compared to weight-matched obese male mice. Male and female C57BL/6 mice were fed either a standard rodent chow or a high-fat diet (HFD) from 6 weeks of age until the HFD-fed group achieved a body weight of 45 g. At that time, both chow- and HFD-fed males (21 weeks old) or females (38 weeks old) were sacrificed and histological analysis was performed on gonadal adipose tissue. Representative H&E stains of gonadal adipose tissue from each of the four treatment groups are presented in panel (a). Sections were used to quantify the presence of crown-like structure (b) and to calculate average adipocyte area (c). Data are reported as mean ± SE; $n = 5$–8 per group; means with different superscripts differ by $P < 0.05$; $^{*}P < 0.05$; bar = 100 μM.

of insulin resistance in these animals is not as severe as that observed in weight-matched obese male mice. In addition, advanced age is associated with the development of insulin resistance [25] suggesting the improvement in glucose tolerance may have been greater if the significant difference in age did not exist between the two groups. This difference in age may explain why glucose tolerance was similar between the male chow and female chow-groups while others have reported differences in glucose tolerance testing between chow-fed male and female mice [26].

Given the strong correlation between metabolic dysfunction in adipose tissue and impaired glucose metabolism; we examined the adipose tissue from the four experimental groups in an attempt to better understand the observed improvement in glucose tolerance in obese females. The experimental design precluded body weight differences between male HFD and female HFD groups; however, body fat content of the female HFD mice was greater due to increased gonadal and subcutaneous adipose tissue mass. This increase in mass was associated with increased adipocyte size in the gonadal adipose tissue and is contrary to our observation in chow-fed animals and the reports of others studying lean animals [26]. Both increased intra-abdominal fat mass and adipocyte size have been associated with insulin resistance in male mice due to an increased infiltration and activation of proinflammatory immune cells in the adipose tissue [6, 7, 19, 27, 28]. Here we observe an apparent disconnect where female mice have increased adipose tissue mass and larger adipocytes but glucose tolerance is improved. When immune cell infiltration and activation were assessed, we observed a reduction in the appearance of immune cells and the formation of CLS in female HFD gonadal adipose tissue. This correlated with reductions in mRNA expression of CD11c and F480 although expression of proinflammatory

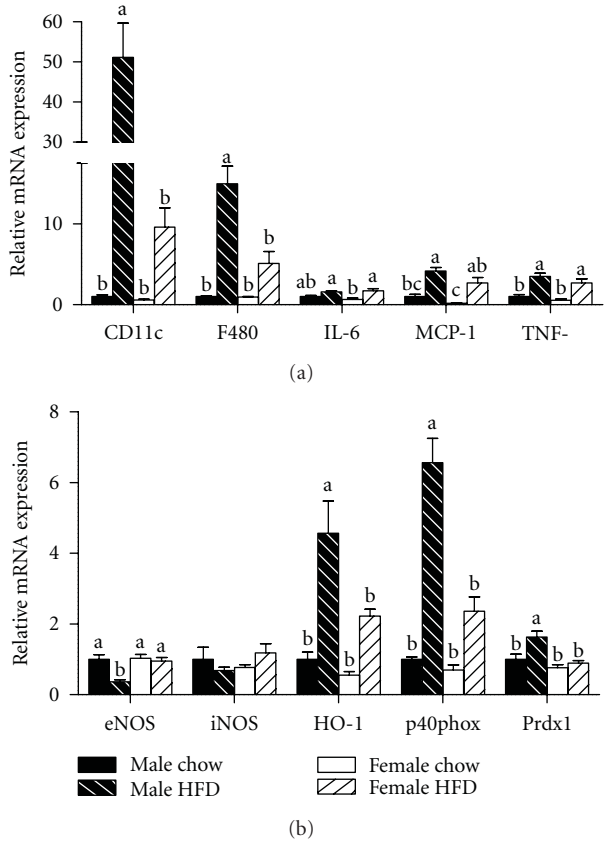

Figure 4: Relative mRNA expression of markers for immune cell infiltration and oxidative stress is decreased in gonadal adipose tissue isolated from obese female mice as compared to obese male mice. Male and female C57BL/6 mice were fed either a standard rodent chow or a high-fat diet (HFD) from 6 weeks of age until the HFD-fed group achieved a body weight of 45 g. At that time, both chow- and HFD-fed males (21 weeks old) or females (38 weeks old) were sacrificed and qRT PCR was performed on gonadal adipose tissue. Relative mRNA expression of markers for immune cell infiltration and inflammation (a) as well as oxidative stress (b) was determined. Data are reported as mean ± SE; $n = 5$–8 per group; means with different superscripts differ by $P < 0.05$. IL-6: interleukin-6; MCP-1: monocyte chemoattractant protein-1; TNF-α: tumor necrosis factor-alpha; eNOS: endothelial nitric oxide synthase; iNOS: inducible nitric oxide synthase; HO-1: heme oxygenase-1; p40phox: NADPH subunit p40phox; Prdx1: peroxiredoxin-1.

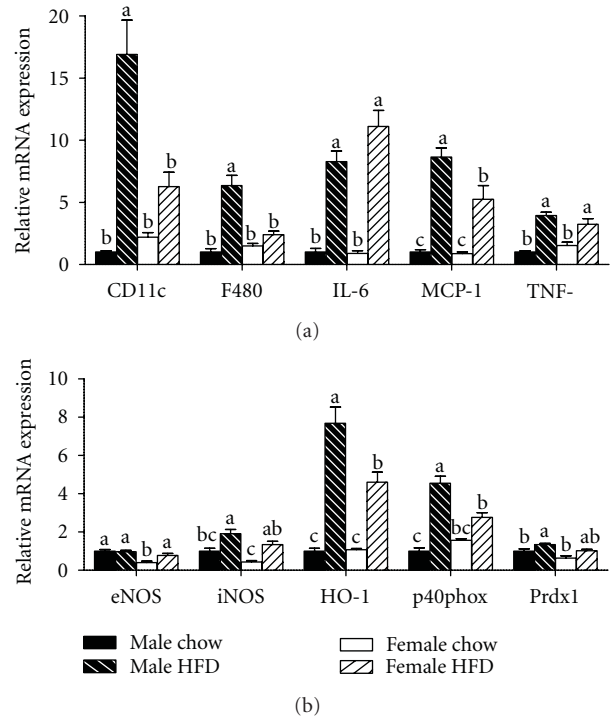

Figure 5: Relative mRNA expression of markers for immune cell infiltration and oxidative stress is altered in subcutaneous adipose tissue isolated from obese female mice as compared to obese male mice. Male and female C57BL/6 mice were fed either a standard rodent chow or a high-fat diet (HFD) from 6 weeks of age until the HFD-fed group achieved a body weight of 45 g. At that time, both chow- and HFD-fed males (21 weeks old) or females (38 weeks old) were sacrificed and qRT PCR was performed on subcutaneous adipose tissue. Relative mRNA expression of markers for immune cell infiltration and inflammation (a) as well as oxidative stress (b) was determined. Data are reported as mean ± SE; $n = 5$–8 per group; means with different superscripts differ by $P < 0.05$. IL-6: interleukin-6; MCP-1: monocyte chemoattractant protein-1; TNF-α: tumor necrosis factor-alpha; eNOS: endothelial nitric oxide synthase; iNOS: inducible nitric oxide synthase; HO-1: heme oxygenase-1; p40phox: NADPH subunit p40phox; Prdx1: peroxiredoxin-1.

cytokines was not different between male HFD and female HFD groups, suggesting that a factor other than these cytokines was potentially responsible for the improvement in glucose tolerance.

We then measured mRNA expression of the adipokines leptin and adiponectin in gonadal adipose tissue. Consistent with previous studies [29], obesity caused an increase in leptin expression in both HFD-fed groups. Interestingly, obesity caused a reduction in adiponectin expression in the male HFD group, but expression was unchanged with obesity in the female HFD group. These data are not surprising as females typically have higher adiponectin levels than males [30, 31] and while this appears to occur independent of estradiol levels, adiponectin is associated with improved insulin sensitivity and suggests a potential mechanism for our observed improvement in the females. However, additional studies investigating circulating concentrations of adiponectin are required to more fully explore this possibility. Endothelial dysfunction and oxidative stress are additional stressors that can influence glucose metabolism and were assessed in adipose tissue. Reduced mRNA expression of eNOS and elevations in HO-1, p40phox, and prdx1 in the adipose tissue of male HFD mice is indicative of oxidative stress within the tissue [32–35]. Alterations in the profile of these genes were not as severe in the female HFD adipose tissue revealing a possible reduction in oxidative stress and another potential mechanism by which estrogen may have provided a beneficial effect. Nominal differences

existed between male chow and female chow adipose tissue and therefore it is unlikely that any of our observations in the obese cohorts were influenced by baseline differences.

Overall, our study demonstrates that if provided enough time, chronic exposure to a hypercaloric diet will induce an obese phenotype in female mice that is characterized by excess abdominal adiposity and enlarged adipocytes as compared to weight-matched obese male mice. However, despite being an older animal, female mice maintained partial protection from the detrimental effects of obesity as demonstrated by improved glucose tolerance testing. Furthermore, immune cell infiltration and oxidative stress were reduced in the adipose tissue of obese female mice, and these changes were associated with increased adiponectin expression. It is likely that a combination of these factors is responsible for the observed improvement in glucose tolerance. While obesity did not alter circulating levels of estrogen we recognize that estrogen may not be the only factor influencing the improved phenotype observed in the female HFD group. However, our data are consistent with studies that have more carefully manipulated circulating levels of estrogen. Future studies in weight-matched obese females will be required to extend and verify these initial findings.

References

[1] F. Abbasi, B. W. Brown Jr., C. Lamendola, T. McLaughlin, and G. M. Reaven, "Relationship between obesity, insulin resistance, and coronary heart disease risk," *Journal of the American College of Cardiology*, vol. 40, no. 5, pp. 937–943, 2002.

[2] K. M. Flegal, B. I. Graubard, D. F. Williamson, and M. H. Gail, "Cause-specific excess deaths associated with underweight, overweight, and obesity," *Journal of the American Medical Association*, vol. 298, no. 17, pp. 2028–2037, 2007.

[3] C. de Luca and J. M. Olefsky, "Inflammation and insulin resistance," *FEBS Letters*, vol. 582, no. 1, pp. 97–105, 2008.

[4] A. W. Ferrante Jr., "Obesity-induced inflammation: a metabolic dialogue in the language of inflammation," *Journal of Internal Medicine*, vol. 262, no. 4, pp. 408–414, 2007.

[5] G. S. Hotamisligil, "Inflammation and metabolic disorders," *Nature*, vol. 444, no. 7121, pp. 860–867, 2006.

[6] K. J. Strissel, Z. Stancheva, H. Miyoshi et al., "Adipocyte death, adipose tissue remodeling, and obesity complications," *Diabetes*, vol. 56, no. 12, pp. 2910–2918, 2007.

[7] C. N. Lumeng, S. M. DeYoung, J. L. Bodzin, and A. R. Saltiel, "Increased inflammatory properties of adipose tissue macrophages recruited during diet-induced obesity," *Diabetes*, vol. 56, no. 1, pp. 16–23, 2007.

[8] M. F. Gregor and G. S. Hotamisligil, "Thematic review series: adipocyte biology. Adipocyte stress: the endoplasmic reticulum and metabolic disease," *Journal of Lipid Research*, vol. 48, no. 9, pp. 1905–1914, 2007.

[9] S. Furukawa, T. Fujita, M. Shimabukuro et al., "Increased oxidative stress in obesity and its impact on metabolic syndrome," *Journal of Clinical Investigation*, vol. 114, no. 12, pp. 1752–1761, 2004.

[10] L. M. Brown, L. Gent, K. Davis, and D. J. Clegg, "Metabolic impact of sex hormones on obesity," *Brain Research*, vol. 1350, pp. 77–85, 2010.

[11] J. M. Bruun, C. B. Nielsen, S. B. Pedersen, A. Flyvbjerg, and B. Richelsen, "Estrogen reduces pro-inflammatory cytokines in rodent adipose tissue: studies in vivo and in vitro," *Hormone and Metabolic Research*, vol. 35, no. 3, pp. 142–146, 2003.

[12] M. R. Meyer, D. J. Clegg, E. R. Prossnitz, and M. Barton, "Obesity, insulin resistance and diabetes: sex differences and role of oestrogen receptors," *Acta Physiologica*, vol. 203, no. 1, pp. 259–269, 2011.

[13] R. E. Stubbins, K. Najjar, V. B. Holcomb, J. Hong, and N. P. Nunez, "Oestrogen alters adipocyte biology and protects female mice from adipocyte inflammation and insulin resistance," *Diabetes, Obesity and Metabolism*, vol. 14, no. 1, pp. 58–66, 2012.

[14] R. E. Stubbins, V. B. Holcomb, J. Hong, and N. P. Nunez, "Estrogenmodulates abdominal adiposity and protects female mice from obesity and impaired glucose tolerance," *European Journal of Nutrition*. In press.

[15] K. L. Grove, S. K. Fried, A. S. Greenberg, X. Q. Xiao, and D. J. Clegg, "A microarray analysis of sexual dimorphism of adipose tissues in high-fat-diet-induced obese mice," *International Journal of Obesity*, vol. 34, no. 6, pp. 989–1000, 2010.

[16] D. J. Clegg, L. M. Brown, S. C. Woods, and S. C. Benoit, "Gonadal hormones determine sensitivity to central leptin and insulin," *Diabetes*, vol. 55, no. 4, pp. 978–987, 2006.

[17] N. H. Rogers, J. W. Perfield, K. J. Strissel, M. S. Obin, and A. S. Greenberg, "Reduced energy expenditure and increased inflammation are early events in the development of ovariectomy-induced obesity," *Endocrinology*, vol. 150, no. 5, pp. 2161–2168, 2009.

[18] Y. Kamei, M. Suzuki, H. Miyazaki et al., "Ovariectomy in mice decreases lipid metabolism-related gene expression in adipose tissue and skeletal muscle with increased body fat," *Journal of Nutritional Science and Vitaminology*, vol. 51, no. 2, pp. 110–117, 2005.

[19] S. P. Weisberg, D. McCann, M. Desai, M. Rosenbaum, R. L. Leibel, and A. W. Ferrante Jr., "Obesity is associated with macrophage accumulation in adipose tissue," *Journal of Clinical Investigation*, vol. 112, no. 12, pp. 1796–1808, 2003.

[20] S. Cinti, G. Mitchell, G. Barbatelli et al., "Adipocyte death defines macrophage localization and function in adipose tissue of obese mice and humans," *Journal of Lipid Research*, vol. 46, no. 11, pp. 2347–2355, 2005.

[21] J. W. Perfield II, Y. Lee, G. I. Shulman et al., "Tumor progression locus 2 (TPL2) regulates obesity-associated inflammation and insulin resistance," *Diabetes*, vol. 60, no. 4, pp. 1168–1176, 2011.

[22] T. T. Tran, Y. Yamamoto, S. Gesta, and C. R. Kahn, "Beneficial effects of subcutaneous fat transplantation on metabolism," *Cell Metabolism*, vol. 7, no. 5, pp. 410–420, 2008.

[23] T. M. D'Eon, S. C. Souza, M. Aronovitz, M. S. Obin, S. K. Fried, and A. S. Greenberg, "Estrogen regulation of adiposity and fuel partitioning: evidence of genomic and non-genomic regulation of lipogenic and oxidative pathways," *The Journal of Biological Chemistry*, vol. 280, no. 43, pp. 35983–35991, 2005.

[24] M. J. Romero-Aleshire, M. K. Diamond-Stanic, A. H. Hasty, P. B. Hoyer, and H. L. Brooks, "Loss of ovarian function in the VCD mouse-model of menopause leads to insulin resistance and a rapid progression into the metabolic syndrome," *American Journal of Physiology*, vol. 297, no. 3, pp. R587–R592, 2009.

[25] L. Lin, P. K. Saha, X. Ma et al., "Ablation of ghrelin receptor reduces adiposity and improves insulin sensitivity during aging by regulating fat metabolism in white and brown adipose tissues," *Aging Cell*, vol. 10, no. 6, pp. 996–1010, 2011.

[26] Y. Macotela, J. Boucher, T. T. Tran, and C. R. Kahn, "Sex and depot differences in adipocyte insulin sensitivity and glucose metabolism," *Diabetes*, vol. 58, no. 4, pp. 803–812, 2009.

[27] K. J. Strissel, J. DeFuria, M. E. Shaul, G. Bennett, A. S. Greenberg, and M. S. Obin, "T-cell recruitment and Th1 polarization in adipose tissue during diet-induced obesity in C57BL/6 mice," *Obesity*, vol. 18, no. 10, pp. 1918–1925, 2010.

[28] C. N. Lumeng, J. L. Bodzin, and A. R. Saltiel, "Obesity induces a phenotypic switch in adipose tissue macrophage polarization," *Journal of Clinical Investigation*, vol. 117, no. 1, pp. 175–184, 2007.

[29] R. S. Ahima and S. Y. Osei, "Adipokines in obesity," *Frontiers of Hormone Research*, vol. 36, pp. 182–197, 2008.

[30] H. Nishizawa, L. Shimomura, K. Kishida et al., "Androgens decrease plasma adiponectin, an insulin-sensitizing adipocyte-derived protein," *Diabetes*, vol. 51, no. 9, pp. 2734–2741, 2002.

[31] F. Bäckhed, H. Ding, T. Wang et al., "The gut microbiota as an environmental factor that regulates fat storage," *Proceedings of the National Academy of Sciences of the United States of America*, vol. 101, no. 44, pp. 15718–15723, 2004.

[32] P. Handa, S. Tateya, N. O. Rizzo et al., "Reduced vascular nitric oxide-cGMP signaling contributes to adipose tissue inflammation during high-fat feeding," *Arteriosclerosis, Thrombosis, and Vascular Biology*, vol. 31, no. 12, pp. 2827–2835, 2011.

[33] A. Georgescu, D. Popov, A. Constantin et al., "Dysfunction of human subcutaneous fat arterioles in obesity alone or obesity associated with type 2 diabetes," *Clinical Science*, vol. 120, no. 10, pp. 463–472, 2011.

[34] J. M. Curtis, P. A. Grimsrud, W. S. Wright et al., "Downregulation of adipose glutathione S-tansferase A4 leads to increased protein carbonylation, oxidative stress, and mitochondrial dysfunction," *Diabetes*, vol. 59, no. 5, pp. 1132–1142, 2010.

[35] D. Pitocco, F. Zaccardi, E. Di Stasio et al., "Oxidative stress, nitric oxide, and diabetes," *Review of Diabetic Studies*, vol. 7, no. 1, pp. 15–25, 2010.

Hindawi Publishing Corporation
Experimental Diabetes Research
Volume 2012, Article ID 430176, 8 pages
doi:10.1155/2012/430176

Research Article

Hepatic Mitochondrial Alterations and Increased Oxidative Stress in Nutritional Diabetes-Prone *Psammomys obesus* Model

Saida Bouderba,[1] M. Nieves Sanz,[2] Carlos Sánchez-Martín,[2] M. Yehia El-Mir,[2] Gloria R. Villanueva,[2] Dominique Detaille,[3,4] and E. Ahmed Koceïr[1]

[1] *USTHB, FSB, Equipe de Bioénergétique et Métabolisme Intermédiaire, Alger 16111, Algeria*
[2] *Departamento de Fisiología y Farmacología, Faculad de Farmacia, Universidad de Salamanca, 37007 Salamanca, Spain*
[3] *Laboratoire de Bioénergétique Fondamentale et Appliquée (LBFA), Université Joseph Fourier, Grenoble 38041, France*
[4] *INSERM U1055, Grenoble cedex 9, Grenoble 38041, France*

Correspondence should be addressed to Dominique Detaille, dominique.detaille@ujf-grenoble.fr

Received 10 January 2012; Accepted 16 March 2012

Academic Editor: Pietro Galassetti

Mitochondrial dysfunction is considered to be a pivotal component of insulin resistance and associated metabolic diseases. *Psammomys obesus* is a relevant model of nutritional diabetes since these adult animals exhibit a state of insulin resistance when fed a standard laboratory chow, hypercaloric for them as compared to their natural food. In this context, alterations in bioenergetics were studied. Using liver mitochondria isolated from these rats fed such a diet for 18 weeks, oxygen consumption rates, activities of respiratory complexes, and content in cytochromes were examined. Levels of malondialdehyde (MDA) and gluthatione (GSH) were measured in tissue homogenates. Diabetic *Psammomys* showed a serious liver deterioration (hepatic mass accretion, lipids accumulation), accompanied by an enhanced oxidative stress (MDA increased, GSH depleted). On the other hand, both ADP-dependent and uncoupled respirations greatly diminished below control values, and the respiratory flux to cytochrome oxydase was mildly lowered. Furthermore, an inhibition of complexes I and III together with an activation of complex II were found. With emergence of oxidative stress, possibly related to a defect in oxidative phosphorylation, some molecular adjustments could contribute to alleviate, at least in part, the deleterious outcomes of insulin resistance in this gerbil species.

1. Introduction

The pathophysiology of type 2 diabetes mellitus (T2DM) is varied and very complex but the association of T2DM with obesity and inactivity indicates a potentially pathogenic link between fuel homeostasis, emergence of insulin resistance, and disease progression. Given the central role for mitochondria in energy production, dysregulated mitochondrial function at the cellular level can impact whole-body metabolism. Three major players are believed to be involved in such a disordered context: hepatocytes, insulin-dependent tissues (skeletal muscle, fat), and β-cells. Evidence pointing to defects in mitochondrial oxidative capacity for all these cell types demonstrates that each of them contributes to glucose imbalance [1]. Nevertheless, the nature, origin, and extent of this dysfunctioning remain controversial. Reduced expression of oxidative phosphorylation genes was observed in muscle and adipose tissue of humans with T2DM [2], while other studies reported on increases in respiration intensity of liver mitochondria from Goto-Kakizaki (GK) rats, a rodent model of diabetes [3], or diabetic patients [4]. In any case, it is important to realize that mitochondrial abnormalities could add to hyperglycemia once the insulin resistance is in place and lead to worsening of the diabetic state.

Due to its strategic position, between the intestinal bed and the systemic circulation, the liver was regarded as buffer organ for the regulation of metabolic fluxes [5, 6]. As glucose and fatty acid metabolisms are largely dependent on mitochondria to generate energy in cells, any impairment in nutrients oxidation, together with a reduced mitochondrial content, could thereby establish a vicious cycle of metabolic

alterations involved in the pathogenesis of T2DM, leading to an increased generation of free radicals. Oxidative stress is recognized to contribute to many pathological processes, and a number of works point to the role of hyperglycaemia in promoting overproduction of mitochondria-derived reactive oxygen species (ROS) [7]. On the other hand, oxidative stress might also result from diminution of the antioxidative capacity in plasma and within the cells of diabetic subjects. Indeed, and in spite of more uncertain data, various reports shown that liver concentrations of reduced glutathione (GSH) decreased in different rodents models of diabetes [8, 9].

Several rodents models have been used to investigate the pathogenesis of metabolic syndrome but they do not reflect the human disease sufficiently. *Psammomys obesus*, a desert gerbil species, is able to subsist on a halophilic plants-based hypocaloric diet. However, in the presence of a relatively high energy regimen such as the standard laboratory diet, this sand rat develops T2DM [10, 11]. Indeed, the potential toxicity of glucose from this exogenous source (high but normal if compared to Wistar rats) will be drastically amplified, leading to a rapid evolution of the disease. Interestingly, prevention of this hyperglycemic state together with an enhancement of hepatic insulin sensitivity was found in diabetes-prone *Psammomys obesus* after exercise training [12]. Through this peculiar behavior, this kind of rodent represents an appropriate biological tool to uncover the features of nutritional diabetes. In addition, a previous experiment with perifused hepatocytes of *Psammomys* reported oxygen consumption rates smaller than those measured from Wistar rats. As well, levels of ATP and ADP were markedly lower in these gerbils [13].

In the light of these above considerations, the aim of the present work was to monitor in parallel the mitochondrial functioning and oxidative damage in diabetes-prone *Psammomys obesus*, by measuring the respiration intensity related to electron transfer chain complexes activities as well as some oxidative stress parameters after 18 weeks of treatment.

2. Materials and Methods

2.1. Animals and Diet. The Algerian sand rats *Psammomys obesus* used for this investigation were housed in suitable cages under controlled temperature and light conditions. Adult animals of both sexes (80–100 g) were divided into two groups: the control group consuming their plants-(*Salsola-foetida*-) based natural food, with a low energy diet (20 kcal/day) but rich in water and minerals—and the group fed the standard laboratory diet of high caloric value (32.5 kcal/day). Food and water were supplied during 18 weeks. Each animal was monitored for body weight and blood glucose in order to select *Psammomys* having a glycaemia superior to 100 mg/dL. All experimental procedures were authorized by the Institutional Animal Care Committee.

2.2. Biochemical Analysis. Fasted *Psammomys* rats were killed by cervical dislocation at the end of treatments, without anesthesia to avoid any further stress, and blood samples were collected in EDTA tubes. Plasma glucose and lipids (triglycerides, total cholesterol, HDL-cholesterol, LDL-c), hepatic and renal function markers (alanine transaminase (ALT), aspartate transaminase (AST), creatinine, urea) were measured by a spectrophotometric method adapted on a Cobas Mira automatic analyser. Plasma insulin was determined by radioimmunoassay. Extraction of hepatic total lipids was carried out using a process earlier described [14], and they were gravimetrically measured.

2.3. Oxidative Stress Assessment. Plasma total antioxidant status (TAS) was analysed in blood samples, using a commercial kit (Randox Laboratories LTD, UK). The principle of this assay is based on the reaction of peroxydase and H_2O_2 with the substrate azinodiethyl-benzothiazoline sulfonic acid (ABTS) to produce a radical cation of stable blue-green colour which was detected at 600 nm. The antioxidant capacity was inversely proportional to this coloration intensity and was expressed as mmol/L.

Lipid peroxidation was estimated from liver homogenates by measuring levels of malondialdehyde (MDA) through the thiobarbituric acid reactive substances method [15].

Liver GSH content was assayed using a commercially available kit (Cayman Chemical Company), based on the reaction with the thiol-specific reagent dithionitrobenzoic acid (DTNB). In this procedure, the sulfhydryl group of GSH reacts with DTNB to form a product which is reduced by glutathione reductase for recycling GSH and producing more thionitro-benzoic acid (TNB). The rate of TNB production was directly proportional to GSH levels, which were expressed as μmoles/mg protein.

The protein content of hepatic samples was determined according to the Lowry method [16], using bovine serum albumin (BSA) solution as a standard.

2.4. Mitochondria Isolation. Liver mitochondria from both *Psammomys* groups were prepared according to a standard differential centrifugation procedure, with all steps carried out at 4°C. After killing the animals, livers were quickly excised, rinsed, and chopped into an isolation medium (250 mM sucrose, 20 mM Tris-HCl, 1 mM EGTA, pH 7.4). The homogenates were centrifuged at 800 g for 10 min to remove nuclei and cell debris. Mitochondria were obtained from the supernatant by spinning twice at 8000 g for 10 min, and the pellet was resuspended in 0.5 mL of isolation buffer, then kept on ice. After measuring protein concentrations as above described, final mitochondrial suspensions were used immediately for respiration or stored at –80°C until enzyme analysis.

2.5. Oxidative Phosphorylation Measurement. Mitochondrial respiration was recorded polarographically, using a sealed oxygraphy chamber equipped with a Clark oxygen electrode and magnetic stirring. Oxygen consumption rates (JO_2) were determined at 37°C in a respiration buffer (125 mM KCl, 20 mM Tris-HCl, 1 mM EGTA, 5 mM Pi) with FFA-BSA to avoid the presence of uncoupled mitochondria. The non-phosphorylating state 2 was initiated by the addition

Table 1: Body weight and biochemical parameters of control ($n = 10$) and high caloric diet-fed *Psammomys* rats ($n = 15$). Each run was performed in duplicate. $^{*}P < 0.05$, $^{**}P < 0.01$, $^{***}P < 0.001$ versus control rat group (natural food).

Parameter	Control (18 weeks)	Diabetic (18 weeks)
Initial body wt (g)	87.8 ± 3.3	85 ± 3.9
Final body wt (g)	121.5 ± 4.1	138.5 ± 8.7*
Hepatic mass/body wt ratio (%)	3.4 ± 0.09	4.05 ± 0.12*
Glucose (mg/dL)	65.2 ± 0.03	267 ± 0.5**
Insulin (pmol/L)	166.5 ± 1.8	1439 ± 3.3***
Triglycerides (mg/dL)	74.6 ± 19	253 ± 45.4**
Cholesterol (mg/dL)	61 ± 4.2	145.7 ± 4.9**
HDL-C (mg/dL)	44.2 ± 3.3	48.5 ± 7.2
LDL-C (mg/dL)	17.8 ± 1.3	29.5 ± 3.2*
Hepatic total lipids (mg/100 g wet wt)	3720 ± 90	4900 ± 190*
Hepatic triglycerides (mg/100 g wet wt)	291 ± 19	654 ± 79**
Hepatic cholesterol (mg/100 g wet wt)	273 ± 11	322 ± 21*
Urea (mg/dL)	53.8 ± 4.6	73.6 ± 6.9*
Creatinine (mg/dL)	0.28 ± 0.05	0.45 ± 0.02*
ALT (U/L)	76 ± 8.4	136 ± 19**
AST (U/L)	86 ± 6.7	167 ± 25**

of either 5 mM glutamate/2.5 mM malate (G/M) or 5 mM succinate/0.5 mM malate (S/M) in presence of 1.25 μM rotenone. The phosphorylating state 3 was obtained after addition of 1 mM ADP while state 4 was measured with 1.25 μg/mL oligomycin, a specific inhibitor of ATP synthase. For uncoupled respiration, 75 μM of dinitrophenol (DNP) was added, while cytochrome c oxidase activity was indirectly evaluated with 1 mM TMPD/5 mM ascorbate. The efficiency of oxidative phosphorylation was then assessed by the state 3-to-state 4 ratio, also called respiratory control index (RCR).

2.6. Electron Transfer Chain Activity and Cytochromes Content. Activities of respiratory complexes were assayed via slight changes of the protocols described by Malgat et al., using liver mitochondrial particles resulting from freezing-thawing cycles [17]. Complex I was assayed as the rate of NADH oxidation at 340 nm in 50 mM KPi buffer containing 3.75 mg/mL BSA, 100 μM decylubiquinone, 100 μM NADH. Rotenone (10 μM) was specifically used to inhibit this complex whose real activity was deduced from difference between NADH oxidation without and with rotenone. Complex II was measured as the rate of 2,6-dichloro-indophenol (DCIP) reduction at 600 nm in 50 mM KPi buffer supplemented with 2.5 mg/mL BSA, 9.3 μM antimycin A, 5 μM rotenone, 100 μM DCIP, 30 mM succinate. Enzyme activity was calculated between the difference before and after addition of 50 μM decylubiquinone. Complex III was assayed by measuring the reduction of cytochrome c at 550 nm, with and without 9.1 μM antimycin A. Isolated mitochondria were incubated in 100 mM KPi medium with 1 mg/mL BSA, 50 μM EDTA, 1 mM KCN, 100 μM oxidized cytochrome c, and the reaction was started by addition of 105.6 μM decylubiquinol.

In parallel, the content in different cytochromes of the electron transfer chain was measured by dual-wavelength spectrophotometry, comparing the spectra of fully oxidized versus fully reduced cytochromes [18].

2.7. Statistical Analysis. All data were reported as mean ± SEM. Differences between both rat groups were determined by Student's t-tests, with a P value of either <0.05, <0.01, or <0.001 considered as statistically significant.

3. Results

3.1. Long-Term Metabolic Effects of High Caloric Diet and Impact on the Liver Redox State. *Psammomys* rats fed a high caloric chow for 18 weeks developed a metabolic syndrome, with significant changes in their body weight ($P < 0.05$), glycemia ($P < 0.01$), and insulinemia ($P < 0.001$) as compared with those of control group (Table 1). Plasma lipids levels, in particular triglyceridemia and cholesterolemia, were also altered. Furthermore, diabetic *Psammomys* exhibited a severe liver deterioration, as evidenced by a substantial increase of transaminases activity ($P < 0.05$), the hepatic mass accretion together with tissue accumulation of triglycerides. A renal injury, characterized by a rise in uremia and creatininemia, was besides showed. On the other hand, such harmful conditions markedly decreased plasma antioxidant capacity (Figure 1), whereas index of lipid peroxidation simultaneously increased (Figure 1). In addition, a depletion in hepatic GSH was found (Figure 1), and the resulting oxidative stress status in the liver, as the GSH/GSSG ratio, was largely diminished by the hypercaloric diet (1.07 ± 0.82 versus 4.29 ± 0.69 for control animals, $P < 0.01$).

3.2. Oxygen Consumption. With mitochondria isolated from diabetic *Psammomys* livers, we noticed a net decline of the respiratory chain activity (Figure 2). Indeed, both basal state

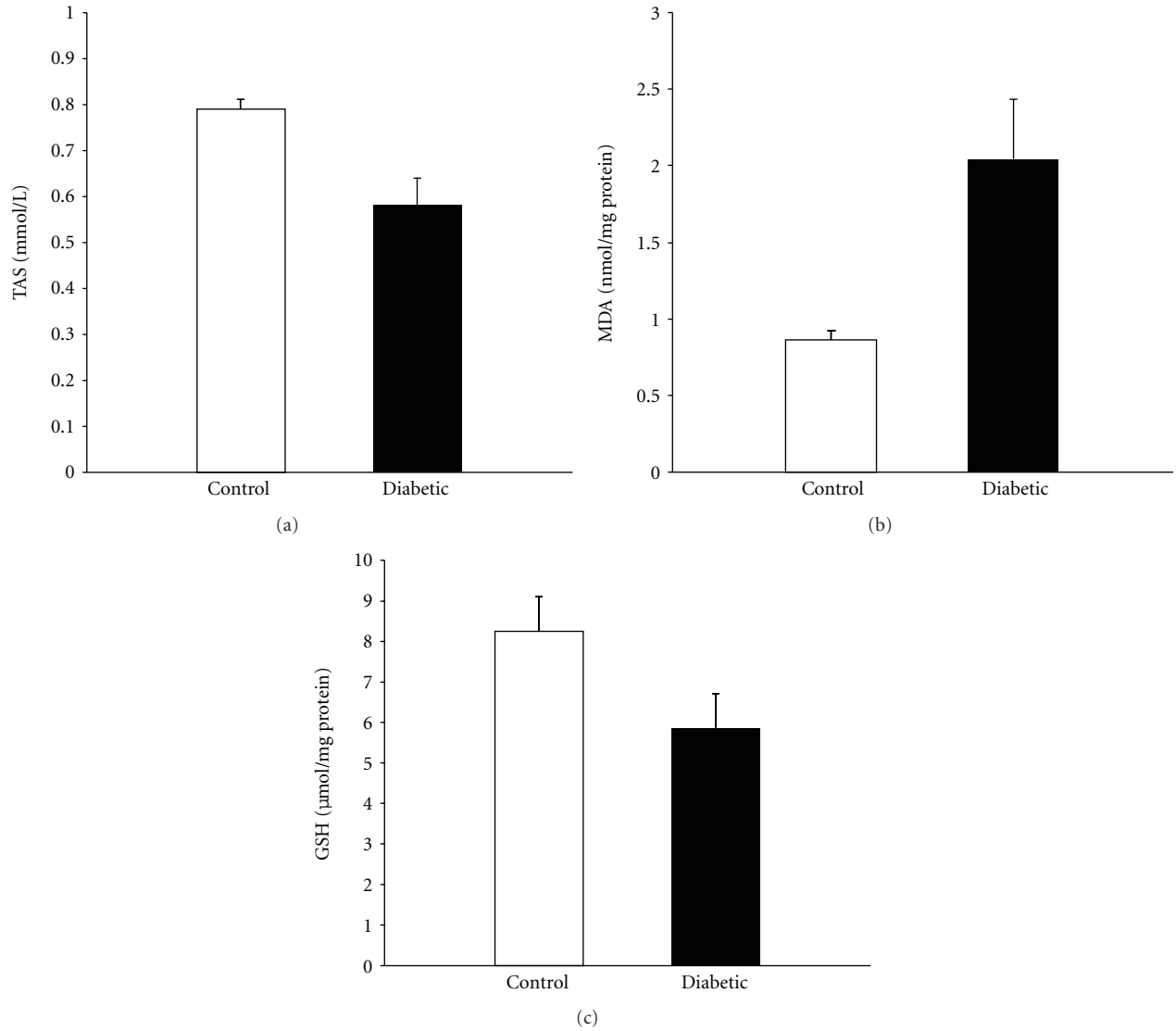

Figure 1: Oxidative stress in plasma and liver tissue. Total antioxidant defences or TAS (a), as well as the intrahepatic contents in MDA (b) and GSH (c), was, respectively, measured in fresh plasma and frozen liver homogenate of control or treated *Psammomys*. $^{*}P < 0.05$ versus control group.

2 and ADP-stimulated state 3 were significantly lower in mitochondria respiring on G/M (−24 and −31%, resp.) but barely decreased with S/M plus rotenone (−8 and −7.5%, resp.). The assessment of oligomycin-induced state 4 showed no modification whatever the substrates. These values led to a decreased RCR (state 3-to-state 4 ratio) for mitochondria only energized with G/M (Table 2). An inhibition of either DNP-uncoupled or TMPD/ascorbate-activated respirations (−25 and −19% resp.) was still observed under this particular condition, suggesting an alteration of some respiratory fluxes which could alter the oxidative phosphorylation machinery.

3.3. Mitochondrial Complexes Activity. To assess whether the above respiration data were directly linked to some defects inside the electron transfer chain, enzyme activities of complexes I, II, III, combined with the level in different cytochromes, were measured in broken liver mitochondria. Complexes I and III were substantially decreased (−32 and −40% resp.) in organelles from diabetic animals as compared to control group, yet complex II unexpectedly increased by 42.4% (Figure 3). Interestingly, a smaller content in cytochrome aa3 was found in diabetic *Psammomys* liver mitochondria (Table 3), a result rather consistent with a reduced activity of cytochrome oxidase that we had above seen through the TMPD-dependent respiration.

4. Discussion

In this work, we have confirmed that *Psammomys obesus* is a reliable biological support for the study of metabolic disorders such as insulin resistance or T2DM, and whose the

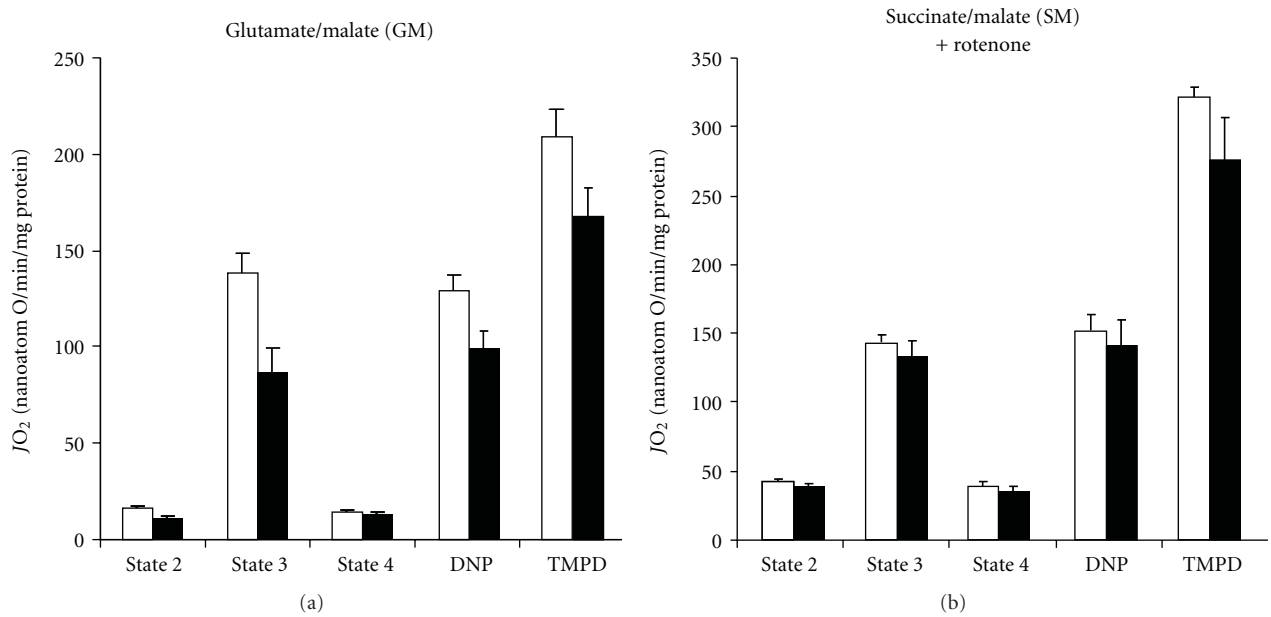

Figure 2: Mitochondrial respiration in *Psammomys*. Oxygen consumption rates (JO_2) were assayed on mitochondria freshly isolated from control (open bars) or treated *Psammomys* (black bars), in the presence of glutamate/malate (a) or succinate/malate with rotenone (b) as energizing substrates. Various respiratory states were next assessed following the addition of different drugs. $^*P < 0.05$ versus control group.

Table 2: Effect of dietary treatment on respiratory control ratios (RCR) of liver mitochondria from both *Psammomys* groups. $^*P < 0.05$ versus control group.

	Oxygen consumption rate (natoms O/min/mg protein)					
	Glutamate/Malate (GM)			Succinate/Malate (SM) + rotenone		
	State 3	State 4	RCR	State 3	State 4	RCR
Control	138.8 ± 9.9	14.8 ± 0.6	9.4 ± 0.9	143.1 ± 5.3	39.3 ± 3.0	3.7 ± 0.3
Diabetic	96.1 ± 7.3*	14.5 ± 0.6	6.6 ± 0.2*	133.0 ± 12.3	35.4 ± 3.5	3.8 ± 0.2

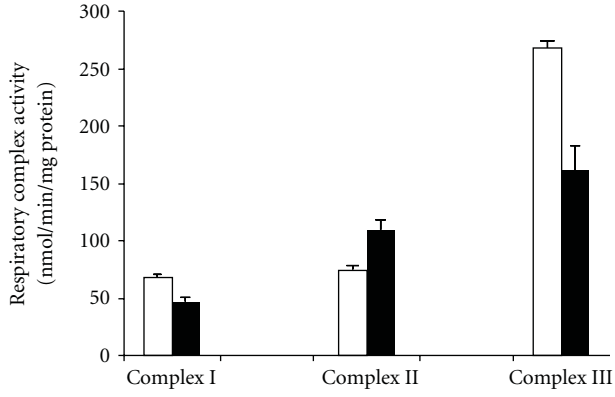

Figure 3: Activities of respiratory complexes I, II, III in liver mitochondria freshly isolated from control (open bars) or treated *Psammomys* (black bars). $^*P < 0.05$ versus control group.

etiology is similar to its manifestation in humans. Our results are in accordance with studies using the Israeli *Psammomys* [19] or the Nile rat [20], even though the latter displayed less pronounced metabolic disturbances than *Psammomys obesus* after feeding a calorie-rich diet for 18 weeks. It may be underlined that the increment in hepatic mass-body weight ratio was positively correlated with hyperinsulinemia and tissue accumulation of lipids, meaning a profound liver injury similar to that reported by others [21]. A high proportion of soluble transaminases was also seen. Knowing that these enzymes are released when hepatocellular damage occurs [22] and, on the other side, that an incomplete oxidation due to chronic fuel excess can be linked to the inability for mitochondria to maintain sufficient ATP levels [23, 24], it seems that these deleterious metabolic defects are consistently associated with a drastic endogenous oxidative stress and subsequent mitochondrial dysfunction, mainly at the inner membrane activity level.

The current work studied oxidative phosphorylation capacity using liver mitochondria isolated from *Psammomys obesus*. Because there existed no or few relevant data about bioenergetics in these rats, it became quite difficult to compare our findings with those of recent literature. We, therefore, tried to discuss them at best with respect to other experimental models involving a mitochondrial dysfunction. Mitochondria from diabetes-prone *Psammomys obesus* showed a lower respiratory rate than that of control

Table 3: Effect of dietary treatment on levels in different cytochromes of liver mitochondria from both *Psammomys* groups.* $P < 0.05$ versus from control group.

	Cytochromes content (pmols/mg protein)			
	a + *a3*	*b*	*c1*	*c*
Control	66.1 ± 3.1	184.2 ± 6.0	95.0 ± 9.2	63.2 ± 21.0
Diabetic	51.3 ± 2.8*	219.4 ± 12.0	79.8 ± 7.9	58.2 ± 7.2

group: the decreases in both state 3 (with ADP) and uncoupled state indicate a loss of oxidative capacity. Similar results were obtained from Wistar rats fed a high-fat diet [25, 26], while no modifications or even higher respiration intensities were found with Zucker rats [27] or GK rats of 6 months age [3]. Cytochrome oxidase, last component of the respiratory chain, is well recognized as a controlling step of nonphosphorylating oxygen consumption [28]. Its activity, when indirectly determined in the presence of TMPD/ascorbate, was lower in diabetic *Psammomys obesus* compared to control animals, and this response was moreover accompanied by a significant loss in cytochrome aa3. Such an observation could reflect a smaller mitochondrial efficiency as evidenced by the reduction of RCR though this fact concerned more particularly the NAD-driven respiration (with glutamate/malate). These findings would be also partially explained by diet-induced changes in membrane lipids composition but this phenomenon merits to be further explored.

High glucose or free fatty acids flux or both impairs metabolic flexibility, which may enhance mitochondrial substrate supply and ROS production [7]. As the harmful effects of ROS on tissues are widely appreciated, the severity of diabetic state for *Psammomys obesus* is likely related to an exacerbated oxidative stress. An increase in lipoperoxidation together with a decline in TAS were reported. In line with these alterations, a decrease of GSH/GSSG ratio was clearly indicative of an impaired liver antioxidant system. Our data are in agreement with several studies using streptozotocin-treated rats [29, 30], rats fed a high fructose diet [31], or diabetic mice [32, 33]. In view of that an increased oxidative stress is also consistent with a slowing-down of oxidative phosphorylation, our bioenergetics results suggest the existence of multiple damaged sites along the electron transfer chain. Indeed, mitochondria from diabetic *Psammomys* revealed an inhibition of complex I and complex III, attributable to an excess in mitochondrial ROS as earlier suggested [34]. Another important finding of this work is that *Psammomys* fed a calorie-rich diet exhibited a net activation of complex II despite a nearly decrease of JO_2 in presence of succinate (FAD-linked substrate), but with comparable RCR between diabetic and control rats. In support of our data, Cunningham et al. observed decreases in all respiratory complexes, except complex II, using liver biopsies from patients with steatosis [35]. Otherwise, complexes II and IV activities were augmented in GK rats or streptozotocin-induced diabetic rats [36].

A large number of studies invoked the involvement of ROS in the pathogenesis of mitochondrial DNA-related disorders [37, 38], and lipid peroxidation products can damage the mitochondrial genome [39]. One may infer that an increasing oxidative stress linked to the diabetic state should lead to mitochondrial DNA damages, altering the function of complexes I and III. Taken into account that the proteins of complex II encoded by nuclear genes are probably spared, any improvement of its activity can alleviate the abnormality or loss of other respiratory parameters, and determine the overall oxidative capacity. Interestingly enough, another kind of adaptative response of mitochondrial metabolism to a high glucose milieu was revealed in pancreatic islets from diabetic *Psammomys obesus* [40]. In this regard, the desert gerbil model could set up metabolic and/or molecular adjustments to circumvent some of the deleterious outcomes of insulin resistance.

It is concluded that a high-caloric diet causes metabolic troubles at the hepatic level in the *Psammomys obesus* rat after an 18-week treatment, and these changes are likely associated with a vast mitochondrial dysfunctioning. The present work is in agreement with an altering expression of oxidative phosphorylation genes, possibly resulting from aggravated oxidative stress, which justifies the performance of further studies to identify some molecular processes responsible for that mitochondrial impairment, and to quantify their relative influence for the liver.

Conflict of Interests

The authors state no conflict of interests.

Acknowledgments

This paper was supported by the Algerian Agency for the Research & Development in Health (ANDRS; Grant no. 03/03/03/10/008) the Program of Interuniversity Cooperation (PCI; Grant no. A/026422/09) as well as by the National Research Program (PNR no. 208/ANDRS/2011 and PNR no. 41/ANDRS/2011) from the National Administration of Algerian Higher Education and Scientific Research (DGRSDT). The authores would like to dedicate this paper to our friend and colleague Professor Yehia El-Mir, recently deceased, with all their love and gratitude.

References

[1] J. A. Kim, Y. Wei, and J. R. Sowers, "Role of mitochondrial dysfunction in insulin resistance," *Circulation Research*, vol. 102, no. 4, pp. 401–414, 2008.

[2] M. E. Patti, A. J. Butte, S. Crunkhorn et al., "Coordinated reduction of genes of oxidative metabolism in humans with insulin resistance and diabetes: potential role of PGC1 and

NRF1," *Proceedings of the National Academy of Sciences of the United States of America*, vol. 100, no. 14, pp. 8466–8471, 2003.

[3] F. M. L. Ferreira, C. M. Palmeira, M. J. Matos, R. Seiç, and M. S. Santos, "Decreased susceptibility to lipid peroxidation of Goto-Kakizaki rats: relationship to mitochondrial antioxidant capacity," *Life Sciences*, vol. 65, no. 10, pp. 1013–1025, 1999.

[4] T. Takamura, H. Misu, N. Matsuzawa-Nagata et al., "Obesity upregulates genes involved in oxidative phosphorylation in livers of diabetic patients," *Obesity*, vol. 16, no. 12, pp. 2601–2609, 2008.

[5] J. Radziuk and S. Pye, "The liver, glucose homeostasis, and insulin action in type 2 diabetes mellitus," in *Contempory Endocrinology: The Metabolic Syndrome: Epidemiology, Clinical Treatment and Underlying Mechanisms*, B. C. Hansen and G. A. Bray, Eds., pp. 343–371, Humana Press, 2007.

[6] G. A. Rutter, "Diabetes: the importance of the liver," *Current Biology*, vol. 10, no. 20, pp. R736–R738, 2000.

[7] M. Brownlee, "Biochemistry and molecular cell biology of diabetic complications," *Nature*, vol. 414, no. 6865, pp. 813–820, 2001.

[8] S. S. Melo, M. R. Arantes, M. S. Meirelles, A. A. Jordao Jr., and H. Vannucchi, "Lipid peroxidation in nicotinamide-deficient and nicotinamide-supplemented rats with streptozotocin-induced diabetes," *Acta Diabetologica*, vol. 37, no. 1, pp. 33–39, 2000.

[9] F. M. Rauscher, R. A. Sanders, and J. B. Watkins, "Effects of coenzyme Q10 treatment on antioxidant pathways in normal and streptozotocin-induced diabetic rats," *Journal of Biochemical and Molecular Toxicology*, vol. 15, no. 1, pp. 41–46, 2001.

[10] G. Marquié, J. Duhault, and B. Jacotot, "Diabetes mellitus in sand rats (*Psammomys obesus*). Metabolic pattern during development of the diabetic syndrome," *Diabetes*, vol. 33, no. 5 I, pp. 438–443, 1984.

[11] E. Ziv, E. Shafrir, R. Kalman, S. Galer, and H. Bar-On, "Changing pattern of prevalence of insulin resistance in *Psammomys obesus*, a model of nutritionally induced type 2 diabetes," *Metabolism*, vol. 48, no. 12, pp. 1549–1554, 1999.

[12] Y. Heled, Y. Shapiro, Y. Shani et al., "Physical exercise enhances hepatic insulin signaling and inhibits phosphoenolpyruvate carboxykinase activity in diabetes-prone *Psammomys obesus*," *Metabolism*, vol. 53, no. 7, pp. 836–841, 2004.

[13] E. A. Koceir, Y. Dahmani, and X. Leverve, "Low rate of glucose 6-phosphate hydrolysis in liver cells is a physiological feature of non-diabetic wild sand rats (*Psammomys obesus*)," *Diabetes and Metabolism*, vol. 29, no. 4, pp. 363–374, 2003.

[14] J. Folch, M. Lees, and G. H. Sloane Stanley, "A simple method for the isolation and purification of total lipides from animal tissues," *The Journal of Biological Chemistry*, vol. 226, no. 1, pp. 497–509, 1957.

[15] R. O. Recknagel and E. A. Glende Jr., "Spectrophotometric detection of lipid conjugated dienes," *Methods in Enzymology*, vol. 105, pp. 331–337, 1984.

[16] O. H. Lowry, N. J. Rosebrough, A. L. Farr, and R. J. Randall, "Protein measurement with the Folin phenol reagent," *The Journal of Biological Chemistry*, vol. 193, no. 1, pp. 265–275, 1951.

[17] M. Malgat, T. Letellier, G. Durrieu, and J. P. Mazat, "Enzymatic and polarographic measurements of the respiratory chain complexes," in *Mitochondrial Diseases: Models and Methods*, P. Lestienne, Ed., pp. 357–377, Springer, Berlin, Germany, 1999.

[18] J. N. Williams Jr., "A method for the simultaneous quantitative estimation of cytochromes a, b, c1, and c in mitochondria," *Archives of Biochemistry and Biophysics*, vol. 107, no. 3, pp. 537–543, 1964.

[19] E. Shafrir and E. Ziv, "Cellular mechanism of nutritionally induced insulin resistance: the desert rodent *Psammomys obesus* and other animals in which insulin resistance leads to detrimental outcome," *Journal of Basic and Clinical Physiology and Pharmacology*, vol. 9, no. 2–4, pp. 347–385, 1998.

[20] F. Chaabo, A. Pronczuk, E. Maslova, and K. Hayes, "Nutritional correlates and dynamics of diabetes in the Nile rat (*Arvicanthis niloticus*): a novel model for diet-induced type 2 diabetes and the metabolic syndrome," *Nutrition & Metabolism*, vol. 7, article 29, 2010.

[21] M. Maislos, V. Medvedovskv, I. Sztarkier, A. Yaari, and E. Sikuler, "*Psammomys obesus* (sand rat), a new animal model of non-alcoholic fatty liver disease," *Diabetes Research and Clinical Practice*, vol. 72, no. 1, pp. 1–5, 2006.

[22] B. J. Song, K. H. Moon, N. U. Olsson, and N. Salem Jr., "Prevention of alcoholic fatty liver and mitochondrial dysfunction in the rat by long-chain polyunsaturated fatty acids," *Journal of Hepatology*, vol. 49, no. 2, pp. 262–273, 2008.

[23] B. Fromenty and D. Pessayre, "Inhibition of mitochondrial beta-oxidation as a mechanism of hepatotoxicity," *Pharmacology and Therapeutics*, vol. 67, no. 1, pp. 101–154, 1995.

[24] S. K. Mantena, D. P. Vaughn, K. K. Andringa et al., "High fat diet induces dysregulation of hepatic oxygen gradients and mitochondrial function *in vivo*," *Biochemical Journal*, vol. 417, no. 1, pp. 183–193, 2009.

[25] G. Vial, H. Dubouchaud, K. Couturier et al., "Effects of a high-fat diet on energy metabolism and ROS production in rat liver," *Journal of Hepatology*, vol. 54, no. 2, pp. 348–356, 2011.

[26] J. Ciapaite, S. J. L. Bakker, G. van Eikenhorst et al., "Functioning of oxidative phosphorylation in liver mitochondria of high-fat diet fed rats," *Biochimica et Biophysica Acta*, vol. 1772, no. 3, pp. 307–316, 2007.

[27] M. Flamment, M. Arvier, Y. Gallois et al., "Fatty liver and insulin resistance in obese Zucker rats: no role for mitochondrial dysfunction," *Biochimie*, vol. 90, no. 9, pp. 1407–1413, 2008.

[28] V. Nogueira, M. Rigoulet, M. A. Piquet, A. Devin, E. Fontaine, and X. M. Leverve, "Mitochondrial respiratory chain adjustment to cellular energy demand," *The Journal of Biological Chemistry*, vol. 276, no. 49, pp. 46104–46110, 2001.

[29] J. A. Herlein, B. D. Fink, Y. O'Malley, and W. I. Sivitz, "Superoxide and respiratory coupling in mitochondria of insulin-deficient diabetic rats," *Endocrinology*, vol. 150, no. 1, pp. 46–55, 2009.

[30] K. R. Shanmugam, K. Mallikarjuna, N. Kesireddy, C. H. Kuo, and K. S. Reddy, "Protective effect of dietary ginger on antioxidant enzymes and oxidative damage in experi-mental diabetic rat tissues," *Food and Chemical Toxicology*, vol. 124, no. 4, pp. 1436–1442, 2011.

[31] P. Rajasekar and C. V. Anuradha, "Effect of L-carnitine on skeletal muscle lipids and oxidative stress in rats fed high-fructose diet," *Experimental Diabetes Research*, vol. 2007, Article ID 72741, 8 pages, 2007.

[32] I. Garcia-Ruiz, C. Rodriguez-Juan, T. Diaz-Sanjuan et al., "Uric acid and anti-TNF antibody improve mitochondrial dysfunction in ob/ob mice," *Hepatology*, vol. 44, no. 3, pp. 581–591, 2006.

[33] D. Du, Y. H. Shi, and G. W. Le, "Oxidative stress induced by high-glucose diet in liver of C57BL/6J mice and its underlying

mechanism," *Molecular Biology Reports*, vol. 37, no. 8, pp. 3833–3839, 2010.

[34] T. A. Young, C. C. Cunningham, and S. M. Bailey, "Reactive oxygen species production by the mitochondrial respiratory chain in isolated rat hepatocytes and liver mitochondria: studies using myxothiazol," *Archives of Biochemistry and Biophysics*, vol. 405, no. 1, pp. 65–72, 2002.

[35] C. C. Cunningham, W. B. Coleman, and P. I. Spach, "The effects of chronic ethanol consumption on hepatic mitochondrial energy metabolism," *Alcohol and Alcoholism*, vol. 25, no. 2-3, pp. 127–136, 1990.

[36] F. M. Ferreira, C. M. Palmeira, R. Seiça, A. J. Moreno, and M. S. Santos, "Diabetes and mitochondrial bioenergetics: alterations with age," *Journal of Biochemical and Molecular Toxicology*, vol. 17, no. 4, pp. 214–222, 2003.

[37] A. P. Rolo and C. M. Palmeira, "Diabetes and mitochondrial function: role of hyperglycemia and oxidative stress," *Toxicology and Applied Pharmacology*, vol. 212, no. 2, pp. 167–178, 2006.

[38] C. Vives-Bauza, R. Gonzalo, G. Manfredi, E. Garcia-Arumi, and A. L. Andreu, "Enhanced ROS production and antioxidant defenses in cybrids harbouring mutations in mtDNA," *Neuroscience Letters*, vol. 391, no. 3, pp. 136–141, 2006.

[39] C. Demeilliers, C. Maisonneuve, A. Grodet et al., "Impaired adaptive resynthesis and prolonged depletion of hepatic mitochondrial DNA after repeated alcohol binges in mice," *Gastroenterology*, vol. 123, no. 4, pp. 1278–1290, 2002.

[40] S. M. Katzman, M. A. Messerli, D. T. Barry et al., "Mitochondrial metabolism reveals a functional architecture in intact islets of Langerhans from normal and diabetic *Psammomys obesus*," *American Journal of Physiology. Endocrinology and Metabolism*, vol. 287, no. 6, pp. E1090–E1099, 2004.

Hindawi Publishing Corporation
Experimental Diabetes Research
Volume 2012, Article ID 302682, 8 pages
doi:10.1155/2012/302682

Research Article

Increased Oxidative Stress and Imbalance in Antioxidant Enzymes in the Brains of Alloxan-Induced Diabetic Rats

Luciane B. Ceretta,[1] Gislaine Z. Réus,[1] Helena M. Abelaira,[1] Karine F. Ribeiro,[1] Giovanni Zappellini,[1] Francine F. Felisbino,[2] Amanda V. Steckert,[1,2] Felipe Dal-Pizzol,[2] and João Quevedo[1]

[1] *Laboratório de Neurociências and Instituto Nacional de Ciência e Tecnologia Translacional em Medicina (INCT-TM), Programa de Pós-Graduação em Ciências da Saúde, Unidade Acadêmica de Ciências da Saúde, Universidade do Extremo Sul Catarinense, 88806-000 Criciúma, SC, Brazil*

[2] *Laboratório de Fisiopatologia Experimental and Instituto Nacional de Ciência e Tecnologia Translacional em Medicina (INCT-TM), Programa de Pós-Graduação em Ciências da Saúde, Unidade Acadêmica de Ciências da Saúde, Universidade do Extremo Sul Catarinense, 88806-000 Criciúma, SC, Brazil*

Correspondence should be addressed to Gislaine Z. Réus, gislainezilli@hotmail.com

Received 14 December 2011; Revised 16 February 2012; Accepted 21 February 2012

Academic Editor: Dan Nemet

Diabetes Mellitus (DM) is associated with pathological changes in the central nervous system (SNC) as well as alterations in oxidative stress. Thus, the main objective of this study was to evaluate the effects of the animal model of diabetes induced by alloxan on memory and oxidative stress. Diabetes was induced in Wistar rats by using a single injection of alloxan (150 mg/kg), and fifteen days after induction, the rats memory was evaluated through the use of the object recognition task. The oxidative stress parameters and the activity of antioxidant enzymes, superoxide dismutase (SOD), and catalase (CAT) were measured in the rat brain. The results showed that diabetic rats did not have alterations in their recognition memory. However, the results did show that diabetic rats had increases in the levels of superoxide in the prefrontal cortex, and in thiobarbituric acid reactive species (TBARS) production in the prefrontal cortex and in the amygdala in submitochondrial particles. Also, there was an increase in protein oxidation in the hippocampus and striatum, and in TBARS oxidation in the striatum and amygdala. The SOD activity was decreased in diabetic rats in the striatum and amygdala. However, the CAT activity was increased in the hippocampus taken from diabetic rats. In conclusion, our findings illustrate that the animal model of diabetes induced by alloxan did not cause alterations in the animals' recognition memory, but it produced oxidants and an imbalance between SOD and CAT activities, which could contribute to the pathophysiology of diabetes.

1. Introduction

Diabetes Mellitus (DM) is a heterogeneous metabolic disorder characterized by hyperglycemia [1]. In type 1 diabetes (DM1), which generally develops at a young age (children and early adulthood), the principal defect is an autoimmune-mediated destruction of pancreatic cells, leading to insulin deficiency [2]. In type 2 diabetes (DM2) the principal defect is insulin resistance, leading to a relative insulin deficiency in the liver and peripheral tissues, which leads to overt hyperglycaemia [3]. The hyperglycaemia in turn causes upto a fourfold increase in neuronal glucose, with intracellular glucose metabolism then leads to neuronal damage [4]. In addition to this, the current therapeutic strategies for DM2 are limited [5].

In both the human and animal models, DM is associated with pathological changes in the central nervous system (SNC) that lead to cognitive and affective deficits, and to an increased risk of brain vascular complications [3]. In the animal models of diabetes, several brain alterations have been described, such as increased hippocampal astrocytic reactivity, impaired synaptic plasticity, vascular changes, decreased

dendritic complexity, and disturbed neurotransmission [6]. Recently, a significant body of evidence has accumulated to indicate that diabetes has detrimental effects on brain function. A number of investigations have been performed to indicate that memory loss is a consequence of both type I and type II diabetes [7]. Some authors have also reported a reduction in the length and a simplification of the dendritic trees of the hippocampal pyramidal cells in diabetic rodents [6]. There is evidence from the animal models showing that changes in dendritic morphology, probably associated with synaptic disturbances, correlate with alterations in memory and learning abilities [8]. Mitochondria are the principal source of reactive oxygen species (ROS) in cells, as the result of imperfectly coupled electron transport. Oxidative stress is widely accepted as playing a key mediatory role in the development and progression of diabetes and its complications, due to the increased production of free radicals and impaired antioxidant defenses [9]. Several mechanisms can contribute to increased oxidative stress in diabetic patients, especially chronic exposure to hyperglycemia. Accumulated evidence points out that hyperglycemia can lead to elevated ROS and reactive nitrogen species (RNS) production by the mitochondrial respiratory system [10], glucose autoxidation [11], activation of the polyol pathway [12], formation of advanced glycation end products (AGEs) [13], antioxidant enzyme inactivation [14] and an imbalance of glutathione redox status [15]. Hyperglycemia can promote an important oxidative imbalance, favoring the production of free radicals and the reduction of antioxidant defenses. At high concentrations, ROS/RNS can lead to damage to the major components of the cellular structure, including nucleic acids, proteins, amino acids, and lipids [16]. Such oxidative modifications in the diabetes condition would affect several cell functions, metabolism, and gene expression, which in turn can cause other pathological conditions [17].

It is important to note that the animal models of diabetes are very useful tools to gain new insights into human diabetes. Animal models induced by chemicals, such as alloxan, exhibit a syndrome of insulin resistance and type 2 diabetes [5]. Thus, the main objective of our study was to evaluate the effects of the animal model of diabetes induced by alloxan on the object recognition task and on the parameters of oxidative stress in the hippocampus, striatum, prefrontal cortex, and amygdala.

2. Material and Methods

2.1. Animals. Male Adult Wistar rats (60 days old) were obtained from the UNESC (Universidade do Extremo Sul Catarinense, Criciúma, SC, Brazil) breeding colony. They were housed five per cage with food and water available *ad libitum* and were maintained on a 12 h light/dark cycle (lights on at 7 : 00 a.m.). All experimental procedures involving animals were performed in accordance with the NIH Guide for the Care and Use of Laboratory Animals and the Brazilian Society for Neuroscience and Behavior (SBNeC) recommendations for animal care and with approval by the local Ethics Committee under protocol number 16/2010.

2.2. Diabetes Induction. Diabetes was induced in rats by using a single intraperitoneal injection of alloxan from Sigma Chemical Co. (St Louis, MO, USA) dissolved in a physiological saline (0.9% NaCl) solution (150 mg/kg), whereas the control group received only a saline injection [18]. Both groups were injected after an 18 h fasting period (60–70 mg/dL blood glucose). Fasting animals are more susceptible to alloxan probably due to partial protection by increased blood glucose [19]. All induced rats showed hyperglycemia (400–600 mg/dL) 48 h after alloxan administration. During the course of the experiment, the blood glucose level was monitored on a daily basis with commercial kits by performing a small puncture in the animals' tail. This methodology is quick and noninvasive, subjecting the rats to a negligible level of stress. At the end of the study, rats with glycemia between 400 and 600 mg/dL were considered diabetic [20]. Fifteen days after the induction of diabetes, based in previous studies [21], all rats were submitted to the object recognition task, after which the animals were killed by decapitation and a biochemical analysis was undertaken of the brain tissues.

2.3. Object Recognition Task. The object recognition task took place in a 40 × 60 cm open field surrounded by 50 cm high walls made of ply wood with a frontal glass wall. The floor of the open field was divided into 12 equal rectangles by black lines. All animals (alloxan or saline; n = 10–15 animals per group) were submitted to a habituation session where they were allowed to freely explore the open field for 5 min. No objects were placed in the box during the habituation trial. Twenty-four hours after habituation, training was conducted by placing the individual rats in the open field for 5 min, in which two identical objects (objects A1 and A2; both being cubes) were positioned in two adjacent corners, 10 cm from the walls. In a short-term recognition memory test given 1.5 h after training, the rats explored the open field for 5 min in the presence of one familiar (A) and one novel (B, a rectangle) object. In a long-term recognition memory test given 24 h after training, the rats explored the open field for 5 min in the presence of one familiar (A) and one novel (C, a pyramid with a square-shaped base) object. All objects had similar textures (smooth), colors (blue), and sizes (weight 150–200 g) but distinctive shapes. A recognition index calculated for each animal was calculated during the test session. It reports the ratio TB/(TA + TB) (TA = time spent exploring the familiar object A; TB = time spent exploring the novel object B) and it reports the ratio TC/(TA + TC) (TA = time spent exploring the familiar object A; TC = time spent exploring the novel object C). Between trials, the objects were washed with 10% ethanol solution. Exploration was defined as sniffing (exploring the object 3–5 cm away from it) or touching the object with the nose and/or forepaws [21].

2.4. Oxidative Stress Parameters. Immediately after the object recognition task, the animals were sacrificed by decapitation and the following brain areas; the prefrontal cortex, amygdala, hippocampus and striatum (n = 4–6 animals per

group) were dissected according to the stereotaxic atlas [22] in ice-cold buffer, in a Petri dish. Submitochondrial particles were prepared in parallel from the four brain regions of each animal. For biochemical analysis in total tissue, the brain structures were rapidly frozen and stored at −70°C.

2.4.1. Mitochondrial Isolation. Rat brain homogenates were centrifuged at 700 g for 10 min to discard nuclei and cell debris and the pellet was then washed to enrich the supernatant that was centrifuged at 700 g for 10 min. The obtained pellet, washed and resuspended in the same buffer, was considered to consist mainly of intact mitochondria able to carry out oxidative phosphorylation. The operations were carried out at 0–2°C. Submitochondrial particles (SMPs) were obtained by freezing and thawing (three cycles) of isolated mitochondria. For superoxide production measurements, SMP were washed twice with 140 mM KCl, 20 mM Tris-HCl (pH 7.4) and suspended in the same medium [23].

2.4.2. Superoxide Production in Submitochondrial Particles of the Rat Brain. Superoxide production was determined in washed brain SMP using a spectrophotometric assay based on superoxide-dependent oxidation of epinephrine to adrenochrome at 37°C ($€_{480\,nm}$ = 4.0 $mM^{-1}\,cm^{-1}$). The reaction medium consisted of 0.23 M mannitol, 0.07 M sucrose, 20 mM Tris-HCl (pH 7.4), SMP (0.3–1.0 mg protein/mL), 0.1 μM catalase, and 1 mM epinephrine. NADH (50 μM) and succinate (7 mM) were used as substrates and rotenone (1 μM) and antimycin (1 μM) were added as specific inhibitors, respectively, to assay O_2^- production at the NADH dehydrogenase and at the ubiquinone-cytochrome b region. Superoxide dismutase (SOD) was used at 0.1–0.3 μM final concentration to give assay specificity [24].

2.4.3. Thiobarbituric Acid Reactive Species Formation. To determine oxidative damage in lipid, we measured the formation of thiobarbituric acid reactive species (TBARS) during an acid-heating reaction, as previously described [25]. The samples were mixed with 1 mL of trichloroacetic acid 10% and 1 mL of thiobarbituric acid 0.67%, and then heated in a boiling water bath for 30 min. Malondialdehyde equivalents were determined in tissue and in submitochondrial particles of the rat brain spectrophotometrically by the absorbance at 532 nm.

2.4.4. Carbonyl Protein Formation. Oxidative damage to proteins was assessed by the determination of carbonyl groups content based on the reaction with dinitrophenylhydrazine (DNPH), as previously described [26]. Proteins were precipitated by the addition of 20% trichloroacetic acid and were redissolved in DNPH. The absorbance was monitored spectrophotometrically at 370 nm.

2.4.5. Superoxide Dismutase Activity. This method for the assay of superoxide dismutase (SOD) activity is based on the capacity of pyrogallol to autoxidize, a process highly dependent on O_2^{-2}; a substrate for SOD [27]. The inhibition of autoxidation of this compound thus occurs when SOD is present, and the enzymatic activity can be then indirectly assayed spectrophotometrically at 420 nm, using a double-beam spectrophotometer with temperature control. A calibration curve was performed using purified SOD as the standard, in order to calculate the specific activity of SOD present in the samples. A 50% inhibition of pyrogallol autoxidation is defined as 1 unit of SOD, and the specific activity is represented as units per mg of protein.

2.4.6. Catalase Activity. The catalase (CAT) activity was assayed using a double-beam spectrophotometer with temperature control. This method is based on the disappearance of H_2O_2 at 240 nm in a reaction medium containing 20 mM H_2O_2, 0.1% Triton X-100, 10 mM potassium phosphate buffer, pH 7.0, and 0.1–0.3 mg protein/mL [28]. One CAT unit is defined as 1 mol of hydrogen peroxide consumed per minute, and the specific activity is reported as units per mg protein.

2.4.7. Protein Determination. All biochemical measures were normalized to the protein content with bovine albumin as standard [29].

2.5. Statistical Analysis. In the open field test, the differences between training test sessions were analyzed by the paired Student's *t*-test. Data for recognition indexes are reported as median ± interquartile ranges (25 and 75). Comparisons among groups were performed using the Kruskal-Wallis test followed by Mann-Whitney test when necessary. The oxidative stress parameters were analyzed by Student's *t*-test for unpaired data and are reported as mean ± S.E.M. *P* values less than 0.05 were considered to be statistically significant.

3. Results

As depicted in Figure 1, in the object recognition task, no statistical differences were observed in the saline or alloxan groups in the training session ($P > 0.05$). In the control rats group, 1.5 h after the training session (short-term recognition memory), we observed an increase in the recognition index compared to the training session, and 24 h after the training session (long-term recognition memory) there was an increase in the recognition index, compared to the training session or to the short-term memory tests ($P < 0.05$; Figure 1). In the diabetic rats induced by alloxan, there was an increase in the recognition index after 24 h, but not 1.5 h after the training session ($P < 0.05$; Figure 1).

In diabetic rats, there was an increase in the superoxide submitochondrial particles in the prefrontal cortex ($P < 0.05$; Figure 2(a)) and an increase in the TBARS submitochondrial particles in the prefrontal cortex and amygdala (Figure 2(b)). In diabetic rats it was shown that there was an increase in the carbonyl proteins in the hippocampus and striatum ($P < 0.05$; Figure 3(a)) and an increase in the TBARS oxidation in the striatum and amygdala ($P < 0.05$; Figure 3(b)). The SOD activity was decreased in diabetic rats in the striatum and amygdala ($P < 0.05$; Figure 4(a)).

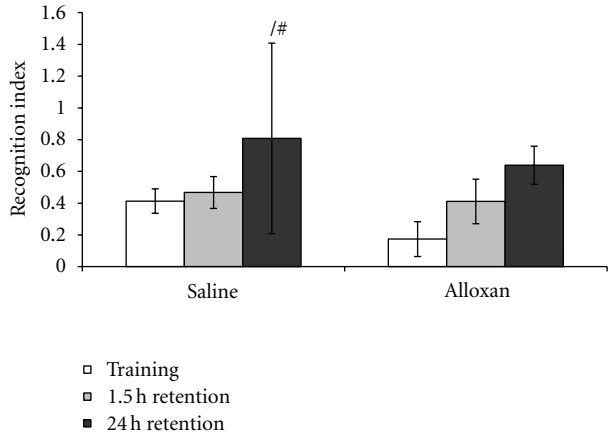

Figure 1: The effects of the animal model of diabetes induced by alloxan on the object recognition task. Results are reported as median ± interquartile ranges of the recognition indexes in training and short- and long-term memory retention test trials. $N = 10$–15 per group, $^{*}P < 0.05$ difference from the training session and $^{\#}P < 0.05$ difference from the training from 1.5 h retention, according to Kruskal-Wallis test.

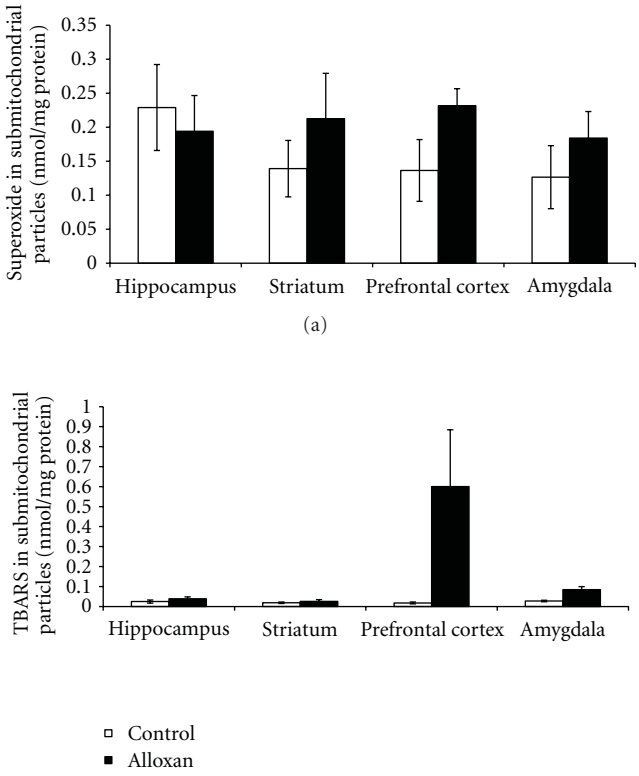

Figure 2: The effects of the animal model of diabetes induced by alloxan on the superoxide (a) and TBARS (b) production in submitochondrial particles in the hippocampus, striatum, prefrontal cortex and amygdala. Results are reported as mean ± S.E.M. $N = 4$–6 per group, $^{*}P < 0.05$ difference from the saline group, according to the Student t-test.

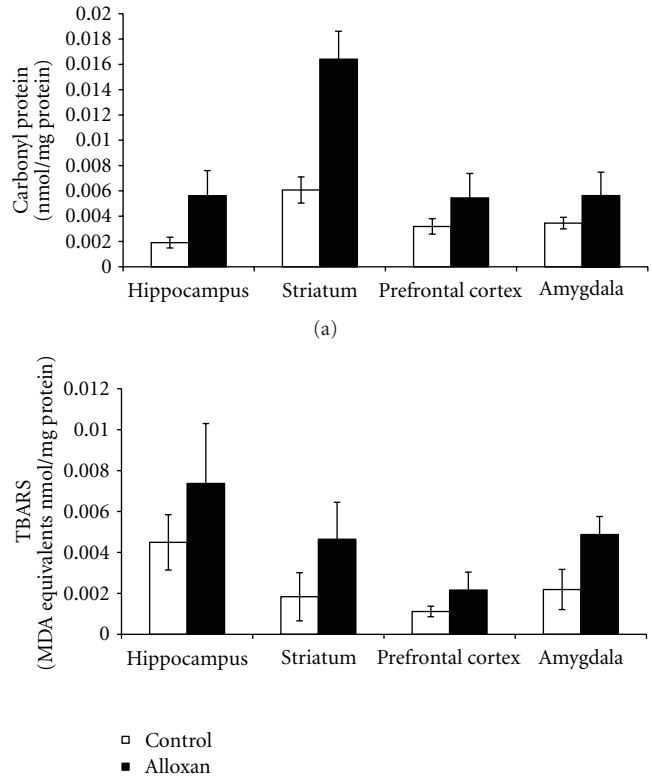

Figure 3: The effects of the animal model of diabetes induced by alloxan on TBARS production (a) and carbonyl formation (b) in the hippocampus, striatum, prefrontal cortex, and amygdala. Results are reported as mean ± S.E.M. $N = 4$–6 per group, $^{*}P < 0.05$ difference from the saline group, according to the Student's t-test.

However, the CAT activity was increased in the hippocampus from diabetic rats ($P < 0.05$; Figure 4(b)).

4. Discussion

Experimental diabetes models can be induced by chemicals that selectively destroy the insulin-producing β-cells in the pancreas [30]. One of the most commonly used chemicals is alloxan. This drug induces diabetes by intracellular generation of ROS formed in a cyclic reaction involving alloxan and its reduced product called dialuric acid [18], with subsequent inhibition of insulin synthesis and secretion.

Recently, a significant body of evidence has accumulated to indicate that diabetes has detrimental effects on brain function. In fact, hypoglycemia and diabetes insults are related with damage in the hippocampus and hypothalamus, which are the brain areas associated with memory and plasticity functions [31]. A number of investigations have been performed to indicate that memory loss is a consequence of both type I and type II diabetes [3, 32]. However, the exact mechanism(s) as to how diabetic conditions could affect memory activity remains to be fully characterized. In the present study our results showed that in diabetic rats, there was an increase in the recognition index 24 h after

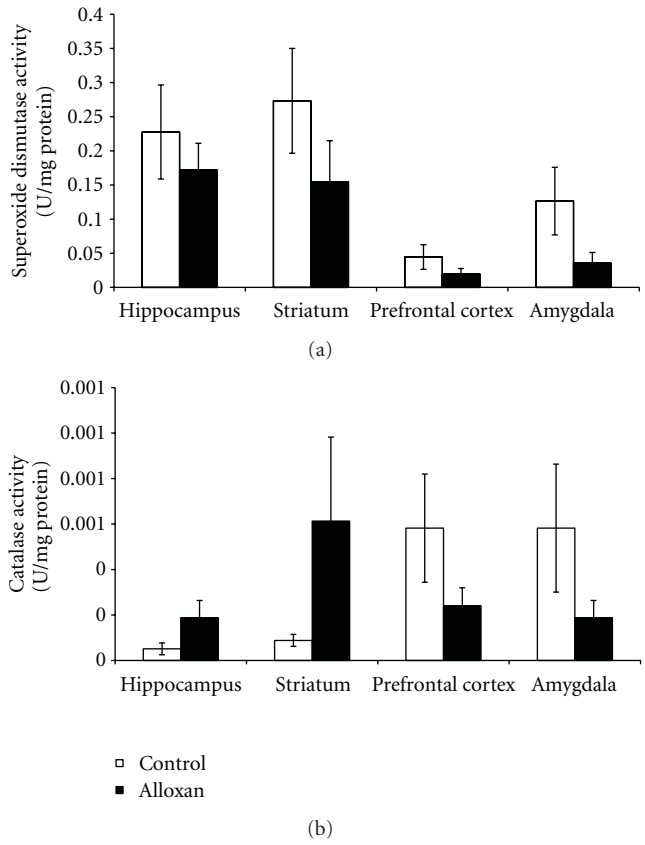

Figure 4: The effects of the animal model of diabetes induced by alloxan on the superoxide dismutase (a) and catalase (b) activities in the hippocampus, striatum, prefrontal cortex, and amygdala. Results are reported as mean ± S.E.M. $N = 4$–6 per group, $^{*}P < 0.05$ difference from the saline group, according to the Student's t-test.

the training session, indicating that diabetic rats did not alter recognition memory, when subjected to the object recognition task. Contrary to this, another study showed a significant reduction of memory formation, evaluated in the passive avoidance test in streptozotocin-induced diabetic mice [7]. The authors suggest that the overexpressed β-amyloid precursor might be one of the underlying factors causing memory deficit.

Differences between these studies could be related with the animal model of diabetes and tests used to evaluate memory. Although some studies have shown that oxidative stress induces significant deficits in cognitive performance (learning ability and memory retention) [33], in the present findings we did not show this correlation. It is important to note that during the formation of memories the activation of specific receptors and of several molecular cascades is required to convert extracellular signals that lead to changes in neuronal connectivity [34], which were probably not altered in the brains of alloxan-induced diabetic rats. For example, we recently demonstrated that brain-derived neurotrophic factor (BDNF) levels did not alter in the hippocampus from alloxan-induced diabetic rats [35]. BDNF is a neurotrophin which has an important role in hippocampal-dependent forms of memory [36]. Thus, the findings of the present study on recognition memory could be related, at least in part, because the animal model of diabetes induced by alloxan did not alter BDNF levels.

A previous study showed that alloxan-induced diabetes is associated with changes in the uptake of insulin by the brain, which includes increased binding to the capillary bed comprising the blood brain barrier and increased transport across the blood brain barrier [37]. Moreover, studies related that oxidative stress impacts several brain areas, such as the forebrain, cerebellum, and brain stem [31, 38]. Thus, in the present study we evaluated oxidative stress parameters in different brain areas, namely, the hippocampus, striatum, prefrontal cortex, and amygdala. Uncontrolled ROS production could lead to damage in cellular macromolecules (DNA, lipids, and protein) and other small antioxidant molecules [39], contributing to the progress of diabetic complications. Still, research indicates that obesity and hyperglycemia are associated with increases in the ROS production [40, 41]. In the present study we observed an increase in the superoxides in the prefrontal cortex and an increase in TBARS in the prefrontal cortex and amygdala in submitochondrial particles. Diabetes causes mitochondrial superoxide overproduction and this increased superoxide production is the major mediator of diabetes tissue damage [41]. In fact, in diabetic cells with a high intracellular glucose concentration, there is more glucose-derived pyruvate being oxidized in the tricarboxylic acid cycle, increasing the flux of electron donors (NADH and FADH2) into the electron transport chain [42]. Thus, electron transfer inside complex III is blocked [43], causing the electrons to use coenzyme Q as a backup, which donates the electrons one at a time to molecular oxygen, thereby generating superoxide [42]. The mitochondria are an organelle and have the ability to generate superoxides at complexes I and III [44, 45]. In addition to this, in brain tissue, complexes I and III have been attributed to major ROS production [44, 45]. In fact, a study from our group demonstrated that in alloxan-induced diabetic rats there were alterations in the mitochondrial respiratory chain [20]. Thus we suggest that alloxan-induced diabetic-like symptoms may provide a useful animal model to test the hypothesis of the involvement of oxidative stress in diabetes. Our results also showed an increase in carbonyl protein in the hippocampus, and amygdala and an increase in TBARS oxidation in the striatum and amygdala from diabetic animals. We discovered from our data that the TBARS levels in mitochondrial particles and in tissues were different, but our analysis was conducted in different areas, involving separate samples from submitochondrial particles and another from tissue. It is known that the mitochondria is a major producer of ROS [42], which in turn causes damage in lipids, which may explain the increase in TBARS in submitochondrial particles in the prefrontal cortex. Recently, Chang et al. [46] showed an increase in the carbonyl protein in the renal tissues from diabetic animals induced by streptozotocin. Additionally, similar to our findings, the TBARS index was increased in the liver of rats that had received a single injection of alloxan (150 mg/kg) [30]. Also,

there was shown to be an increase in the TBARS in the plasma and hippocampus from diabetic animals induced by streptozotocin [47]. Recently, [48] investigated the effects of agmatine, an antihyperglycemic and antioxidant, on MDA and glutathione levels in the cerebral cortex and hippocampus from diabetic rats. The authors found that treatment with agmatine reduced oxidative stress markers in the brain of diabetic rats. In addition, [48] showed that brain regions differ in their response to oxidative stress in obese db/db mice. Still, silibinin, a compound with antioxidant properties, provided efficient neuroprotection in these diabetic rats [48]. Thus, this suggests that diabetes is related to oxidative stress in the brain.

The present findings showed that SOD activity decreased in the striatum and amygdala. On the other hand, the CAT activity increased in the hippocampus in diabetic animals. SOD is a protective enzyme that can selectively scavenge the superoxide anion radical ($O_2^{-\cdot}$) by catalyzing its dismutation to hydrogen peroxide (H_2O_2) [49]. CAT catalyzes degradation of H_2O_2 to water and O_2. Another study showed that SOD and CAT activities were increased in the livers from alloxan-induced diabetic rats [31]. Also, Amer et al. [50] demonstrated that polymorphisms of glutathione S-transferase (an antioxidant enzyme) genes GSTM1 and GSTT1 were associated with an increased risk of type 2 DM. Interestingly, Di Naso et al. [51] reported that exogenous antioxidant copper zinc superoxide dismutase (Cu/Zn SOD) decreased liver peroxidation and increased nitric oxide synthase (NOS) in diabetic rats. Moreover, Gibson et al. [52] showed that N-acetylcysteine (NAC), a biosynthetic precursor of the antioxidant glutathione, reduced thrombotic propensity in type 2 diabetes patients, suggesting that this effect occurred by increasing the platelet antioxidant status as a result of elevated glutathione synthesis.

An imbalance in the SOD/CAT ratio indicates the generation of reactive species [53], which were reported in the present study. In this context, the effects of alloxan on SOD/CAT turnover (by increasing CAT and decreasing SOD activity) may result in antioxidant effects. An imbalance in the SOD/CAT ratio indicates the generation of reactive species, which were reported in the present study. Thus, considering the pathophysiology of diabetes, and the results presented in the present work, it is sensible to suggest that differences in oxidative stress parameters may be related, at least in part, with brain metabolism. Another study from our group also showed a decrease in SOD and an increase in CAT activities in the brain of rats submitted to the chronic mild stress procedure [54]. In fact, studies have reported a relationship between diabetes and stress [55, 56] inclusively, alloxan-induced diabetic rats presented depressive-like behaviour [20].

The cause of the overall oxidative imbalance demonstrated in our study may be due to mitochondrial dysfunction. Recently, it was shown that alloxan-induced diabetic rats presented alterations in the mitochondrial respiratory chain, creatine kinase, and citrate synthase activities [20]. However, mitochondrial alteration could occur by oxidative imbalance. In fact, ROS causes damage in the mitochondrial oxidative phosphorilation [56]. In addition, Bhattacharya et al. [57] reported decreased mitochondrial membrane potential, enhanced cytochrome c release, reciprocal regulation of the Bcl-2 family, and increases of caspases 3 and 9 in alloxan-induced diabetes. The authors also showed that treatment with D-saccharic acid 1,4-lactone, a derivative of D-glucaric acid which has antioxidant properties, counteracted these changes [57].

5. Conclusions

To our knowledge our data describes for the first time, the effects of the animal model of diabetes induced by alloxan on memory and oxidative stress parameters in the rat brain. In conclusion, alloxan-induced diabetes did not alter recognition memory, but induced oxidative damage and an imbalance between antioxidant enzymes, contributing, at least in part, to the pathophysiology of diabetes.

Acknowledgments

This study was supported in part by grants from "Conselho Nacional de Desenvolvimento Científico e Tecnológico" (CNPq-Brazil—J. Quevedo and F. Dal-Pizzol), from the Instituto Cérebro e Mente (J. Quevedo) and UNESC (J. Quevedo and F. Dal-Pizzol). J. Quevedo and F. Dal-Pizzol are recipients of CNPq (Brazil) Productivity Fellowships. G. Z. Réus and A. V. Steckert are holders of a CAPES studentship. Finally, the are grateful to Luciano K. Jornada for assisting in the statistical analysis.

References

[1] G. I. Robles and D. Singh-Franco, "A review of exenatide as adjunctive therapy in patients with type 2 diabetes," *Drug Design, Development and Therapy*, no. 3, pp. 219–240, 2009.

[2] G. J. Biessels, L. P. Van der Heide, A. Kamal, R. L. A. W. Bleys, and W. H. Gispen, "Ageing and diabetes: implications for brain function," *European Journal of Pharmacology*, vol. 441, no. 1-2, pp. 1–14, 2002.

[3] G. J. Biessels and W. H. Gispen, "The impact of diabetes on cognition: what can be learned from rodent models?" *Neurobiology of Aging*, vol. 26, no. 1, supplement, pp. S36–S41, 2005.

[4] D. R. Tomlinson and N. J. Gardiner, "Glucose neurotoxicity," *Nature Reviews Neuroscience*, vol. 9, no. 1, pp. 36–45, 2008.

[5] K. Srinivasan and P. Ramarao, "Animal models in type 2 diabetes research: an overview," *Indian Journal of Medical Research*, vol. 125, no. 3, pp. 451–472, 2007.

[6] A. M. Magariños and B. S. McEwen, "Experimental diabetes in rats causes hippocampal dendritic and synaptic reorganization and increased glucocorticoid reactivity to stress," *Proceedings of the National Academy of Sciences of the United States of America*, vol. 97, no. 20, pp. 11056–11061, 2000.

[7] S. W. Jung, O. K. Han, and S. J. Kim, "Increased expression of β amyloid precursor gene in the hippocampus of streptozotocin-induced diabetic mice with memory deficit and anxiety induction," *Journal of Neural Transmission*, vol. 117, no. 12, pp. 1411–1418, 2010.

[8] B. Kolb, J. Cioe, and W. Comeau, "Contrasting effects of motor and visual spatial learning tasks on dendritic arborization and

spine density in rats," *Neurobiology of Learning and Memory*, vol. 90, no. 2, pp. 295–300, 2008.

[9] A. Ceriello, "New insights on oxidative stress and diabetic complications may lead to a "causal" antioxidant therapy," *Diabetes Care*, vol. 26, no. 5, pp. 1589–1596, 2003.

[10] T. Nishikawa and E. Araki, "Impact of mitochondrial ROS production in the pathogenesis of diabetes mellitus and its complications," *Antioxidants and Redox Signaling*, vol. 9, no. 3, pp. 343–353, 2007.

[11] M. A. Yorek, "The role of oxidative stress in diabetic vascular and neural disease," *Free Radical Research*, vol. 37, no. 5, pp. 471–480, 2003.

[12] N. E. Cameron, M. A. Cotter, and T. C. Hohman, "Interactions between essential fatty acid, prostanoid, polyol pathway and nitric oxide mechanisms in the neurovascular deficit of diabetic rats," *Diabetologia*, vol. 39, no. 2, pp. 172–182, 1996.

[13] V. M. Monnier, "Intervention against the Maillard reaction in vivo," *Archives of Biochemistry and Biophysics*, vol. 419, no. 1, pp. 1–15, 2003.

[14] A. C. Maritim, R. A. Sanders, and J. B. Watkins, "Diabetes, oxidative stress, and antioxidants: a review," *Journal of Biochemical and Molecular Toxicology*, vol. 17, no. 1, pp. 24–38, 2003.

[15] H. Kaneto, J. Fujii, K. Suzuki et al., "DNA cleavage induced by glycation of Cu,Zn-superoxide dismutase," *Biochemical Journal*, vol. 304, no. 1, pp. 219–225, 1994.

[16] M. Valko, D. Leibfritz, J. Moncol, M. T. D. Cronin, M. Mazur, and J. Telser, "Free radicals and antioxidants in normal physiological functions and human disease," *The International Journal of Biochemistry and Cell Biology*, vol. 39, no. 1, pp. 44–84, 2007.

[17] I. S. Young and J. V. Woodside, "Antioxidants in health and disease," *Journal of Clinical Pathology*, vol. 54, no. 3, pp. 176–186, 2001.

[18] G. A. Behr, E. G. Da Silva, A. R. Ferreira, C. T. S. Cerski, F. Dal-Pizzol, and J. C. F. Moreira, "Pancreas β-cells morphology, liver antioxidant enzymes and liver oxidative parameters in alloxan-resistant and alloxan-susceptible Wistar rats: a viable model system for the study of concepts into reactive oxygen species," *Fundamental and Clinical Pharmacology*, vol. 22, no. 6, pp. 657–666, 2008.

[19] T. Szkudelski, "The mechanism of alloxan and streptozotocin action in B cells of the rat pancreas," *Physiological Research*, vol. 50, no. 6, pp. 537–546, 2001.

[20] L. B. Ceretta, G. Z. Réus, G. T. Rezin, G. Scaini, E. L. Streck, and J. Quevedo, "Brain energy metabolism parameters in an animal model of diabetes," *Metabolic Brain Disease*, vol. 25, no. 4, pp. 391–396, 2010.

[21] T. Barichello, M. R. Martins, A. Reinke et al., "Behavioral deficits in sepsis-surviving rats induced by cecal ligation and perforation," *Brazilian Journal of Medical and Biological Research*, vol. 40, no. 6, pp. 831–837, 2007.

[22] G. Paxinos and C. Watson, *The Rat Brain: Stereotaxic Coordinates*, Academic Press, Sydney, Australia, 2nd edition, 1986.

[23] A. Boveris, N. Oshino, and B. Chance, "The cellular production of hydrogen peroxide," *Biochemical Journal*, vol. 128, no. 3, pp. 617–630, 1972.

[24] A. Boveris, "Determination of the production of superoxide radicals and hydrogen peroxide in mitochondria," *Methods in Enzymology*, vol. 105, pp. 429–435, 1984.

[25] H. H. Draper and M. Hadley, "Malondialdehyde determination as index of lipid peroxidation," *Methods in Enzymology*, vol. 186, pp. 421–431, 1990.

[26] R. L. Levine, J. A. Williams, E. R. Stadtman, and E. Shacter, "Carbonyl assays for determination of oxidatively modified proteins," *Methods in Enzymology*, vol. 233, pp. 346–357, 1994.

[27] J. V. Bannister and L. Calabrese, "Assays for superoxide dismutase," in *Methods of Biochemical Analysis*, vol. 32, pp. 279–312, John Wiley & Sons, New York, NY, USA, 1987.

[28] H. Aebi, "Catalase in vitro," *Methods in Enzymology*, vol. 105, no. C, pp. 121–126, 1984.

[29] O. H. Lowry, N. J. Rosebrough, A. L. Farr, and R. J. Randall, "Protein measurement with the Folin phenol reagent," *The Journal of Biological Chemistry*, vol. 193, no. 1, pp. 265–275, 1951.

[30] T. Szkudelski, "The mechanism of alloxan and streptozotocin action in B cells of the rat pancreas," *Physiological Research*, vol. 50, no. 6, pp. 537–546, 2001.

[31] A. J. Bree, E. C. Puente, D. Daphna-Iken, and S. J. Fisher, "Diabetes increases brain damage caused by severe hypoglycemia," *American Journal of Physiology—Endocrinology and Metabolism*, vol. 297, no. 1, pp. E194–E201, 2009.

[32] J. Beauquis, F. Homo-Delarche, M. H. Giroix et al., "Hippocampal neurovascular and hypothalamic-pituitary-adrenal axis alterations in spontaneously type 2 diabetic GK rats," *Experimental Neurology*, vol. 222, no. 1, pp. 125–134, 2010.

[33] K. Fukui, N. O. Omoi, T. Hayasaka et al., "Cognitive impairment of rats caused by oxidative stress and aging, and its prevention by vitamin E," *Annals of the New York Academy of Sciences*, vol. 959, pp. 275–284, 2002.

[34] S. Laroche, "Cellular and molecular mechanisms of memory," *Biologie Aujourd'hui*, vol. 204, no. 2, pp. 93–102, 2010.

[35] L. B. Ceretta, G. Z. Réus, R. B. Stringari et al., "Imipramine treatment reverses depressive-like behavior in alloxan-diabetic rats," *Diabetes/Metabolism Research and Reviews*, vol. 28, no. 2, pp. 139–144, 2012.

[36] B. Lu and K. Martinowich, "Cell biology of BDNF and its relevance to schizophrenia," *Novartis Foundation Symposium*, vol. 289, pp. 119–129, 2008.

[37] W. A. Banks, J. B. Jaspan, and A. J. Kastin, "Effect of diabetes mellitus on the permeability of the blood-brain barrier to insulin," *Peptides*, vol. 18, no. 10, pp. 1577–1584, 1997.

[38] M. L. Haces, T. Montiel, and L. Massieu, "Selective vulnerability of brain regions to oxidative stress in a non-coma model of insulin-induced hypoglycemia," *Neuroscience*, vol. 165, no. 1, pp. 28–38, 2010.

[39] B. Halliwell, "Antioxidant defence mechanisms: from the beginning to the end (of the beginning)," *Free Radical Research*, vol. 31, no. 4, pp. 261–272, 1999.

[40] M. Brownlee, "Biochemistry and molecular cell biology of diabetic complications," *Nature*, vol. 414, no. 6865, pp. 813–820, 2001.

[41] S. Furukawa, T. Fujita, M. Shimabukuro et al., "Increased oxidative stress in obesity and its impact on metabolic syndrome," *Journal of Clinical Investigation*, vol. 114, no. 12, pp. 1752–1761, 2004.

[42] F. Giacco and M. Brownlee, "Oxidative stress and diabetic complications," *Circulation Research*, vol. 107, no. 9, pp. 1058–1070, 2010.

[43] B. L. Trumpower, "The protonmotive Q cycle. Energy transduction by coupling of proton translocation to electron transfer by the cytochrome bc1 complex," *Journal of Biological Chemistry*, vol. 265, no. 20, pp. 11409–11412, 1990.

[44] A. Boveris, E. Cadenas, and A. O. M. Stoppani, "Role of ubiquinone in the mitochondrial generation of hydrogen peroxide," *Biochemical Journal*, vol. 156, no. 2, pp. 435–444, 1976.

[45] J. F. Turrens and A. Boveris, "Generation of superoxide anion by the NADH dehydrogenase of bovine heart mitochondria," *Biochemical Journal*, vol. 191, no. 2, pp. 421–427, 1980.

[46] C.-C. Chang, C.-Y. Chang, Y.-T. Wu, J.-P. Huang, T.-H. Yen, and L.-M. Hung, "Resveratrol retards progression of diabetic nephropathy through modulations of oxidative stress, proinflammatory cytokines, and AMP-activated protein kinase," *Journal of Biomedical Science*, vol. 18, no. 1, article 47, 2011.

[47] C. A. Y. Wayhs, V. Manfredini, A. Sitta et al., "Protein and lipid oxidative damage in streptozotocin-induced diabetic rats submitted to forced swimming test: the insulin and clonazepam effect," *Metabolic Brain Disease*, vol. 25, no. 3, pp. 297–304, 2010.

[48] G. Marrazzo, P. Bosco, F. La Delia et al., "Neuroprotective effect of silibinin in diabetic mice," *Neuroscience Letters*, vol. 504, no. 3, pp. 252–256, 2011.

[49] I. Fridovich, "Superoxide dismutases: regularities and irregularities," *Harvey lectures*, vol. 79, pp. 51–75, 1983.

[50] M. A. Amer, M. H. Ghattas, D. M. Abo-Elmatty, and S. H. Abou-El-Ela, "Influence of glutathione S-transferase polymorphisms on type-2 diabetes mellitus risk," *Genetics and Molecular Research*, vol. 10, no. 4, pp. 3788–3730, 2011.

[51] F. C. Di Naso, A. Simoes Dias, M. Porawski, and N. A. P. Marroni, "Exogenous superoxide dismutase: action on liver oxidative stress in animals with streptozotocin-induced diabetes," *Experimental Diabetes Research*, vol. 2011, Article ID 754132, 6 pages, 2011.

[52] K. R. Gibson, T. J. Winterburn, F. Barrett, S. Sharma, S. M. MacRury, and I. L. Megson, "Therapeutic potential of N-acetylcysteine as an antiplatelet agent in patients with type-2 diabetes," *Cardiovascular Diabetology*, vol. 10, article 43, 2011.

[53] T. M. Michel, J. Thome, D. Martin et al., "Cu, Zn- And Mn-superoxide dismutase levels in brains of patients with schizophrenic psychosis," *Journal of Neural Transmission*, vol. 111, no. 9, pp. 1191–1201, 2004.

[54] G. Lucca, C. M. Comim, S. S. Valvassori et al., "Effects of chronic mild stress on the oxidative parameters in the rat brain," *Neurochemistry International*, vol. 54, no. 5-6, pp. 358–362, 2009.

[55] S. H. Golden, M. Lazo, M. Carnethon et al., "Examining a bidirectional association between depressive symptoms and diabetes," *Journal of the American Medical Association*, vol. 299, no. 23, pp. 2751–2759, 2008.

[56] C. Shen, P. Findley, R. Banerjea, and U. Sambamoorthi, "Depressive disorders among cohorts of women veterans with diabetes, heart disease, and hypertension," *Journal of Women's Health*, vol. 19, no. 8, pp. 1475–1486, 2010.

[57] S. Bhattacharya, P. Manna, R. Gachhui, and P. C. Sil, "D-saccharic acid-1,4-lactone ameliorates alloxan-induced diabetes mellitus and oxidative stress in rats through inhibiting pancreatic beta-cells from apoptosis via mitochondrial dependent pathway," *Toxicology and Applied Pharmacology*, vol. 257, no. 2, pp. 272–283, 2011.

Hindawi Publishing Corporation
Experimental Diabetes Research
Volume 2012, Article ID 216512, 7 pages
doi:10.1155/2012/216512

Review Article

Prevention of Diabetic Complications by Activation of Nrf2: Diabetic Cardiomyopathy and Nephropathy

Bing Li,[1,2,3] Shujun Liu,[2] Lining Miao,[1] and Lu Cai[3]

[1] *Department of Nephrology, Second Hospital of Jilin University, Changchun 130042, China*
[2] *Department of Nephrology, Jilin Province People's Hospital, Changchun 130041, China*
[3] *KCHRI Pediatric Diabetes Research Laboratories, Department of Pediatrics, The University of Louisville, Baxter I, Suite 304F, Louisville, KY 40202, USA*

Correspondence should be addressed to Lining Miao, miaolining@yahoo.com.cn and Lu Cai, l0cai001@louisville.edu

Received 19 December 2011; Accepted 5 April 2012

Academic Editor: Pietro Galassetti

Diabetic cardiomyopathy and nephropathy are two major causes of death of patients with diabetes. Extra generation of reactive oxygen species (ROS), induced by hyperglycemia, is considered as the main reason for the development of these diabetic complications. Transcription factor, NFE2-related factor 2 (Nrf2), is a master regulator of cellular detoxification response and redox status, and also provides a protective action from various oxidative stresses and damages. Recently we have demonstrated its important role in determining the susceptibility of cells or tissues to diabetes-induced oxidative stress and/or damage. Therefore, this review will specifically summarize the information available regarding the effect of Nrf2 on the diabetic complications with a focus on diabetic cardiomyopathy and nephropathy. Given the feature that Nrf2 is easily induced by several compounds, we also discussed the role of different Nrf2 activators in the prevention or therapy of various diabetic complications. These findings suggest that Nrf2 has a potential application in the clinic setting for diabetic patients in the short future.

1. Introduction

Generally speaking, diabetic cardiovascular complications include macrovascular disease (e.g., stroke and atherosclerosis) and microvascular disease (e.g., retinopathy and nephropathy) [1]. Diabetic nephropathy as one of microvascular diseases and diabetic cardiomyopathy as one of macrovascular diseases are two common complications of diabetes and also two main causes of the mortality for diabetic patients. The prevention of diabetic nephropathy and cardiomyopathy has become a global concern for those who are working in diabetic care and management. Although glucose control, blood pressure, lipid lowering, and the blockade of the renin-angiotensin system [2] were used for the treatment of diabetic patients, the development and progression of nephropathy and cardiomyopathy in the patients with diabetes remains unpreventable. Therefore, to develop an effective approach to prevent or delay the development and progression of these lethal complications for diabetic patients is urgently needed.

Hyperglycemia, hyperlipidemia and inflammation were three main metabolic abnormalities in diabetes, all which are able to stimulate generation of reactive oxygen or nitrogen species (ROS or RNS). Extra generation of these species is known to be critically causative of the development of diabetic complications, including diabetic nephropathy and cardiomyopathy [3–6]. Therefore, antioxidant prevention or therapy of diabetic complications has been attractive, but to date, there was no any antioxidant that was found to be efficiently applied in clinics [4–6].

The transcription factor NFE2-related factor 2 (Nrf2) as one member of the cap'n'collar family is a master regulator of cellular detoxification responses and redox status [9, 10]. As illustrated in Figure 1, under physiological conditions Nrf2 locates in the cytoplasm and combines with its inhibitor kelch-like ECH-associated protein 1 (KEAP1) [11]. KEAP1 could mediate a rapid ubiquitination and subsequent degradation of Nrf2 by the proteasome [11]. Upon exposure of cells to oxidative stress or electrophilic compounds, Nrf2 is free from KEAP1 and translocates into the nucleus to

bind to antioxidant-responsive elements (AREs) in the genes encoding antioxidant enzymes such as NADPH quinone oxidoreductase (NQO1), glutathione S-transferase, heme oxygenase-1 (HO1), and γ-glutamylcysteine synthetase, increasing their expression to play a role of detoxification, antioxidation, and anti-inflammation [11, 12].

Recently, several studies have indicated preventive effect of Nrf2 on high glucose- (HG-) induced oxidative damage in the cultured cells and potentially on the diabetic complications in animal models [13]. Although a few good reviews on the general features of Nrf2 in the oxidative stress and damage related to diabetes are available now [14, 15], we would like to briefly review the information in terms of the protective role of Nrf2 in the development of diabetic complications with a specific focus on nephropathy and cardiomyopathy. Given the feature that Nrf2 is easily induced by several compounds, we also discussed the effect of several Nrf2 activators in the prevention or therapy of these two major complications.

2. Diabetes Upregulates Nrf2 Expression and Function in the Heart and Kidney

It is known that Nrf2 expression and function in the cells *in vitro* and tissues *in vivo* are increased in response to oxidative stress. Since several studies have indicated that the induction of ROS and/or RNS by HG in the cultured cardiovascular cells and renal cells, whether HG could elevate the Nrf2 expression and activation and its downstream gene expression in these cells has been investigated [13, 16, 17]. Treatment with glucose at 20 and 40 mM for 24 h increased the expression of Nrf2 mRNA in primary cardiomyocytes or H9C2 cardiac cell line. NQO1, a prototype of Nrf2-regulated chemical-detoxification gene, was induced to be overexpressed in cardiomyocytes by such HG exposure too. Immunoblotting confirmed the protein expression and induction of Nrf2 and HO1 in cardiomyocytes. Immunofluorescent confocal microscopic examination of the cells revealed that HG treatment significantly increased the nuclear and total cell staining of Nrf2 in comparison with the control cells, indicating that glucose indeed increased the protein level and nuclear accumulation of Nrf2 [16]. Used human mesangial cells (HRMCs), Jiang et al. also demonstrated HG-induced elevation of nuclear protein level of Nrf2 along with upregulation of the mRNA level of NQO1, HO-1, and GST [17]. To further confirm the notion that Nrf2 activation by HG is through generation of ROS, N-acetylcysteine (NAC), an ROS scavenger, was included in the medium. As expected, NAC inhibited the activation of HG-induced Nrf2 and NQO1. In addition, HG-induced Nrf2 activation in other cells such as endothelial cells [13, 18] and vascular smooth muscle cells [19] was also reported. Collectively, these results indicate that HG or hyperglycemia is able to activate the Nrf2 pathway through generation of ROS.

Upregulation of Nrf2 and/or its downstream antioxidant genes in response to hyperglycemia were found not only in the cultured cells, but also in the heart and kidney

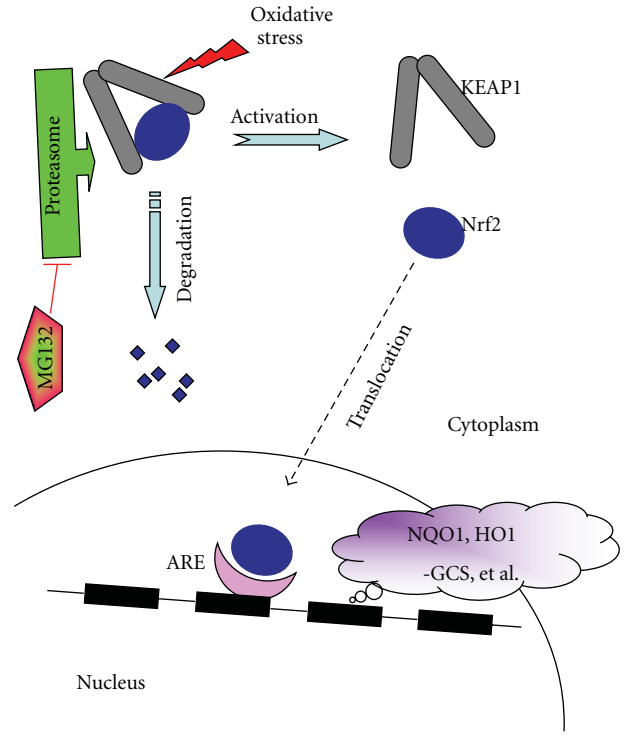

Figure 1: The simplified regulation of Nrf2 by Keap1 and the mechanism of MG132 to activate Nrf2. In general condition, Nrf2 combined with Keap1 in cytoplasm. Under oxidative stress, Nrf2 is free from Keap1 and translocates into nuclear. Through binding with antioxidant response element (ARE), Nrf2 regulates the expression of its downstream target genes to prevent oxidative stress and damage. MG132 could prevent Nrf2 degradation by inhibiting proteasome (adapted from [7, 8]).

of diabetic mice that were also observed. We have used C57BL/6 mice to make type 1 diabetes with a single dose of streptozotocin (STZ). At two weeks after hyperglycemia, we found a significant upregulation of Nrf2 downstream genes NQO1 and HO1 mRNA expression [16]. Jiang et al. have examined if Nrf2 is activated in the kidney of STZ-induced diabetic mice. They used multiple low doses of STZ to induce type 1 diabetes in C57BL/6 mice. At 16 weeks postinjection, Nrf2 expression in the glomeruli of diabetic mice was greatly enhanced and Nrf2 nuclear staining was observed. Activation of Nrf2 was confirmed by upregulation of NQO1 in the glomeruli of diabetic mice [17].

Diabetes-upregulated activation of Nrf2 expression was also observed in the kidney and heart of diabetic patients. In the study by Jiang et al., the diabetic nephropathy kidney tissues were obtained from patients with proteinuria that underwent a renal biopsy for diagnosis of diabetic nephropathy and nondiabetic patients as control. They used these normal and diabetic nephropathy glomeruli to perform immunohistochemical analysis, showing that Nrf2 was hardly expressed in normal glomeruli, whereas it was upregulated in diabetic nephropathy glomeruli. In addition, cells with high expression of Nrf2 in the nucleus were identified as mesangial cells. NQO1 was also activated in

glomeruli of the patients with diabetic nephropathy [17]. In contrast with diabetic nephropathy patients, Tan et al. have demonstrated a different finding in terms of Nrf2 expression in the cardiac tissue from diabetic patients and control [20]. Tissue sections of left ventricles were obtained from autopsy heart specimens of humans with or without diabetes (all diabetic males had histories of hypertension and cardiac dysfunction). Nrf2 expression in the nuclei was significantly downregulated compared to control heart. Reasons for the discrepancy between diabetic kidney and heart remain unclear now based on the limited date. However, several possibilities should be kept in mind: (1) case numbers are too small; (2) organ's different responses may be related; (3) tissues from control groups may be an important issue since what these patients were exposed to were unclear; (4) the last is the period of diabetes history.

In support of the last notion listed above, our recent finding demonstrated that Nrf2 protein expression was slightly increased in the heart of mice with two months hyperglycemia but significantly decreased in the heart of mice with 5 months hyperglycemia [20]. Combined our early study [16] in which Nrf2 downstream genes were increased in the heart of diabetic mice at 2 weeks after STZ-induced hyperglycemia, we assume that Nrf2 is adaptively trying to remain functional to overcome diabetic damage at the early stage of diabetes. At the late stage of diabetes, however, cardiac antioxidant function is further impaired, leading to a decrease in cardiac Nrf2 expression. Therefore, these above studies imply the preventive function of Nrf2 against diabetes-induced oxidative damage.

3. Downregulation of Nrf2 Gene Accelerates Diabetic Pathological Effect on the Heart and Kidney

To gain insight into the role of Nrf2 in prevention of diabetic complication, Yoh et al. have performed the first study using Nrf2-KO mice [21]. They used STZ to induce diabetes in both Nrf2-KO and their wild-type (WT) C57BL/6 mice and found that compared to WT diabetic mice, Nrf2-KO diabetic mice exhibited a deterioration of renal function gradually over the 10-week observation period, along with urinary excretion of nitric oxide metabolites and the occurrence of 8-nitroguanosine, as index of glomerular lesions, during the early stages after treatment. The increased susceptibility of Nrf2-KO mice to diabetes-induced renal damage was further and systemically examined by Jiang et al. [17]. In this study, they used STZ to induce diabetes with Nrf2-KO and WT mice and demonstrated the following evidence: (1) at 16 weeks post-injection, Nrf2-KO diabetic mice showed higher renal ROS production, greater oxidative DNA damage and renal injury compared with WT diabetic mice; (2) Nrf2-KO diabetic mice had more severe glomerular injury than WT diabetic mice, shown by increased glycogen deposition and severe glomerulosclerosis; (3) Nrf2-KO mice had higher TGF-β1 transcription and fibronectin expression, this work clearly indicates a protective role of Nrf2 in diabetic nephropathy; (4) to directly link the Nrf2 to the renal protection from diabetes, particularly hyperglycemia, they used human renal mesangial cells to show that HG-induced significant increase in the expression of several fibrotic mediators, including TGF-β1, could be enhanced by knockdown of Nrf2 by siRNA.

In consistence with the renal protection of Nrf2 from diabetes, we demonstrated that HG-induced ROS generation in both primary neonatal and adult cardiomyocytes from the WT mouse heart, whereas, in the cardiomyocytes from Nrf2-KO mice, ROS was significantly higher under basal conditions and HG remarkably further increased ROS production in concentration and time-dependent manners [16]. In addition, HG also induced significantly higher levels of apoptosis at lower concentrations and in shorter time in Nrf2-KO cardiomyocytes than in WT cardiomyocytes. Primary adult cardiomyocytes from control and diabetic mice that was induced by STZ also showed dependence on Nrf2 function for isoproterenol-stimulated contraction [16].

In fact, Nrf2 activation not only protects the kidney and heart from diabetes-induced oxidative damage, but also the other organs from diabetes. For instance, Ungvari et al. have tried to elucidate the homeostatic role of adaptive induction of Nrf2-driven free-radical detoxification mechanisms in endothelial protection under diabetic conditions. They fed both Nrf2-KO and WT mice with high-fat diet (HFD). HFD-induced increases in vascular ROS levels and endothelial dysfunction were significantly greater or more severe in Nrf2-KO mice than WT mice [18].

4. Prevention of Diabetic Complications by Activation of Nrf2 with Various Activators

The information from the above parts indicates that Nrf2 as an adaptive mechanism is upregulated in the cells exposed to HG or tissues of diabetic animals and patients. Deletion of Nrf2 gene causes a significant increase in the susceptibility of cells or tissues to HG- or diabetes-induced oxidative damage and dysfunction, as illustrated in Figure 2. Therefore, upregulation of Nrf2 expression and function by various approaches may provide a preventive effect on diabetes-induced oxidative damage and consequent complications, to support of which several studies have been done with very multiple beneficial effects on the diabetic complications, as summarized in Table 1.

4.1. In Vitro Evidence. The first study using Nrf2 activator to prevent HG-induced damage was done by Xue et al. [13]. They used sulforaphane (SNF) to induce nuclear translocation of Nrf2 with significant increases in its downstream antioxidant genes such as three- to five-fold increased expression of transketolase and glutathione reductase [13]. SNF treatment significantly prevented HG: increased the formation of ROS and the activation of the hexosamine and PKC pathways, both which have been well defined as important cellular changes in diabetic effect on the target organs. After this study, several other studies with different Nrf2 activators in different kinds of cells also reported similar preventive effects on HG-induced oxidative

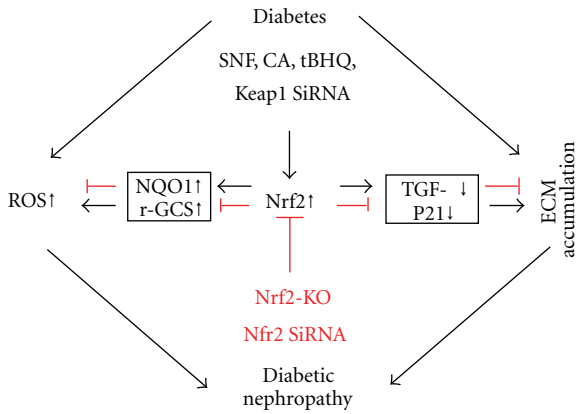

Figure 2: The protection by Nrf2 activation from diabetic nephropathy. Two main pathogenic factors leading to diabetic nephropathy in diabetic patients are increased ROS/RNS and extracellular matrix (ECM) accumulation. Activation of Nrf2 by SNF, CA, tBHQ, and Keap1 SiRNA or activation of Nrf2's downstream targets genes such as NQO1 and r-GCS plays an important role in preventing ROS/RNS-induced damage. At the same time, the expression of TGF-β and P21 was inhibited, leading to a prevention of ECM accumulation. Inhibition of Nrf2 in Nrf2-KO animals or by Nfr2 siRNA resulted in an enhancing diabetic effects. This illustration was made mainly based on a published study [22].

damage (see Table 1). For instance, the effects of magnesium lithospermate B (LAB) against HG-induced oxidative stress and damage via activation of Nrf2 have been evaluated in vascular smooth muscle cells [19].

Zheng et al. have systemically examined the preventive effect of Nrf2 activation with its activators on HG-mediated mesangial cell growth inhibition and hypertrophy. They used human mesangial cell line (HRMC) and three kinds of Nrf2 activators, *tert*-Butylhydroquinone (*t*BHQ), SNF, or cinnamic aldehyde (CA). The growth curve for HRMCs growing in HG media was found to be below compared to those either growing in control or in HG with Nrf2 activators. Staining with Ki67 showed that hyperglycemia inhibited cell proliferation, which was counteracted by activation of Nrf2. The size of HRMCs growing in HG was larger than those in control media, and the increased HRMCs' size induced by HG was significantly improved by three Nrf2 activators. Collectively, these results demonstrate that hyperglycemia-induced cell growth inhibition, and that hypertrophy can be attenuated by activation of the Nrf2 pathway. To gain molecular understanding of how Nrf2 activation relieves HRMC hypertrophy and growth inhibition under HG conditions, the expressions of TGF-β1 and its downstream effectors were further analyzed. They found that HG-induced upregulation of TGF-β1, fibronectin, collagen IV, and p21 in HRMCs was suppressed by treatment with three Nrf2 activators.

4.2. In Vivo Evidence. The preventive effect of Nrf2 activation on diabetic complications in animal models has been explored recently by several groups with different activators (see Table 1). Resveratrol, a red wine antioxidant and a natural phytoalexin, has already been used in prevention and therapy of cancer [33], regulation of blood platelet functions, and protection of cardiovascular diseases [34]. By treating STZ-induce diabetic rats with resveratrol, Palsamy and Subramanian not only confirmed the protection of resveratrol to diabetic nephropathy but also found that resveratrol could normalize the protein expression of Nrf2, and its downstream genes such as γ-GCS and HO-1 in diabetic kidney [31]. Similarly by treating with 1% *t*BHQ in STZ-induce diabetic mice diet, Li et al. also demonstrated that renal expression of Nrf2 and downstream antioxidants increased along with significant decreases in the extracellular matrix deposition and malondialdehyde concentrations in the glomeruli compared to the diabetic mice with regular diet [28].

As mentioned in Section 1, under physiological conditions, Nrf2 locates in the cytoplasm and combines with its inhibitor Keap1 that leads to Nrf2 degradation by the proteasome (Figure 1). It is known that MG132 acts as a proteasome inhibitor, so that it may activate Nrf2 through decreasing the degradation of Nrf2. Luo et al. have first explored the possible prevention of diabetic nephropathy by activation of Nrf2 with MG132 [8]. They treated STZ-induced diabetic rats with MG132 (10 μg/kg) for 12 weeks and they found the following important outcomes. (1) Diabetes-increased 24-h urinary protein excretion rate and renal pathological changes were all improved after MG132 administration. (2) Diabetes-enhanced renal 26S proteasome activity and concentration were effectively reduced after MG132 administration. (3) Diabetes-increased nitrosative damages in kidneys were decreased after MG132 treatment. (4) Renal mRNA and protein expressions of Nrf2 in diabetic rats were upregulated by MG132 compared to diabetes alone. Accordingly, diabetes-decreased renal mRNA expression of superoxide dismutase 1 (SOD1), catalase, and glutathione peroxidase (GPx) was restored after MG132 intervention. (5) Diabetes-increased renal nuclear factor κB (NF-κB) activity was inhibited after MG132 administration. These data suggest that inhibition of the proteasome by MG132 has a preventive effect on the development and progression of diabetic nephropathy in rats through the upregulation of Nrf2-dependent antioxidant genes (Figure 1).

In line with the above findings for the renal protection by MG132 activation of Nrf2, a series of synthetic triterpenoids, CDDO, and CDDO-imidazolide as potent inducers of Nrf2/ARE signaling has been developed and used to prevent several diseases related to inflammatory and oxidative damage [35–38]. Recently, a novel synthetic triterpenoid derivative, dihydro-CDDO-trifluoroethyl amide (dh404), has been developed to activate Nrf2 and suppresses oxidative stress. Dh404 interrupted the Keap1-Cul3-Rbx1 E3 ligase complex-mediated Nrf2 ubiquitination and subsequent degradation saturating the binding capacity of Keap1 to Nrf2, thereby rendering more Nrf2 to be translocated into the nuclei to activate Nrf2-driven gene transcription [39]. We have shown that activation of cardiac Nrf2 by Dh404 in STZ-induced diabetic mice significantly prevented diabetes-induced cardiac oxidative damage and insulin resistance [20]. More importantly, Bardoxolone methyl (aka CDDO-Me or RTA 402) has been clinically

Table 1: Nrf2 activators were treated to diabetic animals and cells.

Nrf2 activators	Mechanisms	Target organs	Species	Ways and volume	References
Insulin	Nuclear translocation	Brain endothelial cell	Human	100 nM, 30 min	[23]
Sulforaphane	Disrupt the Keap1-Nrf2 complex nuclear translocation	HMEC-1 endothelial cell	Human	4 mol/L, 6–48 h	[13]
		Pancreatic islet RIN cells	Mice Rat	40 μg /kg, IP daily, 8 days 10 μM , 3 h	[24]
		Kidney	Mice	12.5 mg/kg, p.o. 16 weeks	[22]
		Mesangial cells	Human	1.25 mmol/L	
		Nerve Neuro2a cell	Rat	0.5 and 1 mg/kg, 6 weeks 5.5 mM	[25]
Oltipraz	Nuclear translocation	Liver	Mice	150 mg/kg, IP tertian, 5 times	[26]
		Adipose/muscle	Mice	0.75 g/kg p.o., 28 weeks	[27]
tBHQ	Enhance expression and nuclear accumulation	Kidney	Mice	1% p.o., 4 and 12 week	[28]
		Renal mesangial cells	Human	6.25 mmol/L	[22]
MG132	Decrease degradation	Kidney	Rat	10 μg /kg IP, daily, 12 weeks	[8]
PETN	Induce HO-1	Blood vessel	Rat	15 mg/kg/day, p.o. 7 weeks	[29]
LAB	Activate NQO1	Vascular smooth muscle cells Vessel tissue	Rat	50 μmol/L 50 mg/kg IP. daily, 15 days	[19]
AGE-BSA	Nuclear translocation	Aortic endothelial cells	Bovine	100 μg mL^{-1}, 0–24 hours	[30]
Resveratrol	Increase expression	Kidney	Rat	5 mg/kg, p.o., 30 days	[31]
DH404	Disrupt the Keap1-Nrf2 complex	HL-1 cells Heart	Mice	200 nmol/L, 12 hour 10 mg/kg, IP., tertian 2 weeks	[20]
CA	Increase the expression	kidney mesangial cells	Mice Human	25/50 mg/kg, p.o., 16 weeks 5 mmol/L	[22]
Telmisartan	Suppression of NAD(P)H oxidase	Kidney	Mice	5 mg/kg, p.o., 4 weeks	[32]

Notes. RIN cells: rat pancreatic β-cell line RINm5F; HMEC-1 cells: human microvascular endothelial cells; tBHQ: tert-butylhydroquinone; PETN: pentaerithrityl tetranitrate; LAB: magnesium lithospermate B; AGE-BSA: AGE-modified bovine albumin; CA: cinnamic aldehyde; HL-1 cells: adult murine atrial cardiomyocyte tumor lineage p.o.: diet; IP: intraperitoneal injection.

explored and extensively discussed for its preventive and therapeutic effects on diabetic nephropathy [40–45].

Although the studies discussed above and others listed in Table 1 have phenomenally suggested the involvement of Nrf2 activation in the preventing diabetic nephropathy, it remains unclear whether upregulated Nrf2 by these activators such as resveratrol, *t*BHQ, or MG132 is really or not the mediator to prevent complications. This uncertain conclusion was solved by a recent systemic study by Zheng et al. The beauty of the Zhang et al. study is that they used two activators of Nrf2: SNF and CA to treat STZ-induce diabetic model in both Nrf2-KO and WT mice [22]. They demonstrated that the activation of Nrf2 and its downstream targets NQO1 and γ-GCS could improve metabolic disorder and alleviate renal damage in STZ-induced WT diabetic mice, but not in Nrf2-KO diabetic mice. This study conclusively indicates the requirement of Nrf2 for SNF- and CA-induced renal protection against diabetes [22].

Besides the studies discussed above, several other studies also demonstrated the preventive effects of Nrf2 activation on diabetic complications with different Nrf2 activators, which are summarized in Table 1. It should be noted that not all Nrf2 activators have the same effects on the activation of Nrf2 and its downstream target genes. For instance, AGE-modified bovine albumin (AGE-BSA) could induce Nrf2 nuclear translocation and enhanced mRNA and protein expression of HO-1 and NQO1, but not glutathione peroxidase-1. Treated with AGE-BSA (100 μg/mL for 24 h), bovine aortic endothelial cells exhibited an adaptive endogenous defense against oxidative stress in diabetes [30]. Pentaerithrityl tetranitrate (PETN), although did not activate Nrf2, significantly activated the expression and function of HO-1, which significantly improved endothelial dysfunction in diabetes by reducing oxidative stress [29].

To further address the importance of Nrf2 downstream protective genes in preventing diabetic complications, there was a very important human study. It is known that NQO1, one important Nrf2 downstream protective components, is an important detoxifying enzyme. To address whether the functional variants of NQO1 can reflect the development of diabetic complications, Ramprasath et al. have analyzed the genotypes of 539 type 2 patients and 285 controls in South Indian population. It is found that the functional variants of NQO1 were associated with the development of coronary artery disease in people with type 2 diabetes [46]. There was

an study, in which nonobese and hypoinsulinemic C57BL/6-Ins2(Akita) (C57BL/6-Akita) diabetic mice were treated with telmisartan, an angiotensin II type 1 receptor blocker, for 4 weeks. Vehicle-treated C57BL/6-Akita mice exhibited higher renal NAD(P)H oxidase (NOX) and lower renal SOD activity with increased levels of renal superoxide than the C57BL/6-wild-type nondiabetic mice. Interestingly, telmisartan treatment not only reduced NOX activity but also enhanced SOD activity in C57BL/6-Akita mouse kidneys, leading to a reduction of renal superoxide levels. Furthermore, telmisartan-treated C57BL/6-Akita mice increased the renal protein expression of SOD and Nrf2. In parallel with the reduction of renal superoxide levels, a reduction of urinary albumin levels and a normalization of elevated glomerular filtration rate were observed in telmisartan-treated C57BL/6-Akita mice. Finally, treatment of C57BL/6-Akita mice with apocynin, an NOX inhibitor, also increased the renal protein expression of SOD and Nrf2. Collectively, our data suggest that NOX negatively regulates renal SOD, possibly by downregulation of Nrf2, and that telmisartan could upregulate renal SOD by the suppression of NOX and subsequent upregulation of Nrf2, leading to the amelioration of renal oxidative stress and diabetic renal changes [32].

5. Conclusions

The prevalence of diabetes dramatically increases in worldwide and its complications significantly affect the life quality of diabetic patients. Diabetic nephropathy and cardiomyopathy are the two major causes for the mortality of diabetic patients. However, there was no an effective approach to prevent the development of these complications for the patients with diabetes. Recently, studies have indicated that Nrf2 as a pivotal mediator for the antioxidant defense system in our body plays a critical role in preventing diabetes-induced oxidative stress/damage, inflammation, and organ's dysfunction. Although there remain many questions to be further investigated, the potential beneficial effects of upregulation of Nrf2 and/or its downstream protective components has attracted the attention of basic scientists and clinical physicians to consider its potential application in the clinic.

Acknowledgment

Cited work from the authors's laboratory was supported in part by grants from ADA (1-11-BA-0117 to LC) and the Starting-Up Fund for Chinese-American Research Institute for Diabetic Complications from Wenzhou Medical College (to L. Cai). B. Li is a recipient of Scholarship under State Scholarship Fund from China Scholarship Council.

References

[1] G. Orasanu and J. Plutzky, "The pathologic continuum of diabetic vascular disease," *Journal of the American College of Cardiology*, vol. 53, no. 5, supplement, pp. S35–S42, 2009.

[2] J. F. Mann, R. E. Schmieder, M. McQueen et al., "Renal outcomes with telmisartan, ramipril, or both, in people at high vascular risk (the ONTARGET study): a multicentre, randomised, double-blind, controlled trial," *The Lancet*, vol. 372, no. 9638, pp. 547–553, 2008.

[3] L. Cai and Y. J. Kang, "Oxidative stress and diabetic cardiomyopathy: a brief review," *Cardiovascular Toxicology*, vol. 1, no. 3, pp. 181–193, 2001.

[4] T. Inoguchi, P. Li, F. Umeda et al., "High glucose level and free fatty acid stimulate reactive oxygen species production through protein kinase C-dependent activation of NAD(P)H oxidase in cultured vascular cells," *Diabetes*, vol. 49, no. 11, pp. 1939–1945, 2000.

[5] T. Nishikawa, D. Edelstein, X. L. Du et al., "Normalizing mitochondrial superoxide production blocks three pathways of hyperglycaemic damage," *Nature*, vol. 404, no. 6779, pp. 787–790, 2000.

[6] C. Rask-Madsen and G. L. King, "Mechanisms of disease: endothelial dysfunction in insulin resistance and diabetes," *Nature Clinical Practice Endocrinology & Metabolism*, vol. 3, no. 1, pp. 46–56, 2007.

[7] K. A. Jung and M. K. Kwak, "The Nrf2 system as a potential target for the development of indirect antioxidants," *Molecules*, vol. 15, no. 10, pp. 7266–7291, 2010.

[8] Z. F. Luo, W. Qi, B. Feng et al., "Prevention of diabetic nephropathy in rats through enhanced renal antioxidative capacity by inhibition of the proteasome," *Life Sciences*, vol. 88, no. 11-12, pp. 512–520, 2011.

[9] M. Kobayashi and M. Yamamoto, "Nrf2-Keap1 regulation of cellular defense mechanisms against electrophiles and reactive oxygen species," *Advances in Enzyme Regulation*, vol. 46, no. 1, pp. 113–140, 2006.

[10] G. P. Sykiotis and D. Bohmann, "Stress-activated cap'n'collar transcription factors in aging and human disease," *Science Signaling*, vol. 3, no. 112, article re3, 2010.

[11] M. McMahon, K. Itoh, M. Yamamoto, and J. D. Hayes, "Keap1-dependent proteasomal degradation of transcription factor Nrf2 contributes to the negative regulation of antioxidant response element-driven gene expression," *The Journal of Biological Chemistry*, vol. 278, no. 24, pp. 21592–21600, 2003.

[12] J. B. de Haan, "Nrf2 activators as attractive therapeutics for diabetic nephropathy," *Diabetes*, vol. 60, no. 11, pp. 2683–2684, 2011.

[13] M. Xue, Q. Qian, A. Adaikalakoteswari, N. Rabbani, R. Babaei-Jadidi, and P. J. Thornalley, "Activation of NF-E2-related factor-2 reverses biochemical dysfunction of endothelial cells induced by hyperglycemia linked to vascular disease," *Diabetes*, vol. 57, no. 10, pp. 2809–2817, 2008.

[14] G. Negi, A. Kumar, R. P. Joshi, and S. S. Sharma, "Oxidative stress and Nrf2 in the pathophysiology of diabetic neuropathy: old perspective with a new angle," *Biochemical and Biophysical Research Communications*, vol. 408, no. 1, pp. 1–5, 2011.

[15] J. Pi, Q. Zhang, J. Fu et al., "ROS signaling, oxidative stress and Nrf2 in pancreatic beta-cell function," *Toxicology and Applied Pharmacology*, vol. 244, no. 1, pp. 77–83, 2010.

[16] X. He, H. Kan, L. Cai, and Q. Ma, "Nrf2 is critical in defense against high glucose-induced oxidative damage in cardiomyocytes," *Journal of Molecular and Cellular Cardiology*, vol. 46, no. 1, pp. 47–58, 2009.

[17] T. Jiang, Z. Huang, Y. Lin, Z. Zhang, D. Fang, and D. D. Zhang, "The protective role of Nrf2 in streptozotocin-induced diabetic nephropathy," *Diabetes*, vol. 59, no. 4, pp. 850–860, 2010.

[18] Z. Ungvari, L. Bailey-Downs, T. Gautam et al., "Adaptive induction of NF-E2-related factor-2-driven antioxidant genes in endothelial cells in response to hyperglycemia," *American Journal of Physiology*, vol. 300, no. 4, pp. H1133–H1140, 2011.

[19] K. Y. Hur, S. H. Kim, M. A. Choi et al., "Protective effects of magnesium lithospermate B against diabetic atherosclerosis via Nrf2-ARE-NQO1 transcriptional pathway," *Atherosclerosis*, vol. 211, no. 1, pp. 69–76, 2010.

[20] Y. Tan, T. Ichikawa, J. Li et al., "Diabetic downregulation of Nrf2 activity via ERK contributes to oxidative stress-induced insulin resistance in cardiac cells in vitro and in vivo," *Diabetes*, vol. 60, no. 2, pp. 625–633, 2011.

[21] K. Yoh, A. Hirayama, K. Ishizaki et al., "Hyperglycemia induces oxidative and nitrosative stress and increases renal functional impairment in Nrf2-deficient mice," *Genes to Cells*, vol. 13, no. 11, pp. 1159–1170, 2008.

[22] H. Zheng, S. A. Whitman, W. Wu et al., "Therapeutic potential of Nrf2 activators in streptozotocin-induced diabetic nephropathy," *Diabetes*, vol. 60, no. 11, pp. 3055–3066, 2011.

[23] M. Okouchi, N. Okayama, J. S. Alexander, and T. Y. Aw, "NRF2-dependent glutamate-L-cysteine ligase catalytic subunit expression mediates insulin protection against hyperglycemia-induced brain endothelial cell apoptosis," *Current Neurovascular Research*, vol. 3, no. 4, pp. 249–261, 2006.

[24] M. Y. Song, E. K. Kim, W. S. Moon et al., "Sulforaphane protects against cytokine- and streptozotocin-induced β-cell damage by suppressing the NF-κB pathway," *Toxicology and Applied Pharmacology*, vol. 235, no. 1, pp. 57–67, 2009.

[25] G. Negi, A. Kumar, and S. S. Sharma, "Nrf2 and NF-κB modulation by sulforaphane counteracts multiple manifestations of diabetic neuropathy in rats and high glucose-induced changes," *Current Neurovascular Research*, vol. 8, no. 4, pp. 294–304, 2011.

[26] L. M. Aleksunes, S. A. Reisman, R. L. Yeager, M. J. Goedken, and C. D. Klaassen, "Nuclear factor erythroid 2-related factor 2 deletion impairs glucose tolerance and exacerbates hyperglycemia in type 1 diabetic mice," *Journal of Pharmacology and Experimental Therapeutics*, vol. 333, no. 1, pp. 140–151, 2010.

[27] Z. Yu, W. Shao, Y. Chiang et al., "Oltipraz upregulates the nuclear factor (erythroid-derived 2)-like 2 (NRF2) antioxidant system and prevents insulin resistance and obesity induced by a high-fat diet in C57BL/6J mice," *Diabetologia*, vol. 54, no. 4, pp. 922–934, 2011.

[28] H. Li, L. Zhang, F. Wang et al., "Attenuation of glomerular injury in diabetic mice with tert-butylhydroquinone through nuclear factor erythroid 2-related factor 2-dependent antioxidant gene activation," *American Journal of Nephrology*, vol. 33, no. 4, pp. 289–297, 2011.

[29] S. Schuhmacher, M. Oelze, F. Bollmann et al., "Vascular dysfunction in experimental diabetes is improved by pentaerithrityl tetranitrate but not isosorbide-5-mononitrate therapy," *Diabetes*, vol. 60, no. 10, pp. 2608–2616, 2011.

[30] M. He, R. C. Siow, D. Sugden, L. Gao, X. Cheng, and G. E. Mann, "Induction of HO-1 and redox signaling in endothelial cells by advanced glycation end products: a role for Nrf2 in vascular protection in diabetes," *Nutrition, Metabolism and Cardiovascular Diseases*, vol. 21, no. 4, pp. 277–285, 2011.

[31] P. Palsamy and S. Subramanian, "Resveratrol protects diabetic kidney by attenuating hyperglycemia-mediated oxidative stress and renal inflammatory cytokines via Nrf2-Keap1 signaling," *Biochimica et Biophysica Acta*, vol. 1812, no. 7, pp. 719–731, 2011.

[32] H. Fujita, H. Fujishima, T. Morii et al., "Modulation of renal superoxide dismutase by telmisartan therapy in C57BL/6-*Ins2*(^{Akita}) diabetic mice," *Hypertension Research*, vol. 35, no. 2, pp. 213–220, 2012.

[33] B. B. Aggarwal, A. Bhardwaj, R. S. Aggarwal, N. P. Seeram, S. Shishodia, and Y. Takada, "Role of resveratrol in prevention and therapy of cancer: preclinical and clinical studies," *Anticancer Research*, vol. 24, no. 5, pp. 2783–2840, 2004.

[34] P. Palsamy and S. Subramanian, "Resveratrol, a natural phytoalexin, normalizes hyperglycemia in streptozotocin-nicotinamide induced experimental diabetic rats," *Biomedicine & Pharmacotherapy*, vol. 62, no. 9, pp. 598–605, 2008.

[35] K. Liby, T. Hock, M. M. Yore et al., "The synthetic triterpenoids, CDDO and CDDO-imidazolide, are potent inducers of heme oxygenase-1 and Nrf2/ARE signaling," *Cancer Research*, vol. 65, no. 11, pp. 4789–4798, 2005.

[36] S. Shin, J. Wakabayashi, M. S. Yates et al., "Role of Nrf2 in prevention of high-fat diet-induced obesity by synthetic triterpenoid CDDO-Imidazolide," *European Journal of Pharmacology*, vol. 620, no. 1–3, pp. 138–144, 2009.

[37] T. E. Sussan, T. Rangasamy, D. J. Blake et al., "Targeting Nrf2 with the triterpenoid CDDO-imidazolide attenuates cigarette smoke-induced emphysema and cardiac dysfunction in mice," *Proceedings of the National Academy of Sciences of the United States of America*, vol. 106, no. 1, pp. 250–255, 2009.

[38] R. K. Thimmulappa, R. J. Fuchs, D. Malhotra et al., "Preclinical evaluation of targeting the Nrf2 pathway by triterpenoids (CDDO-Im and CDDO-Me) for protection from LPS-induced inflammatory response and reactive oxygen species in human peripheral blood mononuclear cells and neutrophils," *Antioxidants & Redox Signaling*, vol. 9, no. 11, pp. 1963–1970, 2007.

[39] T. Ichikawa, J. Li, C. J. Meyer, J. S. Janicki, M. Hannink, and T. Cui, "Dihydro-CDDO-trifluoroethyl amide (dh404), a novel Nrf2 activator, suppresses oxidative stress in cardiomyocytes," *PloS One*, vol. 4, no. 12, Article ID e8391, 2009.

[40] G. M. McMahon and J. P. Forman, "Bardoxolone methyl, chronic kidney disease, and type 2 diabetes," *The New England Journal of Medicine*, vol. 365, no. 18, pp. 1746–1747, 2011.

[41] P. E. Pergola, M. Krauth, J. W. Huff et al., "Effect of bardoxolone methyl on kidney function in patients with T2D and stage 3b-4 CKD," *American Journal of Nephrology*, vol. 33, no. 5, pp. 469–476, 2011.

[42] P. E. Pergola, P. Raskin, R. D. Toto et al., "Bardoxolone methyl and kidney function in CKD with type 2 diabetes," *The New England Journal of Medicine*, vol. 365, no. 4, pp. 327–336, 2011.

[43] K. S. Rogacev, J. T. Bittenbring, and D. Fliser, "Bardoxolone methyl, chronic kidney disease, and type 2 diabetes," *The New England Journal of Medicine*, vol. 365, no. 18, pp. 1745–1747, 2011.

[44] A. Upadhyay, M. J. Sarnak, and A. S. Levey, "Bardoxolone methyl, chronic kidney disease, and type 2 diabetes," *The New England Journal of Medicine*, vol. 365, no. 18, pp. 1746–1747, 2011.

[45] S. van Laecke and R. Vanholder, "Bardoxolone methyl, chronic kidney disease, and type 2 diabetes," *The New England Journal of Medicine*, vol. 365, no. 18, pp. 1745–1747, 2011.

[46] T. Ramprasath, P. S. Murugan, E. Kalaiarasan, P. Gomathi, A. Rathinavel, and G. S. Selvam, "Genetic association of Glutathione peroxidase-1 (GPx-1) and NAD(P)H : quinone oxidoreductase 1(NQO1) variants and their association of CAD in patients with type-2 diabetes," *Molecular and Cellular Biochemistry*, vol. 361, no. 1-2, pp. 143–150, 2011.

Hindawi Publishing Corporation
Experimental Diabetes Research
Volume 2012, Article ID 316384, 4 pages
doi:10.1155/2012/316384

Research Article

Increased Caspase-3 Immunoreactivity of Erythrocytes in STZ Diabetic Rats

Uğur Fırat,[1] Savaş Kaya,[2] Abdullah Çim,[3] Hüseyin Büyükbayram,[1] Osman Gökalp,[4] Mehmet Sinan Dal,[5] and Mehmet Numan Tamer[6]

[1] *Department of Pathology, School of Medicine, Dicle University, Diyarbakır 21000, Turkey*
[2] *Department of Immunology, School of Medicine, Dicle University, Diyarbakır 21000, Turkey*
[3] *Department of Hepatology and Transplantation, Division of Gene and Cell Based Therapy, School of Medicine, King's College London, London SE5 9NU, UK*
[4] *Department of Medical Pharmacology, School of Medicine, Dicle University, Diyarbakır 21000, Turkey*
[5] *Department of Internal Medicine, Division of Endocrinology, School of Medicine, Dicle University, Diyarbakır 21000, Turkey*
[6] *Department of Internal Medicine, Division of Endocrinology, School of Medicine, Süleyman Demirel University, Isparta 32260, Turkey*

Correspondence should be addressed to Uğur Fırat, dijlefirat@hotmail.com

Received 16 February 2012; Accepted 26 March 2012

Academic Editor: Pietro Galassetti

Eryptosis is a term to define apoptosis of erythrocytes. Oxidative stress and hyperglycemia, both of which exist in the diabetic intravascular environment, can trigger eryptosis of erythrocytes. In this experimental study, it is presented that the majority of erythrocytes shows caspase-3 immunoreactivity in streptozocin- (STZ)-induced diabetic rats. Besides that, caspase-3 positive erythrocytes are aggregated and attached to vascular endothelium. In conclusion, these results may start a debate that eryptosis could have a role in the diabetic complications.

1. Introduction

Hyperglycemia and oxidative stress are the prominent features of diabetes mellitus (DM) and seems to play a crucial role in DM-related microvascular complications. In addition, complications of DM like nephropathy, retinopathy, and macrovascular disease are associated with anemia [1, 2].

Eryptosis, a term used for apoptosis of erythrocyte, is triggered with osmotic shock, oxidative stress, or energy depletion [3]. Moreover, eryptosis is characterized with cell shrinkage, membrane blebbing, membrane phospholipids scrambling, and phosphatidylserine (PS) shifting from inner to outer membrane of the erythrocyte [4]. It is demonstrated that death receptor initiated pathway of apoptosis takes a role in eryptosis involving Fas, caspase-8, and caspase-3 [5]. Caspase-3, an executioner caspase, immunoreactivity is observed in the lysate of erythrocytes obtained from type 2 DM patients [6]. Besides that, previous reports show the evidence that eryptosis underlies anemia and microvascular injury both of which may be related with endothelial adhesion and increased aggregation of erythrocytes, in DM patients [3, 7–9].

In this study, it is presented that increased caspase-3 activity is detected in erythrocytes in the vasculature of cerebrum and cerebellum of STZ-induced DM rats. In other words, eryptotic erythrocytes number is increased in DM rats. This finding can explain the anemia and the underlying or accompanying factors of microvascular injury, such as erythrocyte aggregation and endothelial erythrocyte adhesion in DM.

2. Materials and Methods

2.1. Animals. Female Wistar Albino rats are obtained from the Laboratory Animals Facility of Dicle University. In this study, rats are handled in accordance with the Animal Welfare Act and the Guide for the Care and Use of Laboratory animals prepared by the Animal Ethical Committee of Dicle University. Rats are distributed into following groups with

$n = 7$ each: non-DM group and DM group. Rats in non-DM group received citrate buffer intraperitoneal (i.p.) injections. Rats of DM group were injected with STZ (50 mg/kg, i.p.; in 0.1 M citrate buffer, pH 4.5) for induction of DM. Blood glucose level of rats in DM group is confirmed before sacrifice and it is over 250 mg/mL. Thirty days after i.p. administration rats are executed for the analysis.

2.2. Biochemical Analysis. The excised cerebrum for biochemical analyses were weighed, immediately stored at −80°C. The cerebral tissues are perfused with 1.15% ice-cold KCl (w/v) and sliced into minute pieces then homogenized in five volumes of the same solution. The homogenate is centrifuged at 14.000 rpm at 4°C for 30 minutes (min). The supernatants are used for the assay. Lipid peroxidation level, indicator of oxidative tissue damage, in the cerebrum is defined with malondialdehyde (MDA) amount as mentioned by Ohkawa et al. [10].

2.3. Immunohistochemical Staining. Cerebrum and cerebellum are fixated in 10% formaldehyde for 48 hours. Then, they are dehydrated and embedded in paraffin. Paraffin blocks are sliced in 4 μm thickness with microtome. Tissue slices are located on positive-charged glasses and incubated at 60°C for 60 min to deparaffinize. Then, slides are treated with xylene (3×5 min) and hydrated with alcohol. Antigen retrieving process is done in citrate buffer (10 mM Citric Acid, 0.05% Tween 20, pH 6.0) by boiling and cooling down (x3) in microwave oven. After this and every other processes slides are washed with Phosphate-Buffered Saline twice for 5 min each. Endogenous peroxidase blocking is done with Peroxide Block (ACA500, ScyTek, UT, USA) for 10 min at room temperature (RT). Then, slides are treated with Super Block (AAA125, ScyTek, UT, USA) for 20 min at RT. Then, slides are treated with rabbit anti-human Caspase-3 polyclonal Antibody (1 : 750) (cat#. GTX73090, Gene Tex, Inc.; CA92606, USA) cross reacting with rat caspase-3 for 20 min at RT. Then, biotinylated SensiTek polyvalent antibodies (ABF125, ScyTek, UT, USA) are applied for 20 min at RT before SensiTek HRP, streptavidin-HRP complex (ABG125, ScyTek, UT, USA) treated for 20 min at RT. Finally, AEC Chromogen/Substrate Bulk Kit (ACJ125, ScyTek, Utah, USA) working solution is applied for 10 min at RT. Counterstaining is performed with Mayer hematoxylin (cat#. 05-M06002, Bio-Optica, Milano, Italy). Slides are evaluated under the light microscope (Nikon ECLIPSE 80i, Japan) at ×400 magnification by a pathologist blinded to study groups.

2.4. Statistics. Caspase-3 positive and negative erythrocytes are counted in vascular spaces at randomly selected 8 regions for each slide. The averages of percentage of positive cell are calculated for each slide. Then, the means of percentages of positive cells of the groups are compared with Student's t-test. The difference of the means of MDA levels is also calculated with Student's t-test. Data are presented as mean ± S.D.

3. Results

In this study, MDA levels, showing lipid peroxidation representing oxidative tissue destruction, in cerebral tissues are significantly higher in DM group than non-DM group, 451 ± 66 nmol/gr protein, and 263 ± 55 nmol/gr protein, respectively ($P < 0.0001$). In addition, immunohistochemical staining of the cerebral and cerebellar tissues demonstrates that a few number of erythrocytes show immunoreactivity to caspase-3 in non-DM group (Figure 1(a)), that is physiological outcome of senescence of erythrocytes, possibly. However, the number of capase-3 immunoreactive erythrocytes is elevated in DM group (Figure 1(b)). In addition, majority of the erythrocytes with caspase-3 immunoreactivity attached each other in DM group (Figure 1(c)). Furthermore, these aggregated erythrocytes adhered to endothelium of the vessels (Figure 1(c)). What is more, some of the vessels are totally occluded with caspase-3 positive erythrocytes in these rats in DM group (Figure 1(d)). The statistical picture of our finding is as follows: 31.33 ± 9.03% of the erythrocytes show immunoreactivity to caspase-3 in DM group; nonetheless, 7.43 ± 3.36% of the erythrocytes stained with caspase-3 in non-DM group (Figure 2). In addition, the mean of percentages of caspase-3 positive cells is significantly different in DM group than other group ($P < 0.0001$). These findings suggest that eryptosis, ignited with either high serum glucose level or oxidative stress or bought of them and defined with prominent caspase-3 immunoreactivity, is a considerable underlying cause of the diabetic complications, such as microangiopathy and anemia.

4. Discussion

In this study, in brief, caspase-3 immunoreactivity in erythrocytes, aggregation, and endothelial adhesion of erythrocytes are shown with immunohistochemical staining of cerebral and cerebellar tissues in the diabetic rats. In diabetic rats, presence of caspase-3 immunoreactivity in erythrocytes may be an indirect evidence of eryptosis accompanying conditions like PS exposure and caspase-8 activity.

Up to date, according to our literature search, this is the first report that demonstrates caspase-3 activity in erythrocytes with immunohistochemical study in diabetic rat. Beside that, there are two other reports supporting our finding, caspase-3 activity in erythrocytes [6, 11]. First report presents that caspase-3 activity is significantly higher in type 2 DM than healthy subjects [6]. Second report shows that even erytrhocytes of type 2 DM patients without chronic kidney disease are stained with annexin V, bind PS, and show early apoptotic cells [11]. Our results suggest that hyperglycemia, a kind of hyperosmalar state, and oxidative stress may initiate the cascade of eryptosis. Hyperglycemia and oxidative stress are a well-documented trigger of eryptosis; however, how they do succeed that is not clearly demonstrated yet [6]. One explanation of that may be death receptor based. Previously, it was reported that Fas, caspase-8, and caspase-3 exist in erythrocytes and take role in eryptosis [5]. In the same study, it is also reported that erythrocytes expresses FasL. In the line with

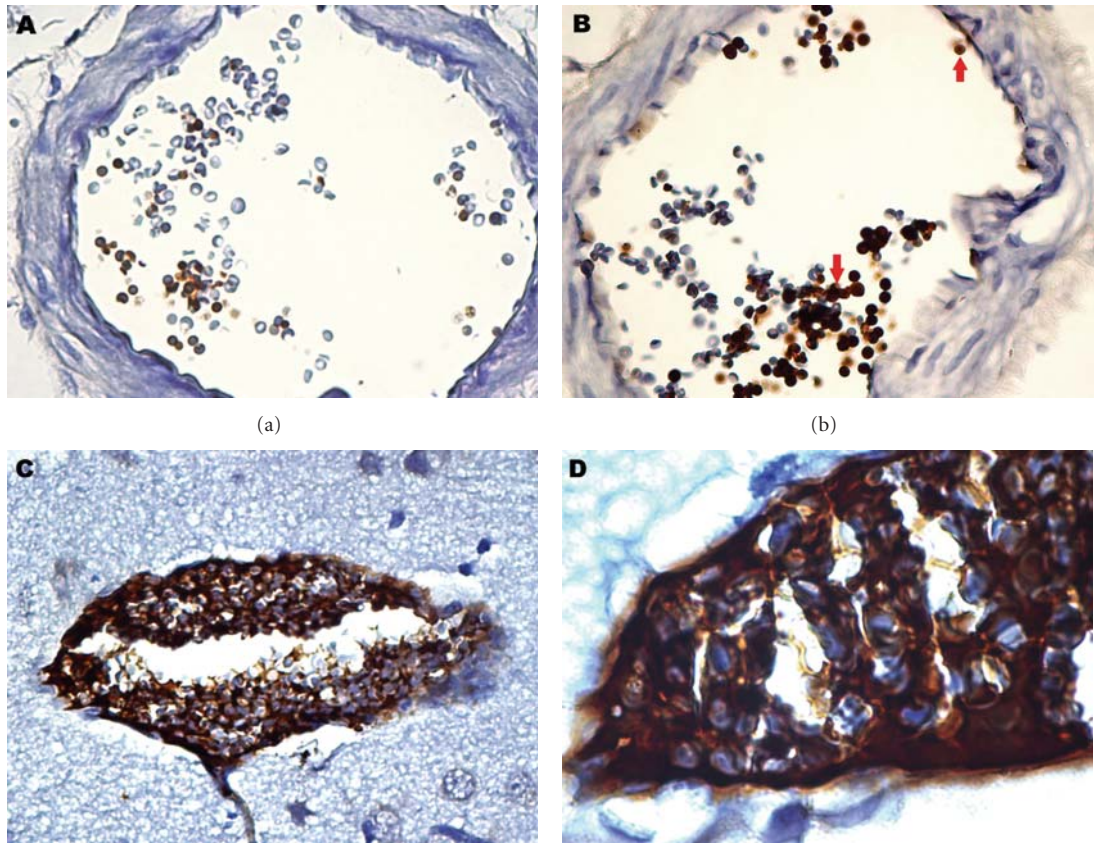

Figure 1: Caspase-3 immunoreactivity of erythrocytes (immunoperoxidase). Baseline caspase-3 positivity of erythrocytes in rats of non-DM group (a). Red arrows show caspase-3 positive erythrocytes in brown color in rats of DM group (b). Caspase-3 positive erythrocytes, aggregated and adhered to vascular endothelium in diabetic rat (c). Caspase-3 positive erythrocytes occluding vascular spaces presented in higher magnification endothelium in diabetic rat (d). Magnifications are 400 in (a), (b), and (c), and 1000 in (d).

this and our result, it may be thought that hyperglycemia and oxidative stress direct erythrocytes into hemolytic pathway, very parallel to eryptotic pathway. Then, PS is exposed on the outer membrane of the erythrocyte during hemolysis which results in erythrocyte-to-erythrocyte attachment. Thus, Fas-FasL interaction starts eryptosis, which may protect microcirculation from occlusion and be pointed with caspase-3 positivity, in erythrocytes to escape hemolysis in the process of erythrocyte aggregation. In short, eryptosis may work as a mechanism saving erythrocytes from hemolysis. On the other hand, hyperglycemia and oxidative stress may induce eryptosis independent of hemolysis beginning with death receptor pathway.

It is clearly seen in our study that diabetic rat erythrocytes attached each other and endothelial surface (Figure 1(c)). In reports, increased aggregability was observed in the red blood cells of diabetic patients [8, 9]. In one report, it is shown that PS decreases energy to need erythrocyte-erythrocyte attachment [7]. In addition to these reports, it is claimed that PS exposure is responsible for increased erythrocyte adhesion to endothelium in central retinal vein occlusion [12]. Here, we do not present direct evidence of PS presence on erythrocytes; nonetheless, caspase-3 immunoreactivity may be accepted as indirect evidence of its existence. As a result, we conclude the reason of increased aggregability and adhesiveness may be PS presence in outer membrane of eryptotic erythrocytes. Besides all, it is worthy to say that caspase-3 immunoreactivity is observed in the vascular endothelium of the cerebrum and cerebellum in many areas (unpresented data) in DM group. In line with this, high aggregability and adhesiveness of erythrocytes may cause vascular occlusion which may explain the underlying pathology in microangiopathic complications of diabetes.

Anemia in diabetics is generally overlooked and thought to be developed due to nephropathic complication of diabetes. In addition, low or nonfunctional erythropoietin is accused of anemia [1, 13]. On the other hand, hyperglycemia itself can be the reason of anemia if diabetic treatment is not given properly or absent. As an example, we have seen once a case: 70-year-old female who is diagnosed as having diabetes without nephropathy after hospital admittance is presented with severe anemia (hemoglobin = 8 g/dL) and recovered from anemia (hemoglobin = 12.5 g/dL) with diabetic prescription (unpublished case). We believe that our result, high frequency of eryptotic erythrocytes in diabetics, is a reflection of functional anemia, undetectable with

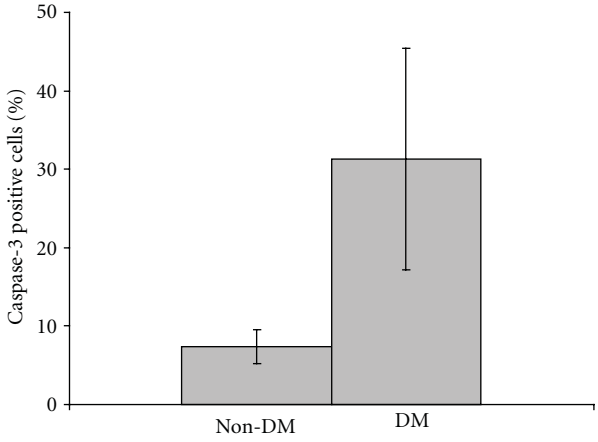

Figure 2: Percentages of Caspase-3 immunoreactive erythrocytes in diabetic and nondiabetic rats. Means ± SD of the percentages of caspase-3 positive cells are compared with student's t-test ($P < 0.0001$; $n = 7$).

routine laboratory tests, which is also mentioned elsewhere as anemia masked by dehydration [14]. Consequently, to diagnose anemia in diabetics, calculation of intravascular total volume with red blood cell count may be taken into consideration. Alternatively, caspase-3 positive erythrocyte count may be another solution to diagnose functional anemia in diabetics.

5. Conclusions

In short, it is presented here that the number of eryptotic erythrocyte in diabetic rat is higher than non-DM group. This result may help us to understand the bases of anemia and microangiopathy in diabetics. In conclusion, the treatment of masked anemia in diabetes may lead to improvement of diabetic complications in these patients.

Conflict of Interests

All authors fully disclose that there is no financial or ethical conflict of interest.

Acknowledgments

This project is supported by a grant from Dicle University Scientific Research Project Coordination Unit (DÜBAP), Turkey (10-VF-155). All authors fully disclose that there is no financial or ethical conflict of interest.

References

[1] S. Thomas and M. Rampersad, "Anaemia in diabetes," *Acta Diabetologica*, vol. 41, supplement 1, pp. S13–S17, 2004.

[2] M. C. Thomas, M. E. Cooper, K. Rossing, and H. H. Parving, "Anaemia in diabetes: is there a rationale to TREAT?" *Diabetologia*, vol. 49, no. 6, pp. 1151–1157, 2006.

[3] K. S. Lang, P. A. Lang, C. Bauer et al., "Mechanisms of suicidal erythrocyte death," *Cellular Physiology and Biochemistry*, vol. 15, no. 5, pp. 195–202, 2005.

[4] F. Lang, E. Gulbins, H. Lerche, S. M. Huber, D. S. Kempe, and M. Föller, "Eryptosis, a window to systemic disease," *Cellular Physiology and Biochemistry*, vol. 22, no. 5-6, pp. 373–380, 2008.

[5] D. Mandal, A. Mazumder, P. Das, M. Kundu, and J. Basu, "Fas-, caspase 8-, and caspase 3-dependent signaling regulates the activity of the aminophospholipid translocase and phosphatidylserine externalization in human erythrocytes," *Journal of Biological Chemistry*, vol. 280, no. 47, pp. 39460–39467, 2005.

[6] E. Maellaro, S. Leoncini, D. Moretti et al., "Erythrocyte caspase-3 activation and oxidative imbalance in erythrocytes and in plasma of type 2 diabetic patients," *Acta Diabetologica*. In press.

[7] A. Othmane, M. Bitbol, P. Snabre, and P. Mills, "Influence of altered phospholipid composition of the membrane outer layer on red blood cell aggregation: relation to shape changes and glycocalyx structure," *European Biophysics Journal*, vol. 18, no. 2, pp. 93–99, 1990.

[8] M. Martinez, A. Vayá, R. Server, A. Gilsanz, and J. Aznar, "Alterations in erythrocyte aggregability in diabetics: the influence of plasmatic fibrinogen and phospholipids of the red blood cell membrane," *Clinical Hemorheology and Microcirculation*, vol. 18, no. 4, pp. 253–258, 1998.

[9] N. Babu and M. Singh, "Influence of hyperglycemia on aggregation, deformability and shape parameters of erythrocytes," *Clinical Hemorheology and Microcirculation*, vol. 31, no. 4, pp. 273–280, 2004.

[10] H. Ohkawa, N. Ohishi, and K. Yagi, "Assay for lipid peroxides in animal tissues by thiobarbituric acid reaction," *Analytical Biochemistry*, vol. 95, no. 2, pp. 351–358, 1979.

[11] J. V. Calderón-Salinas, E. G. Muñoz-Reyes, J. F. Guerrero-Romero et al., "Eryptosis and oxidative damage in type 2 diabetic mellitus patients with chronic kidney disease," *Molecular and Cellular Biochemistry*, vol. 357, no. 1-2, pp. 171–179, 2011.

[12] M. P. Wautier, E. Héron, J. Picot, Y. Colin, O. Hermine, and J. L. Wautier, "Red blood cell phosphatidylserine exposure is responsible for increased erythrocyte adhesion to endothelium in central retinal vein occlusion," *Journal of Thrombosis and Haemostasis*, vol. 9, no. 5, pp. 1049–1055, 2011.

[13] M. C. Thomas, C. Tsalamandris, R. MacIsaac, and G. Jerums, "Functional erythropoietin deficiency in patients with Type 2 diabetes and anaemia," *Diabetic Medicine*, vol. 23, no. 5, pp. 502–509, 2006.

[14] M. M. Christopher, "Hematologic complications of diabetes mellitus," *Veterinary Clinics of North America*, vol. 25, no. 3, pp. 625–637, 1995.

Hindawi Publishing Corporation
Experimental Diabetes Research
Volume 2012, Article ID 375673, 10 pages
doi:10.1155/2012/375673

Research Article

Fagopyrum tataricum (Buckwheat) Improved High-Glucose-Induced Insulin Resistance in Mouse Hepatocytes and Diabetes in Fructose-Rich Diet-Induced Mice

Chia-Chen Lee, Wei-Hsuan Hsu, Siou-Ru Shen, Yu-Hsiang Cheng, and She-Ching Wu

Department of Food Science, National Chiayi University, Chiayi City 60004, Taiwan

Correspondence should be addressed to She-Ching Wu, scwu@mail.ncyu.edu.tw

Received 9 October 2011; Accepted 11 January 2012

Academic Editor: Pietro Galassetti

Fagopyrum tataricum (buckwheat) is used for the treatment of type 2 diabetes mellitus in Taiwan. This study was to evaluate the antihyperglycemic and anti-insulin resistance effects of 75% ethanol extracts of buckwheat (EEB) in FL83B hepatocytes by high-glucose (33 mM) induction and in C57BL/6 mice by fructose-rich diet (FRD; 60%) induction. The active compounds of EEB (100 μg/mL; 50 mg/kg bw), quercetin (6 μg/mL; 3 mg/kg bw), and rutin (23 μg/mL; 11.5 mg/kg bw) were also employed to treat FL83B hepatocytes and animal. Results indicated that EEB, rutin, and quercetin + rutin significantly improved 2-NBDG uptake via promoting Akt phosphorylation and preventing PPARγ degradation caused by high-glucose induction for 48 h in FL83B hepatocytes. We also found that EEB could elevate hepatic antioxidant enzymes activities to attenuate insulin resistance as well as its antioxidation caused by rutin and quercetin. Finally, EEB also inhibited increases in blood glucose and insulin levels of C57BL/6 mice induced by FRD.

1. Introduction

Type 2 diabetes mellitus (T2DM) is a chronic disease caused by deficient insulin secretion or ineffective insulin activity, which negatively affects carbohydrate metabolism. Medicinal plants are used as a common alternative treatment for T2DM in many parts of the world. Insulin resistance is associated with inflammatory factors such as tumor necrosis factor-α (TNF-α) and interleukin-6 (IL-6) in T2DM patients. Cellular stress due to obesity is thought to be associated with the disturbance of homeostasis in the endoplasmic reticulum (ER). Hepatic regulation of glucose homeostasis is the major factor controlling plasma glucose concentrations, and the induction of hepatic ER stress and oxidative stress resulting in insulin resistance has been investigated [1].

High-fructose diet upregulates hepatic expression of the sterol regulatory element binding protein-1c (SREBP-1c), a key transcription factor for hepatic expression of lipogenic enzymes, but down regulates the expression of PPARα (promoting fatty acid oxidation) [2, 3]. The study also investigates the fructose-inducing effect in C57BL/6 mice and has found that fructose would promote SREBP-1c promoter activity resulting in hepatic lipogenesis [4]. Moreover, fructose is employed to induce insulin resistance, hepatic steatosis, and the metabolic syndrome [5]. Fructose is a highly lipogenic sugar that has profound metabolic effects in the liver resulting in metabolic syndrome, and fructose does not stimulate insulin secretion [6]. The rate of hepatic uptake of fructose from portal circulation is greater than the rate of glucose uptake, and because fructose metabolism bypasses phosphofructokinase, fructose metabolism is not under the regulatory control of insulin [7]. On the other hand, fructose may activate SREBP-1c which activates genes involved in de novo lipogenesis, and triglyceride [8].

Fagopyrum tataricum (buckwheat) is a herbaceous plant that belongs to the Polygonaceae family. It has now been introduced in many countries, because the seeds of this herb are a healthy and nutritionally important food item. Rutin has been found to be the major ingredient of buckwheat [9]. Tartary buckwheat (*F. tataricum*) contains more rutin and quercetin than common buckwheat (*F. esculentum*) dose; rutin is known to have antioxidative activity [10]. Due to

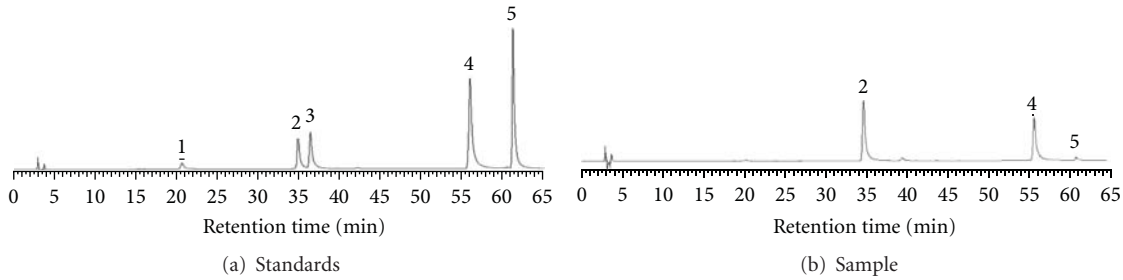

(a) Standards (b) Sample

Figure 1: (a) The HPLC chromatogram of standards (rutin and quercetin): (1) caffic acid, (2) rutin, (3) quercetin-3-glucoside, (4) quercetin, and (5) kaempferol. (b) The HPLC chromatogram of sample (75% ethanol extracts of *F. tataricum*).

the rise in recent years to investigate the anti-diabetic activity of antioxidants, anti-insulin resistance of rutin, quercetin, and the 75% ethanol extracts from buckwheat (EEB) *in vivo* and *in vitro* were investigated in this study.

2. Materials and Methods

2.1. Materials and Chemicals. 3-(4,5-Dimethylthiazol-2-yl)-2,5-diphenyltetrazolium bromide (MTT), glucose, quercetin, Triton-X 100, rutin, and trypsin were purchased from Sigma Co. (St. Louis, MO, USA). Sodium bicarbonate, fetal bovine serum (FBS), F12-K medium, penicillin, and streptomycin were purchased from HyClone Laboratories (Logan, UT, USA). The Bio-Rad protein assay dye was from Bio-Rad Laboratories (Hercules, CA, USA). 2-[N-(7-Nitrobenz-2-oxa-1,3-diazol-4-yl)amino]-2-deoxy-d-glucose (2-NBDG) was from Invitrogen (Carlsbad, CA, USA).

2.2. Preparation of Sample. The seeds of *F. tataricum* (buckwheat) were provided by Taiwan Golden Buckwheat Limited company) and then were freeze-dried and ground. Approximately 2.5 kg of the buckwheat powder was extracted by 25 L of 75% ethanol for 2 days. After extraction, the ethanol extracts were vacuum-concentrated and freeze-dried. The extract powder was stored at −20°C until used. The 75% ethanol extracts of buckwheat was shown as EEB in this study.

2.3. Cell Culture. FL83B cells were seeded in 10 cm dishes at a density of 5×10^5 per well and grown until 80% confluence was reached. Subsequently, insulin resistance was induced in these cells and glucose uptake was determined [11]. FL83B cell line is a mouse normal liver cell from the Bioresource Collection and Research Center (BCRC) in Taiwan (Hsinchu, Taiwan), which is cultured in the F12-K medium supplemented with 10% heat-inactivated FBS and antibiotics (100 unit/mL penicillin and 100 μg/mL streptomycin). Cells were cultured at 37°C in a humidified atmosphere of 5% CO_2.

2.4. High-Performance Liquid Chromatography (HPLC) Assay. HPLC was performed with a Hitachi liquid chromatograph (Hitachi, Ltd., Tokyo, Japan) consisting of a model L-6200 pump and a model L-4200 UV-Vis detector set at 320 nm. The analyses were carried out on a LiChrospher RP-18 column (250 mm·4.6 mm i.d., 5 μm, E. Merck Co., Darmstadt, Germany). Extracts were filtered through a 0.45 μm filter before use. The mobile phase A was 2% acetic acid, and the mobile phase B was 0.5% acetic acid/water (1 : 1; v/v). Caffic acid, rutin, quercetin, kaempferol, and quercetin-3-glucoside were determined by ultraviolet detector (Hitachi L-7455 diode array detector). Caffic acid, rutin, quercetin, kaempferol, and quercetin-3-glucoside were identified by comparison of their retention time (Rt) values and UV spectra with those of known standards and determined by peak areas from the chromatograms [12]. Results suggested that 228.8 mg/g of rutin and 58.6 mg/g of quercetin were contained in EEB (Figure 1).

2.5. Cell Viability. Mouse FL83B cells (1.5×10^5 cells per well) were seeded into 24-well plates overnight. Cells were treated with high glucose (33 mM) and sample (quercetin/rutin/EEB) in free-serum F12-K medium for 48 h. Subsequently, cells were washed with phosphate buffered saline (PBS) twice, and the supernatants were exchanged with 1 mL of medium and MTT (0.5 mg/mL) to react for 2 h at 37°C. After reaction, removing medium, and washing cells with PBS, the MTT reacted product (formazan crystals) was dissolved with 0.5 mL of dimethyl sulfoxide (DMSO), and the absorption was measured at 570 nm by an ELISA reader for cell viability assay.

2.6. Insulin Resistance Induction and Glucose (2-NBDG) Uptake. Glucose uptake of FL83B cells was assessed using the fluorescent glucose analog, 2-NBDG. Briefly, cells were treated with high glucose (33 mM) and sample in serum-free medium for 48 hours, and then the medium was replaced with Krebs-Ringer-Bicarbonate (KRB) buffer containing insulin (500 nM; final concentration) and 2-NBDG (160 μM; final concentration) for 20 min for incubation at 37°C. Free 2-NBDG was washed out from cultures after treatment and measured 2-NBDG with a FACS flow cytometer (BD Biosciences, San Jose, CA, USA) and analyzed using CellQuest software [11].

2.7. Western Blot Analysis. FL83B cells were lysed in ice-cold lysis buffer containing 20 mM of Tris-HCl (pH 7.4), 1% of Triton X-100, 0.1% of SDS, 2 mM of EDTA, 10 mM of NaF, 1 mM of phenylmethylsulfonyl fluoride (PMSF), 500 μM of sodium vanadate, and 10 μg/mL of aprotinin overnight. And then the cell lysates were sonicated with ice cooling (four

times each 15 s) and then centrifuged (12,000 ×g, 10 min) to recover the supernatant. The supernatant was taken as the cell extract. The protein concentration in the cell extract was determined using a Bio-Rad protein assay kit. The samples were subjected to 10% sodium dodecyl sulfate-polyacrylamide gel electrophoresis (SDS-PAGE). The protein spots were electrotransferred to a polyvinylidene difluoride (PVDF) membrane. The membrane was incubated with block buffer (PBS containing 0.05% of Tween-20 and 5% w/v nonfat dry milk) for 1 h, washed with PBS containing 0.05% Tween-20 (PBST) three times, and then probed with anti-Akt antibody, anti-PTP1B, anti-GS, anti-p-PKC, anti-PKC, anti-AMPK, anti-p-Akt, anti-GLUT2, and anti-PPAR-γ antibodies (Cell Signaling Technology, Beverly, MA, USA) overnight at 4°C. In addition, the intensity of the blots probed with 1 : 1000 diluted solution of mouse monoclonal antibody to bind GAPDH (Cell Signaling Technology) was used as the control to ensure that a constant amount of protein was loaded into each lane of the gel. The membrane was washed three times each for 5 min in PBST, shaken in a solution of HRP-linked anti-rabbit IgG secondary antibody, and washed three more times each for 5 min in PBST. The expressions of proteins were detected by enhanced chemiluminescent (ECL) reagent (Millipore, Billerica, MA, USA).

2.8. Animals Study. C57BL6 mice (4 weeks old) were obtained from BioLASCO, Taiwan Co., Ltd. in this study. Animals were provided with food and water ad libitum. Animals were subjected to 12 h light/dark cycle with a maintained relative humidity of 60% and a temperature at 25°C. The experiments were carried out in a qualified animal breeding room in the animal center at our institute. Hyperglycemia and hyperinsulinemia in mice were induced by fructose-rich diet (FRD; 60%) for 8 weeks of induction [13]. The animals were randomly divided into 6 groups ($n = 12$), including (a) control, (b) fructose-rich diet (FRD), (c) FRD + quercetin (3 mg/kg bw), (d) FRD + rutin (11.5 mg/kg bw), (e) FRD + EEB (50 mg/kg bw), and (f) FRD + rutin + quercetin. The doses of rutin and quercetin were equivalent to those administered to the EEB administration group.

2.9. Oral Glucose Tolerance Test (OGTT). The OGTT was performed at week 4 and week 8. The experiment was performed on animals after fasting for 12 h (free access to water). Animals were given glucose (2 g/kg of body weight) with an oral administration. Blood samples were collected from the tail vein at times 0, 30, 60, 90, and 120 min after glucose administration. Homeostasis model assessment of insulin resistance (HOMA-IR) was calculated according to the formula HOMA-IR = fasting insulin × fasting blood glucose/22.5 [14, 15].

2.10. Assays for Blood Glucose. Blood glucose was immediately determined by the glucose oxidase method, using an analyzer [16].

2.11. Assay for Antioxidase Activity. Glutathione peroxidase (GPx) activity was determined as previously described [17]. Glutathione reductase (GR) activity determination was according to Bellomo et al. (1987) [18]. The catalase (CAT) activity was determined by the method of Aebi (1984) [19]. SOD activity was determined by the method of S. Marklund and G. Marklund (1974) [20].

2.12. Assay for Hepatic and Pancreatic Reactive Oxygen Species (ROS). The ROS levels were assayed with nitroblue tetrazolium (NBT), which is reduced to form blue-black formazan. In this assay, 100 μL of homogenates reacted with 10 mg/mL of NBT and measured by the absorbance at 570 nm [21].

2.13. Assay for Insulin Level. Insulin was determined by the insulin kit derived from Mercodia AB (Uppsala, Sweden).

2.14. Histopathologic Studies. Liver tissues were trimmed (2 mm thickness) and fixed (buffer formaldehyde). The fixed tissues were processed including those embedded in paraffin, sectioned, and rehydrated. The histological examination by the previous conventional methods evaluated the index of ethanol-induced necrosis by assessing the morphological changes in the liver sections stained with hematoxylin and eosin (H and E) [22].

2.15. Statistical Analysis. Experimental results were averaged triplicate analysis. The data were recorded as mean ± standard deviation (SD) and analysis by statistical analysis system (SAS Inc., Cary, NC, USA). One-way analysis of variance was performed by ANOVA procedures. Significant differences between means were determined by Duncan's multiple range tests. Results were considered statistically significant at $P < 0.05$.

3. Results and Discussion

3.1. Effects of EEB, Rutin, and Quercetin on High-Glucose-Induced Insulin Resistance in the FL83B Hepatocytes for 48 h. Caffic acid, rutin, quercetin, kaempferol, and quercetin-3-glucoside of EEB were identified by HPLC. Results suggested that 228.8 mg/g of rutin and 58.6 mg/g of quercetin were contained in EEB (Figure 1). We performed a 2-NBDG uptake test involving FL83B cells with high-glucose (33 mM)-induced insulin resistance to evaluate the effects of EEB (100 μg/mL), rutin (23 μg/mL; 37 μM), and quercetin (6 μg/mL; 20 μM) on improving insulin sensitivity. The results showed that EEB, quercetin, and rutin significantly increased glucose uptake in these cells (Figure 2(a)). Furthermore, the treating concentrations of EEB, rutin, and quercetin without cytotoxic effects were found in FL83B hepatocytes (data not shown).

Akt is a Ser/Thr protein kinase that plays a key role in the translocation of glucose transporter (GLUT) to the plasma membrane via a signal transduction cascade involving insulin treatment [23]. We determined whether activated Akt was involved in the anti-insulin resistance effect of EEB, rutin, quercetin, and rutin + quercetin on glucose uptake. The treatment of high glucose significantly inhibited Akt phosphorylation in FL83B hepatocytes (Figure 2(b)). These results showed that exposure to high concentrations of glucose induces an insulin resistance-like condition including inhibition of the Akt pathway and EEB, rutin, quercetin,

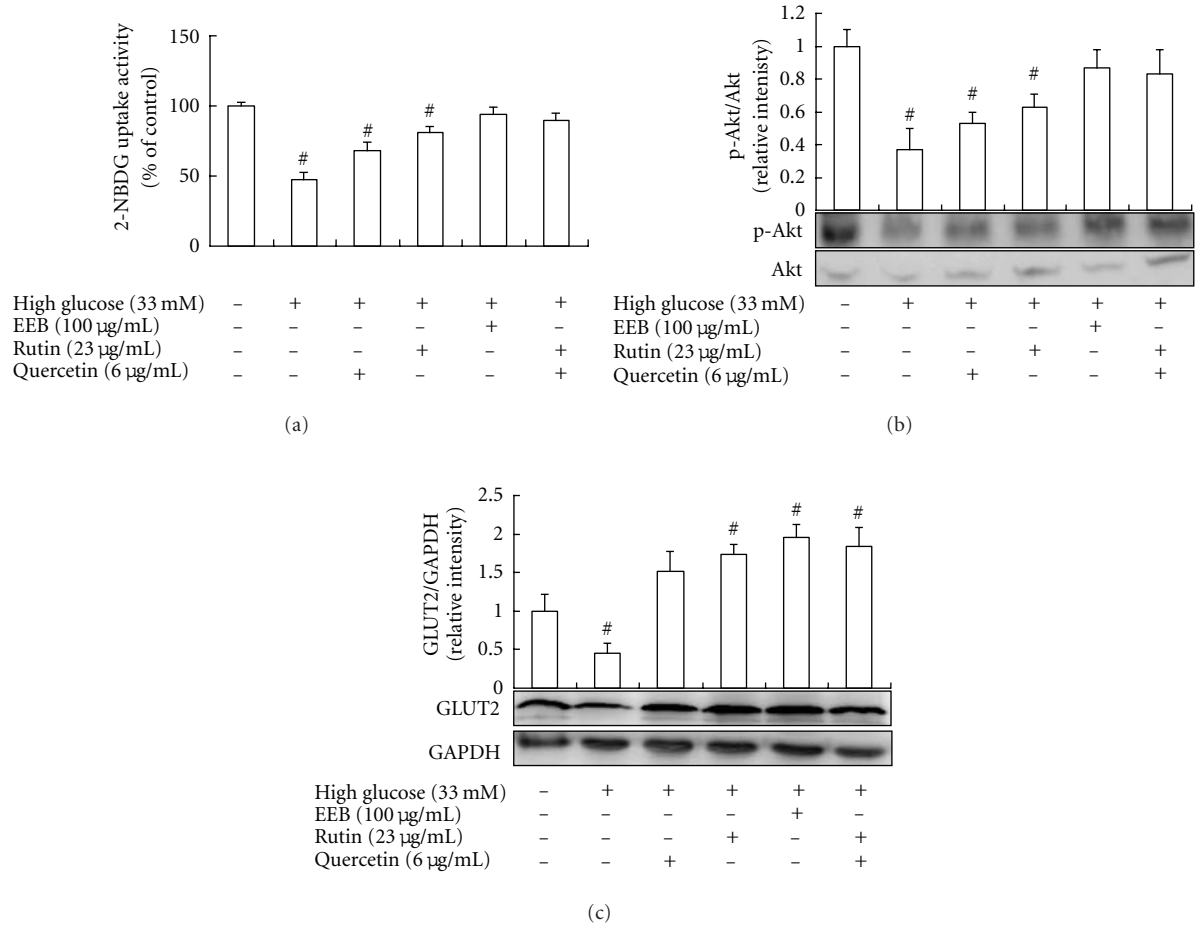

Figure 2: Effects of EEB on 2-NBDG uptake (a), Akt phosphorylation (b), and GLUT2 expression (c) of FL83B hepatocytes induced by high glucose. FL83B cells were incubated in serum-free F12K medium with glucose (33 mM; final concentration) with or without EEB, quercetin, rutin, and quercetin + rutin for 48 h. EEB: 75% ethanol extracts of buckwheat. #Significantly different ($P < 0.05$) from normal; *significantly different ($P < 0.05$) from high-glucose treating group.

and rutin + quercetin could overcome the insulin resistance by activating the Akt pathways, thus resulting in increased glucose uptake.

GLUT2 is the major glucose transporter expressed in hepatocytes, insulin-secreting pancreatic β-cells and absorptive epithelial cells of the intestinal mucosa and kidney. GLUT2 is thought to act as a glucose-sensing apparatus that plays a role in blood glucose homeostasis, by responding to changes in blood glucose concentration and altering the rate of glucose uptake by hepatocytes. High-glucose levels decreased GLUT2 protein expression in FL83B cells, but EEB, rutin, quercetin, and rutin + quercetin markedly increased GLUT2 protein expression (Figure 2(c)). Results showed that EEB, rutin, and quercetin promoted Akt phosphorylation, in turn promoting GLUT2 translocation into plasma membrane of FL83B cells thereby increasing glucose uptake and alleviating insulin resistance induced by high-glucose. Although rutin + quercetin treatment did not show the synthetic effect on 2-NBDG uptake, Akt phosphorylation, and GLUT2 expression in high-glucose-induced FL83B hepatocytes compared to quercetin- or rutin-treated groups.

3.2. Effects of EEB, Rutin, and Quercetin on AMP-Dependent Protein Kinase (AMPK), Protein Tyrosine Phosphatase 1B (PTP1B), and Glycogen Synthase (GS) Expressions in FL83B Hepatocytes. AMPK is a conserved intracellular energy sensor that plays a central role in the regulation of glucose and lipid metabolism, and AMPK has multiple biological effects, including the regulation of intracellular glucose transport [24]. Recent investigations suggest that AMPK could potentially be beneficial as a therapeutic target in the treatment of diabetes and obesity [25]. However, AMPK expression would be inhibited by oxidative stress and ER stress in inflammatory factors or high-glucose induction downregulating AMPK expression and phosphorylation [1, 5, 6, 8]. On the other hand, hepatic specific PTP1B plays a pivotal role in glucose and lipid metabolism. Inhibition of PTP1B in the peripheral tissues may be beneficial with respect to the treatment of diabetes as well as the treatment of metabolic syndrome and

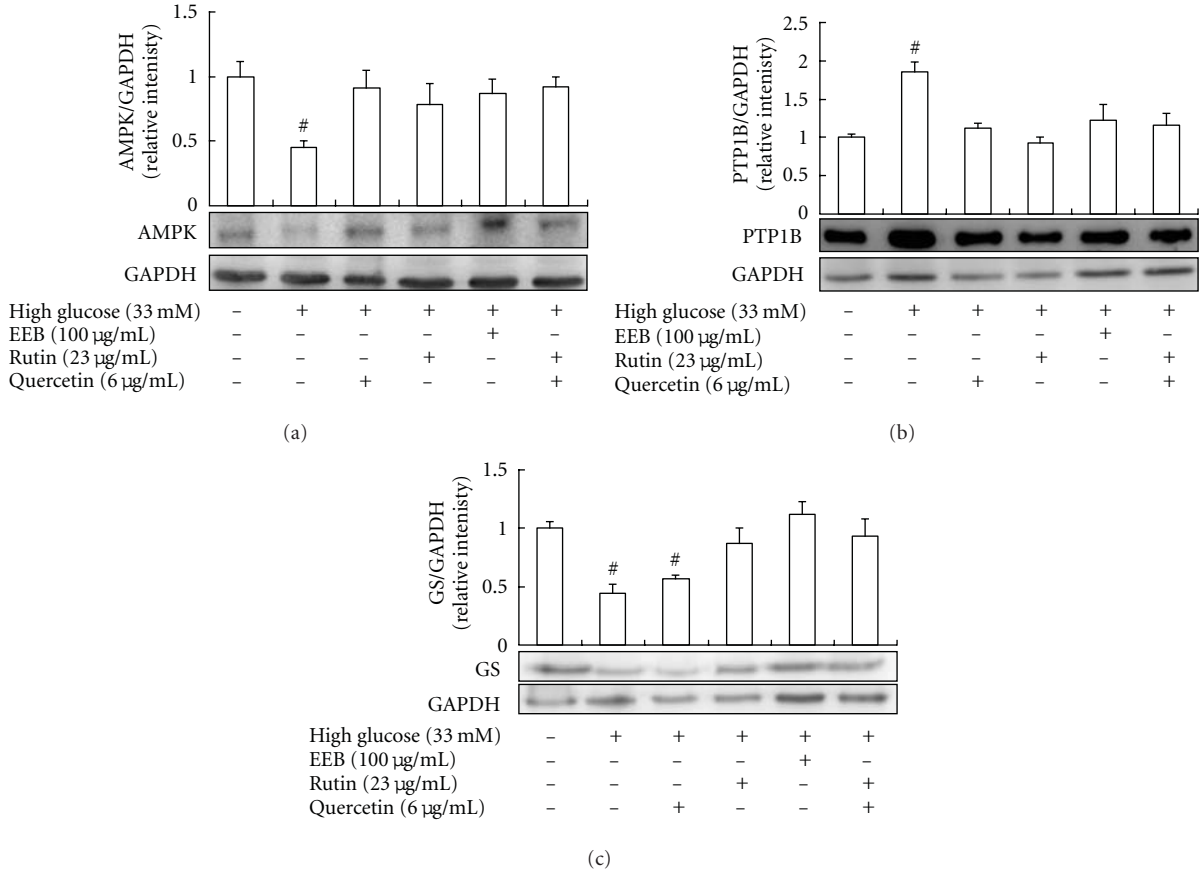

Figure 3: Effects of EEB on AMPK (a), PTP1B (b), and GS expressions (c) of FL83B hepatocytes induced by high glucose. FL83B cells were incubated in serum-free F12K medium with glucose (33 mM; final concentration) with or without EEB, quercetin, rutin, and quercetin + rutin for 48 h. EEB: 75% ethanol extracts of buckwheat. #Significantly different ($P < 0.05$) from normal; *significantly different ($P < 0.05$) from high-glucose-treated group.

reduction of cardiovascular risk. Study has demonstrated that PTP1B expression involved in ER stress in high-glucose induction [1, 24]. In addition, the natural product, monascin, identified from *Monascus*-fermented products has been demonstrated to show the inhibitory activity for PTP1B expression in insulin-resistance-induced C2C12 cells [26].

We evaluated the effects of EEB, rutin, and quercetin on AMPK and PTP1B expression of FL83B hepatocytes induced by high-glucose treatment for 48 h. Results indicated that EEB, rutin, and quercetin significantly prevented a decrease in AMPK (Figure 3(a)), and the inhibition of PTP1B was found in EEB, rutin, and quercetin treatments in high-glucose-induced FL83B hepatocytes (Figure 3(b)). These results showed that EEB, rutin, and quercetin could significantly regulate AMPK and PTP1B activity in FL83B hepatocytes thereby attenuating insulin resistance and promoting 2-NBDG uptake.

Moreover, we investigated the GS expression of FL83B hepatocytes induced by high-glucose treatment for 48 h. Results indicated that EEB, rutin, and rutin + quercetin could promote GS expression compared to the high-glucose-induced group; however, this effect was not found in the quercetin-treated group (Figure 3(c)).

3.3. Antioxidative Stress and Anti-PPARγ Phosphorylation by EEB, Rutin, and Quercetin in FL83B Hepatocytes. High-glucose levels have been shown to induce the activities of inflammatory cytokines, chemokines, p38 mitogen-activated protein kinase, reactive oxygen species (ROS), protein kinase C (PKC), and nuclear factor-κB (NF-κB) activity in clinical and experimental systems [27–29]. We evaluated the inhibitory effect of EEB on ROS production in this study. High-glucose levels significantly increased ROS production, whereas EEB, rutin, quercetin, and rutin + quercetin treatments could decrease ROS production in high-glucose-induced FL83B hepatocytes (Figure 4). Activation of p-PKC directly contributes to the oxidative stress and membrane-associated NADPH oxidases, which further leads to excessive ROS production. Results suggested that EEB, rutin, quercetin, and rutin + quercetin markedly inhibited PKC

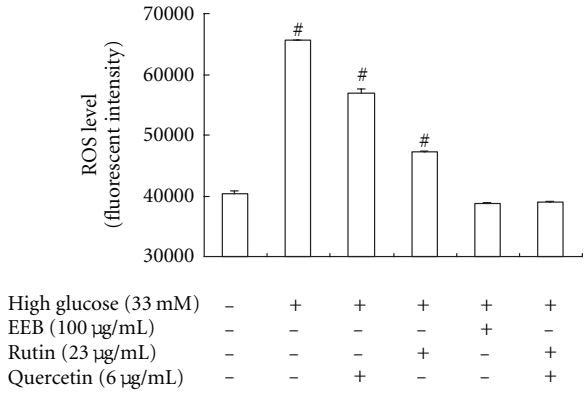

Figure 4: Effects of EEB on ROS level in FL83B hepatocytes induced by high glucose. FL83B cells were incubated in serum-free F12K medium with glucose (33 mM; final concentration) with or without EEB, quercetin, rutin, and quercetin + rutin for 48 h. EEB: 75% ethanol extracts of buckwheat. #Significantly different ($P < 0.05$) from normal; *significantly different ($P < 0.05$) from high-glucose-treated group.

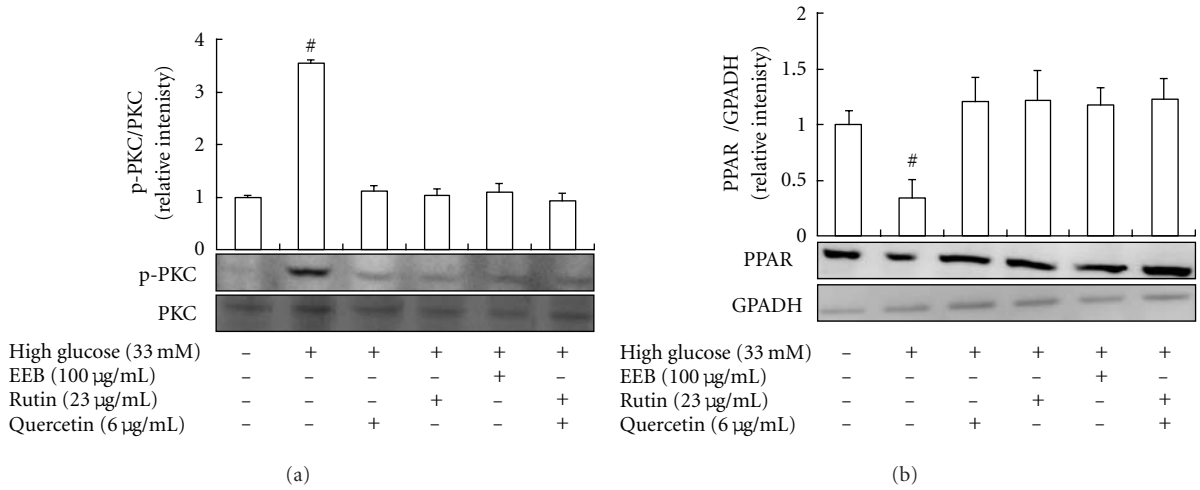

Figure 5: Effects of EEB on PKC phosphorylation (a) and PPARγ expressions (b) of FL83B hepatocytes induced by high glucose. FL83B cells were incubated in serum-free F12K medium with glucose (33 mM; final concentration) with or without EEB, quercetin, rutin, and quercetin + rutin for 48 h. EEB: 75% ethanol extracts of buckwheat. #Significantly different ($P < 0.05$) from normal; *significantly different ($P < 0.05$) from high-glucose-treated group.

phosphorylation caused by high-glucose induction for 48 h (Figure 5(a)).

Peroxisome proliferator-activated receptors (PPARs) regulate cellular development and differentiation and govern cellular bioenergetics by modulating fat and glucose metabolism and inflammatory responses [30]. There are three PPAR subtypes, including PPAR-α, PPAR-γ, and PPAR-δ. All three subtypes can modulate DNA transcription by binding to specific peroxisome-proliferator-response elements (PPREs) on target genes. Moreover, PPAR-γ plays an important role in the development of insulin resistance. PPARγ plays a key role in adipogenesis, survival of mature adipocytes, fatty acid uptake, lipid storage, and systemic energy homeostasis. The metabolic regulation of PPAR-γ for glucose homeostasis is investigated in the study [31]. High-glucose induction attenuating insulin sensitivity has been found via activating PKC [26]. PKC inhibits PPAR-γ function via direct phosphorylation at serine residues, affecting DNA-binding activity and increasing PPAR-γ degradation by the ubiquitin-proteasome-dependent pathway [26, 31].

Therefore, we postulated that the EEB, rutin, quercetin, and rutin + quercetin could prevent a decrease in PPAR-γ of high-glucose-induced FL83B hepatocytes; this result may attribute to EEB, rutin, quercetin, and rutin + quercetin significantly inhibiting p-PKC activation thereby attenuating PPARγ phosphorylation and degradation (Figure 5(b)).

3.4. The Regulation of EEB, Rutin, Quercetin, and Rutin + Quercetin on Blood Glucose In Vivo . Fructose is employed to induce insulin resistance, hepatic steatosis, and the metabolic syndrome [32]. Fructose is a highly lipogenic sugar that has profound metabolic effects in the liver resulting in metabolic syndrome, and fructose does not stimulate insulin secretion [6]. The rate of hepatic uptake of fructose from portal

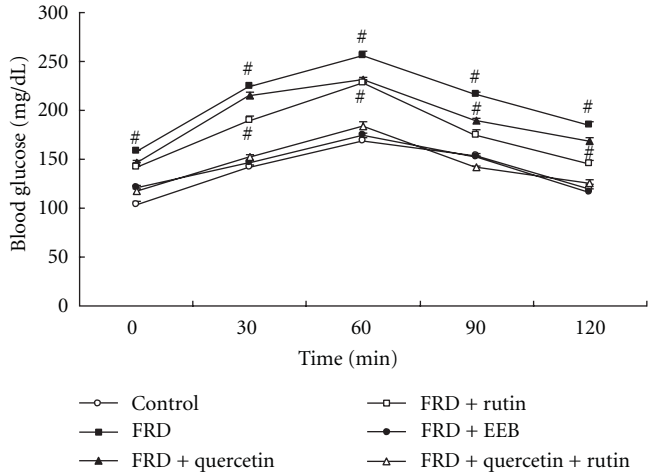

Figure 6: The regulatory effect of EEB, quercetin, rutin, and quercetin + rutin on OGTT in C57BL/6 mice induced by fructose-rich diet (FRD; 60%) for 8 weeks. The animals were randomly divided into 6 groups ($n = 12$), including (a) control, (b) fructose-rich diet (FRD), (c) FRD + quercetin (3 mg/kg bw), (d) FRD + rutin (11.5 mg/kg bw), (e) FRD + EEB (50 mg/kg bw), and (f) FRD + rutin + quercetin. The doses of rutin and quercetin were equivalent to those administered to the EEB administration group. EEB: 75% ethanol extracts of buckwheat. Data are presented as the mean ± SEM. #Significantly different ($P < 0.05$) from control group.

Table 1: Effects of EEB on HOMA-IR by levels of blood glucose and insulin in FRD-induced rats.

Groups	Week 8		
	Glucose (mmol/L)	Insulin (mIU/L)	HOMA-IR
Normal	6.4 ± 0.4	10.3 ± 0.4	2.9 ± 0.4
HFD	7.8 ± 0.0#	18.1 ± 0.5#	6.3 ± 0.7#
HFD + quercetin	7.5 ± 0.1#	17.1 ± 0.7#	5.7 ± 0.2#
HFD + rutin	7.2 ± 0.1#*	15.3 ± 0.4#*	4.9 ± 0.4#*
HFD + EEB	6.9 ± 0.4#*	11.2 ± 0.3*	3.4 ± 0.8#*
HFD + quercetin + rutin	7.0 ± 0.3#*	13.6 ± 0.2*	4.2 ± 0.1#*

Hyperglycemia and hyperinsulinemia in mice were induced by fructose-rich diet (FRD; 60%) for 8 weeks. The animals were randomly divided into 6 groups ($n = 12$), including (a) control, (b) fructose-rich diet (FRD), (c) FRD + quercetin (3 mg/kg bw), (d) FRD + rutin (11.5 mg/kg bw), (e) FRD + EEB (50 mg/kg bw), and (f) FRD + rutin + quercetin. The doses of rutin and quercetin were equivalent to those administered to the EEB administration group. Data are presented as the mean ± SEM. #Significant difference from the control group ($P < 0.05$). *Significant difference form the FRD group ($P < 0.05$). The statistics were shown by the t-test.

circulation is greater than the rate of glucose uptake, and because fructose metabolism bypasses phosphofructokinase, fructose metabolism is not under the regulatory control of insulin [7].

The levels of blood glucose and insulin in the FRD-induced group were significantly increased compared with the normal group, suggesting that the FRD markedly induced hyperinsulinemia and hyperglycemia, and the elevations of blood glucose and insulin both were inhibited by EEB and rutin/quercetin + rutin treatments; moreover, the HOMA-IR value by FRD induction was significantly reduced by EEB and rutin/quercetin + rutin treatments (Table 1). On the other hand, the improvement of EEB and rutin/quercetin + rutin administrations for regulating blood glucose in OGTT test was significantly observed compared to the control group and FRD-induced group, suggesting that the hypoglycemic activity of rutin + quercetin and EEB are both greater than rutin or quercetin administration from 30 min to 120 min (Figure 6). However, these effects were not found in quercetin administration group, indicating that EEB and which active compound (rutin) both improved insulin sensitivity in C57BL/6 mice induced by FRD.

3.5. The Improvements of EEB, Rutin, Quercetin, and Rutin + Quercetin on Fatty Acid/Cholesterol Generation and Accumulation. Plasma and hepatic fatty acid/cholesterol are commonly associated with impaired insulin-mediated glucose uptake in related tissues and coexist with type 2 diabetes and obesity [33]. As shown in Table 2, EEB and rutin/quercetin + rutin could improve plasma and hepatic TC, TG, HDL-C, and LDL-C levels compared to the FRD-induced group, thereby showing antihyperglycemic and antihyperinsulinemic activities. In addition, FRD induction for 8 weeks significantly increased fatty degeneration and

Table 2: Effect of EEB on hepatic and serum TC, TG, HDL, and LDL levels in FRD-induced rats at week 8.

Groups	Hepatic TG	Hepatic TC	Hepatic HDL-C	Hepatic LDL-C
	Concentration (mg/g)			
Normal	298.2 ± 3.6	26.6 ± 1.6	17.9 ± 0.2	373.4 ± 1.2
FRD	385.2 ± 7.1$^{\#}$	39.5 ± 1.3$^{\#}$	17.7 ± 0.8	457.2 ± 3.9$^{\#}$
FRD + quercetin	359.8 ± 4.2$^{\#*}$	38.9 ± 2.6$^{\#}$	16.0 ± 0.3	429.7 ± 4.6$^{\#}$
FRD + rutin	322.2 ± 7.4$^{\#*}$	29.6 ± 1.9$^{\#*}$	17.1 ± 0.4	393.1 ± 3.4$^{\#*}$
FRD + EEB	310.0 ± 6.2*	24.7 ± 1.4*	15.7 ± 0.4*	378.5 ± 2.0*
FRD + quercetin + rutin	317.9 ± 7.3*	27.9 ± 1.1*	16.7 ± 0.1	359.8 ± 10.1*
Groups	Plasma TG	Plasma TC	Plasma HDL-C	Plasma LDL-C
	Concentration (mg/dL)			
Normal	124.6±1.7	69.0 ± 1.1	71.8 ± 2.5	126.5 ± 1.5
FRD	238.0 ± 1.1*	94.3 ± 3.1$^{\#}$	52.6 ± 1.6$^{\#}$	239.5 ± 4.7$^{\#}$
FRD + quercetin	193.5 ± 6.6$^{\#*}$	89.0 ± 5.3$^{\#}$	54.1 ± 3.7$^{\#}$	235.5 ± 5.6$^{\#}$
FRD + rutin	172.0 ± 3.3$^{\#*}$	82.7 ± 2.8$^{\#*}$	52.5 ± 5.3$^{\#}$	211.4 ± 1.6$^{\#*}$
FRD + EEB	148.5 ± 8.7$^{\#*}$	76.6 ± 2.4$^{\#*}$	62.8 ± 2.2$^{\#*}$	187.5 ± 3.9$^{\#*}$
FRD + quercetin + rutin	138.2 ± 6.4*	80.5 ± 2.4$^{\#*}$	59.4 ± 1.5$^{\#*}$	193.2 ± 1.8$^{\#*}$

Hyperglycemia and hyperinsulinmia in mice were induced by fructose-rich diet (FRD; 60%) for 8 weeks. The animals were randomly divided into 6 groups ($n = 12$), including (a) control, (b) fructose-rich diet (FRD), (c) FRD + quercetin (3 mg/kg bw), (d) FRD + rutin (11.5 mg/kg bw), (e) FRD + EEB (50 mg/kg bw), and (f) FRD + rutin + quercetin. The doses of rutin and quercetin were equivalent to those administered to the EEB administration group. Data are presented as the mean ± SEM. $^{\#}$Significant difference from the control group ($P < 0.05$). *Significant difference form the FRD group ($P < 0.05$). The statistics were shown by the t-test.

Table 3: Effects of EEB on hepatic antioxidase activity in FRD-induced rats at week 8.

Groups	Hepatic antioxidant enzyme activity			
	CAT	GR	GPx	SOD
	nmol H_2O_2/min/mg protein	nmol NADPH/min/mg protein		U/mg protein
Normal	126.3 ± 1.6	5963 ± 11	5438 ± 32	65.8 ± 0.7
FRD	90.4 ± 3.0$^{\#}$	4543 ± 56$^{\#}$	4019 ± 57$^{\#}$	50.3 ± 0.6$^{\#}$
FRD + quercetin	120.8 ± 1.8*	4326 ± 52$^{\#}$	4089 ± 34$^{\#}$	58.5 ± 1.9$^{\#*}$
FRD + rutin	117.9 ± 2.9*	5107 ± 60$^{\#*}$	4101 ± 55$^{\#}$	65.0 ± 2.6*
FRD + EEB	127.1 ± 3.7*	6211 ± 58*	4739 ± 38$^{\#*}$	67.1 ± 1.4*
FRD + quercetin + rutin	121.0 ± 2.0*	5842 ± 32*	4997 ± 22$^{\#*}$	62.2 ± 1.7*

Hyperglycemia and hyperinsulinemia in mice were induced by fructose-rich diet (FRD; 60%) for 8 weeks. The animals were randomly divided into 6 groups ($n = 12$), including (a) control, (b) fructose-rich diet (FRD), (c) FRD + quercetin (3 mg/kg bw), (d) FRD + rutin (11.5 mg/kg bw), (e) FRD + EEB (50 mg/kg bw), and (f) FRD + rutin + quercetin. The doses of rutin and quercetin were equivalent to those administered to the EEB administration group. Data are presented as the mean ± SEM. $^{\#}$Significant difference from the control group ($P < 0.05$). *Significant difference form the FRD group ($P < 0.05$). The statistics were shown by the t-test.

accumulation provided histopathological evidence of liver tissue; however, these histopathologic injuries were improved by EEB, rutin/quercetin + rutin administration (Figure 7).

3.6. Effects of EEB on Hepatic Antioxidant Enzymes Activity. Several lines of evidence have established that excessive oxidative stress caused by reactive oxygen species (ROS) and reactive nitrogen species (RNS) can promote disease progression through oxidation of biomolecules such as DNA, lipids, and proteins [34, 35]. Oxidative stress contributes to diabetes and other human diseases [36]. Elevated levels of free fatty acid have been inhibiting insulin secretion by mitochondrial oxidation in the establishment of insulin resistance in diabetes mellitus [37]. An association between oxidative stress and insulin resistance has been reported in diabetes [38]. The results described above indicated that FRD induction resulted in lipid accumulation in the liver, resulting in insulin resistance. Therefore, the preventive

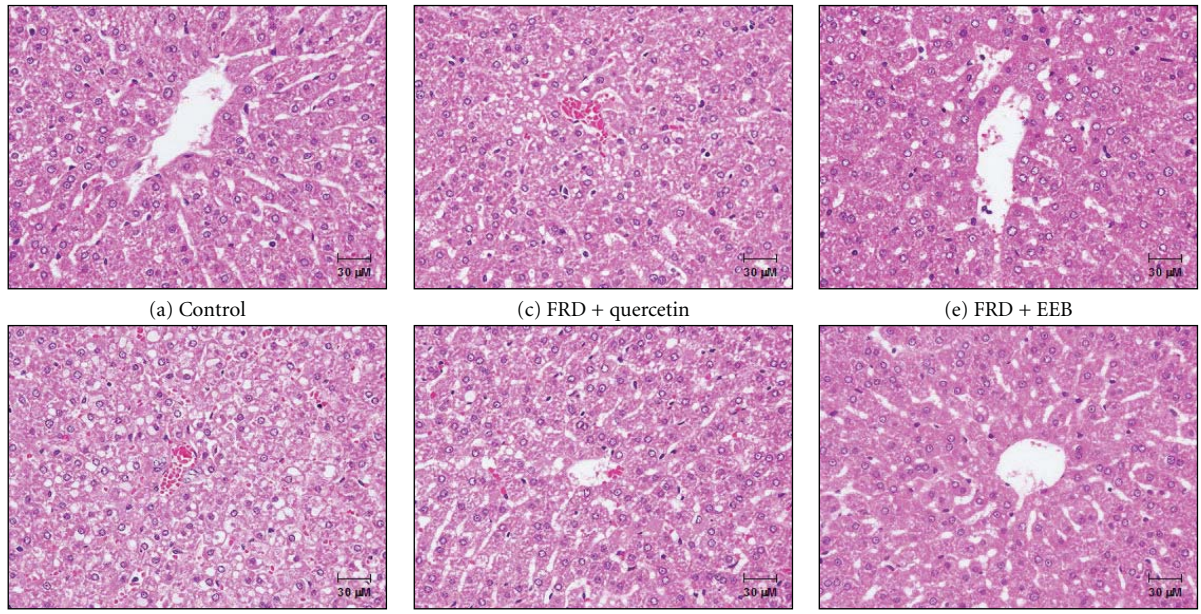

Figure 7: The effects of EEB, quercetin, rutin, and quercetin + rutin on fatty acid accumulation in liver of C57BL/6 mice induced by fructose-rich diet (FRD; 60%) for 8 weeks. The animals were randomly divided into 6 groups ($n = 12$), including (a) control, (b) fructose-rich diet (FRD), (c) FRD + quercetin (3 mg/kg bw), (d) FRD + rutin (11.5 mg/kg bw), (e) FRD + EEB (50 mg/kg bw), and (f) FRD + rutin + quercetin. EEB: 75% ethanol extracts of buckwheat. The doses of rutin and quercetin were equivalent to those administered to the EEB administration group.

effects of EEB and rutin/quercetin + rutin on oxidative stress in the liver of FRD-induced mice were evaluated in this study. The results suggested that EEB and rutin/quercetin + rutin administration significantly increased CAT, GR, GPx, and SOD activities in liver of FRD-induced C57BL/6 mice (Table 3).

4. Conclusion

In conclusion, we evaluated the effects of EEB, rutin, and quercetin on the insulin resistance pathway in FL83B hepatocytes with high-glucose-level-induced insulin resistance. We found that EEB, rutin, and quercetin may alleviate insulin resistance by improving insulin signaling via p-PKC activity inhibition and glucose uptake enhancement in insulin-resistant cells. In addition, we proposed that alleviation of insulin resistance was involved in the antioxidative effect of these phenolic acids in C57BL/6 mice induced by FRD (60%) for 8 weeks. We found that EEB and rutin/quercetin + rutin could improve hyperglycemia and hyperinsulinemia but quercetin administration did not show these activities, suggesting that rutin was major active compound of EEB. Taken together, the present study showed that EEB, rutin, and quercetin exerted antihyperglycemic and antioxidant activities because of their multiple effects, including antioxidative capacity and promotion of antioxidation enzymes, for protecting oxidative stress-induced insulin resistance in FL83B hepatocytes.

References

[1] E. H. Jang, J. H. Ko, C. W. Ahn et al., "In vivo and in vitro application of black soybean peptides in the amelioration of endoplasmic reticulum stress and improvement of insulin resistance," *Life Sciences*, vol. 86, no. 7-8, pp. 267–274, 2010.

[2] P. Zimmet, K. G. M. M. Alberti, and J. Shaw, "Global and societal implications of the diabetes epidemic," *Nature*, vol. 414, no. 6865, pp. 782–787, 2001.

[3] Y. Nagai, Y. Nishio, T. Nakamura, H. Maegawa, R. Kikkawa, and A. Kashiwagi, "Amelioration of high fructose-induced metabolic derangements by activation of PPARα," *American Journal of Physiology*, vol. 282, no. 5, pp. E1180–E1190, 2002.

[4] R. Nagata, Y. Nishio, O. Sekine et al., "Single nucleotide polymorphism (-468 Gly to Ala) at the promoter region of sterol regulatory element-binding protein-1c associates with genetic defect of fructose-induced hepatic lipogenesis," *Journal of Biological Chemistry*, vol. 279, no. 28, pp. 29031–29042, 2004.

[5] M. J. Dekker, Q. Su, C. Baker, A. C. Rutledge, and K. Adeli, "Fructose: a highly lipogenic nutrient implicated in insulin resistance, hepatic steatosis, and the metabolic syndrome," *American Journal of Physiology*, vol. 299, no. 5, pp. E685–E694, 2010.

[6] S. H. Adams, K. L. Stanhope, R. W. Grant, B. P. Cummings, and P. J. Havel, "Metabolic and endocrine profiles in response

to systemic infusion of fructose and glucose in rhesus macaques," *Endocrinology*, vol. 149, no. 6, pp. 3002–3008, 2008.

[7] M. B. Vos and C. J. McClain, "Fructose takes a toll," *Hepatology*, vol. 50, no. 4, pp. 1004–1006, 2009.

[8] D. Faeh, K. Minehira, J. M. Schwarz, R. Periasami, P. Seongsu, and L. Tappy, "Effect of fructose overfeeding and fish oil administration on hepatic de novo lipogenesis and insulin sensitivity in healthy men," *Diabetes*, vol. 54, no. 7, pp. 1907–1913, 2005.

[9] M. Holasova, V. Fiedlerova, H. Smrcinova, M. Orsak, J. Lachman, and S. Vavreinova, "Buckwheat—the source of antioxidant activity in functional foods," *Food Research International*, vol. 35, no. 2-3, pp. 207–211, 2002.

[10] C. L. Liu, Y. S. Chen, J. H. Yang, and B. H. Chiang, "Antioxidant activity of tartary (*Fagopyrum tataricum* (L.) gaertn.) and common (*Fagopyrum esculentum* moench) buckwheat sprouts," *Journal of Agricultural and Food Chemistry*, vol. 56, no. 1, pp. 173–178, 2008.

[11] B.-H. Lee, W.-H. Hsu, and T.-M. Pan, "Inhibitory effects of dioscorea polysaccharide on TNF-α-induced insulin resistance in mouse FL83B cells," *Journal of Agricultural and Food Chemistry*, vol. 59, no. 10, pp. 5279–5285, 2011.

[12] A. Schieber, P. Keller, and R. Carle, "Determination of phenolic acids and flavonoids of apple and pear by high-performance liquid chromatography," *Journal of Chromatography A*, vol. 910, no. 2, pp. 265–273, 2001.

[13] T. P. Liu, I. M. Liu, and J. T. Cheng, "Improvement of insulin resistance by Panax ginseng in fructose-rich chow-fed rats," *Hormone and Metabolic Research*, vol. 37, no. 3, pp. 146–151, 2005.

[14] A. K. Sharma and B. P. Srinivasan, "Triple verses glimepiride plus metformin therapy on cardiovascular risk biomarkers and diabetic cardiomyopathy in insulin resistance type 2 diabetes mellitus rats," *European Journal of Pharmaceutical Sciences*, vol. 38, no. 5, pp. 433–444, 2009.

[15] D. R. Matthews, J. P. Hosker, and A. S. Rudenski, "Homeostasis model assessment: insulin resistance and β-cell function from fasting plasma glucose and insulin concentrations in man," *Diabetologia*, vol. 28, no. 7, pp. 412–419, 1985.

[16] R. Jalal, S. M. Bagheri, A. Moghimi, and M. B. Rasuli, "Hypoglycemic effect of aqueous shallot and garlic extracts in rats with fructose-induced insulin resistance," *Journal of Clinical Biochemistry and Nutrition*, vol. 41, no. 3, pp. 218–223, 2007.

[17] J. Mohandas, J. J. Marshall, and G. G. Duggin, "Low activities of glutathione-related enzymes as factors in the genesis of urinary bladder cancer," *Cancer Research*, vol. 44, no. 11, pp. 5086–5091, 1984.

[18] G. Bellomo, F. Mirabelli, and D. DiMonte, "Formation and reduction of glutathione-protein mixed disulfides during oxidative stress. A study with isolated hepatocytes and menadione (2-methyl-1,4-naphthoquinone)," *Biochemical Pharmacology*, vol. 36, no. 8, pp. 1313–1320, 1987.

[19] H. Aebi, "Catalase in vitro," *Methods in Enzymology*, vol. 105, pp. 121–126, 1984.

[20] S. Marklund and G. Marklund, "Involvement of the superoxide anion radical in the autoxidation of pyrogallol and a convenient assay for superoxide dismutase," *European Journal of Biochemistry*, vol. 47, no. 3, pp. 469–474, 1974.

[21] B. H. Lee, B. Y. Ho, C. T. Wang, and T. M. Pan, "Red mold rice promoted antioxidase activity against oxidative injury and improved the memory ability of zinc-deficient rats," *Journal of Agricultural and Food Chemistry*, vol. 57, no. 22, pp. 10600–10607, 2009.

[22] P. Gray, *Handbook of Basic Microtechnique*, McGraw-Hill, New York, NY, USA, 3rd edition, 1964.

[23] D. R. Alessi and P. Cohen, "Mechanism of activation and function of protein kinase B," *Current Opinion in Genetics and Development*, vol. 8, no. 1, pp. 55–62, 1998.

[24] B. Kola, M. Boscaro, G. A. Rutter, A. B. Grossman, and M. Korbonits, "Expanding role of AMPK in endocrinology," *Trends in Endocrinology and Metabolism*, vol. 17, no. 5, pp. 205–215, 2006.

[25] B. B. Kahn, T. Alquier, D. Carling, and D. G. Hardie, "AMP-activated protein kinase: ancient energy gauge provides clues to modern understanding of metabolism," *Cell Metabolism*, vol. 1, no. 1, pp. 15–25, 2005.

[26] B.-H. Lee, W.-H. Hsu, T.-H. Liao, and T.-M. Pan, "The Monascus metabolite monascin against TNF-α-induced insulin resistance via suppressing PPAR-γ phosphorylation in C2C12 myotubes," *Food and Chemical Toxicology*, vol. 49, no. 10, pp. 2609–2617, 2011.

[27] I. Jialal and S. K. Venugopal, "Oxidative strees, inflammation, and diabetic vasculopathies: the role of alpha tocopherol therapy," *Free Radical Research*, vol. 36, no. 12, pp. 1331–1336, 2002.

[28] S. K. Jain, K. Kannan, G. Lim, J. Matthews-Greek, R. McVie, and J. A. Bocchini, "Elevated blood interleukin-6 levels in hyperketonemic type 1 diabetic patients and secretion by acetoacetate-treated cultured U937 monocytes," *Diabetes Care*, vol. 26, no. 7, pp. 2139–2143, 2003.

[29] N. Shanmugam, M. A. Reddy, M. Guha, and R. Natarajan, "High glucose-induced expression of proinflammatory cytokine and chemokine genes in monocytic cells," *Diabetes*, vol. 52, no. 5, pp. 1256–1264, 2003.

[30] J. N. Feige, L. Gelman, L. Michalik, B. Desvergne, and W. Wahli, "From molecular action to physiological outputs: peroxisome proliferator-activated receptors are nuclear receptors at the crossroads of key cellular functions," *Progress in Lipid Research*, vol. 45, no. 2, pp. 120–159, 2006.

[31] J. Díaz-Delfín, M. Morales, and C. Caelles, "Hypoglycemic action of thiazolidinediones/peroxisome proliferator-activated receptor γ by inhibition of the c-Jun NH2-terminal kinase pathway," *Diabetes*, vol. 56, no. 7, pp. 1865–1871, 2007.

[32] M. J. Dekker, Q. Su, C. Baker, A. C. Rutledge, and K. Adeli, "Fructose: a highly lipogenic nutrient implicated in insulin resistance, hepatic steatosis, and the metabolic syndrome," *American Journal of Physiology*, vol. 299, no. 5, pp. E685–E694, 2010.

[33] B. Salgin, M. L. Marcovecchio, R. M. Williams et al., "Effects of growth hormone and free fatty acids on insulin sensitivity in patients with type 1 diabetes," *Journal of Clinical Endocrinology and Metabolism*, vol. 94, no. 9, pp. 3297–3305, 2009.

[34] A. Burke and G. A. FitzGerald, "Oxidative stress and smoking-induced vascular injury," *Progress in Cardiovascular Diseases*, vol. 46, no. 1, pp. 79–90, 2003.

[35] L. S. Nakao, L. K. Iwai, J. Kalil, and O. Augusto, "Radical production from free and peptide-bound methionine sulfoxide oxidation by peroxynitrite and hydrogen peroxide/iron(II)," *FEBS Letters*, vol. 547, no. 1–3, pp. 87–91, 2003.

[36] D. M. Niedowicz and D. L. Daleke, "The role of oxidative stress in diabetic complications," *Cell Biochemistry and Biophysics*, vol. 43, no. 2, pp. 289–330, 2005.

[37] A. Shah, N. Mehta, and M. P. Reilly, "Adipose inflammation, insulin resistance, and cardiovascular disease," *Journal of Parenteral and Enteral Nutrition*, vol. 32, no. 6, pp. 638–644, 2008.

[38] L. A. Videla, "Oxidative stress signaling underlying liver disease and hepatoprotective mechanisms," *World Journal of Hepatology*, vol. 1, pp. 72–78, 2009.

Hindawi Publishing Corporation
Experimental Diabetes Research
Volume 2012, Article ID 386831, 5 pages
doi:10.1155/2012/386831

Research Article

Comparison of Oxidant/Antioxidant, Detoxification Systems in Various Tissue Homogenates and Mitochondria of Rats with Diabetes Induced by Streptozocin

Veysel Kenan Çelık,[1] Zeynep Deniz Şahın,[2] İsmail Sari,[1] and Sevtap Bakir[1]

[1] *Departments of Biochemistry, Cumhuriyet University School of Medicine, 58140 Sivas, Turkey*
[2] *Department of Histology and Embryology, Cumhuriyet University School of Medicine, 58140 Sivas, Turkey*

Correspondence should be addressed to Veysel Kenan Çelık, kenanim123@yahoo.com

Received 17 October 2011; Revised 31 January 2012; Accepted 2 February 2012

Academic Editor: Pietro Galassetti

Objective. Oxidative stress is considered to be the main factor in the development of diabetic complications and tissue injury. our objective was to investigate and compare the oxidant/antioxidant conditions and detoxification mechanisms of the liver, lung, kidney, cardiac tissues, and mitochondria of rats with diabetes induced by streptozocin (STZ). *Methods*. Rats with diabetes induced by streptozocin were anesthetized by administering 90 mg/kg ketamine hydrochloride and 3 mg/kg xylazine hydrochloride. Thoracic cavities were incised open; liver, lung, kidney, and cardiac tissues were removed and stored at −70°C. All samples were homogenized and mitochondrial fractions were separated. Total Antioxidant Status (TAS), Total Oxidant Status (TOS), Oxidative Stress Index (OSI), Paraoxonase (PON), Arylesterase, Catalase (Cat), Malondialdehyde (MDA), and Glutathion-S-transferase were measured in each fraction. *Results*. MDA and TOS levels were significantly increased in liver tissues, and TOS and OSI were increased in the mitochondrial fractions of diabetic rats. These increases were not statistically significant compared to the control group. No significant differences were determined in the antioxidant and GST activities. *Conclusion*. According to our results, oxidative stress has not developed in rats with diabetes induced by streptozocin. The detoxification system was induced; however, this induction did not differ significantly from the controls.

1. Introduction

Diabetes is a rapidly spreading disease due to current adverse living conditions and unbalanced nutrition habits. The incidence and prevalence of type II diabetes are increasing particularly in industrializing and developing nations, and this increase is estimated to exceed 200 million as of the end of 2011 [1]. Chronic complications of diabetes affect several organ and systems creating the primary causes of morbidity and mortality. Overall, chronic complications are grouped into two categories as vascular and nonvascular complications [2–4].

Diabetes is a metabolic disease; however, it has long been known that its complications are associated with oxidative stress [5]. Chronic hyperglycemia leads to increased oxidative stress particularly in tissues where complications of diabetes develop [6]. The mechanisms that increase oxidative stress in diabetes include nonenzymatic glycation, autooxidative glycation, metabolic stress secondary to the changes in energy metabolism, activity of the sorbitol pathway, levels of inflammatory mediators, and tissue injury resulting from the changes in antioxidant defense system [7–13].

In this study, our objective was to investigate and compare the antioxidant-oxidant systems (TAS,TOS, OSI, PON, Arylesterase, Catalase, and MDA) and levels of GST enzyme that plays an important role in detoxification mechanisms in heart, liver, lung, and kidney tissues and mitochondrial fractions in rats with hyperglycemia (not chronic) developed with STZ, a diabetogenic chemical agent.

2. Material and Methods

2.1. Development of Experimental Diabetes. Twelve female and male *Wistar albino* rats of 250–300 grams in weight,

reproduced in the Experimental Animals Laboratory of Cumhuriyet University, Medical Faculty were used in this study. Rats were separated into two groups as control and study groups and were provided with free access to food and water. An approval document dated November 1st; 2007 and numbered B.30.2.CUM.0.01.00.00-50/214 was obtained from the Cumhuriyet University, Experimental Animals Ethics Committee.

Blood glucose levels of rats were measured following and overnight fasting (Lever Check TD-4222). Rats with blood glucose levels 80–110 mg/dL were considered normal. A single dose of intraperitoneal 60 mg/kg streptozocin (STZ; Sigma Chemical Co., St. Louis Missouri, USA) resolved in 0.1 M citrate buffer of 4.5 pH was used to develop diabetes in the experimental group of animals without sex distinction. Blood glucose levels were measured in the intravenous blood samples obtained from the tails of rats at 48 hours of streptozocin injection. Rats with blood glucose levels of 250 mg/dL were considered diabetic.

2.2. Surgical Procedure. All rats were anesthetized at week two with an intramuscular injection of 90 mg/kg ketamine hydrochloride, 3 mg/kg of xylazine hydrochloride into left fore leg muscle. Thoracic cavities were incised open; liver, lung, kidney, and heart tissues were removed and stored at −70°C.

2.3. Mitochondria Extract. All defrosted tissues were homogenized in ice shower containing 4 mL of 0.2 M phosphate buffer at pH 7.4. Homogenates were centrifuged at 3000 g for 15 minutes at 4°C to remove tissue remnants. Activities were determined in the supernatant.

Mitochondria were extracted according to the method defined by Max et al. [14] and modified by Mousa [15]. Samples of 1 gram was obtained from each tissue and homogenized in 5 mL of 0.25 M sucrose solution. Homogenates were centrifuged at 800 g for 15 minutes at 4°C, supernatant was later recentrifuged at 20 000 g for 10 minutes. Following the removal of the supernatant, the mildly swollen layer on top of the mitochondrial pellet was removed with the gentle addition of sucrose solution. Pellet was later prepared for analyses by suspension with 1.2 mL of 0.02 M phosphate buffer at pH 7.4.

2.4. Activity Analyses. MDA were measured spectrophotometrically according to the thiobarbituric acid (TBA) method [16]. TAS, TOS, PON, and arylesterase activities were measured using the commercial kit (Rel Assay Diagnostic) Syncron LX autoanalyzer. OSI was calculated according to the following formula: OSI: TOS/TASX100.

Catalase activity was determined by measuring the amount of H_2O_2 decreased at 240 nm wavelength according to the method defined by Beers and Sizer [17]. GST activities were calculated spectrophotometrically at 340 nm according to the method defined by Habig et al. [18].

2.5. Statistical Analysis. Statistical analysis was performed using the Kruskal Wallis analysis (SPSS, 14.0). Paired comparisons were performed with Mann-Whitney U test, when a P value of ≤ 0.05 was obtained. A P value of ≤ 0.05 was considered significant.

3. Results

In the comparison of parameters measured in control group by tissue types as shown in Table 1 (lung, liver, kidney, and heart), no significant differences were determined in terms of MDA and PON. Paired comparisons with Mann-Whitney U test demonstrated that level of MDA was significantly higher in heart tissue compared to the lung and kidney tissues ($P < 0.05$), and PON activity was significantly higher in the kidney tissue compared to the liver and lung tissues ($P < 0.05$). Kruskal Wallis analysis was used to determine significant differences between the groups, and no significant differences were determined in the paired comparison of other tissue types ($P > 0.05$).

No significant differences were determined in terms of MDA and TOS between the groups in the evaluation of parameters measured in diabetic group by tissue types. Paired comparisons with Mann-Whitney U test demonstrated that MDA level of liver tissue was significantly higher compared to that of the heart tissue ($P < 0.05$). TOS level of liver tissue was significantly higher compared to that of the heart and lung tissues ($P < 0.05$). Renal TOS level was also significantly higher compared to the lung and heart ($P < 0.05$). Kruskal Wallis analysis was used to determine significant differences between the groups, and no significant differences were determined in the paired comparison of other tissue types ($P > 0.05$) (Table 1).

A significant difference was determined in terms of TOS, OSI (%), GST, and Catalase between the groups in the evaluation of parameters measured in mitochondrial tissue fractions by tissue types in the diabetic group, as shown in Table 2. In the paired comparison of these groups with the Mann-Whitney U test, TOS and OSI levels were significantly higher in the mitochondrial fraction of liver tissue compared to the heart tissue and kidney tissue, respectively ($P < 0.05$). Catalase-specific activity in the mitochondrial fraction of liver tissue was significantly higher compared to that of the mitochondrial fraction of lung tissue. GST-specific-activity was appointed to be significantly higher in the mitochondrial fraction liver tissue compared to mitochondrial fractions of all tissue types. Kruskal Wallis analysis was used to determine significant differences between the groups, and no significant differences were determined in the paired comparison of other tissue types ($P > 0.05$).

Significant difference was determined in terms of MDA, OSI (%) and Catalase between the groups in the evaluation of parameters measured in mitochondrial tissue fractions of control group by different tissue types (Table 2). Paired comparisons with Mann-Whitney U test in these groups demonstrated that OSI (%) level was significantly higher in mitochondrial fraction of liver tissue compared to kidney and heart tissues ($P < 0.05$). Catalase-specific activity in mitochondrial fraction of kidney tissue was significantly higher compared to that of lung tissue. MDA level was determined to be significantly higher in the mitochondrial fraction of liver tissue compared to mitochondrial fractions

Table 1: Evaluation of parameters measured in both group by tissue types.

Measurement	Lung X ± S	Liver X ± S	Kidney X ± S	Heart X ± S
MDA (nmol/mL)				
Control	3,81 ± 1,1[§]	3,22 ± 0,7	5,22 ± 0,8[ξ]	1,29 ± 0,4[ξ]
Diabetic	3,22 ± 3,1	9,01 ± 7,8*	3,30 ± 1,5	0,50 ± 0,4*
TAS (mmol trolox Equiv/L)				
Control	0,423 ± 0,54	0,406 ± 0,21	0,376 ± 0,10	0,143 ± 0,03
Diabetic	0,19 ± 0,06	0,53 ± 0,28	0,45 ± 0,28	0,18 ± 0,04
TOS (μmol H_2O_2 Equiv/L)				
Control	7,75 ± 10,4	4,46 ± 1,2	6,40 ± 2,4	2,53 ± 0,9
Diabetic	2,22 ± 0,03[#]	6,29 ± 1,05[#]	4,59 ± 0,78[#]	1,49 ± 0,6[#]
OSİ (%)				
Control	16,83 ± 2,35	13,12 ± 6,70	16,97 ± 4,12	17,35 ± 3,42
Diabetic	12,05 ± 3,4	15,82 ± 11,4	12,49 ± 6,99	8,07 ± 1,44
PON (U/L)				
Control	4,33 ± 3,2*	4,33 ± 1,5*	9,33 ± 0,5*	7,66 ± 1,5
Diabetic	6,00 ± 3,0	6,00 ± 4,3	8,00 ± 1,0	7,33 ± 1,5
Arylesterase (U/L)				
Control	4365,0 ± 410,7	4347,6 ± 738,5	4093,3 ± 359,1	4068,3 ± 380,6
Diabetic	4785,0 ± 111,8	4088,3 ± 541,0	4350,0 ± 172,4	4249,0 ± 483,0
GST (U/mgPrt)				
Control	0,0032 ± 0,002	0,0547 ± 0,040	0,0073 ± 0,004	0,0062 ± 0,003
Diabetic	0,0011 ± 0,001	0,0238 ± 0,020	0,0020 ± 0,003	0,0173 ± 0,029
Catalase (U/mgPrt)				
Control	0,545 ± 0,07	0,1176 ± 0,04	0,0371 ± 0,02	0,0188 ± 0,01
Diabetic	0,012 ± 0,003	0,0665 ± 0,029	0,0381 ± 0,036	0,0488 ± 0,04

* $P = 0.05$, § $P = 0,03$, # $P = 0.01$.

of all other tissue types. Additionally, MDA level of mitochondrial fraction of lung tissue was also significantly higher compared to the MDA levels in the mitochondrial fraction of kidney and heart tissues ($P < 0.05$). Kruskal Wallis analysis was used to determine significant differences between the groups, and no significant differences were determined in the paired comparison of other tissue types ($P > 0.05$).

No significant differences were determined between the diabetic and control groups in the statistical analysis of parameters measured in all tissue types (tissue-mitochondrial) ($P > 0.05$).

4. Discussion

Male and female rats were equally distributed to each group to prevent the influence of confounding factors including sex. The most significant increase in the level of MDA among rats with chemically induced diabetes was observed in the liver when the results were evaluated between different tissues and within the same group (Table 1). Studies on rats with STZ-induced diabetes have demonstrated that MDA levels were significantly increased in the liver [19] and kidney mitochondria [19, 20]. According to our results this increase was limited to the liver; however it was not statistically significant. The increase in TOS in both liver and mitochondrial fractions in the diabetic group led to an increase also in the OSI. Although MDA, TOS, and OSI were increased, these were not statistically significant increases compared to the control group ($P > 0.05$). No significant differences were noted between the two groups, tissues and mitochondrial fractions when levels of TAS were compared.

A significant increase only in the catalase activity of liver mitochondria of the diabetic group was noted in the comparison of the antioxidative enzymes PON, arylesterase, and catalase ($P = 0.03$). The lack of difference in OSI levels in between the groups suggested us the contribution of the increased catalase activity. A study on acute diabetic rats has demonstrated that catalase activity is not altered [21]; however another time-dependent study has demonstrated an increase in the first week followed by a decrease compared to the controls [22]. In the long term, this will affect the OSI and trigger oxidative injury. Planning of a time-dependent study is important to demonstrate the alterations in OSI.

On the other hand, in terms of the data of GST, liver mitochondrial fraction was increased in the diabetic group, although not statistically significantly compared to the controls. This increase in GST is in response to STZ and causes a reflex in the detoxification system. It is known that medications and endogenous-exogenous chemical substances are first metabolized by the liver microsomal oxidase

Table 2: Evaluation of parameters measured in the mitochondrial fraction of both group by tissue types.

Measurement	Lung X ± S	Liver X ± S	Kidney X ± S	Heart X ± S
MDA (nmol/L)				
Control	4,23 ± 0,59$^{\#}$	6,04 ± 0,12$^{\#}$	2,54 ± 0,67$^{\#}$	1,21 ± 0,29$^{\#}$
Diabetic	2,90 ± 2,00	6,21 ± 4,63	4,43 ± 3,81	1,61 ± 0,99
TAS (mmol trolox Equiv/L)				
Control	0,79 ± 0,86	0,69 ± 0,55	1,46 ± 0,32	0,83 ± 0,59
Diabetic	0,51 ± 0,10	2,11 ± 1,65	1,28 ± 0,20	0,42 ± 0,15
TOS (μmol H_2O_2 Equiv/L)				
Control	8,83 ± 11,79	7,82 ± 9,31	2,27 ± 0,79	1,57 ± 1,28
Diabetic	1,87 ± 0,35	10,00 ± 7,09$^{\triangle}$	2,19 ± 0,76	0,85 ± 0,33
OSİ (%)				
Control	8,66 ± 5,03	16,10 ± 21,67§	1,52 ± 0,28§	1,82 ± 0,32§
Diabetic	3,84 ± 1,44	5,59 ± 2,15*	1,68 ± 0,22*	2,20 ± 1,0
PON (U/L)				
Control	6,00 ± 2,00	11,66 ± 12,50	7,33 ± 2,08	8,00 ± 1,00
Diabetic	7,33 ± 0,57	10,66 ± 5,85	7,33 ± 1,52	9,66 ± 2,88
Arylesterase (U/L)				
Control	5006,6 ± 742,0	4330,6 ± 951,4	4636,3 ± 210,7	3996,3 ± 183,9
Diabetic	3583,6 ± 1487,6	4460,6 ± 449,5	4348,0 ± 165,3	3996,6 ± 136,0
GST (U/mgPrt)				
Control	0,0027 ± 0,001	0,0307 ± 0,016	0,0063 ± 0,004	0,0077 ± 0,005
Diabetic	0,0023 ± 0,0007$^{\triangle}$	0,0272 ± 0,003$^{\triangle}$	0,0038 ± 0,001$^{\triangle}$	0,0087 ± 0,004$^{\triangle}$
Catalase (U/mgPrt)				
Control	0,0126 ± 0,004$^{\xi}$	0,0655 ± 0,032	0,1005 ± 0,047$^{\xi}$	0,0254 ± 0,02
Diabetic	0,0086 ± 0,003§	0,0575 ± 0,024§	0,0429 ± 0,0094	0,0266 ± 0,009

$^{\#}P = 0.01$, $^{\triangle}P = 0.02$, $^{\S}P = 0.03$, $^{\xi}P = 0.04$, $^{*}P = 0.05$.

systems leading to the formation of several toxic intermediate products. This is the phase 1 reaction needed for the metabolism of xenobiotics. These toxic substances are conjugated and transformed in to polar compounds that dissolve in water in order to excrete in urine in phase 2 reactions. GST is one of the most important phase 2 systems [23]. The increase in GST activity will both prevent the cells from the toxic effects of harmful compounds and prevent the development of oxidative injury. The lack of difference in terms of OSI in between the groups possibly resulted from the increased GST activity. Although we did not find any other study investigating the relationship between GST and diabetes, there is one study on the effect of STC on GST. This study has suggested that GST activity was decreased [24]. The lack of more studies on this topic is a limitation in terms of the comparison of our results. Further studies on this topic will be very important to remove the uncertainties, since the reported result contradicts with ours.

Consequently, although partial differences were observed between the tissues within the same group, no statistically significant difference was determined between the tissues and mitochondrial fractions. However, oxidative stress might develop in the long term in a chronic picture of diabetes and lead to tissue injury in addition to reduction in catalase and GST activity.

5. Conclusion

Consequently, although partial differences have been noted in both oxidant/antioxidant systems and detoxification enzyme (i.e., GST) activity in tissue and mitochondria of rats with experimental diabetes, these differences are not statistically significant compared to the control group. According to our results, oxidative stress has not developed in acute diabetes induced by a chemical agent, suggesting that oxidative stress might develop in long term and lead to tissue injury in a chronic picture of diabetes.

References

[1] H. King, R. E. Aubert, and W. H. Herman, "Global burden of diabetes, 1995—2025: prevalence, numerical estimates, and projections," *Diabetes Care*, vol. 21, no. 9, pp. 1414–1431, 1998.

[2] B. K. Tripathi and A. K. Srivastava, "Diabetes mellitus: complications and therapeutics," *Medical Science Monitor*, vol. 12, no. 7, pp. RA130–RA147, 2006.

[3] P. J. Thornalley, "Glycation in diabetic neuropathy: characteristics, consequences, causes, and therapeutic options," *International Review of Neurobiology*, vol. 50, pp. 37–57, 2002.

[4] A. F. Milano, "Diabetes mellitus and life insurance," *Journal of Insurance Medicine*, vol. 33, no. 1, pp. 50–103, 2001.

[5] A. M. Vincent, J. W. Russell, P. Low, and E. L. Feldman, "Oxidative stress in the pathogenesis of diabetic neuropathy," *Endocrine Reviews*, vol. 25, no. 4, pp. 612–628, 2004.

[6] R. Memisoğullari, S. Taysi, E. Bakan, and I. Capoglu, "Antioxidant status and lipid peroxidation in type II diabetes mellitus," *Cell Biochemistry and Function*, vol. 21, no. 3, pp. 291–296, 2003.

[7] A. K. Mohamed, A. Bierhaus, S. Schiekofer, H. Tritschler, R. Ziegler, and P. P. Nawroth, "The role of oxidative stress and NF-κB activation in late diabetic complications," *BioFactors*, vol. 10, no. 2-3, pp. 157–167, 1999.

[8] J. W. Baynes, "Role of oxidative stress in development of complications in diabetes," *Diabetes*, vol. 40, no. 4, pp. 405–412, 1991.

[9] G. L. King and N. K. Banskota, "Mechanism of diabetic microvascular complications," in *Joslin's Diabetes Mellitus*, C. R. Kahn and G. C. Weir, Eds., pp. 634–648, Lippincott Williams & Wilkins, Philadelphia, Pa, USA, 30th edition, 1994.

[10] A. M. Armstrong, J. E. Chestnutt, M. J. Gormley, and I. S. Young, "The effect of dietary treatment on lipid peroxidation and antioxidant status in newly diagnosed noninsulin dependent diabetes," *Free Radical Biology and Medicine*, vol. 21, no. 5, pp. 719–726, 1996.

[11] D. Giugliano, A. Ceriello, and G. Paolisso, "Oxidative stress and diabetic vascular complications," *Diabetes Care*, vol. 19, no. 3, pp. 257–267, 1996.

[12] S. R. J. Maxwell, H. Thomason, D. Sandler et al., "Poor glycaemic control is associated with reduced serum free radical scavenging (antioxidant) activity in non-insulin-dependent diabetes mellitus," *Annals of Clinical Biochemistry*, vol. 34, no. 6, pp. 638–644, 1997.

[13] N. N. Orie, W. Zidek, and M. Tepel, "Increased intracellular generation of reactive oxygen species in mononuclear leukocytes from patients with diabetes mellitus type 2," *Experimental and Clinical Endocrinology and Diabetes*, vol. 108, no. 3, pp. 175–180, 2000.

[14] S. R. Max, J. Garbus, and H. J. Wehman, "Simple procedure for rapid isolation of functionally intact mitochondria from human and rat skeletal muscle," *Analytical Biochemistry*, vol. 46, no. 2, pp. 576–584, 1972.

[15] H. M. Mousa, *Cyanide detoxification in domestic fowl (Gallus domesticus)*, Ph.D. thesis, University of London, London, UK, 1982.

[16] H. Ohkawa, N. Ohishi, and K. Yagi, "Assay for lipid peroxides in animal tissues by thiobarbituric acid reaction," *Analytical Biochemistry*, vol. 95, no. 2, pp. 351–358, 1979.

[17] R. F. Beers Jr. and I. W. Sizer, "A spectrophotometric method for measuring the breakdown of hydrogen peroxide by catalase," *The Journal of Biological Chemistry*, vol. 195, no. 1, pp. 133–140, 1952.

[18] W. H. Habig, M. J. Pabst, and W. B. Jakoby, "Glutathione S transferases: the first enzymatic step in mercapturic acid formation," *The Journal of Biological Chemistry*, vol. 249, no. 22, pp. 7130–7139, 1974.

[19] Y. Y. Jang, J. H. Song, Y. K. Shin, E. S. Han, and C. S. Lee, "Protective effect of boldine on oxidative mitochondrial damage in streptozotocin-induced diabetic rats," *Pharmacological Research*, vol. 42, no. 4, pp. 361–371, 2000.

[20] X.-F. Zhang and B. K.-H. Tan, "Antihyperglycaemic and antioxidant properties of Andrographis paniculata in normal and diabetic rats," *Clinical and Experimental Pharmacology and Physiology*, vol. 27, no. 5-6, pp. 358–363, 2000.

[21] K. Volkovova, V. Chorvathova, M. Jurcovicova, L. Koszeghyova, and P. Bobek, "Antioxidative state of the myocardium and kidneys in acute diabetic rats," *Physiological Research*, vol. 42, no. 4, pp. 251–255, 1993.

[22] R. Kakar, S. V. Mantha, J. Radhi, K. Prasad, and J. Karla, "Antioxidant defens system in diabetic kidney: a time course study," *Life Sciences*, vol. 60, no. 9, pp. 667–679, 1997.

[23] R. K. Murray, P. A. Mayes, D. K. Granner, and V. W. Rodwell, *Harper's Biochemistry*, Section in Xenobiotics Metabolism, Apleton & Longe, Norwalk, Conn, USA, 22nd edition, 1990.

[24] C. Agius and A. S. Gidari, "Effect of streptozotocin on the glutathione S-transferase of mouse liver cytosol," *Biochemical Pharmacology*, vol. 34, no. 6, pp. 811–819, 1985.

Hindawi Publishing Corporation
Experimental Diabetes Research
Volume 2012, Article ID 941304, 8 pages
doi:10.1155/2012/941304

Research Article

Insulin Resistance Promotes Early Atherosclerosis via Increased Proinflammatory Proteins and Oxidative Stress in Fructose-Fed ApoE-KO Mice

Beatriz Cannizzo,[1] Agustín Luján,[1] Natalia Estrella,[1] Carina Lembo,[2] Montserrat Cruzado,[1] and Claudia Castro[1]

[1] *Laboratory of Vascular Biology, Institute of Medicine and Experimental Biology of Cuyo (IMBECU)-CONICET, Faculty of Medical Sciences, National University of Cuyo, 5500 Mendoza, Argentina*
[2] *Laboratory of Cardiovascular Pathophysiology, Institute of Medicine and Experimental Biology of Cuyo (IMBECU)-CONICET, Faculty of Medical Sciences, National University of Cuyo, 5500 Mendoza, Argentina*

Correspondence should be addressed to Claudia Castro, ccastro@fcm.uncu.edu.ar

Received 31 October 2011; Accepted 13 December 2011

Academic Editor: Galassetti Pietro

High fructose intake induces an insulin resistance state associated with metabolic syndrome (MS). The effect of vascular inflammation in this model is not completely addressed. The aim of this study was to evaluate vascular remodeling, inflammatory and oxidative stress markers, and atheroma development in high-fructose diet-induced insulin resistance of ApoE-deficient mice (ApoE-KO). Mice were fed with either a normal chow or a 10% w/v fructose (HF) in drinking water over a period of 8 weeks. Thereafter, plasma metabolic parameters, vascular remodeling, atheroma lesion size, inflammatory markers, and NAD(P)H oxidase activity in the arteries were determined. HF diet induced a marked increase in plasma glucose, insulin, and triglycerides in ApoE-KO mice, provoked vascular remodeling, enhanced expression of vascular cell-adhesion molecule-1 (VCAM-1) and matrix metalloprotease 9 (MMP-9) and enlarged atherosclerotic lesion in aortic and carotid arteries. NAD(P)H oxidase activity was enhanced by fructose intake, and this effect was attenuated by tempol, a superoxide dismutase mimetic, and losartan, an Angiotensin II receptor antagonist. Our study results show that high-fructose-induced insulin resistance promotes a proinflammatory and prooxidant state which accelerates atherosclerotic plaque formation in ApoE-KO mice.

1. Introduction

Insulin-resistant states, including the metabolic syndrome (MS) and type 2 diabetes, have been strongly associated with subclinical and clinical cardiovascular disease (CVD)[1]. Elevated blood glucose, hyperinsulinemia, dyslipidemia and, oxidative stress are central components of MS which are additionally associated with a "proatherogenic" phenotype [2]. There are evidences indicating that structural and functional changes in the vascular wall are involved in cardiovascular alterations associated with MS [3], but the mechanisms underlying are not completely addressed. Previous studies from our group showed that chronic fructose-fed rats exhibited dyslipidemia, hyperglycemia, and endothelial dysfunction, and it was suggested an important role for the renin-angiotensin system (RAS) in the pathogenic mechanisms involved in this model [4].

Arterial remodeling occurs under an atherosclerotic plaque formation [5]. The propensity to accelerated lesion formation in MS may involve altered vascular structure and increased vascular inflammatory response. Delbosc et al. [6] reported that mesenteric arterial media/lumen ratio was higher in fructose-fed rats, and a potential association of soluble adhesion molecules with atherosclerosis has been postulated [7]. Vascular cell adhesion molecule-1 (VCAM-1) is a cytokine-inducible member of the immunoglobulin gene superfamily that is expressed by endothelial cells in regions predisposed to atherosclerosis and at the borders

of atherosclerotic plaques [7, 8]. VCAM-1 functions in combination with other adhesion molecules during chronic inflammation, activating NAD(P)H oxidase and endothelial MMPs [9]. Oxidative stress and associated vascular damage are mediators of vascular injury and inflammation in many CVD including atherosclerosis [10]. NAD(P)H oxidase is the major source of vascular reactive oxygen species (ROS) and is expressed in endothelial cells, vascular smooth muscle cells (VSMCs), fibroblasts, and monocyte/macrophages [11]. Extent data strongly support the hypothesis that oxidative stress, induced via activation of NAD(P)H oxidase, plays a causative role in atherosclerosis [12, 13]. ROS are able to regulate cellular growth (hyperplastic or hypertrophic), endothelial dysfunction, cell migration, and inflammation [14]. ROS also induce the expression of matrix-degrading enzymes such as matrix metalloproteinases (MMPs) which are involved in vascular remodeling and are postulated to participate in the pathogenesis of atherosclerosis [15]. We aimed to study the association of fructose intake-induced insulin resistance with the development of atherosclerotic plaque in ApoE-KO mice, an experimental model of cardiovascular complications related to MS, and the relationship between metabolic parameters, vascular inflammation, and oxidative stress.

2. Methods

2.1. Animals and Diets. All animals were cared in accordance with the *Guiding Principles in the Care and Use of Animals* of the US National Institutes of Health. All procedures were approved by the Animal Research Committee of the Universidad Nacional de Cuyo (protocol approval no. 10089 CICUAL/2009). Male C57/BL6J wild type and ApoE-KO mice 8 weeks of age (20 to 22 g; The Jackson Laboratories, Bar Harbor, ME) were used for this study. The animals were maintained in a 22°C room with a 12 hour light/dark cycle and received drinking water *ad libitum* and were fed a standard commercial chow diet (GEPSA, Argentina). During 8 weeks, animals from each genotype were randomly divided into two groups: control mice ($n = 10$), with free access to tap water; fructose-fed (HF) mice ($n = 10$) receiving 10% (w/v) fructose (Parafarm, Argentina) in their drinking water. Additional group of age-matched ApoE-KO mice were given a control diet or HF during 4 weeks and then were randomized to no treatment, Tempol (Sigma Aldrich, St. Louis, MO, USA; 1 mg/kg of body weight per day), or losartan (Roemmers, Argentina, 10 mg/kg of body weight per day), during 4 more weeks.

2.2. Biochemical Determinations. After overnight fasting blood samples for glucose, insulin, triglycerides, and cholesterol determinations were taken from mice, collected from cardiac puncture under anesthesia at the end of the experimental period. The plasma glucose, cholesterol, and triglyceride concentrations were determined using commercial kits by enzymatic colorimetric methods (GT Lab, BuenosAires, Argentina). Insulin was measured by ELISA (Crystal Chem, USA).

2.3. Histomorphometric Studies. Mice were euthanized by cervical dislocation and were perfused *in situ* with chilled phosphate-buffered saline. The proximal aorta and the mesenteric artery tree were fixed with 2% paraformaldehyde, paraffin embedded, and mounted in a Micron microtome. Consecutive sections (5 μm thickness) were taken from 2 to 3 regions of the aortic arch separated by ~60 μm and from the mesenteric vascular tree. Three cross-sections from each region were stained with hematoxylin/eosin or with Masson's trichrome solution and examined the diameters of the wall and the lumen, displayed in 20X optical microscope and digitized images with the software Image Pro. The linear relationship of superficial lumen/media was calculated for each vessel with the Scion Image software.

2.4. Quantification of Atherosclerotic Plaques. Plaque area was quantified by Oil-red-O staining of lipid deposits. Aortas and whole right carotid arteries were incubated for 45 min with Oil red O (0.5% in 60% isopropyl alcohol). Excess stain was removed with 60% isopropyl alcohol. Quantification of atherosclerosis was performed in the aortic arch region up to the descending abdominal aorta and on the bifurcation of the right common carotid arteries by computer-assisted image analysis as previously described in detail [16]. Subsequently images of en face preparations of the whole mounted aorta and the carotid arteries were taken and the percentage of plaques in relation to the entire aortic surface was calculated as plaque score in percent of total area using ImageJ 1.37 v software (NIH).

In another group of animals the whole aorta and right carotid arteries were dissected from mice, perfusion fixed in situ with 2% paraformaldehyde, paraffin embedded, and mounted in a microtome. Atherosclerotic lesion size in cross-sections of the aortic sinus was quantified as the area occupied by hematoxylin/eosin staining.

2.5. Determination of Vascular Markers of Inflammation. Paraformaldehyde-fixed sections of aorta or mesenteric arteries were incubated with murine monoclonal antibody against VCAM-1(1 : 500; BD) or rabbit polyclonal antibody against MMP-9 (1 : 200; Santa Cruz), overnight at 4°C, followed by 1 h incubation with FITC or Alexa red conjugated secondary antibody, respectively. Sections were mounted and visualized using fluorescence microscopy. Total area of antigen-specific fluorescence staining per section was quantified using WCIF ImageJ imaging software. Positively stained areas were selected and measured using program-specific tools. Two replicate measurements were averaged for each tissue type per mouse ($n = 4$–6) to obtain data for statistical analysis. MMP-9 expression was also determined by Western Blot analysis. Aortic tissues were homogenized in 100 μL lysis buffer supplemented with protease inhibitors (Complete Mini; 1 tablet/1.5 mL; Roche Diagnostics, Mannheim, Germany). Samples were run on 12.5% Tris-HCl gels with Tris/glycine/SDS buffer and the proteins detected; after transfer to PDVF membranes, using rabbit-anti MMP-9 antibody (1 : 500; Santa Cruz Biotechnology, Santa Cruz, CA) and HRP-conjugated secondary

Table 1: Average plasma glucose, insulin, and lipid levels in WT and ApoE-KO mice fed with control diet or high fructose diet.

	Glucose (mg/dL)	Insulin(ng/mL)	Cholesterol (mg/dL)	Triglycerides (mg/dL)
WT-control diet	161.2 ± 0.6	nd	71.41 ± 1.5	91 ± 1.2
WT-fructose fed	142.7 ± 5.4	nd	130.35 ± 6.3$^\sharp$	83.8 ± 0.7
ApoE-control diet	143.4 ± 25.9	0.85 ± 0.03	391.6 ± 6.0	114.10 ± 3.5
ApoE-fructose fed	216.2 ± 22.2*	1.27 ± 0.19*	382.0 ± 34.5	190.2 ± 18.2*

Values are the mean ± SD ($n = 12$)$^\sharp P < 0.05$ versus WT control diet, $^* P < 0.001$ versus ApoE control diet.

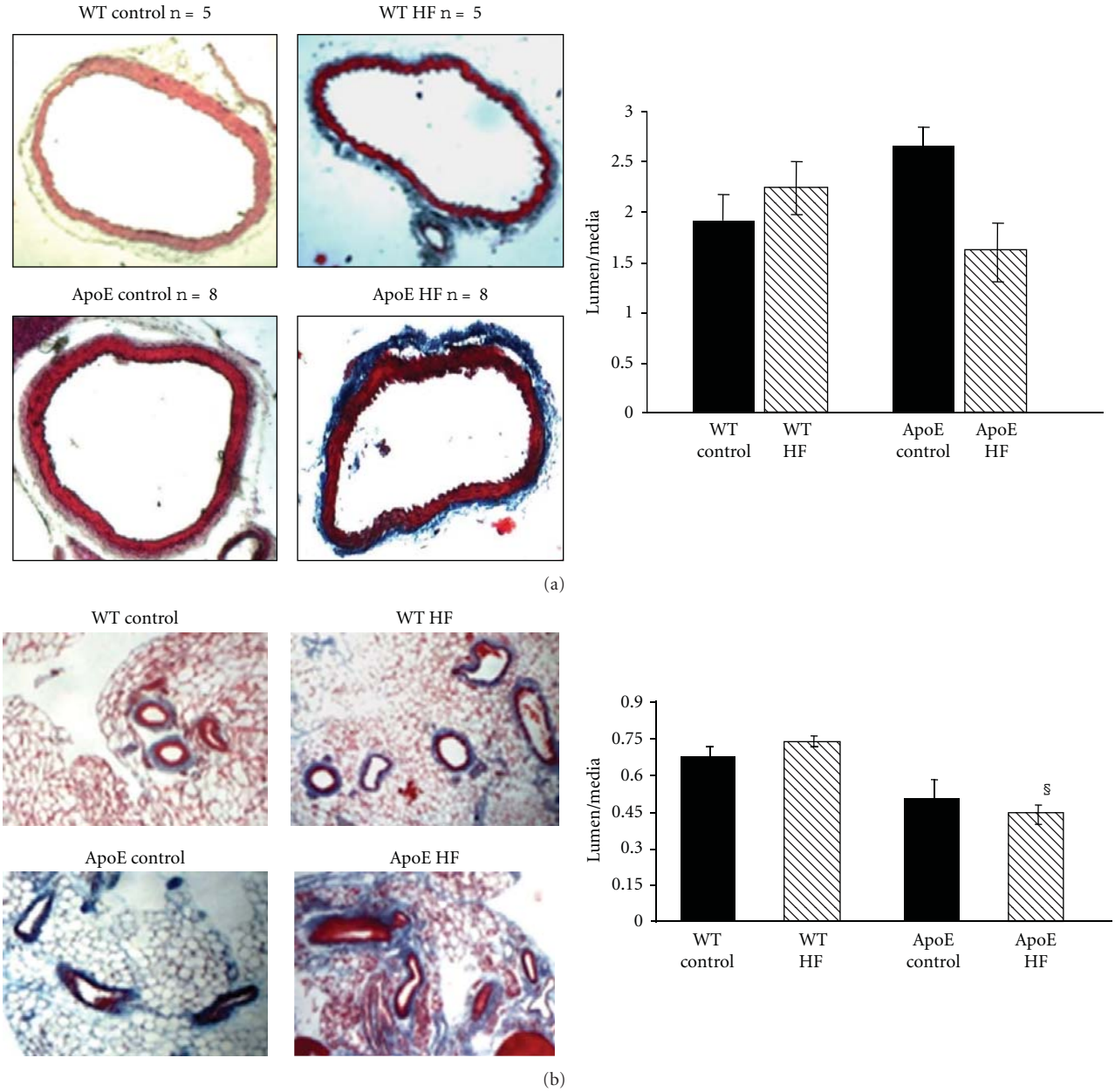

Figure 1: Morphometric analysis of the middle layer of aorta (a) and mesenteric arteries (b) from WT and ApoE-KO mice fed regular chow (Control diet) or high fructose diet (HF). ApoE-KO mice display a decreased lumen/media ratio in vessels walls from fructose-fed ApoE-KO mice. Results are expressed as means ($n = 8$) ± S.E.M $^{**}P < 0.001$ versus ApoE control in aortic rings; $^* P < 0.05$ versus WT, $^{\S}P < 0.05$ versus ApoE control in mesenteric arteries rings.

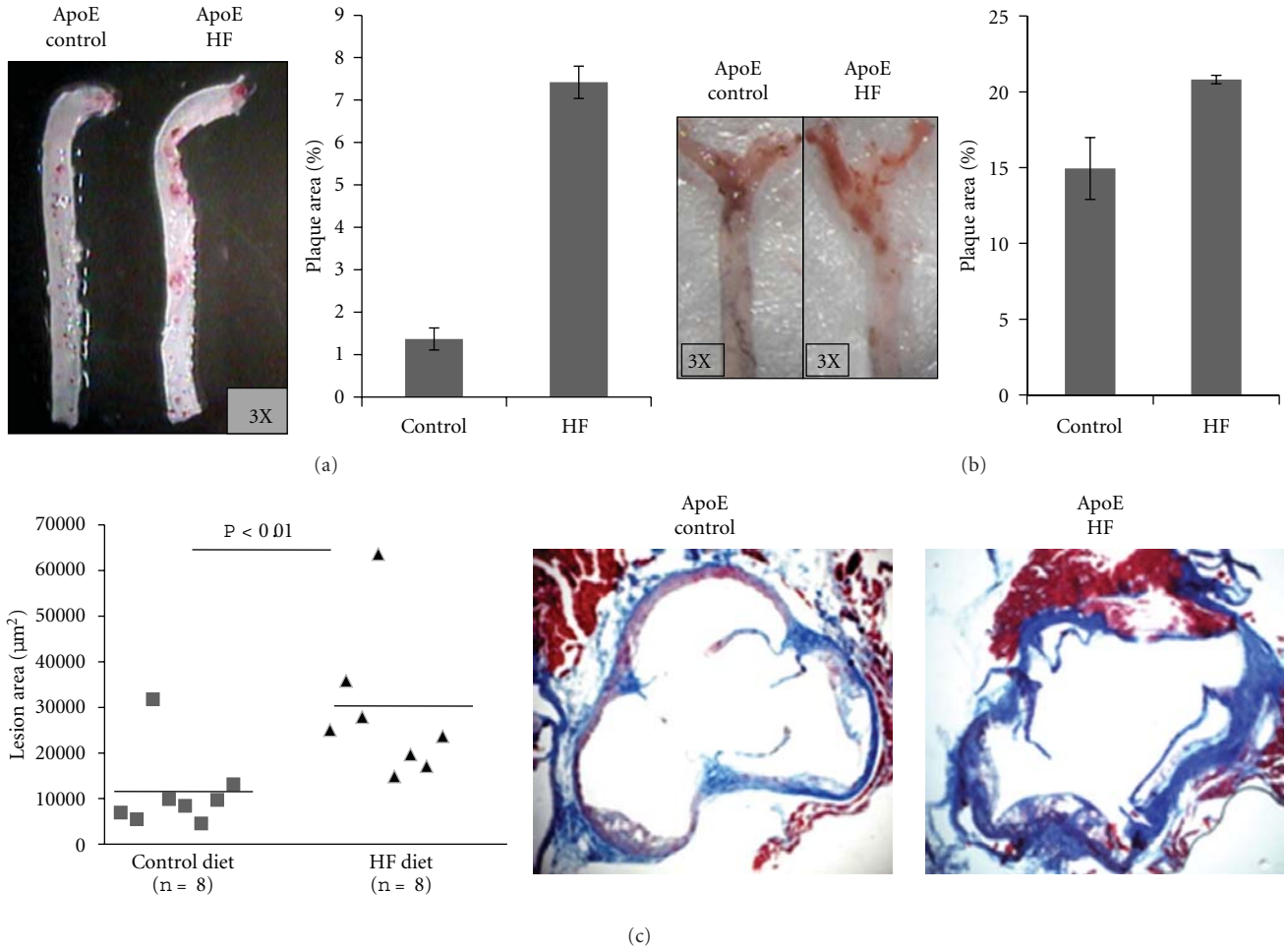

Figure 2: High fructose intake enhances atheroma development. (a) Representative of whole aorta artery and (b) representative of right carotid artery staining with Oil-red O. Extent of atherosclerosis quantified as percent of plaque area in ApoE-KO mice fed control diet and HF diet. (c) Cross-sections from the aortic sinus were stained with hematoxylin and eosin to quantify the lesion area. Results are expressed as means ($n = 8$) ± S.E.M $^{*}P < 0.05$; $^{**}P < 0.01$ versus control diet.

antibody (1 : 10.000 Jackson laboratory, US) for 1 h, proteins were visualized by performing luminal-enhanced chemiluminescence. Loading of equal amounts of proteins was confirmed by reproving the membrane with an antibody against tubulin antibody (1 : 100; Santa Cruz Biotechnology, Santa Cruz, CA) and secondary HRP-conjugated antibody (1 : 10.000 Jackson laboratory, US).

2.6. Detection of Tissue NAD(P)H Oxidase Activity. The NAD(P)H-driven superoxide production, an estimate of NAD(P)H oxidase activity, was measured in freshly dissected aorta using lucigenin-enhanced chemiluminescence. Longitudinally cut aortas were transferred to 96-well optiplates (Packard, USA) containing 50 mM phosphate buffer, 150 mM sucrose, 100 μM NAD(P)H, and 5 μM lucigenin (N,N′-dimethyl-9-9′-biacridianium, Sigma Aldrich, St. Louis, MO, USA). Luminescence generated by the reaction of tissue-derived superoxide and lucigenin was counted at 20°C with a microplate scintillation counter (Fluoroskan Ascent, Thermo) running in kinetic mode with a 1 min interval for each sample. Luminescence measurements were obtained every 15 s for 25 minutes. Basal chemiluminescence was measured in the tissue placed in the 96-well optiplate (dark-adapted) with phosphate-sucrose buffer and 5 μM lucigenin before 100 μM NAD(P)H addition and subtracted from NAD(P)H-stimulated luminescence. Dried tissues were weighed for calculation of normalized superoxide production expressed as counts per minute and per milligram of dry tissue.

2.7. Statistical Analysis. Results are reported as mean ± S.E.M. Significance was determined by nonparametric analysis using Mann-Whitney U test to detect a statistical difference between group of interest and its control. Analyses involving more than two groups were done by ANOVA and Bonferroni's post hoc test using Prism-4 software. Differences were considered significant at $P < 0.05$.

3. Results

3.1. Effects of High Fructose Diet on Biochemical Parameters. Fructose intake slightly increased cholesterol levels in WT

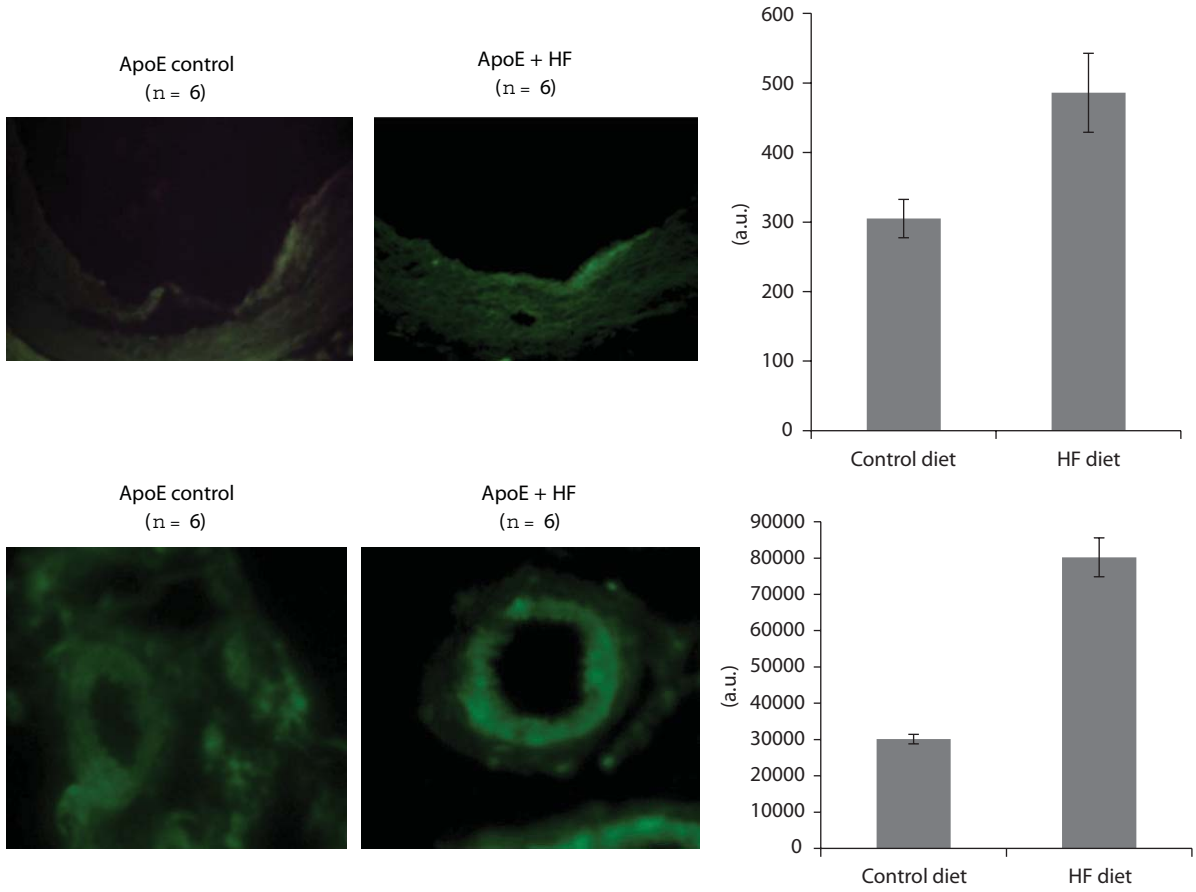

Figure 3: Immunofluorescence detection of VCAM-1 expression (green) in aorta and mesenteric arteries of ApoE KO mice fed control diet or fructose-rich diet (HF). Quantification of the fluorescent signal was performed by ImageJ software. Results are expressed as means ± S.E.M $^{*}P < 0.05$; $^{**}P < 0.01$ versus control diet.

mice compared to WT in a control diet, without changing any of the others variables measured. In ApoE-KO mice 8 weeks of 10% fructose feeding in drinking water significantly increased the concentration of plasma glucose, insulin, and triglycerides, compared to ApoE-KO mice in control diet, with no changes in cholesterol levels (Table 1).

3.2. Effects of High Fructose Diet on Vascular Remodeling. We determined the structural changes in the arterial wall by histological analysis of aorta and the mesenteric arteries. In ApoE-KO mice fed with fructose, thickness of the middle layer of both aorta (Figure 1(a)) and mesenteric arteries (Figure 1(b)) significantly increased compared to ApoE-KO mice in a control diet, producing a lower ratio of lumen/media in the vessels of fructose-fed ApoE-KO mice.

3.3. High Fructose Diet Enhances Atherosclerosis. We determined the effects of fructose feeding on the development of atherosclerosis in arteries from ApoE-KO mice. We quantified the area of atheroma plaque by computerized morphometry using two independent approaches: (1) *en face* Oil red O-stained mouse aortas and right carotid arteries and (2) quantification of the lesion area in aortic sinus cross-sections. Fructose-treated mice displayed a significant induction in the area of Oil Red O-stained atherosclerotic plaques in both aorta and right carotid arteries (Figures 2(a) and 2(b), resp.), as compared with untreated mice. HF diet increased the lesion area in the aortic sinus in ApoE-KO mice (Figure 2(c)).

3.4. Effect of Fructose on Vascular Inflammation. Vascular adhesion molecule (VCAM-1) is a hallmark of vascular inflammation. Immunofluorescence detection revealed a markedly increased VCAM-1 expression in aorta, especially on the endothelium, and within the vascular wall in mesenteric arteries from ApoE-KO mice fed with HF diet (Figure 3).

We also evaluated the expression of metalloproteinase 9 (MMP-9), another vascular inflammatory marker involved in remodeling. MMP-9 expression, examined by immunohistochemistry and western blot, clearly increased in fructose-fed ApoE-KO aorta tissue (Figure 4).

3.5. Effect of Fructose on NAD(P)H Oxidase Activity. NAD(P)H oxidase contributes to basal vascular superoxide production. HF diet increased significantly the NAD(P)H

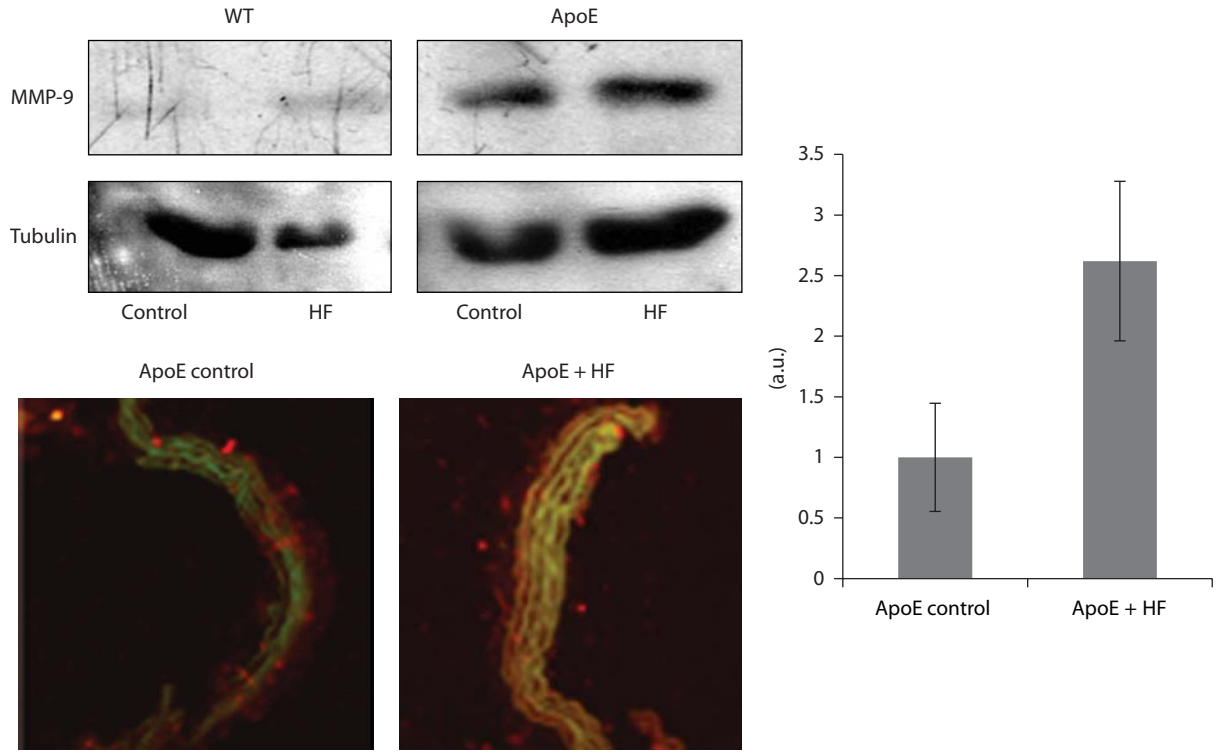

Figure 4: Expression of MMP-9 in aorta from ApoE KO and WT mice fed control diet or fructose-rich diet (HF) determined by Western Blot and immunoflorescence detection. Quantification of the fluorescent signal was performed by ImageJ software. Results are expressed as means ± S.E.M $^{*}P < 0.05$ versus control diet. (MMP-9: red; Actin: green).

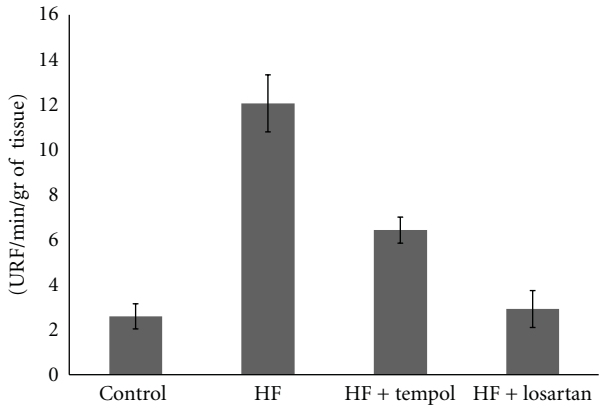

Figure 5: NAD(P)H oxidase activity (relative light units: RLU/mg dry tissue) in aorta of mice fed with control diet ($n = 8$) and mice fed with HF diet ($n = 8$) alone or with Tempol ($n = 8$) or losartan ($n = 8$). Results are expressed as means ± S.E.M. $P < 0.001$ versus control.

oxidase activity, suggesting the involvement of oxidative stress in this model. Four-week treatment with Tempol, a membrane permeable superoxide dismutase mimetic, or with losartan, an Angiotensin-II receptor 1 (AT1) antagonist, significantly reduced vascular NAD(P)H oxidase activity in aortas from ApoE KO mice in a HF diet (Figure 5).

4. Discussion

Most of the studies that utilize fructose intake to develop an experimental model of MS use rat, an animal model that is resistant to develop atheroma plaques and is not suitable for studying inflammatory pathways implicated in the development of atherosclerosis [17]. In this study we induce a MS, characterized by hyperglycemia, hypertriglyceridemia, and hyperinsulinemia in ApoE-deficient mice, an atherogenic-prone animal model, to investigate the effect of insulin resistance induced by fructose feeding on vascular remodeling, vascular inflammation, oxidative stress, and atheroma development. We first noticed that high-fructose diet promoted vascular remodeling, which is involved in the pathogenesis of atherosclerosis. Due to the hemodynamic, histological, and biological particularities in large and small vessels, it is of great interest to investigate structural changes in our model. Turnover of extracellular matrix components and cell migration causes structural changes in the vessel wall with either outward (adventitial/media) or inward (lumenal) protrusion. It is postulated that outgrowth remodeling occurred also in mesenteric artery [18], so we measured the medial thickness of both large and small arteries. We demonstrated that in fructose-fed ApoE-KO mice, the media cross-section area from aortas and mesenteric arteries were significantly increased while lumen diameter was normal. This remodeling format is similar to that found in fructose-fed rats by Puyo et al. [19].

One important feature we found was that fructose-rich diet promotes a proatherogenic state in ApoE-KO mice, independently of hypercholesterolemia, leading to accelerate aortic and carotid atheroma development. It has been demonstrated the involvement of inflammation in vascular remodeling and atherogenesis, with the expression of VCAM-1 in the vascular wall [17, 20]. Here we observed that intimal VCAM-1 expression in small and large caliber arteries was significantly increased in fructose-treated ApoE KO mice compared with control chow mice.

Different components of the MS have been identified as possible stimulus for the synthesis and activity of MMPs. Diverse MMPs have been identified in atherosclerotic plaques and in regions of foam cell accumulation and have been directly associated with plaque remodeling [21] as well as plaque vulnerability [22]. In our study we found that high fructose diet enhanced expression of MMP-9, a gelatinase enzyme, in atheroma-free area of the vessels during early stages of atherosclerosis development.

Oxidative stress and inflammation processes are key components of atherosclerosis, from fatty streak formation to plaque rupture and thrombosis [23, 24]. Diets rich in fructose can alter cellular metabolism via several pathways, thereby accelerating oxidative stress. Fructose feeding results in the activation of the renin-angiotensin system [25], and it is well established that angiotensin II is associated with oxidative stress [26]. This oxidative stress is characterized by overproduction of ROS and is dependent on the activation of NAD(P)H oxidase. We found that fructose-rich diet increased NAD(P)H oxidase activity in ApoE-KO mice, and this enhancement is diminished by Tempol, a superoxide dismutase mimetic, and by losartan, an Angiotensin-II receptor 1 (AT1) inhibitor, corroborating the role of superoxide generation in fructose-induced insulin resistance and suggesting the involvement of the renin-angiotensin system in the enhanced oxidative stress in our model.

Our results show that insulin resistance associated with MS promotes the initial stages of a proinflammatory and a prooxidant state. These changes potentially contribute to enhancing vascular remodeling and atheroma plaque development and placing the insulin resistance as a potent atherogenic risk factor.

Abbreviations

ApoE-KO:	ApoE-deficient mice
NAD(P)H:	Nicotinamide adenine dinucleotide phosphate
ROS:	Reactive oxygen species
VCAM-1:	Vascular cell adhesion molecule-1
MMPs:	Matrix metalloproteases.

Acknowledgments

This work was supported by Grant 06/J246 (to M. Cruzado), 2007–2009 from Secretaría de Ciencia y Técnica, Universidad Nacional de Cuyo. B. cannizzo is a recipient of a doctoral fellowship from CONICET, and C. Lembo is a recipient of a doctoral fellowship from National Agency of Scientific and Technological Promotion. The authors gratefully acknowledge the technical assistance of Mrs. Miriam García and Miss. Analía Redondo.

References

[1] A. Z. Fan, "Metabolic syndrome and progression of atherosclerosis among middle-aged US adults," *Journal of Atherosclerosis and Thrombosis*, vol. 13, no. 1, pp. 46–54, 2006.

[2] E. A. Schwartz and P. D. Reaven, "Molecular and signaling mechanisms of atherosclerosis in insulin resistance," *Endocrinology and Metabolism Clinics of North America*, vol. 35, no. 3, pp. 525–549, 2006.

[3] G. M. Reaven, "Insulin resistance/compensatory hyperinsulinemia, essential hypertension, and cardiovascular disease," *Journal of Clinical Endocrinology and Metabolism*, vol. 88, no. 6, pp. 2399–2403, 2003.

[4] R. Miatello, M. Cruzado, and N. Risler, "Mechanisms of cardiovascular changes in an experimental model of syndrome X and pharmacological intervention on the renin-angiotensin-system," *Current Vascular Pharmacology*, vol. 2, no. 4, pp. 371–377, 2004.

[5] S. Kiechl and J. Willeit, "The natural course of atherosclerosis—part II: vascular remodeling," *Arteriosclerosis, Thrombosis, and Vascular Biology*, vol. 19, no. 6, pp. 1491–1498, 1999.

[6] S. Delbosc, E. Paizanis, R. Magous et al., "Involvement of oxidative stress and NADPH oxidase activation in the development of cardiovascular complications in a model of insulin resistance, the fructose-fed rat," *Atherosclerosis*, vol. 179, no. 1, pp. 43–49, 2005.

[7] K. Peter, U. Weirich, T. K. Nordt, J. Ruef, and C. Bode, "Soluble vascular cell adhesion molecule-1 (VCAM-1) as potential marker of atherosclerosis," *Thrombosis and Haemostasis*, vol. 82, suppl. 1, pp. 38–43, 1999.

[8] Y. Nakashima, E. W. Raines, A. S. Plump, J. L. Breslow, and R. Ross, "Upregulation of VCAM-1 and ICAM-1 at atherosclerosis-prone sites on the endothelium in the ApoE-deficient mouse," *Arteriosclerosis, Thrombosis, and Vascular Biology*, vol. 18, no. 5, pp. 842–851, 1998.

[9] T. L. Deem and J. M. Cook-Mills, "Vascular cell adhesion molecule 1 (VCAM-1) activation of endothelial cell matrix metalloproteinases: role of reactive oxygen species," *Blood*, vol. 104, no. 8, pp. 2385–2393, 2004.

[10] I. M. Fearon and S. P. Faux, "Oxidative stress and cardiovascular disease: novel tools give (free) radical insight," *Journal of Molecular and Cellular Cardiology*, vol. 47, no. 5, pp. 372–381, 2009.

[11] K. K. Griendling, D. Sorescu, B. Lassègue, and M. Ushio-Fukai, "Modulation of protein kinase activity and gene expression by reactive oxygen species and their role in vascular physiology and pathophysiology," *Arteriosclerosis, Thrombosis, and Vascular Biology*, vol. 20, no. 10, pp. 2175–2183, 2000.

[12] G. Muller and H. Morawietz, "Nitric oxide, NAD(P)H oxidase, and atherosclerosis," *Antioxidants and Redox Signaling*, vol. 11, no. 7, pp. 1711–1731, 2009.

[13] B. Collin, D. Busseuil, M. Zeller et al., "Increased superoxide anion production is associated with early atherosclerosis and cardiovascular dysfunctions in a rabbit model," *Molecular and Cellular Biochemistry*, vol. 294, no. 1-2, pp. 225–235, 2007.

[14] D. Sorescu, K. Szocs, and K. K. Griendling, "NAD(P)H oxidases and their relevance to atherosclerosis," *Trends in Cardiovascular Medicine*, vol. 11, no. 3-4, pp. 124–131, 2001.

[15] M. H. Shin, Y. J. Moon, J. E. Seo, Y. Lee, K. H. Kim, and J. H. Chung, "Reactive oxygen species produced by NADPH oxidase, xanthine oxidase, and mitochondrial electron transport system mediate heat shock-induced MMP-1 and MMP-9 expression," *Free Radical Biology and Medicine*, vol. 44, no. 4, pp. 635–645, 2008.

[16] C. Castro, J. M. Campistol, D. Sancho, F. Sanchez-Madrid, E. Casals, and V. Andres, "Rapamycin attenuates atherosclerosis induced by dietary cholesterol in apolipoprotein-deficient mice through a p27Kip1-independent pathway," *Atherosclerosis*, vol. 172, no. 1, pp. 31–38, 2004.

[17] A. Soliman and P. Kee, "Experimental models investigating the inflammatory basis of atherosclerosis," *Current Atherosclerosis Reports*, vol. 10, no. 3, pp. 260–271, 2008.

[18] S. Schnee, K. Sass, H. Moellmer, R. Hohenfellner, and K. Spanel-Borowski, "Heterogeneity of atherosclerosis in mesenteric arteries and outgrowth remodeling," *Cardiovascular Pathology*, vol. 19, no. 6, pp. e195–e203, 2010.

[19] A. M. Puyo, M. A. Mayer, S. Cavallero, A. S. Donoso, and H. A. Peredo, "Fructose overload modifies vascular morphology and prostaglandin production in rats," *Autonomic and Autacoid Pharmacology*, vol. 24, no. 2, pp. 29–35, 2004.

[20] E. Galkina and K. Ley, "Vascular adhesion molecules in atherosclerosis," *Arteriosclerosis, Thrombosis, and Vascular Biology*, vol. 27, pp. 2292–2301, 2007.

[21] D. Wagsater, C. Zhu, J. Bjorkegren, J. Skogsberg, and P. Eriksson, "MMP-2 and MMP-9 are prominent matrix metalloproteinases during atherosclerosis development in the Ldlr(-/-Apob)(100/100) mouse," *International Journal of Molecular Medicine*, vol. 28, no. 2, pp. 247–253, 2011.

[22] G. Berg, V. Miksztowicz, and L. Schreier, "Metalloproteinases in metabolic syndrome," *Clinica Chimica Acta*, vol. 412, no. 11, pp. 1731–1739, 2011.

[23] K. K. Koh, P. C. Oh, and M. J. Quon, "Does reversal of oxidative stress and inflammation provide vascular protection?" *Cardiovascular Research*, vol. 81, no. 4, pp. 649–659, 2009.

[24] J. A. Piedrahita, S. H. Zhang, J. R. Hagaman, P. M. Oliver, and N. Maeda, "Generation of mice carrying a mutant apolipoprotein E gene inactivated by gene targeting in embryonic stem cells," *Proceedings of the National Academy of Sciences of the United States of America*, vol. 89, no. 10, pp. 4471–4475, 1992.

[25] S. Ishibashi, "The vascular renin-angiotensin system as a possible source of vascular inflammation in fructose-fed rats," *Hypertension Research*, vol. 30, no. 5, pp. 375–376, 2007.

[26] K. Shinozaki, K. Ayajiki, Y. Nishio, T. Sugaya, A. Kashiwagi, and T. Okamura, "Evidence for a causal role of the renin-angiotensin system in vascular dysfunction associated with insulin resistance," *Hypertension*, vol. 43, pp. 255–262, 2004.

Hindawi Publishing Corporation
Experimental Diabetes Research
Volume 2012, Article ID 653678, 6 pages
doi:10.1155/2012/653678

Research Article

Oxidative/Nitrosative Stress and Protein Damages in Aqueous Humor of Hyperglycemic Rabbits: Effects of Two Oral Antidiabetics, Pioglitazone and Repaglinide

Anna Gumieniczek, Beata Owczarek, and Bernadeta Pawlikowska

Department of Medicinal Chemistry, Medical University of Lublin, Jaczewskiego 4, 20-090 Lublin, Poland

Correspondence should be addressed to Anna Gumieniczek, anna.gumieniczek@umlub.pl

Received 14 October 2011; Revised 28 December 2011; Accepted 29 December 2011

Academic Editor: Pietro Galassetti

The present study was undertaken to determine oxidative/nitrosative stress in aqueous humor of alloxan-induced hyperglycemic rabbits and to investigate the effects of two oral antidiabetic drugs, pioglitazone from peroxisome proliferator-activated receptor gamma (PPARγ) agonists and repaglinide from nonsulfonylurea K_{ATP} channel blockers. Ascorbic acid (AA), glutathione (GSH), total antioxidant status (TAS), lipid peroxidation products (LPO), total nitrites (NO_2), advanced oxidized protein products (AOPP), and protein carbonyl groups (PCG) were determined using respective colorimetric and ELISA methods. In our hyperglycemic animals, AA decreased by 77%, GSH by 45%, and TAS by 66% as compared to control animals. Simultaneously, LPO increased by 78%, PCG by 60%, AOPP by 84%, and NO_2 by 70%. In pioglitazone-treated animals, AA and TAS increased above control values while GSH and PCG were normalized. In turn, LPO was reduced by 54%, AOPP by 84%, and NO_2 by 24%, in relation to hyperglycemic rabbits. With repaglinide, AA and TAS were normalized, GSH increased by 20%, while LPO decreased by 45%. Our results show that pioglitazone and repaglinide differ significantly in their ability to ameliorate the parameters like NO_2, PCG, and AOPP. In this area, the multimodal action of pioglitazone as PPARγ agonist is probably essential.

1. Introduction

The eye is a unique organ since it is constantly exposed to radiation, atmospheric oxygen, environmental chemicals, and physical abrasion. In consequence, the eye provides a unique situation for generation of reactive oxygen species (ROS). In particular, oxidative stress is implicated in the etiology of many ocular diseases such as glaucoma, retinal degeneration, ocular inflammation, cataracts, and diabetic complications [1–3]. Also nitrogen reactive species (RNS) play an important role in different oxidative alterations [4, 5]. Nitric oxide (NO) is an important messenger in vascular and nervous systems or in immunological reactions including these in the eye. On the other hand, NO formed in excess by inducible NO synthase (iNOS) may cause serious ocular injuries [6].

Ocular tissues and fluids contain antioxidants that play a key role in protecting them against these oxidative/nitrosative damages. Aqueous and vitreous humors as well as lens contain high amounts of ascorbic acid (AA). It is generally accepted that it offers significant protection for the eye by suppressing generation of free radicals [7]. Also ocular glutathione (GSH) participates in neutralization of reactive species and maintains other antioxidants in their active forms. Unfortunately, these antioxidants are not able to eliminate free radicals completely and if oxidative stress is severe, it may cause cell damage or death [3].

Protein carbonyls groups (PCG), markers of early protein oxidation, and advanced oxidized protein products (AOPP) have been recently described as closely related to different pathological situations [8–10]. Some findings also suggest

that the changes in proteins may be important in development of ocular diabetic complications [11].

Therefore, the present study was undertaken to determine several markers of oxidative/nitrosative stress in aqueous humor of alloxan-induced hyperglycemic rabbits where such experiments have not been performed previously. We wanted to explore potent relationship between some commonly studied parameters of oxidative alterations: AA, GSH, total antioxidant status (TAS), lipid peroxidation products (LPO), total nitrites (NO_2), and two markers of oxidative protein modification, PCG and AOPP, and search for this which showed more expressive correlations.

It is known that structures through which aqueous humor leaves the anterior chamber may be a target of pharmacological manipulations. Thus, reducing ROS/RNS overproduction and its consequences may be an effective strategy for protection against severe ocular injuries [11, 12]. Therefore, the second goal of the present study was to investigate which of two oral antidiabetic drugs, a peroxisome proliferator-activated receptor gamma (PPARγ) agonist pioglitazone or a nonsulfonylurea K_{ATP} channel blocker repaglinide could be more effective in ameliorating these oxidative/nitrosative changes. Pioglitazone belonging chemically to 2,4-thiazolidinediones family (TZDs) acts in diabetes mainly by decreasing insulin resistance at the level of the muscle and liver. It has been shown to be potent antioxidant in different pathological situations connected with oxidative/nitrosative stress including diabetes [13, 14]. Repaglinide, from nonsulfonylurea K_{ATP} channel blockers, is a carbamoyl methyl benzoic acid derivative with the effect on early insulin secretion and reducing postprandial glucose directly [15]. Additionally, some results from the literature have previously demonstrated that it may have positive effects on parameters of oxidative/nitrosative stress [16, 17].

2. Material and Methods

2.1. Animals and Chemicals. White male New Zealand rabbits (the mean weight 3.1 kg) were housed in a controlled environment with 12 h light and dark cycles. They were provided with standard diet and water *ad libitum*. Animal care was in accordance with the "Principles of Laboratory Animal Care" (NIH publication No. 86-23, revised 1985) and with the Guidelines of Medical University of Lublin Animal Ethics Committee. The rabbits were divided into six groups of 5 animals: normal control (Group C), control treated with pioglitazone (Group CP), control treated with repaglinide (Group CR), hyperglycemic (Group H), hyperglycemic treated with pioglitazone (Group HP), and hyperglycemic treated with repaglinide (Group HR). Hyperglycemia was induced by a single intravenous injection of 80 mg/kg of alloxan. Two weeks after the injection when hyperglycemia was verified by blood glucose concentration higher than 11 mmol/L, administration of pioglitazone at a dose of 1 mg/kg and repaglinide at a dose of 0.3 mg/kg was started and continued for 4 weeks (the start of experiment). The drugs were given directly to oral cavity using a syringe without a needle, every day before the morning feeding. During experiment, glucose concentration was monitored once a week. At the end of experiment, the animals were sacrificed with pentobarbital sodium at a dose of 60 mg/kg. The aqueous humor was collected by a 26-G needle attached to a tuberculin syringe with special care to avoid blood contamination. The needle was introduced into anterior chamber and ca. 100 μL aqueous humor was withdrawn. The samples were stored at -70°C until analysis.

TAS was assessed using a commercially available test from Randox Laboratories Ltd. (UK) while AA estimation was performed according to Kyaw [18]. GSH and LPO were determined using Bioxytech GSH-400 and LPO-586 kits from Oxis Research (USA). The stable metabolites of NO were estimated using a Nitrate/Nitrite Assay Kit from Fluka Chemicals (UK). Nitrates were reduced to nitrites by incubation of each sample for 120 min in the presence of nitrate reductase and NADPH. Then, total nitrites were assayed by adding of Griess reagent and measuring the absorbance at 540 nm. PCG and AOPP levels were determined using respective ELISA or colorimetric kits from Immundiagnostik AG (Germany). Protein content was determined by the method of Lowry et al. [19] using bovine serum albumin as standard.

Two spectrophotometers, UV-Vis CE-6000 from CECIL Instruments (UK) and a Microplate Reader PowerWave XS from Bio-Tek Instruments Inc. (USA), were used.

2.2. Statistical Analysis. All numerical data are presented as the mean with respective standard error (SEM). The significance of differences was determined with Kruskal-Wallis and Mann-Whitney's U tests. Multiple regression and Spearman's rank coefficients were used to investigate the possible correlations between AOPP or PCG level and other parameters. Probability P less than 0.05 were considered significant. For all statistical evaluation, statistica software was used.

3. Results

In hyperglycemic animals, there were decreases of AA by 77%, GSH by 45%, and TAS by 66% as compared to control animals. Simultaneously, there were increases of LPO by 78%, PCG by 60%, AOPP by 84%, and NO_2 by 70%. Pioglitazone increased AA and TAS above control values and normalized GSH and PCG. In turn, LPO was reduced by 54%, AOPP by 84% and NO_2 by 24% in relation to hyperglycemic rabbits. With repaglinide treatment, AA and TAS were normalized while GSH increased by 20% and LPO decreased by 45% in relation to hyperglycemic rabbits. However, repaglinide did not affect the levels of PCG, AOPP, and NO_2 (Table 1).

Multiple regression analysis did not show significant correlations. However, some correlations were observed when respective pairs of parameters were taken into account. In hyperglycemic group, we observed a negative correlation between AOPP and GSH, and positive correlations in pairs AOPP-LPO and AOPP-NO_2 (Figures 1(a)–1(c)). In hyperglycemic pioglitazone-treated group, similar correlations were observed between AOPP and LPO, and AOPP and NO_2. In the case of PCG, correlations for both hyperglycemic

Table 1: Effects of pioglitazone and repaglinide on oxidative/nitrosative stress parameters in the aqueous humor of control and hyperglycemic rabbits.

	Group C	Group CP	Group CR	Group H	Group HP	Group HR
TAS (mmol/mL)	1.99 ± 0.10	1.96 ± 0.15	1.90 ± 0.15	0.67 ± 0.09[a]	2.37 ± 0.14[a,b]	1.56 ± 0.15[b]
AA (μg/mL)	12.90 ± 1.05	13.94 ± 0.93	10.03 ± 1.05	3.02 ± 0.38[a]	21.87 ± 1.18[a,b]	12.62 ± 1.36[b]
GSH (nmol/mL)	138.7 ± 4.49	144.2 ± 12.84	117.7 ± 3.32[a]	76.14 ± 6.56[a]	131.4 ± 5.86[b]	91.06 ± 8.17[a,b]
NO_2 (nmol/mL)	39.04 ± 2.84	43.67 ± 4.09	37.44 ± 2.5	113.4 ± 7.63[a]	102.0 ± 8.78[a]	142.5 ± 2.54[a]
LPO (nmol/mL)	0.57 ± 0.27	0.89 ± 0.25	0.68 ± 0.023	2.64 ± 0.14[a]	1.21 ± 0.11[a,b]	1.45 ± 0.17[a,b]
PCG (nmol/mg protein)	17.86 ± 1.36	16.98 ± 1.30	24.13 ± 1.63[a]	44.49 ± 2.15[a]	20.46 ± 2.96[b]	40.46 ± 3.57[a]
AOPP (nmol/mg protein)	2.53 ± 0.26	2.44 ± 0.26	2.76 ± 0.32	16.15 ± 2.24[a]	4.31 ± 0.18[a,b]	19.29 ± 0.88[a,b]

Values are mean ± SEM ($n = 5$). TAS: total antioxidant status, AA: ascorbic acid, GSH: glutathione, NO_2: total nitrites, PCG: protein carbonyls, AOPP: advanced oxidized protein products. C: control rabbits, CP: control rabbits treated with pioglitazone, CR: control rabbits treated with repaglinide, H: hyperglycemic rabbits, HP: hyperglycemic rabbits treated with pioglitazone, HR: hyperglycemic rabbits treated with repaglinide. [a]Significant at $P < 0.05$ versus Group C. [b]Significant at $P < 0.05$ versus Group H.

and hyperglycemic pioglitazone-treated animals were also significant, although respective r values were lower than these for AOPP (Figures 1(d) and 1(e)). Because repaglinide did not affect the altered protein oxidation, in this case respective correlations were not calculated.

4. Discussion

In the eye of diabetic subjects, the occurrence of oxidative stress was demonstrated as depletion of GSH, an important aqueous antioxidant [20]. Between others, GSH maintains the second major antioxidant AA in its active form [21]. Relation between these two antioxidants was confirmed in the present study where diminished levels of GSH and AA were stated in aqueous humor of our hyperglycemic animals. Some reports suggest that intracellular GSH level may be decreased by RNS derived from NO produced in excess by iNOS. As a consequence, production of nitrosoglutathione and formation of protein-mixed disulfides with glutathione have been reported [22]. Previously, excessive levels of NO were stated in vitreous fluid of patients with proliferative diabetic retinopathy [6]. It was also observed in the present study together with a decreased level of GSH. The altered antioxidant balance in aqueous humor of our hyperglycemic rabbits was additionally confirmed by a significant increase in lipid peroxidation. Previously, elevated concentrations of LPO were stated in vitreous fluid of diabetic db/db mice [23] and in aqueous fluid of glaucoma patients [20].

Under situation of oxidative stress, many attention is devoted to oxidative damages in proteins [24]. They may result, between others, from formation of different protein adducts. Early modifications often bring carbonyl groups to proteins and may be estimated as 2,4-dinitrophenylhydrazine derivatives or PCG [25]. Recently, a large interest lies on latter products of protein oxidation (AOPP) which are defined as dityrosine-containing cross-linked protein products [10, 26]. In aqueous humor of our hyperglycemic animals, the both markers, PCG and AOPP, were elevated in comparison with respective controls. Previously, similar changes were found in plasma of type 2 diabetic patients where higher increase in the level of AOPP compared with PCG was found. It was explained by lower susceptibility of AOPP cross-linked proteins to proteolysis and their subsequent accumulation in plasma [10]. In the present study, we additionally concluded that AOPP correlated better than PCG to other examined parameters (Figure 1).

In our study AA, TAS, GSH, and LPO were ameliorated by the two drugs, pioglitazone and repaglinide. However, only after pioglitazone, significant changes in NO_2, PCG, and AOPP were observed. It is known that AOPP are formed by action of chloraminated oxidants, mainly hypochlorous acid and chloramines, produced by myeloperoxidase (MPO) [26, 27]. On the other hand, it has been showed that pioglitazone inhibits proinflammatory factors including MPO. Therefore, its present effect on AOPP in aqueous humor of hyperglycemic animals may be, at least in part, a consequence of the above ability.

It is known that expression of many genes including proinflammatory cytokines, adhesion molecules, and others such as iNOS was regulated by a nuclear factor NF-κB. It is also supposed that beneficial effects of antioxidants against oxidative complications may involve effective inhibition of NF-κB [6]. Such mechanism for antioxidative and anti-inflammatory properties of PPARγ agonists, including pioglitazone, has been proposed [28–30]. Previous data about decreased levels of NO_2 and MPO after pioglitazone in lung and testis of our hyperglycemic animals confirm this [31, 32]. However, the exact mechanism whereby the drug exerts its antioxidant effect is still unclear. In this area, the multimodal action of PPARγ agonists is probably essential [33].

As far as concerning K_{ATP} channel blockers, it cannot be excluded that they may affect oxidative/nitrosative stress. After repaglinide, total serum antioxidant capacity [17] and lipid peroxidation were ameliorated [15, 16]. After another drug mitiglinide, significant decreases of lipid peroxidation and nitrotyrosine were also observed [34]. However, all these effects occurred in type 2 diabetes where they could be probable by better controlling postprandial hyperglycemia and thus by the cluster of oxidative stress. Additionally, it has been stated that insulin *per se* reduces the level of NF-κB. Because NF-κB regulates the expression of enzymes involved in ROS/RNS generation, in this way, insulin can modulate the mechanisms involved in oxidative/nitrosative

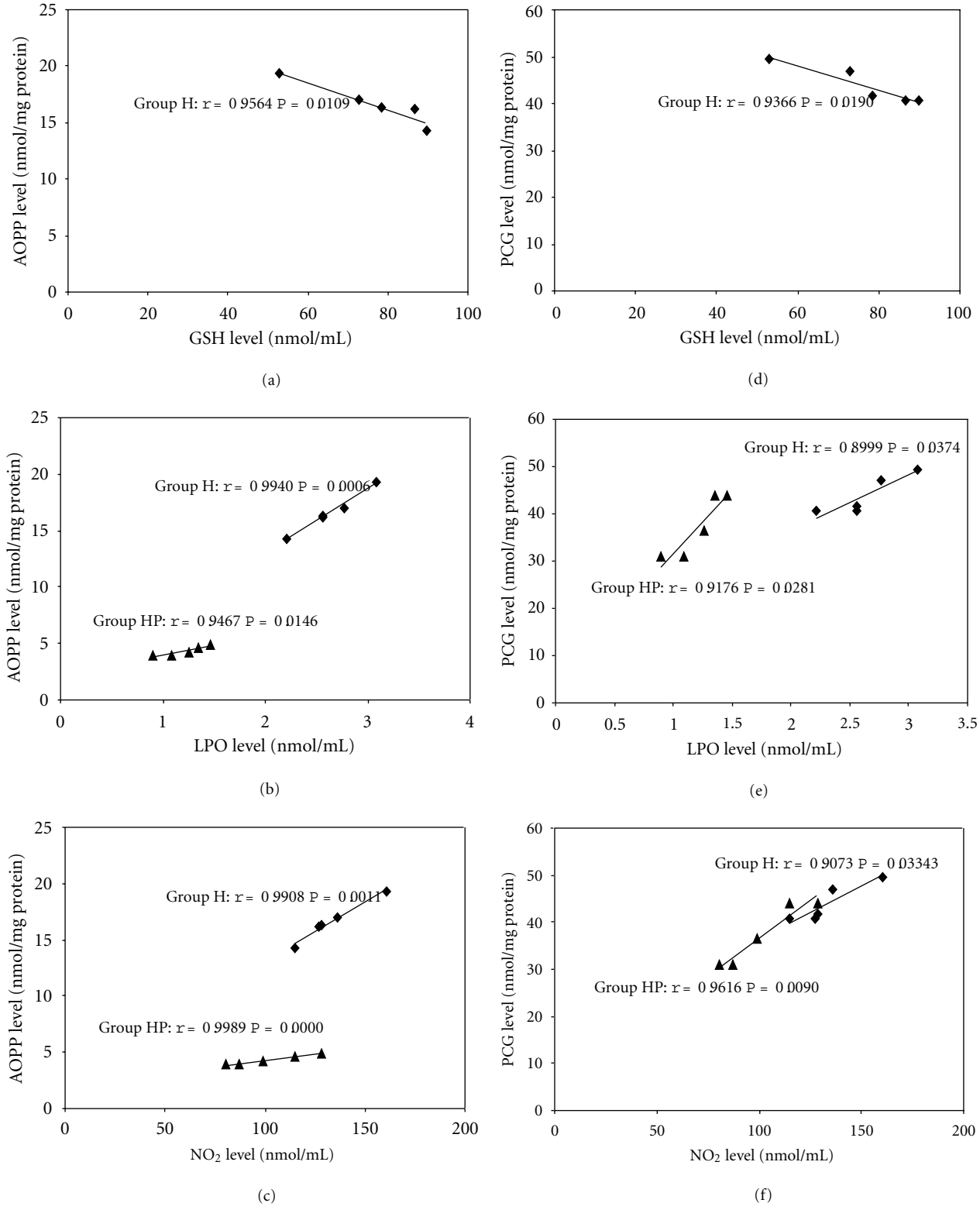

Figure 1: Correlations between GSH, LPO, and NO_2 and respective protein oxidation marker, AOPP ((a)–(c)) or PCG ((d)–(f)), in hyperglycemic (Group H) and hyperglycemic pioglitazone-treated (Group HP) animals.

Table 2: Blood glucose and plasma insulin concentrations in control and hyperglycemic rabbits at the start and the end of experiment.

Group	Glucose (mmol/L)		Insulin (mU/L)	
	Start	End	Start	End
Control (C)	6.2 ± 0.1	5.7 ± 0.3	13.16 ± 1.26	13.30 ± 1.12
Control-pioglitazone (CP)	6.5 ± 0.3	5.9 ± 0.3[b]	11.74 ± 0.72	14.12 ± 0.98[b]
Control-repaglinide (CR)	6.3 ± 0.2	4.0 ± 0.3[a,b,*]	12.83 ± 1.01	20.0 ± 1.42[a,b,*]
Hyperglycemic (H)	26.3 ± 2.3[a]	24.9 ± 2.8[a]	3.21 ± 0.63[a]	2.79 ± 0.79[a]
Hyperglycemic-pioglitazone (HP)	27.2 ± 0.3[a]	23.9 ± 1.8[a]	2.31 ± 0.15	2.01 ± 0.34[a]
Hyperglycemic-repaglinide (HR)	26.4 ± 1.2[a]	24.0 ± 2.3[a]	2.32 ± 0.15[a]	2.02 ± 0.04[a]

Values are mean ± SEM ($n = 5$). [a]Significant at $P < 0.05$ versus Group C. [b]Significant at $P < 0.05$ versus Group H. *Significant at $P < 0.05$ versus start.

stress [35]. In our previous studies concerning heart, lung, and testis, repaglinide significantly affected nitrotyrosine and LPO levels but did not affect NO_2 and PCG levels [31, 32]. It was confirmed in the present study by the lack of any effect on PCG, AOPP, and NO_2.

What is important in the present study is that pioglitazone and repaglinide did not significantly affect glucose concentration in our hyperglycemic animals. After alloxan injection, these animals preserved insulin secretion but its amount was very low because of destruction of many B cells by alloxan. Therefore, repaglinide could not stimulate its secretion in sufficient way and pioglitazone failed to affect its sensitivity (Table 2). This lack of antihyperglycemic activity was expected and used by us to differentiate, at least in part, some direct antioxidative/antinitrosative effects of the drugs from effects mediated via increased insulin action. When animals with type 2 diabetes were used, these two kinds of effects could not be separated.

5. Conclusions

In aqueous humor of our hyperglycemic animals, the decreased AA, GSH, and TAS as well as increased LPO, NO_2, PCG, and AOPP were observed confirming the exposition of ocular structures on oxidative/nitrosative stress. It was observed that correlations between AOPP and other factors were more expressive than the same correlations for PCG. We concluded that AOPP which was easy to obtain, corresponded better than PCG to other examined parameters. In addition, antioxidative/antinitrosative properties of pioglitazone and repaglinide were compared. The results obtained in the present study confirm that pioglitazone and repaglinide differ significantly in their ability to ameliorate the examined markers of oxidative/nitrosative stress in aqueous humor, especially in respect to protein modifications. It cannot be excluded that K_{ATP} channel blockers like repaglinide may affect oxidative/nitrosative stress but PPARγ agonists like pioglitazone seem to act more comprehensively which was confirmed independently on their action oh hyperglycemia.

References

[1] P. Geraldine, B. B. Sneha, R. Elanchezhian et al., "Prevention of selenite-induced cataractogenesis by acetyl-L-carnitine: an experimental study," *Experimental Eye Research*, vol. 83, no. 6, pp. 1340–1349, 2006.

[2] I. Grattagliano, G. Vendemiale, F. Boscia, T. Micelli-Ferrari, L. Cardia, and E. Altomare, "Oxidative retinal products and ocular damages in diabetic patients," *Free Radical Biology and Medicine*, vol. 25, no. 3, pp. 369–372, 1998.

[3] S. E. Ohia, C. A. Opere, and A. M. LeDay, "Pharmacological consequences of oxidative stress in ocular tissues," *Mutation Research*, vol. 579, no. 1-2, pp. 22–36, 2005.

[4] N. Ahmed, R. Babaei-Jadidi, and S. K. Howell, "Degradation products of proteins damaged by glycation, oxidation and nitration in clinical type 1 diabetes," *Diabetologia*, vol. 48, no. 8, pp. 1590–1603, 2005.

[5] R. A. Kowluru, "Diabetes-induced elevations in retinal oxidative stress, protein kinase C and nitric oxide are interrelated," *Acta Diabetologica*, vol. 38, no. 4, pp. 179–185, 2001.

[6] N. Toda and M. Nakanishi-Toda, "Nitric oxide: ocular blood flow, glaucoma, and diabetic retinopathy," *Progress in Retinal and Eye Research*, vol. 26, no. 3, pp. 205–238, 2007.

[7] X. M. Zhang, K. Ohishi, and T. Hiramitsu, "Microdialysis measurement of ascorbic acid in rabbit vitreous after photodynamic reaction," *Experimental Eye Research*, vol. 73, no. 3, pp. 303–309, 2001.

[8] B. Anderstam, A. C. Bragfors-Helin, A. Valli, P. Stenvinkel, B. Lindholm, and M. E. Suliman, "Modification of the oxidative stress biomarker AOPP assay: application in uremic samples," *Clinica Chimica Acta*, vol. 393, no. 2, pp. 114–118, 2008.

[9] H. Kaneda, J. Taguchi, K. Ogasawara, T. Aizawa, and M. Ohno, "Increased level of advanced oxidation protein products in patients with coronary artery disease," *Atherosclerosis*, vol. 162, no. 1, pp. 221–225, 2002.

[10] A. Piwowar, M. Knapik-Kordecka, and M. Warwas, "AOPP and its relations with selected markers of oxidative/antioxidative system in type 2 diabetes mellitus," *Diabetes Research and Clinical Practice*, vol. 77, no. 2, pp. 188–192, 2007.

[11] M. Stefek, Z. Kyselova, L. Rackova, and L. Krizanova, "Oxidative modification of rat eye lens proteins by peroxyl radicals in vitro: protection by the chain-breaking antioxidants stobadine and trolox," *Biochimica et Biophysica Acta*, vol. 1741, no. 1-2, pp. 183–190, 2005.

[12] S. A. Madsen-Bouterse and R. A. Kowluru, "Oxidative stress and diabetic retinopathy: pathophysiological mechanisms and treatment perspectives," *Reviews in Endocrine and Metabolic Disorders*, vol. 9, no. 4, pp. 315–327, 2008.

[13] I. Inoue, S. Goto, T. Matsunaga et al., "The ligands/activators for peroxisome proliferator-activated receptor α (PPARα) and PPARγ increase Cu^{+2},Zn^{+2}-superoxide dismutase and decrease

p22^{phox} message expression in primary endothelial cells," *Metabolism*, vol. 50, no. 1, pp. 3–11, 2001.

[14] J. B. Majithiya, A. N. Paramar, and R. Balaraman, "Pioglitazone, a PPARγ agonist, restores endothelial function in aorta of streptozotocin-induced diabetic rats," *Cardiovascular Research*, vol. 66, no. 1, pp. 150–161, 2005.

[15] Y. Li, L. Xu, J. Shen et al., "Effects of short-term therapy with different insulin secretagogues on glucose metabolism, lipid parameters and oxidative stress in newly diagnosed type 2 diabetes mellitus," *Diabetes Research and Clinical Practice*, vol. 88, no. 1, pp. 42–47, 2010.

[16] D. Manzella, A. M. Abbatecola, R. Grella, and G. Paolisso, "Repaglinide administration improves brachial reactivity in type 2 diabetic patients," *Diabetes Care*, vol. 28, no. 2, pp. 366–371, 2005.

[17] T. Tankova, D. Koev, L. Dakovska, and G. Kirilov, "The effect of repaglinide on insulin secretion and oxidative stress in type 2 diabetic patients," *Diabetes Research and Clinical Practice*, vol. 59, no. 1, pp. 43–49, 2003.

[18] A. Kyaw, "A simple colorimetric method for ascorbic acid determination in blood plasma," *Clinica Chimica Acta*, vol. 86, no. 2, pp. 153–157, 1978.

[19] O. H. Lowry, N. J. Rosenbrough, A. L. Farr, and R. J. Randall, "Protein measurement with the Folin phenol reagent," *The Journal of Biological Chemistry*, vol. 193, no. 1, pp. 265–275, 1951.

[20] S. M. Ferreira, S. F. Lerner, R. Brunzini, P. A. Evelson, and S. F. Llesuy, "Oxidative stress markers in aqueous humor of glaucoma patients," *American Journal of Ophthalmology*, vol. 137, no. 1, pp. 62–69, 2004.

[21] C. Livingstone and J. Davis, "Targeting therapeutics against glutathione depletion in diabetes and its complications," *The British Journal of Diabetes and Vascular Disease*, vol. 7, no. 6, pp. 258–265, 2007.

[22] T. Fujii, R. Hamaoka, J. Fujii, and N. Taniguchi, "Redox capacity of cells affects inactivation of glutathione reductase by nitrosative stress," *Archives of Biochemistry and Biophysics*, vol. 378, no. 1, pp. 123–130, 2000.

[23] M. P. Cohen, E. Hud, E. Shea, and C. W. Shearman, "Vitreous fluid of *db/db* mice exhibits alterations in angiogenic and metabolic factors consistent with early diabetic retinopathy," *Ophthalmic Research*, vol. 40, no. 1, pp. 5–9, 2008.

[24] M. Aslan, A. Cort, and I. Yucel, "Oxidative and nitrative stress markers in glaucoma," *Free Radical Biology and Medicine*, vol. 45, no. 4, pp. 367–376, 2008.

[25] R. L. Levine, D. Garland, C. N. Oliver et al., "Determination of carbonyl content in oxidatively modified proteins," *Methods in Enzymology*, vol. 186, pp. 464–478, 1990.

[26] T. Nguyen-Khoa, Z. A. Massy, J. P. de Bandt et al., "Oxidative stress and haemodialysis: role of inflammation and duration of dialysis treatment," *Nephrology Dialysis Transplantation*, vol. 16, no. 2, pp. 335–340, 2001.

[27] M. Kalousova, J. Skrha, and T. Zima, "Advanced glycation end-products and advanced oxidation protein products in patients with diabetes mellitus," *Physiological Research*, vol. 51, no. 6, pp. 597–604, 2002.

[28] T. Shiojiri, K. Wada, A. Nakajima et al., "PPARγ ligands inhibit nitrotyrosine formation and inflammatory mediator expressions in adjuvant-induced rheumatoid arthritis mice," *European Journal of Pharmacology*, vol. 448, no. 2-3, pp. 231–238, 2002.

[29] B. Sung, S. Park, B. P. Yu, and H. Y. Chung, "Amelioration of age-related inflammation and oxidative stress by PPARγ activator: Suppression of NF-κB by 2,4-thiazolidinedione," *Experimental Gerontology*, vol. 41, no. 6, pp. 590–599, 2006.

[30] L. Tao, H. Liu, E. Gao et al., "Antioxidative, antinitrative, and vasculoprotective effects of a peroxisome proliferator-activated receptor-γ agonist in hypercholesterolemia," *Circulation*, vol. 108, no. 22, pp. 2805–2811, 2003.

[31] A. Gumieniczek, Ł. Komsta, and M. R. Chehab, "Effects of two oral antidiabetics, pioglitazone and repaglinide, on aconitase inactivation, inflammation and oxidative/nitrosative stress in tissues under alloxan-induced hyperglycemia," *European Journal of Pharmacology*, vol. 659, no. 1, pp. 89–93, 2011.

[32] A. Gumieniczek, M. Krzywdzińska, and M. Nowak, "Modulation of nitrosative/oxidative stress in the lung of hyperglycemic rabbits by two antidiabetics, pioglitazone and repaglinide," *Experimental Lung Research*, vol. 35, no. 5, pp. 371–379, 2009.

[33] B. Gross and B. Staels, "PPAR agonists: multimodal drugs for the treatment of type-2 diabetes," *Best Practice and Research in Clinical Endocrinology and Metabolism*, vol. 21, no. 4, pp. 687–710, 2007.

[34] R. Assaloni, R. da Ros, L. Quagliaro et al., "Effects of S21403 (mitiglinide) on postprandial generation of oxidative stress and inflammation in type 2 diabetic patients," *Diabetologia*, vol. 48, no. 9, pp. 1919–1924, 2005.

[35] J. E. da Silva-Santos, M. C. Santos-Silva, F. Cunha, and J. Assreuy, "The role of ATP-sensitive potassium channels in neutrophil migration and plasma exudation," *The Journal of Pharmacology and Experimental Therapeutics*, vol. 300, no. 3, pp. 946–951, 2002.

Hindawi Publishing Corporation
Experimental Diabetes Research
Volume 2012, Article ID 793783, 5 pages
doi:10.1155/2012/793783

Research Article

Oxidative Metabolism Genes Are Not Responsive to Oxidative Stress in Rodent Beta Cell Lines

Faer Morrison, Karen Johnstone, Anna Murray, Jonathan Locke, and Lorna W. Harries

Institute of Biomedical and Clinical Sciences, Peninsula College of Medicine and Dentistry, University of Exeter, Barrack Road, Exeter EX2 5DW, UK

Correspondence should be addressed to Lorna W. Harries, l.w.harries@exeter.ac.uk

Received 21 October 2011; Revised 18 November 2011; Accepted 19 November 2011

Academic Editor: Dan Nemet

Altered expression of oxidative metabolism genes has been described in the skeletal muscle of individuals with type 2 diabetes. Pancreatic beta cells contain low levels of antioxidant enzymes and are particularly susceptible to oxidative stress. In this study, we explored the effect of hyperglycemia-induced oxidative stress on a panel of oxidative metabolism genes in a rodent beta cell line. We exposed INS-1 rodent beta cells to low (5.6 mmol/L), ambient (11 mmol/L), and high (28 mmol/L) glucose conditions for 48 hours. Increases in oxidative stress were measured using the fluorescent probe dihydrorhodamine 123. We then measured the expression levels of a panel of 90 oxidative metabolism genes by real-time PCR. Elevated reactive oxygen species (ROS) production was evident in INS-1 cells after 48 hours ($P < 0.05$). TLDA analysis revealed a significant ($P < 0.05$) upregulation of 16 of the 90 genes under hyperglycemic conditions, although these expression differences did not reflect differences in ROS. We conclude that although altered glycemia may influence the expression of some oxidative metabolism genes, this effect is probably not mediated by increased ROS production. The alterations to the expression of oxidative metabolism genes previously observed in human diabetic skeletal muscle do not appear to be mirrored in rodent pancreatic beta cells.

1. Introduction

Type 2 diabetes (T2D) occurs when the pancreatic beta cells can no longer compensate for peripheral insulin resistance by increasing insulin production and is associated with hyperglycemia and an altered lipid profile (dyslipidemia) [1]. The T2D "microenvironment" is detrimental to cells and tissues and is thought to contribute to further beta cell dysfunction and reduced beta cell mass, as well as microvascular and macrovascular complications. Increased levels of reactive oxygen species (ROS) are hypothesized to have a role in causing beta cell dysfunction due to altered glucose levels and lipid profiles, leading to T2D [2]. ROS have a physiological role in normal intracellular signal transduction. However, excessive ROS production causes damage to cellular components, of which RNA is especially vulnerable, potentially leading to gene expression changes [3].

Mitochondrial dysfunction is thought to contribute to beta cell dysfunction and has been observed in beta cells and in other tissues of individuals with T2D [4, 5]. Moreover, several groups have found that components of the electron transport chain and other genes involved in oxidative metabolism were altered in tissues from individuals with T2D [6–8]. For example, decreases in the expression of oxidative phosphorylation genes regulated by the transcriptional coactivator PGC1 (PPARGC1A), which is involved in regulation of energy metabolism, have been observed in T2D skeletal muscle [6, 7]. Increases in the expression of these genes were observed in liver from patients with T2D and were correlated with blood glucose levels [8].

The beta cells of the pancreas are particularly vulnerable to the effects of ROS as they contain lower levels of antioxidant enzymes (catalase, superoxide dismutase, glutathione peroxidase) compared with other tissues, including skeletal muscle and liver [9]. ROS-mediated mitochondrial dysfunction, as observed in T2D islets, has been shown to disrupt glucose-induced insulin secretion from beta cells [10]. Therefore, the beta cells, as well as being the central tissue in T2D pathogenesis, might be expected to be particularly susceptible to ROS-mediated gene expression changes.

The vulnerable state of the beta cell and the importance of oxidative metabolism in relation to insulin secretion and ROS production led us to investigate whether the expression of genes involved in oxidative metabolism is altered in response to hyperglycemia-induced oxidative stress in a rodent pancreatic beta cell line INS-1. We hypothesized that hyperglycemia-induced oxidative stress in the pancreatic beta cell may contribute to beta cell dysfunction and impaired insulin secretion because of deregulation in the expression of oxidative metabolism genes.

2. Materials and Methods

2.1. Cell Culture and Experimental Procedure. The rat pancreatic beta cell line INS-1 was cultured in RPMI 1640 medium (Invitrogen) supplemented with 11 mmol/L glucose, 10% fetal calf serum and 1% penicillin/streptomycin at 37°C in a humidified atmosphere. After 72 hours, the cells were seeded in 25 cm^2 flasks at a density of 3.5×10^5 cells/flask (for gene expression analysis) or in 96-well plates at a density of 2×10^4 cells/well (for cell viability and ROS production measurements). Cells were then incubated under the conditions already described but with low (5.6 mmol/L), ambient (11 mmol/L) or high (28 mmol/L) glucose for a further 48 hours (conditions previously used to model hyperglycemia in T2D) [11].

2.2. Cell Viability. Cell viability was measured using (3-(4,5-dimethylthiazol-2-yl)-2,5-diphenyltetrazolium bromide (MTT) assay [12]. Briefly, MTT was added to cells at a final concentration of 0.5 mg/mL. Cells were incubated for 1 hour at 37°C. The medium was then aspirated and 100 μL DMSO added to each well to solubilize the blue formazan product. Absorbance was measured using an OPTIMA reader (BMG LABTECH) at an excitation wavelength of 540 nm. Three biological replicates were carried out, each with five technical replicates.

2.3. ROS Production. Intracellular ROS production was measured using the fluorescent probe dihydrorhodamine 123 (DHR123) (Invitrogen), which, when oxidized, localizes in the mitochondria and fluoresces green, indicating the presence of ROS. In brief, DHR was added to cells in 100 μL fresh RPMI medium to a final concentration of 1 μM. Cells were incubated for 30 minutes at 37°C. Fluorescence was measured using a PHERAstar reader (BMG LABTECH) at an excitation wavelength of 485 nm and an emission wavelength of 520 nm. Three biological replicates were carried out, each with five technical replicates.

2.4. Gene Expression Analysis. The genes selected for this study are given in Table 1. Choice of targets was made on the basis that these 90 genes have shown evidence in the literature that they may be effected by some of the physiological changes that occur with T2D. The first set of targets (indicated in Table 1 by bold type) were taken from a study where microarray analysis of skeletal muscle samples from matched diabetic and nondiabetic subjects was undertaken [7]. Using a pathways analysis approach, they identified a set of genes involved in oxidative phosphorylation whose expression was decreased in diabetic muscle. The majority of these targets were genes responsive to the transcriptional coactivator PGC1. We therefore chose to study these, together with other PPAR genes (*Ppara*, *Ppard,* and *Pparg*) and their targets. This is relevant because the Pro12Ala variant of PPARG has been associated with T2D [13]. A very similar pattern of gene expression was also noted by a second group, who carried out an analogous experiment, also in skeletal muscle [6]. In concordance with the Mootha study, this study demonstrated deregulation of a group of genes involved in oxidative phosphorylation regulated by nuclear respiratory factor-1 (NRF1) and PGC1 (indicated in Table 1 by underlined type). Genes that appear in both studies are marked in Table 1 by bold and underlined type. Other targets have been selected on the basis of involvement in response to oxidative stress and with roles in oxidative metabolism. Most of these genes can be subdivided into activation of the antioxidant defense system, cell cycle arrest, DNA repair, damaged protein repair, or activation of the NFκB pathway. The final category of genes were selected on the basis that they are key players in pathways involved in T2D. These include genes involved in cell cycle and apoptosis, immune and inflammatory processes, energy metabolism and homeostasis, including glucose metabolism, and insulin signaling and homeostasis. Expression of the 90 target genes were analyzed with the Micro Fluidic Card system (Taqman low density array (TLDA) custom array, Applied Biosystems).

2.5. Statistical Analysis. Comparisons of ROS production and gene expression between the three glucose culture conditions were determined using the Kruskal-Wallis H test.

3. Results and Discussion

We found that although ROS were increased at both high and low glucose compared with ambient glucose ($P < 0.05$) (Figure 1), this was not accompanied by concomitant alterations in the expression levels of the 90 test genes. TLDA analysis revealed deregulation of 16 out of 90 (18%) of genes analyzed ($P < 0.05$) (Figure 2), but the patterns of deregulation did not mirror changes in ROS production. If increased ROS production was responsible for the changes in gene expression, then we would expect the pattern of ROS production to mirror the pattern of gene expression. This, however, was not the case, which leads us to conclude that the expression changes are probably due to effects of glycemia, rather than a specific effect of ROS. The lack of response in the remaining 82% of genes tested may indicate that these genes are not responsive to ROS or glucose in beta cells. A decrease in cell viability was observed at low glucose after 48 hours, whereas high glucose increased cell viability compared with ambient glucose (results not shown). The effects on cell viability could explain some of the gene expression changes observed.

This study provides evidence that increasing glycemia affects expression of a proportion of genes involved in oxidative metabolism in the pancreatic beta cell line INS-1. A number of genes were upregulated in response to

Table 1: Panel of 90 target genes for analysis by TLDA expression profiling. Candidate genes have been shown by pathway-based microanalysis to be deregulated in T2D skeletal muscle, are reported in the literature to be involved in oxidative metabolism or the oxidative stress response, or are reported in the literature to be key players in diabetes pathways/deregulated in T2D.

Panel of 90 target genes for analysis by TLDA expression profiling							
Deregulated in T2D skeletal muscle	***Alas1***	***Atp5c1***	***Atp5g1***	***Atp5g2***	***Atp5g3***	***Ckmt1***	***Cox4i1***
	Cox6a1	***Cox6c***	***Nrf1***	***Pdx1***	***Pkm2***	***Por***	***Sdhc***
	Slc25a4	***Ucp2***	***Uros***	***Eif2ak3***	***Sdhb***	***Uqcrc1***	***Cox5b***
	Atp5o	*Cox7b*	*Cyc1*	*Atp5j*	*Ndufa5*	*Ndufa8*	*Ndufb5*
	Ndufb6	*Ndufs2*	*Ndufs3*	*Ppara*	*Ppard*	*Pparg*	*Ppargc1a*
	Sdha						
Involved in oxidative metabolism and the oxidative stress response	*Aco1*	*Ccng1*	*Cdkn1a*	*Cxcl10*	*Ddit3*	*Dnaja1*	*Fmo1*
	Gck	*Gsr*	*Hspa4*	*Hspa5*	*Igfbp2*	*Il18*	*Ins1*
	Ireb2	*Nfkb1*	*Nfkbia*	*Pck1*	*Rad23a*	*Sod1*	*Tnf*
	Tp53	*Txn2*	*Txnip*	*Ung*	*Xbp1*	*Ercc1*	*Mtor*
	Nampt	*Ndufaf1*	*Nfe2l2*	*Prkcd*	*Prkcz*	*Shc1*	
Key players in T2D pathways							
Cell cycle and apoptosis	*Crls1*	*Hdac4*	*Hdac5*	*Hgf*	*Igf1*	*Suv39h1*	
Cellular and energy metabolism and homeostasis, including glucose homeostasis	*Foxo1*	*Gckr*	*Hagh*	*Hk1*	*Prkaa2*	*Sirt1*	
Immune and inflammatory processes	*Crp*	*Il1b*	*Il1rn*	*Il6*	*Rage*		
Insulin signaling and homeostasis	*Gcg*	*Insr*	*Kcnj11*				

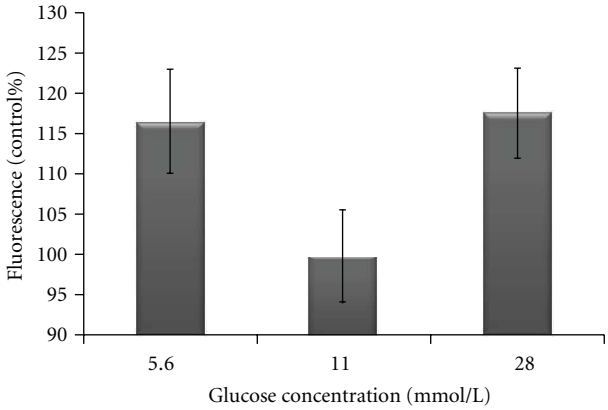

Figure 1: The production of ROS in INS-1 cells cultured in low, ambient, and high glucose concentrations for 48 hours. Intracellular ROS production was measured using the fluorogenic probe dihydrorhodamine 123. Differences in ROS production were statistically analyzed by the Kruskal-Wallis H test. Significant results ($P < 0.05$) relative to control are indicated by*.

increasing glycemia, including several components of the electron transport chain (*Atp5g3, Atp5g2, Cox4i1, Cox6a1, Ndufs2, Sdhb*) (Figures 2(a)–2(f)) and genes involved in oxidative metabolism or cellular antioxidant defense (*Gsr, Nfkb1, Sod1*). Also upregulated with high glucose were genes involved in energy homeostasis or metabolism (*Pkm2, Prkaa2*) (Figures 2(g)–2(k)). Deregulation of these genes in beta cells could potentially contribute to impaired mitochondrial metabolism and insulin secretion. *Prkaa2* is a catalytic subunit of the AMP-activated protein kinase (AMPK), a key regulator of energy homeostasis, which has been shown to decrease glucose-stimulated insulin secretion, insulin content, and mitochondrial metabolism [14].

Also up-regulated in response to increasing glycemia are *Cdkn1a* which is involved in p53-mediated cell cycle arrest in response to cellular stress and has already been shown to be induced by H_2O_2 [15], *Crls1* which is important in maintaining the integrity of the mitochondrial membrane, and is thought to be involved in apoptosis, *Gcg* which encodes four distinct proteins including glucagon, and the inflammatory marker *Crp* (Figures 2(l)–2(o)). Interestingly, the only gene that is significantly downregulated in response to high glucose, compared with ambient glucose, is the promoter of beta cell function and survival, *Pdx1* (Figure 2(p)). It has been shown previously that *Pdx1* deficiency causes beta cell dysfunction and beta cell death and that both hyperglycemia and hyperlipidemia lead to decreased *Pdx1* expression and consequent beta cell dysfunction [16]. The glycolysis gene *Pkm2* is worth mentioning in more detail, as it was the only gene which was significantly deregulated between low and ambient glucose, ambient and high glucose, and low and high glucose (Figure 2(j)). *Pkm2* has previously been shown to be glucose-responsive so acts here as a positive control [17].

Although we saw evidence of deregulated gene expression in response to altered glycemia, we found little evidence to suggest that ROS were involved in mediating these gene

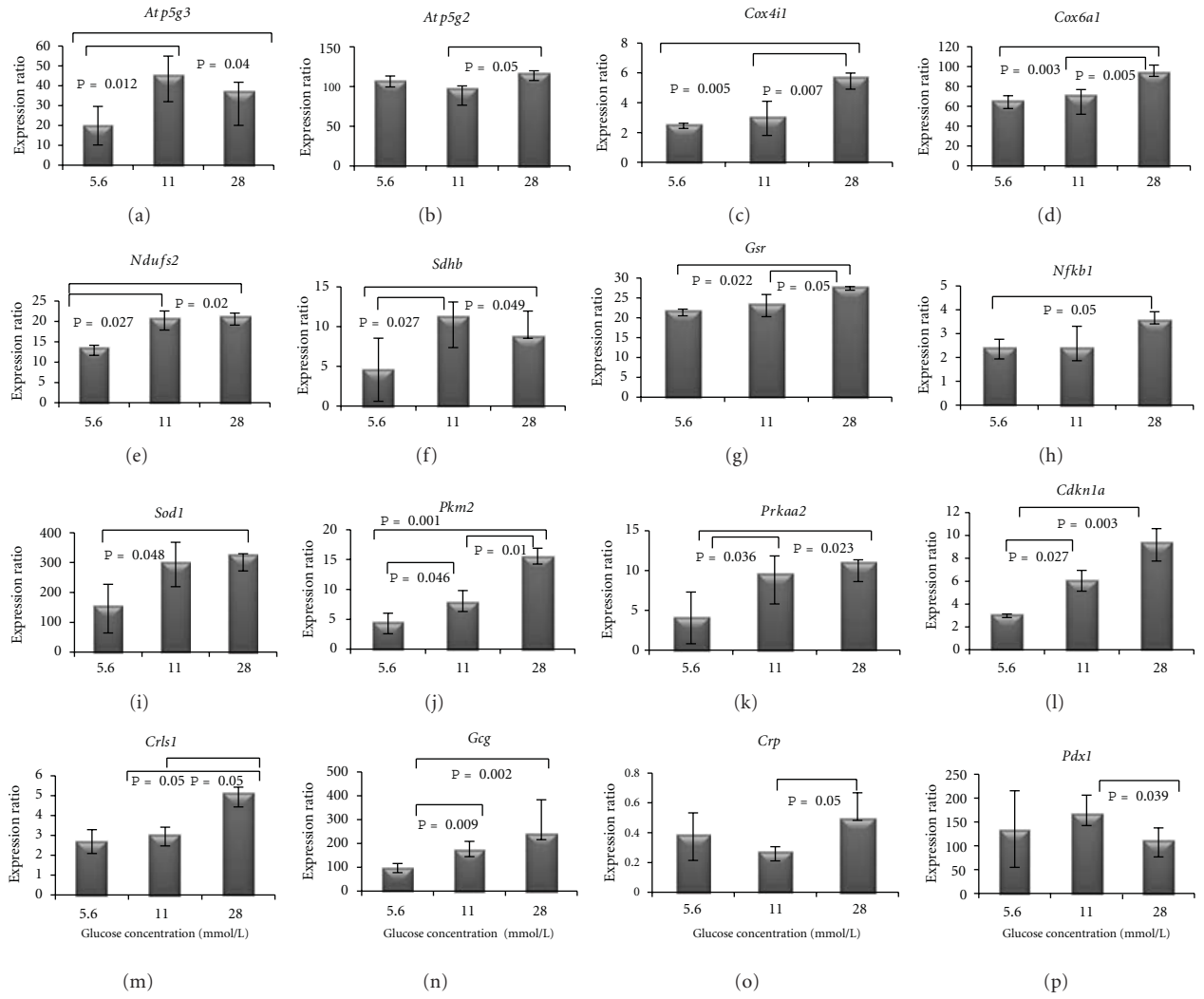

Figure 2: Gene expression in INS-1 cells cultured in low (5.6 mmol/L), ambient (11 mmol/L), and high (28 mmol/L) glucose concentrations for 48 hours (gene name above each graph). Gene expression changes were analyzed using TLDA expression profiling on a panel of 90 target genes. Gene expression differences were statistically analyzed by the Kruskal-Wallis *H* test and were normalized to the mean expression of the endogenous controls *B2m* and *Tbp,* as they were found to be most stable using the GeNorm algorithm (Statminer, Integromics). Note that the scales of the graphs differ between genes as the expression is shown relative to mean expression across all genes. Significant results ($P < 0.05$) are indicated by*.

expression changes. This is interesting because ROS production and oxidative stress have been strongly associated with mitochondrial dysfunction, and H_2O_2-induced oxidative stress has previously been shown to alter expression of some of these genes in beta cells [15, 18]. For instance, H_2O_2-induced oxidative stress in rat pancreatic islet cells has been demonstrated to induce *Cdkn1a* mRNA expression [15]. Elevated *Cdkn1a* expression may result in a suppression of beta cell proliferation and insulin biosynthesis, which provides an important link between oxidative stress and beta cell dysfunction in T2D [15]. A transient exposure of the rat insulinoma cell line INS-1E to H_2O_2 significantly increased mitochondrial ROS production and impaired glucose-stimulated insulin secretion, which persisted for several days after the exposure [18]. This occurred alongside a concomitant decrease in expression of genes involved in mitochondrial biogenesis and a compensatory increase in expression of respiratory chain subunit mRNAs [18].

Moreover, there are examples of ROS altering signaling pathways in other tissues which are relevant to diabetes, such as adipose tissue and liver. For instance, *in vivo* exposure to high glucose in rats increased the mRNA levels of several inflammatory genes in the adipose, and this effect was partially prevented by the free radical scavenger N-acetyl-cysteine [19]. The authors suggest that exposure to ROS-induced damage over the lifetime of an adipocyte could contribute to the pathological state seen in metabolic disorders such as T2D [19]. ROS levels have been shown to be elevated in the liver of *db/db* mice and in a human hepatic cell line treated with the fatty acid palmitate. The NADPH oxidase NOX3 was found to be the predominant source of ROS production, and the increase in ROS was found to induce p38MAPK and JNK

pathways, which was shown to contribute to hepatic insulin resistance [20].

Our panel of 90 genes were selected on the basis that they have already been shown to be deregulated in T2D tissues or are involved in the oxidative stress response, therefore, were strong candidates for this study. Although ROS appear to have little role in mediating the expression of these genes under the conditions described, it should be highlighted that ROS may influence the expression of other genes involved in beta cell function. It would be interesting to further investigate the effect of hyperglycemia-induced ROS production on expression of other genes with important roles in beta cell function, such as maintenance of beta cell mass and regulation of apoptosis, as both hyperglycemia and oxidative stress are thought to be crucial in mediating beta cell apoptosis and subsequent loss of beta cell mass in T2D [21].

In conclusion, our study provides further evidence that hyperglycemia induces ROS production in the pancreatic beta cell. Although 18% of the oxidative metabolism genes tested were shown to be deregulated in response to increasing glycemia, there was little evidence that ROS or oxidative stress was involved in mediating these gene expression changes, indicating that gene expression changes noted in diabetic tissues may be more attributable to differences in glucose or lipid concentration than to increases in oxidative stress.

Acknowledgments

This study was funded by the Wellcome Trust Project Grant WT081278MA to L. W. Harries and by a charitable donation from the Mendip Golf Club.

References

[1] M. Cnop, "Fatty acids and glucolipotoxicity in the pathogenesis of Type 2 diabetes," *Biochemical Society Transactions*, vol. 36, no. 3, pp. 348–352, 2008.

[2] A. P. Robertson, "Chronic oxidative stress as a central mechanism for glucose toxicity in pancreatic islet beta cells in diabetes," *Journal of Biological Chemistry*, vol. 279, no. 41, pp. 42351–42354, 2004.

[3] Q. Kong and C. L. G. Lin, "Oxidative damage to RNA: mechanisms, consequences, and diseases," *Cellular and Molecular Life Sciences*, vol. 67, no. 11, pp. 1817–1829, 2010.

[4] M. Anello, R. Lupi, D. Spampinato et al., "Functional and morphological alterations of mitochondria in pancreatic beta cells from type 2 diabetic patients," *Diabetologia*, vol. 48, no. 2, pp. 282–289, 2005.

[5] D. E. Kelley, J. He, E. V. Menshikova, and V. B. Ritov, "Dysfunction of mitochondria in human skeletal muscle in type 2 diabetes," *Diabetes*, vol. 51, no. 10, pp. 2944–2950, 2002.

[6] M. E. Patti, A. J. Butte, S. Crunkhorn et al., "Coordinated reduction of genes of oxidative metabolism in humans with insulin resistance and diabetes: potential role of PGC1 and NRF1," *Proceedings of the National Academy of Sciences of the United States of America*, vol. 100, no. 14, pp. 8466–8471, 2003.

[7] V. K. Mootha, C. M. Lindgren, K. F. Eriksson et al., "PGC-1α-responsive genes involved in oxidative phosphorylation are coordinately downregulated in human diabetes," *Nature Genetics*, vol. 34, no. 3, pp. 267–273, 2003.

[8] H. Misu, T. Takamura, N. Matsuzawa et al., "Genes involved in oxidative phosphorylation are coordinately upregulated with fasting hyperglycaemia in livers of patients with type 2 diabetes," *Diabetologia*, vol. 50, no. 2, pp. 268–277, 2007.

[9] S. Lenzen, "Oxidative stress: the vulnerable β-cell," *Biochemical Society Transactions*, vol. 36, no. 3, pp. 343–347, 2008.

[10] K. Sakai, K. Matsumoto, T. Nishikawa et al., "Mitochondrial reactive oxygen species reduce insulin secretion by pancreatic β-cells," *Biochemical and Biophysical Research Communications*, vol. 300, no. 1, pp. 216–222, 2003.

[11] D. A. Cunha, P. Hekerman, L. Ladrière et al., "Initiation and execution of lipotoxic ER stress in pancreatic β-cells," *Journal of Cell Science*, vol. 121, no. 14, pp. 2308–2318, 2008.

[12] T. Mosmann, "Rapid colorimetric assay for cellular growth and survival: application to proliferation and cytotoxicity assays," *Journal of Immunological Methods*, vol. 65, no. 1-2, pp. 55–63, 1983.

[13] J. C. Florez, J. Hirschhorn, and D. Altshuler, "The inherited basis of diabetes mellitus: implications for the genetic analysis of complex traits," *Annual Review of Genomics and Human Genetics*, vol. 4, pp. 257–291, 2003.

[14] G. A. Rutter, G. Da Silva Xavier, and I. Leclerc, "Roles of 5′-AMP-activated protein kinase (AMPK) in mammalian glucose homoeostasis," *Biochemical Journal*, vol. 375, no. 1, pp. 1–16, 2003.

[15] H. Kaneto, Y. Kajimoto, Y. Fujitani et al., "Oxidative stress induces p21 expression in pancreatic islet cells: possible implication in beta-cell dysfunction," *Diabetologia*, vol. 42, no. 9, pp. 1093–1097, 1999.

[16] K. Fujimoto and K. S. Polonsky, "Pdx1 and other factors that regulate pancreatic β-cell survival," *Diabetes, Obesity and Metabolism*, vol. 11, no. 4, pp. 30–37, 2009.

[17] K. Yamada and T. Noguchi, "Nutrient and hormonal regulation of pyruvate kinase gene expression," *Biochemical Journal*, vol. 337, no. 1, pp. 1–11, 1999.

[18] N. Li, T. Brun, M. Cnop, D. A. Cunha, D. L. Eizirik, and P. Maechler, "Transient oxidative stress damages mitochondrial machinery inducing persistent β-cell dysfunction," *Journal of Biological Chemistry*, vol. 284, no. 35, pp. 23602–23612, 2009.

[19] Y. Lin, A. H. Berg, P. Iyengar et al., "The hyperglycemia-induced inflammatory response in adipocytes: the role of reactive oxygen species," *Journal of Biological Chemistry*, vol. 280, no. 6, pp. 4617–4626, 2005.

[20] D. Gao, S. Nong, X. Huang et al., "The effects of palmitate on hepatic insulin resistance are mediated by NADPH oxidase 3-derived reactive oxygen species through JNK and p38 MAPK pathways," *Journal of Biological Chemistry*, vol. 285, no. 39, pp. 29965–29973, 2010.

[21] R. Lupi and S. Del Prato, "β-cell apoptosis in type 2 diabetes: quantitative and functional consequences," *Diabetes and Metabolism*, vol. 34, no. 2, pp. S56–S64, 2008.

Hindawi Publishing Corporation
Experimental Diabetes Research
Volume 2012, Article ID 230342, 7 pages
doi:10.1155/2012/230342

Research Article

Protective Effects of Beta Glucan and Gliclazide on Brain Tissue and Sciatic Nerve of Diabetic Rats Induced by Streptozosin

Harun Alp,[1] Sefer Varol,[2] Muhammet Murat Celik,[3] Murat Altas,[4] Osman Evliyaoglu,[5] Orhan Tokgoz,[6] Mehmet Halis Tanrıverdi,[7] and Ertugrul Uzar[2]

[1] *Department of Pharmacology and Toxicology, Veterinary Faculty, Dicle University, 21103 Diyarbakir, Turkey*
[2] *Department of Neurology, Faculty of Medicine, Dicle University, 21103 Diyarbakir, Turkey*
[3] *Department of Internal Medicine, Faculty of Medicine, Mustafa Kemal University, 31000 Hatay, Turkey*
[4] *Department of Neurosurgery, Faculty of Medicine, Mustafa Kemal University, 31000 Hatay, Turkey*
[5] *Department of Biochemistry, Faculty of Medicine, Dicle University, 21103 Diyarbakir, Turkey*
[6] *Department of Anesthesiology, Faculty of Medicine, Dicle University, 21103 Diyarbakir, Turkey*
[7] *Department of Family Medicine, Faculty of Medicine, Dicle University, 21103 Diyarbakir, Turkey*

Correspondence should be addressed to Harun Alp, alpharun@gmail.com

Received 26 September 2011; Accepted 7 December 2011

Academic Editor: Pietro Galassetti

There have not been yet enough studies about effects of beta glucan and gliclazide on oxidative stress created by streptozotocin in the brain and sciatic nerve of diabetic rats. The aim of this paper was to investigate the antioxidant effects of gliclazide and beta glucan on oxidative stress and lipid peroxidation created by streptozotosin in brain and sciatic nerve. Total of 42 rats were divided into 6 groups including control, diabetic untreated (DM) (only STZ, diabetic), STZ (DM) + beta glucan, STZ (DM) + gliclazide, only beta glucan treated (no diabetic), and only gliclazide treated (no diabetic). The brain and sciatic nerve tissue samples were analyzed for malondialdehyde (MDA), total oxidant status (TOS), total antioxidant status (TAS), oxidative stress index (OSI), and paraoxonase (PON-1) levels. We found a significant increase in MDA, TOS, and OSI along with a reduction in TAS level, catalase, and PON-1 activities in brain and sciatic nerve of streptozotocin-induced diabetic rats. Also, this study shows that in terms of these parameters both gliclazide and beta glucan have a neuroprotective effect on the brain and sciatic nerve of the streptozotocin-induced diabetic rat. Our conclusion was that gliclazide and beta glucan have antioxidant effects on the brain and sciatic nerve of the streptozotocin-induced diabetic rat.

1. Introduction

Diabetes mellitus (DM) is one of the most common chronic metabolic disorders leading to complications in a number of organ and systems. DM characterised by disturbed glucose metabolism due to an absolute or relative insulin deficiency affects the central and peripheral nervous systems [1]. It is reported that encephalopathy is the long-term neurological complication of diabetes and is associated with cognitive decline and increased risk of dementia [2]. Brain and nerve tissues are two sites of diabetic organ damage [3]. Also, it is reported that oxidative stress and apoptosis play an important role in diabetes-induced tissue damage [4, 5]. DM, in hyperglicemia uncontrolled, initiates degenerative processes that causes damage of brain and nerve tissues because of excess oxidative stress. In diabetic complications, oxidative stress results from an overproduction of reactive oxygen/nitrogen species generated by glucose autoxidation, mitochondria dysfunction, protein glycation and from decreased antioxidant defenses [6].

One of the important goals of DM treatment is to prevent its complications. To this end, there is accumulating evidence that supplementation antioxidant compounds may offer some protection against diabetic complications [7]. Therefore, beta-glucan and gliclazide were selected as possible protective materials of this study. Beta-glucans are glucose polymers that are found in the cell walls of yeast, fungi, and cereal plants. They are known to have beneficial

effects on the immune system and are claimed to have no toxic or adverse effects. Natural products containing beta-glucans have been used for thousands of years for the benefits of human health, but beta-glucans were only identified as active components recently [8]. Beta-glucans have been investigated extensively for immune stimulation effects and developed for the treatment of several diseases including cancer, decubitus ulcer, and infectious diseases. Recent studies have reported that beta-glucans could reduce hyperglicemia, hyperlipidemia, and hypertension [9]. Several mechanisms were suggested for the protective effect of beta-glucan; one of these mechanisms is related to antioxidant capacity of this molecule. It was found that β-glucan is an antioxidant with the scavenging ability lying between that of α-tocopherol, which is known to be incorporated in the lipid bilayer, and the water-soluble antioxidant, mannitol [10]. Therefore, beta-glucans have great potential for the treatment of diabetes and associated neurological diseases including diabetic neuropathy and encephalopathy. Thus, beta glucan can lead new approaches for the prevention of diabetic neurologic complications and vascular risk factors by reducing oxidative damage of this molecule. However, there have not been yet enough studies for its antioxidant actions on diabetic brain and sciatic norve tissues. The aim of this study was to investigate the antioxidant protective effects of beta glucan on brain and sciatic nerve tissues of streptozotocin-induced diabetic rats.

Gliclazide which is another possible protective material of this study, is a second-generation sulfonylurea hypoglycemic agent. It may show effect as reduction in free radical generation or an increase in free radical scavenging. Also, gliclazide may contribute to the control of the physiopathological mechanisms underlying both the process of aging and type 2 diabetes by reducing oxidant stress and DNA damage, improving antioxidant status [11]. In diabetic experimental models, it has been reported that gliclazide potentially protects the vasculature through improvements in plasma lipids and platelet function [12]. However, there have not been yet enough studies about its antioxidant actions on diabetic brain and sciatic nerve tissues. Therefore, in the present study, the protective effects of gliclazide against oxidative stress and lipid peroxidation created by streptozotocin on brain and sciatic nerve in diabetic rats were investtigated.

2. Materials and Methods

2.1. Animals, Care, and Nutrition. This study was approved by Dicle University Animal Ethical Committee and was carried out in accordance with the "Animal Welfare Act and the Guide for the Care and Use of Laboratory animals prepared by the Dicle University, Animal Ethical Committee." Female Wistar Albino rats (250 ± 50 g) were obtained from the Animal labaratuary of Dicle University. The rats were housed in clean polypropylene cages having six rats per cage and maintained under temperature controlled room (23 ± 2°C) with a photoperiod of 12 h light and 12 h dark cycle. The rats were given standard pellets diet and water ad libitum throughout the experimental period. All efforts were made to minimize animal suffering and to use only the number of animals necessary to produce reliable scientific data.

2.2. Animals and Treatment. The rats were fasted overnight, and diabetes was induced by a single dose via intraperitoneal injection of streptozotocin solution (STZ). The experiment was designed as a total of 28 days. A week after STZ administration, their blood glucose values were measured and were defined as diabetic rats, that is, their blood glucose values were above 250 mg/dL. STZ caused the death of some rats. At the end, 42 rats were divided into 6 groups including control, diabetic untreated (only STZ, diabetic), diabetics treated with beta glucan (STZ + beta glucan), diabetics treated with gliclazide (STZ + gliclazide), only beta glucan treated (beta glucan control, no diabetic), and only gliclazide treated (gliclazide control, no diabetic). The beta-glucan (Mustafa Nevzat Company, Turkey) used in this study is 1,3-1,6 beta-D-glucan in the microparticulate form, which was prepared from the S. cerevisiae yeast. Beta glucan was administered orally (50 mg/kg body weight) with a gavage for 21 days in the STZ + beta glucan and beta glucan groups. The gliclazide (DIAMICRON, Mustafa Nevzat Company, Turkey) used in the tablet form was administered orally (10 mg/kg body weight) with a gavage for 21 days in the STZ + gliclazide and only gliclazide groups. STZ solution was prepared as follows: 24 mg of STZ was dissolved in 1 mL of 5 mM citrate buffer (pH 4.5) before the injection, and a volume of 2.5 mL/kg was administrated into each rat. The animals were fasted overnight and diabetes was induced by a single i.p. injection of a freshly prepared solution of STZ (CAS number: 133 18883-66-4, 85882, Sigma-Aldrich) (50 mg/kg body weight) in 0.1 M cold citrate buffer (pH 4.5). One week after STZ administration, blood was taken from the lateral veins of the tail, their blood glucose levels were measured by a glucometer (ACCU-CHEK, Roche Diagnostics) using a glucose oxidase method and the rats whose blood glucose values were above 250 mg/dL were accepted as diabetic [13]. After completion of 21 days for drug treatments, the animals were sacrificed by cervical dislocation, and the brain and sciatic nerve tissues were excised at 4°C. The tissues were washed with ice-cold saline and immediately stored at −50°C for biochemical analyses.

2.3. Biochemical Analyses. The excised cerebrum and sciatic nerve tissue samples for biochemical analyses were weighed, immediately stored at −50°C. The cerebrum tissues cleaned with 1.15% ice-cold KCl, minced, then homogenized in five volumes (w/v) of the same solution. Assays were performed on the supernatant of the homogenate that is prepared at 14.000 rpm for 30 min at +4°C. The protein concentration of the tissue was measured by the method of Lowry [14]. Lipid peroxidation level in the cerebrum was expressed as malondialdehyde (MDA). It was measured according to procedure of Ohkawa et al. [15]. Catalase activity was measured according to the method of Aebi [16]. Serum paraoxonase (PON-1) activity was measured spectrophotometrically by modified Eckerson method [17]. The TAS of supernatant fractions was evaluated by using a novel automated and colorimetric measurement method developed by Erel [18]. Hydroxyl

radicals, the most potent biological radicals, are produced in this method. In the assay, the ferrous ion solution present in reagent 1 is mixed with hydrogen peroxide, which is present in reagent 2. The subsequently produced radicals, such as brown-colored dianisidine radical cations produced by the hydroxyl radicals, are also potent radicals. Using this method, the antioxidative effect of the sample is measured against the potent-free radical reactions initiated by the produced hydroxyl radicals. The assay has excellent precision values lower than 3%. The total antioxidant status (TAS) results are expressed as nmol Trolox equivalent/mg protein. The total oxidant status (TOS) of supernatant fractions was evaluated by using a novel automated and colorimetric measurement method developed by Erel [19]. Oxidants present in the sample oxidize the ferrous ion-o-dianisidine complex to ferric ion. The oxidation reaction is increased by glycerol molecules, which are abundantly present in the reaction medium. The ferric ion makes a colored complex with xylenol orange in an acidic medium. The color intensity, which can be measured spectrophotometrically, is related to the total amount of oxidant molecules present in the sample. The assay is calibrated with hydrogen peroxide, and the results are expressed in terms of nmol H_2O_2 equivalent/mg protein [20]. The TOS level to TAS level ratio was regarded as the oxidative stress index (OSI). The unit of cerebrum tissue TOS and TAS was μmole H_2O_2 Equiv./gram protein and mmole H_2O_2 Equiv./gram protein, respectively. The cerebrum tissue OSI value was calculated as follows: OSI = ((TOS, μmole H_2O_2 Equiv./gram protein)/(TAS, μmole H_2O_2 Equiv./gram protein) $\times$ 100) [21].

2.4. Statistical Analyses. The data was analyzed by using Statistical Package for the Social Sciences version 11.5 (SPSS 11.5 for Windows, Chicago, IL, USA). The variables between the groups were tested by Mann Whitney U test. A value of $P < 0.05$ indicates a significant difference. Data are expressed as mean ± S.D.

3. Results

In the rat brain, the MDA, TOS, TAS, and OSI level, catalase and PON-1 enzyme activities are presented in Table 1. There was a significant depletion in the PON-1, catalase, and TAS levels in the brain of the diabetic rat compared to the control groups (for both parameters $P < 0.05$). However, beta glucan-treated diabetic rats significantly reversed the catalase, PON-1 and TAS back to normal levels compared to untreated diabetic rats (for both parameters $P < 0.05$). PON-1 activity was significantly higher in gliclazide-treated diabetic group than untreated diabetic group in the brain ($P < 0.05$), but catalase activity and TAS level were not significant (for both parameters $P > 0.05$). As can be seen from Table 1, the level of MDA, TOS, and OSI in the brain tissue was increased in untreated diabetic rats compared with the rats of control group (for both parameters $P < 0.05$). However, MDA, TOS, and OSI levels were significantly reduced to gliclazide-treated diabetic group compared with the untreated-diabetic group in brain tissue (for both parameters $P < 0.05$). Likewise, MDA, TOS, and OSI levels were significantly reduced to beta-glucan-treated diabetic group compared with the untreated-diabetic group in brain tissue (for both parameters $P < 0.05$).

It was observed that medication similarly affected both tissue in the rat sciatic nerve compared with brain tissue. In the rat sciatic nerve, the MDA, TOS, TAS, and OSI levels as well as catalase and PON-1 enzyme activities are presented in Table 2. There were no significant differences in brain tissue MDA, TOS, TAS, OSI, catalase, and PON-1 in both beta glucan-treated group and gliclazide-treated group compared to control group rats ($P > 0.05$). There was a significant depletion in the PON-1, catalase, and TAS levels in the sciatic nerve of the diabetic rat compared to the control groups (for both parameters $P < 0.05$). However, beta-glucan-treated diabetic rats significantly reversed catalase, PON-1, and TAS back to normal levels compared to untreated diabetic rats (for both parameters $P < 0.05$). PON-1 activity was significantly higher in gliclazide-treated diabetic group than untreated diabetic group in the brain ($P < 0.05$), but catalase activity and TAS level were not significant (for both parameters $P > 0.05$). As can be seen from Table 2, the levels of MDA, TOS, and OSI in the sciatic nerve tissue were increased in untreated diabetic rats compared with the rats of control group (for both parameters $P < 0.05$). However, MDA, TOS, and OSI levels were significantly reduced to gliclazide-treated diabetic group compared with the untreated-diabetic group in sciatic nerve tissue (for both parameters $P < 0.05$). Likewise, MDA, TOS, and OSI levels were significantly reduced to beta-glucan-treated diabetic group compared with the untreated-diabetic group in sciatic nerve tissue (for both parameters $P < 0.05$).

4. Discussion

DM is a metabolic disorder with a globally rising prevalence which can affect the peripheral and central nervous system [2, 22]. It is well known that oxidative stress is a contributor to the development of complications in DM. There are several lines of evidence indicating that oxidative stress is increased in diabetic neuropathy and encephalopathy [23, 24]. Streptozotocin-induced diabetes is a well-described model of experimental diabetes that provides a relevant example of endogenous chronic oxidative stress as a result of hyperglycemia in diabetic brain [4].

Previous experimental studies in STZ-induced diabetic rats have been suggested that the increased oxidative stress is an important factor in the pathogenesis of the complications [4]. For example, increased lipid peroxidation impairs membrane function by decreasing membrane fluidity and causes free-radical-induced membrane lipid peroxidation including increased membrane rigidity, decreased cellular deformability, leading to various diseases [25]. Lipid peroxidation is initiated by free radicals attack to membrane lipids, generating large amounts of reactive products, which have been implicated in diabetes and its complications. MDA is a decomposition product of peroxidized polyunsaturated fatty acids, end product of lipid peroxidation. Thus, MDA is a marker of lipid peroxidation. In this study, the level of MDA significantly increased in the untreated diabetic rat sciatic

Table 1: Biochemical parameters in all groups in the brain of rats.

Groups	MDA (nmol/gr protein)	TOS (mmol H_2O_2 Eq./g protein)	TAS (mmol Trolox Eq./g protein)	OSI	Catalase (U/g protein)	PON-1 activity (U/mg protein)
Control (I)	259.9 ± 60.5	22.0 ± 8.2	0.44 ± 0.1	53.6 ± 25.5	1.19 ± 0.14	0.72 ± 0.29
Diabetic (II)	454.7 ± 62.8	39.7 ± 3.5	0.22 ± 0.08	204.9 ± 96.3	0.65 ± 0.15	0.30 ± 0.05
Diabetic + gliclazide (III)	367.4 ± 47.6	32.2 ± 2.8	0.29 ± 0.04	113.7 ± 17.1	0.73 ± 0.12	0.40 ± 0.10
Diabetic + Beta glucan (IV)	329.2 ± 45.3	27.0 ± 5.9	0.38 ± 0.08	75.0 ± 26.9	1.02 ± 0.09	0.59 ± 0.26
Gliclazide (V)	242.0 ± 36.7	20.5 ± 6.3	0.44 ± 0.1	51.01 ± 28.7	1.34 ± 0.23	0.80 ± 0.18
Beta glucan (VI)	257.0 ± 55.0	21.8 ± 6.8	0.46 ± 0.11	52.7 ± 33.4	1.30 ± 0.26	0.71 ± 0.20
P values						
I-II	0.002	0.004	0.003	0.002	0.002	0.004
II-III	0.009	0.009	N.S.	0.009	N.S.	0.046
II–IV	0.002	0.004	0.012	0.002	0.002	0.016
I–VI	N.S.	N.S.	N.S.	N.S.	N.S.	N.S.
I–V	N.S.	N.S.	N.S.	N.S.	N.S.	N.S.

N.S: not significant, MDA: malondialdehyde, TOS: total oxidant status, TAS: total antioxidant status, OSI: oxidative stress index, PON-1: paraoxonase.

Table 2: Biochemical parameters in all groups in the sciatic nerve of rats.

Groups	MDA (nmol/gr protein)	TOS (mmol H_2O_2 Eq./g protein)	TAS (mmol Trolox Eq./g protein)	OSI	Catalase (U/g protein)	PON-1 activity (U/mg protein)
Control (I)	17.6 ± 3.1	11.4 ± 3.5	0.16 ± 0.01	70.7 ± 23.0	0.36 ± 0.07	0.11 ± 0.02
Diabetic (II)	30.2 ± 4.2	20.6 ± 1.9	0.08 ± 0.03	299.4 ± 161.9	0.19 ± 0.05	0.04 ± 0.01
Diabetic + gliclazide (III)	25.0 ± 2.9	17.7 ± 2.5	0.11 ± 0.02	162.3 ± 37.2	0.21 ± 0.03	0.06 ± 0.01
Diabetic + Beta glucan (IV)	23.0 ± 1.3	14.1 ± 2.7	0.14 ± 0.03	108.4 ± 41.5	0.29 ± 0.03	0.09 ± 0.03
Gliclazide (V)	16.1 ± 2.4	10.7 ± 3.2	0.16 ± 0.04	71.5 ± 40.8	0.39 ± 0.07	0.12 ± 0.03
Beta glucan (VI)	17.1 ± 3.6	11.3 ± 3.5	0.17 ± 0.04	73.6 ± 45.2	0.38 ± 0.08	0.10 ± 0.03
P values						
I-II	0.002	0.004	0.002	0.002	0.002	0.002
II-III	0.017	0.025	N.S.	0.018	N.S.	0.021
II–IV	0.002	0.004	0.012	0.002	0.002	0.006
I–V	N.S.	N.S.	N.S.	N.S.	N.S.	N.S.
I–VI	N.S.	N.S.	N.S.	N.S.	N.S.	N.S.

N.S: not significant, MDA: malondialdehyde, TOS: total oxidant status, TAS: total antioxidant status, OSI: oxidative stress index, PON-1: paraoxonase.

and brain tissues. And it was concluded that the increase in lipid peroxidation might be a reflection of the decrease in enzymatic and nonenzymatic antioxidants of defense systems in diabetic rats. Similarly, in previous studies, increased MDA levels have been found in brain and sciatic nerve of diabetic rats [4, 26]. Also, in our study, the reduced MDA levels by both gliclazide and beta glucan likely demonstrate that beta glucan and gliclazide might be agents to protect the brain and nerve tissues against diabetic oxidative stress. In one study, it has been reported that treatment with gliclazide prevented the increase level of lipid peroxidation marker in plasma and pancreas of diabetic rats. In another a study, it has been found that MDA level decreased following gliclazide treatment in patients with diabetes [25, 27]. Also, it has been reported that gliclazide may be beneficial by inhibition of lipid and protein denaturation [28]. Similar to our study, Delibas et al. reported that gliclazide treatment prevented the elevation of MDA levels in hippocampus of diabetic rats [29]. In addition to MDA level, measurement of TOS, TAS, and OSI provides novel and reliable index of oxidative stress. The levels of oxidants can already be measured separately in the laboratory, but these measurements are time-consuming and costly. The number of different oxidants in all biological samples makes it difficult to measure each oxidant separately. Assessment of TOS may be indicating the level of all free oxidant radicals caused by diabetes-related oxidative stress [30]. Likewise, the number of different antioxidants in all biological samples makes it difficult to measure each antioxidant separately. Thereby, TAS may be an important factor providing protection from neurological

damage caused by diabetes-related oxidative stress [31]. Therefore, we investigated both TAS and TOS by using new measurement methods developed by Erel (2004, 2005) to more accurately assess oxidative stress in this study [18, 19]. Also we evaluated oxidative stress with OSI, detected by using both TOS and TAS parameters. We found increased TOS and OSI levels and decreased TAS level and catalase activity in the diabetic rats compared to control rats in the brain and sciatic nerve tissues. At the same time, this study confirms that brain and sciatic nerve of diabetic rats show increased MDA, TOS, and OSI levels along with reduced TAS and catalase. These increases may be due to overproduction or decreased excretion of oxidant substances. Because of the increase in these oxidants and the decrease in total antioxidants, the oxidative/antioxidative balance demonstrated to shift towards the oxidative status in brain and sciatic nerve tissues of diabetic rats in this study. Treatment with beta glucan of diabetic rats was significantly reduced to TOS and OSI along with increased TAS level and catalase activity compared to untreated diabetic rats in brain and sciatic tissues. Because of the decrease in these oxidants and the increase in these antioxidants, the oxidative/antioxidative balance demonstrated to shift towards the antioxidative status with beta glucan treatment in brain and sciatic nerve tissues of diabetic rats. Additionally, there was no difference in beta glucan group between control group regarding sciatic and brain oxidant/antioxidant parameters. These findings show no toxic effect treatment with beta glucan in brain and sciatic nerve tissues of diabetic rats. Thus, it may be preferred to use natural products in treating and preventing various diseases.

Owing to their useful effects on the immune system, antioxidant, and anti-inflammatory properties, and because they lack any toxic effects, beta glucans have been used in previous many studies [32, 33]. It has been suggested that beta-glucans lowered postprandial glycemia, hyperlipidemia, and hypertension [34, 35]. Also, it is reported that beta glucan improves wound healing in diabetic mice [36]. In addition, it has been suggested that beta-glucans may be used to prevent or treat excessive microglial activation during chronic inflammatory conditions [37]. The present study is the first experimental research demonstrating the protective effectiveness of beta glucan to protect diabetes-induced oxidative stress in brain and sciatic nerve of rats.

Gliclazide which is a another marker of drug of the present study, second-generation sulfonylurea, might exert antioxidant effect. It has been demonstrated that gliclazide prevents, through its antioxidant properties, oxidized low-density lipoprotein-associated endothelial dysfunction, apoptosis, and plaque rupture [38]. It has been found that gliclazide was able to significantly reduce high glucose-induced apoptosis, mitochondrial alterations, and nitrotyrosine concentration increase [39]. It has been suggested that it decreases hyperglycemia and hyperinsulinemia and inhibits oxidative stress. It is also a promising therapeutic candidate for the prevention of vascular complications of diabetes, by decreasing the level of DNA damage induced by reactive oxygen species [13, 40]. Also it has been found that gliclazide reduced oxidative stress in liver and kidney tissues of diabetic rats [11, 41]. But the protective effect of gliclazide on diabetic brain and sciatic nerve tissues has not been reported so far, it is interested in whether antioxidative properties of gliclazide may occur to reduction in oxidative damage, in the context of prevention of diabetes-associated neuropathy and encephalopathy. In the present study, treatment with gliclazide of diabetic rats significantly reduced TOS and OSI levels compared to untreated diabetic rats in brain and sciatic tissues but insignificant increased TAS level and catalase activity. Because of the decrease in these oxidants and the increase in these antioxidants, the oxidative/antioxidative balance demonstrated to shift towards the antioxidative status with gliclazide treatment in brain and sciatic nerve tissues of diabetic rats. This study is the first experimental research demonstrating the effectiveness of gliclazide to protect diabetes-induced oxidative stress in brain and sciatic nerve of rats. As a result, we may explain these results due to the antioxidant and antidiabetic effects of gliclazide.

Paraoxonase is one of the important antioxidant enzymes. PON-1 hydrolyses lipid peroxides in oxidized lipoproteins. A close relationship between PON-1 deficiency and accelerated progression of arteriosclerosis has been found in experimental and human studies [42, 43]. Although microangiopathy plays a role in the pathogenesis of diabetic neuropathy, there has been little research on PON-1 activity in patients with DM. Therefore, PON-1 was selected as a marker agent of antioxidant defences system in present study. In a previous study, it has been found that serum PON-1 decreased in diabetic rats and spermine reversed the decline of PON-1 spermine-treated diabetic rats [44]. Also, it has been indicated that cerebrospinal fluid (CSF) levels of β-glucan and gliclazide correlated in a dose-dependent pattern with therapeutic response, and they penetrated to blood-brain barrier [45, 46]. To our knowledge, brain and sciatic nerve injury relationship between PON-1 activities has not been studied in diabetic rats. In this study, we found decreased PON-1 activity in the brain and sciatic tissues of diabetic rats compared to control rats. Both beta glucan and gliclazide treatments were reversed to decrement activity of PON-1 in diabetic rats.

5. Conclusions

Hyperglicemia in STZ-induced diabetic rats can cause oxidative damage in brain and sciatic nerve tissues, which may play vital roles in the pathogenesis of diabetic neuropathy and encephalopathy. Also treatment of beta glucan and/or gliclazide inhibits lipid peroxidation and regulates total oxidant/antioxidant status in diabetic rat brain and sciatic nerve tissues. This study results suggested that beta glucan and gliclazide may be considered to reduce oxidative stress in diabetic brain and sciatic nerve and may be used as a protective agent against diabetic damage of brain and sciatic nerve.

Ethical Approval

This paper was approved by Dicle University Animal Ethical Committee.

Acknowledgment

This research was supported financially by the Dicle University.

References

[1] B. A. Perkins and V. Bril, "Emerging therapies for diabetic neuropathy: a clinical overview," *Current Diabetes Reviews*, vol. 1, no. 3, pp. 271–280, 2005.

[2] Y. D. Reijmer, E. van den Berg, J. de Bresser et al., "Accelerated cognitive decline in patients with type 2 diabetes: MRI correlates and risk factors," *Diabetes/Metabolism Research and Reviews*, vol. 27, no. 2, pp. 195–202, 2011.

[3] K. R. Shanmugam, K. Mallikarjuna, N. Kesireddy, and K. Sathyavelu Reddy, "Neuroprotective effect of ginger on antioxidant enzymes in streptozotocin-induced diabetic rats," *Food and Chemical Toxicology*, vol. 49, no. 4, pp. 893–897, 2011.

[4] E. Arnal, M. Miranda, J. Barcia, F. Bosch-Morell, and F. J. Romero, "Lutein and docosahexaenoic acid prevent cortex lipid peroxidation in streptozotocin-induced diabetic rat cerebral cortex," *Neuroscience*, vol. 166, no. 1, pp. 271–278, 2010.

[5] Z. Zheng, H. Chen, H. Wang et al., "Improvement of retinal vascular injury in diabetic rats by statins is associated with the inhibition of mitochondrial reactive oxygen species pathway mediated by peroxisome proliferator-activated receptor γ coactivator 1α," *Diabetes*, vol. 59, no. 9, pp. 2315–2325, 2010.

[6] F. Giacco and M. Brownlee, "Oxidative stress and diabetic complications," *Circulation Research*, vol. 107, no. 9, pp. 1058–1070, 2010.

[7] A. Cumaoğlu, G. Ozansoy, A. M. Irat, A. Aricioğlu, Ç. Karasu, and N. Arı, "Effect of long term, non cholesterol lowering dose of fluvastatin treatment on oxidative stress in brain and peripheral tissues of streptozotocin-diabetic rats," *European Journal of Pharmacology*, vol. 654, no. 1, pp. 80–85, 2011.

[8] J. Chen and K. Raymond, "Beta-glucans in the treatment of diabetes and associated cardiovascular risks," *Vascular Health and Risk Management*, vol. 4, no. 6, pp. 1265–1272, 2008.

[9] J. Chen and R. Seviour, "Medicinal importance of fungal β-(1 → 3), (1 → 6)-glucans," *Mycological Research*, vol. 111, no. 6, pp. 635–652, 2007.

[10] M. Babincová, Z. Bacová, E. Machová, and G. Kogan, "Antioxidant properties of carboxymethyl glucan: comparative analysis," *Journal of Medicinal Food*, vol. 5, no. 2, pp. 79–83, 2002.

[11] G. Alper, S. Irer, E. Duman, O. Caglayan, and C. Yilmaz, "Effect of I-deprenyl and gliclazide on oxidant stress/antioxidant status and DNA damage in a diabetic rat model," *Endocrine Research*, vol. 31, no. 3, pp. 199–212, 2005.

[12] S. Pennathur and J. W. Heinecke, "Mechanisms of oxidative stress in diabetes: implications for the pathogenesis of vascular disease and antioxidant therapy," *Frontiers in Bioscience*, vol. 9, pp. 565–574, 2004.

[13] E. Uzar, H. Alp, M. U. Cevik et al., "Ellagic acid attenuates oxidative stress on brain and sciatic nerve and improves histopathology of brain in streptozotocin-induced diabetic rats," *Neurological Sciences*. In press.

[14] O. H. Lowry, N. J. Rosebrough, A. L. Farr, and R. J. Randall, "Protein measurement with the Folin phenol reagent," *The Journal of Biological Chemistry*, vol. 193, no. 1, pp. 265–275, 1951.

[15] H. Ohkawa, N. Ohishi, and K. Yagi, "Assay for lipid peroxides in animal tissues by thiobarbituric acid reaction," *Analytical Biochemistry*, vol. 95, no. 2, pp. 351–358, 1979.

[16] H. Aebi, "Catalase in vitro," *Methods in Enzymology*, vol. 105, pp. 121–126, 1984.

[17] H. W. Eckerson, C. M. Wyte, and B. N. La Du, "The human serum paraoxonase/arylesterase polymorphism," *American Journal of Human Genetics*, vol. 35, no. 6, pp. 1126–1138, 1983.

[18] O. Erel, "A novel automated method to measure total antioxidant response against potent free radical reactions," *Clinical Biochemistry*, vol. 37, no. 2, pp. 112–119, 2004.

[19] O. Erel, "A new automated colorimetric method for measuring total oxidant status," *Clinical Biochemistry*, vol. 38, no. 12, pp. 1103–11111, 2005.

[20] E. Ozturk, O Balat, Y. G. Acılmıs, C. Ozcan, S. Pence, and Ö. Erel, "Measurement of the placental total antioxidant status in preeclamptic women using a novel automated method," *Journal of Obstetrics and Gynaecology Research*, vol. 37, no. 4, pp. 337–342, 2011.

[21] A. Aycicek, O. Erel, and A. Kocyigit, "Increased oxidative stress in infants exposed to passive smoking," *European Journal of Pediatrics*, vol. 164, no. 12, pp. 775–778, 2005.

[22] D. W. Zochodne, "Diabetes mellitus and the peripheral nervous system: manifestations and mechanisms," *Muscle & Nerve*, vol. 36, no. 2, pp. 144–166, 2007.

[23] A. Ozkul, M. Ayhan, C. Yenisey, A. Akyol, E. Guney, and F. A. Ergin, "The role of oxidative stress and endothelial injury in diabetic neuropathy and neuropathic pain," *Neuroendocrinology Letters*, vol. 31, no. 2, pp. 261–264, 2010.

[24] W. H. Hoffman, S. L. Siedlak, Y. Wang, R. J. Castellani, and M. A. Smith, "Oxidative damage is present in the fatal brain edema of diabetic ketoacidosis," *Brain Research*, vol. 1369, pp. 194–202, 2011.

[25] G. Saravanan and P. Ponmurugan, "Beneficial effect of S-allylcysteine (SAC) on blood glucose and pancreatic antioxidant system in streptozotocin diabetic rats," *Plant Foods for Human Nutrition*, vol. 65, no. 4, pp. 374–378, 2010.

[26] X. P. Cui, B. Y. Li, H. Q. Gao, N. Wei, W. L. Wang, and M. Lu, "Effects of grape seed proanthocyanidin extracts on peripheral nerves in streptozocin-induced diabetic rats," *Journal of Nutritional Science and Vitaminology*, vol. 54, no. 4, pp. 321–328, 2008.

[27] L. L. Chen, F. Yu, T. S. Zeng, Y. F. Liao, Y. M. Li, and H. C. Ding, "Effects of gliclazide on endothelial function in patients with newly diagnosed type 2 diabetes," *European Journal of Pharmacology*, vol. 659, no. 2-3, pp. 296–301, 2011.

[28] Y. Noda, A. Mori, and L. Packer, "Gliclazide scavenges hydroxyl, superoxide and nitric oxide radicals: an ESR study," *Research Communications in Molecular Pathology and Pharmacology*, vol. 96, no. 2, pp. 115–124, 1997.

[29] N. Delibas, I. Kilinc, Z. Yonden, R. Sutcu, F. Gultekin, and H. Koylu, "NMDA receptor subunits 2A and 2B decrease and lipid peroxidation increase in the hippocampus of streptozotocin-diabetic rats: effects of insulin and gliclazide treatments," *International Journal of Neuroscience*, vol. 114, no. 3, pp. 391–401, 2004.

[30] M. Aslan, T. Sabuncu, A. Kocyigit, H. Celik, and S. Selek, "Relationship between total oxidant status and severity of diabetic nephropathy in type 2 diabetic patients," *Nutrition, Metabolism and Cardiovascular Diseases*, vol. 17, no. 10, pp. 734–740, 2007.

[31] J. Nourooz-Zadeh, D. Ziegler, C. Sohr, J. D. Betteridge, J. Knight, and J. Hothersall, "The use of pholasin as a probe

for the determination of plasma total antioxidant capacity," *Clinical Biochemistry*, vol. 39, no. 1, pp. 55–61, 2006.

[32] J. Saluk-Juszczak, K. Krolewska, B. Wachowicz et al., "(1 → 3)-β-D-Glucan inhibits a dual mechanism of peroxynitrite stroke," *International Journal of Biological Macromolecules*, vol. 48, no. 3, pp. 488–494, 2011.

[33] N. Senoglu, M. F. Yuzbasioglu, M. Aral et al., "Protective effects of N-acetylcysteine and β-glucan pretreatment on oxidative stress in cecal ligation and puncture model of sepsis," *Journal of Investigative Surgery*, vol. 21, no. 5, pp. 237–243, 2008.

[34] S. Panahi, A. Ezatagha, F. Temelli, T. Vasanthan, and V. Vuksan, "β-glucan from two sources of oat concentrates affect postprandial glycemia in relation to the level of viscosity," *Journal of the American College of Nutrition*, vol. 26, no. 6, pp. 639–644, 2007.

[35] A. L. Jenkins, D. J. A. Jenkins, U. Zdravkovic, P. Würsch, and V. Vuksan, "Depression of the glycemic index by high levels of β-glucan fiber in two functional foods tested in type 2 diabetes," *European Journal of Clinical Nutrition*, vol. 56, no. 7, pp. 622–628, 2002.

[36] M. Berdal, H. I. Appelbom, J. H. Eikrem et al., "Aminated β-1,3-D-glucan improves wound healing in diabetic db/db mice," *Wound Repair and Regeneration*, vol. 15, no. 6, pp. 825–832, 2007.

[37] V. B. Shah, D. L. Williams, and L. Keshvara, "β-Glucan attenuates TLR2- and TLR4-mediated cytokine production by microglia," *Neuroscience Letters*, vol. 458, no. 3, pp. 111–115, 2009.

[38] L. Li and G. Renier, "The oral anti-diabetic agent, gliclazide, inhibits oxidized LDL-mediated LOX-1 expression, metalloproteinase-9 secretion and apoptosis in human aortic endothelial cells," *Atherosclerosis*, vol. 204, no. 1, pp. 40–46, 2009.

[39] S. Del Guerra, M. Grupillo, M. Masini et al., "Gliclazide protects human islet beta-cells from apoptosis induced by intermittent high glucose," *Diabetes/Metabolism Research and Reviews*, vol. 23, no. 3, pp. 234–238, 2007.

[40] A. Sliwinska, J. Blasiak, J. Kasznicki, and J. Drzewoski, "In vitro effect of gliclazide on DNA damage and repair in patients with type 2 diabetes mellitus (T2DM)," *Chemico-Biological Interactions*, vol. 173, no. 3, pp. 159–165, 2008.

[41] M. L. Onozato, A. Tojo, A. Goto, and T. Fujita, "Radical scavenging effect of gliclazide in diabetic rats fed with a high cholesterol diet," *Kidney International*, vol. 65, no. 3, pp. 951–960, 2004.

[42] C. Zhang, W. Peng, M. Wang et al., "Studies on protective effects of human paraoxonases 1 and 3 on atherosclerosis in apolipoprotein E knockout mice," *Gene Therapy*, vol. 17, no. 5, pp. 626–633, 2010.

[43] M. Inoue, T. Suehiro, T. Nakamura, Y. Ikeda, Y. Kumon, and K. Hashimoto, "Serum arylesterase/diazoxonase activity and genetic polymorphisms in patients with type 2 diabetes," *Metabolism*, vol. 49, no. 11, pp. 1400–1405, 2000.

[44] A. Jafarnejad, S. Z. Bathaie, M. Nakhjavani, and M. Z. Hassan, "Effect of spermine on lipid profile and HDL functionality in the streptozotocin-induced diabetic rat model," *Life Sciences*, vol. 82, no. 5-6, pp. 301–307, 2008.

[45] R. Petraitiene, V. Petraitis, W. W. Hope et al., "Cerebrospinal fluid and plasma (1 → 3)-β-D-glucan as surrogate markers for detection and monitoring of therapeutic response in experimental hematogenous *Candida* meningoencephalitis," *Antimicrobial Agents and Chemotherapy*, vol. 52, no. 11, pp. 4121–4129, 2008.

[46] H. Al-Salami, G. Butt, I. Tucker, and M. Mikov, "Influence of the semisynthetic bile acid (MKC) on the ileal permeation of gliclazide in healthy and diabetic rats," *Pharmacological Reports*, vol. 60, no. 4, pp. 532–541, 2008.